

**GAF-Tandem Signal Transduktion in Chimeren mit der CyaB1
Adenylat Cyclase als Reporter**

**Interdomain Signal Transduction in GAF Tandem Chimeras
Using the CyaB1 Adenylyl Cyclase as a Reporter**

DISSERTATION

der Fakultät für Chemie und Pharmazie
der Eberhard-Karls-Universität Tübingen

zur Erlangung des Grades eines Doktors
der Naturwissenschaften

2008

vorgelegt von

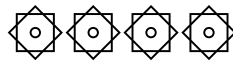
Iman Mansi

Tag der mündlichen Prüfung:	18. Juli 2008
Dekan:	Prof. Dr.L.Wesemann
Erster Berichterstatter:	Prof. Dr. J.E. Schultz
Zweiter Berichterstatter:	Prof.Dr. P. Ruth

Allah sagte:

”ihr Menschen! Wir erschufen euch aus einem Mann und einer Frau und machten euch zu Völkern und Stämmen, damit ihr einander kennenlernt. Doch der vor Allah am meisten Geehrte von euch ist der Gottesfürchtigste unter euch. Allah ist fürwahr wissend, kundig”

(Quran, 49:13)



All thanks goes to Allah who created me, send me my living, guided me to the right path and gave me power and good health to finish this work.



Acknowledgment

The experimental part of this work was performed within the period from August 2004 to September 2007 under the supervision of Prof. Dr. J.E.Schultz.

I would like to thank prof. Schultz for accepting me in his lab., for the beneficial scientific discussions and the different subjects he gave.

I am so grateful to prof. Ruth for taking part in the evaluation of my thesis.

Prof. Werz and prof. Laufer, I do appreciate your participation in the thesis examination.

I express my gratitude to Jost Weber and Jürgen Linder for the great help and interest they showed at the beginning of my work in the lab and for training me on the handling of the different kits and methods. Special thanks to J.Linder for the beneficial discussions, support and interest and for providing some of the constructs and templates. Anita Schultz, thanks a lot for providing some of the templates and your help in the cloning of three of my constructs.

And not to forget to thank Gottlieb Daimler und Karl Benz Foundation represented by the company managers Prof. Putlitz and Dr. Schade, the manager of the foundation, Dr. Klein and his secretary Mrs. Jung and all other employees in the foundation for providing my personal finance for two years and for the annual nice meetings with beneficial lectures and interesting journeys.

I am so thankful to Dr. I.Tews and his four-week diploma student, F.Voigts-Hoffmann from Heidelberg University, for the efforts they spent to solve the crystal structure of CyaB1 PAS domain and from the department of Biochemistry (Tübingen University), Dr. C.Schal for measuring the crystals of CyaB2 GAF ($\Delta 253$ -A255) and J.Romer for his help in operating the crystallization robot.

‘Meine Deutsch Lehrerin, Frau. Voegt, Ich danke ihnen sehr für ihre Bemühung und Geduld während Deutsch Unterrichte’

My Lab colleagues, my friends in Germany and in Jordan, my family in Germany and in Jordan, thank you all, without your love, encouragement and prayers, I will never be able to finish this work.

Content

Content.....	I
List of Constructs.....	IX
Abbreviations.....	XII
Amino acid abbreviations.....	XIV
1. Introduction.....	1
Signal transduction.....	1
1.1. Small molecule binding domains.....	2
1.1.1. GAF domains.....	3
1.1.2. PAS domains.....	5
1.2. Phosphodiesterases.....	6
1.2.1. PDE regulatory domain.....	8
1.2.2. PDE catalytic domain.....	10
1.3. Class III adenylyl cyclase.....	12
1.4. Cyanobacterium anabaena sp. PCC 7120 Adenylyl cyclases, CyaB1 and CyaB2.....	12
1.5. Aim of work.....	14
2. Materials and equipments.....	17
2.1. Chemicals and Materials.....	17
2.2. Equipments.....	19
2.3. Bacterial strains.....	20
2.4. Plasmids.....	21

2.5. Oligonucleotides.....	21
2.5.1. Sequencing primers.....	22
2.5.2. Cloning primers.....	23
2.5.2.1.CyaB1 holoenzyme.....	23
2.5.2.2.CyaB2 holoenzyme and mutants.....	24
2.5.2.3.hPDE5 GAF domain.....	26
2.5.2.4.rPDE2 GAF domain.....	27
2.5.2.5.hPDE2 GAF domain.....	28
2.6. Buffers and solutions.....	29
2.6.1. Molecular biology.....	29
2.6.1.1.solutions for DNA treatment.....	29
2.6.1.2.Solutions for bacterial culture media.....	29
2.6.1.3.Solutions for blue/white screening.....	29
2.6.2. Protein chemistry.....	30
2.6.2.1.Protein purification with Ni ⁺² –NTA- Agarose.....	30
2.6.2.2.SDS-Polyacrylamide gel electrophoresis.....	30
2.6.2.3.Western blot.....	31
2.6.2.4.Cyclase enzyme Assay.....	31
2.6.2.5.Dimerization buffers.....	32
2.6.2.6.Other solutions.....	33
3. Methods.....	33
3.1. Bioinformatics and databases.....	33
3.2. Molecular biology methods.....	33
3.2.1. Polymerase chain reaction.....	33
3.2.2. Isolation of DNA by agarose gel electrophoresis.....	35
3.2.3. Purification of DNA fragment from agarose gel.....	36
3.2.3.1.Use of DNA purification kit.....	36
3.2.3.2.Use of squeeze-freeze method.....	36
3.2.4. Generation of blunt ends.....	36
3.2.5. 5'-phosphorylation of the PCR product.....	36
3.2.6. Dephosphorylation of the plasmid vector.....	37
3.2.7. Photometric determination of the DNA concentration.....	37
3.2.8. Ligation of the DNA fragments.....	37
3.2.9. Transformation of the recombinant DNA.....	37
3.2.9.1.Preparation of competent cells.....	37

3.2.9.2. Transformation of DNA plasmid into competent cells.....	38
3.2.10. White-blue colony screen.....	38
3.2.11. Isolation of DNA.....	38
3.2.11.1. Isolation and purification of DNA from bacterial cultures (minipreps).....	38
3.2.11.2. Phenol/chloroform extraction.....	38
3.2.11.3. Ethanol precipitation.....	39
3.2.12. Enzymatic digestion.....	39
3.2.13. Sequencing.....	39
3.2.13.1. Chain terminating sequencing.....	39
3.2.13.2. Capillary DNA sequencing.....	40
3.2.14. Glycerol stock.....	41
3.3. Protein chemistry.....	41
3.3.1. Preculture.....	41
3.3.2. Expression.....	41
3.3.3. Cell harvesting and washing.....	42
3.3.4. Purification of soluble protein from <i>E.coli</i>	42
3.3.5. Protein dialysis.....	42
3.3.6. Bio-Rad protein determination.....	42
3.3.7. Sample concentration.....	42
3.3.8. SDS-PAGE.....	43
3.3.9. Western blot.....	44
3.3.10. Adenylyl cyclase enzyme assay.....	45
3.3.11. Crystallization.....	46
3.3.11.1. Hanging-drop vapour diffusion method.....	46
3.3.11.2. Sitting-drop vapour diffusion method.....	46
3.3.12. Size exclusion chromatography (Gel filtration).....	47
3.3.13. Dimerization studies.....	49
3.4. Cloning.....	50
3.4.1. Cloning of hPDE2 constructs.....	53
3.4.1.1. Cloning of hPDE2NGAF/CyaB1 chimera.....	53
3.4.1.2. Cloning of Δ N-hPDE2GAF/CyaB1 chimera.....	54
3.4.1.3. Cloning of hPDE5N-hPDE2GAF/CyaB1 chimera.....	55
3.4.1.4. Cloning of rPDE2GAF/CyaB1.....	57
3.4.2. Cloning of CyaB2 constructs and mutants.....	58
3.4.2.1. Cloning of (Δ aa or + aa)/CyaB1.....	58
3.4.2.2. Cloning of CyaB2 (Δ R253-A254)/CyaB1.....	60

3.4.2.3. Cloning of CyaB2 (Δ R253-A255) GAFcr for crystallization...	61
3.4.2.4. Cloning of CyaB2 (256 + NAA)cr, CyaB2 (M258L/M259L)GAF and CyaB2 (M258S/M259T)GAF.....	62
3.4.2.5. Cloning of CyaB2 (M74G/L75G)/CyaB1 and CyaB2 (M74S/L75T)/CyaB1.....	63
3.4.2.6. Cloning of CyaB2 α 2-mutants (CyaB2 (M87S)/CyaB1, CyaB2 (L88S)/CyaB1 and CyaB2(M87A/L88S)/CyaB1).....	65
3.4.2.7. Cloning of CyaB2 connecting helix-mutants (CyaB2 (M258A/M259A)/CyaB1, CyaB2 (M258L/M259L)/CyaB1, CyaB2 (M258G/M259G)/CyaB1 and CyaB2 (M258S/M259T)/ CyaB1.....	66
3.4.2.8. Cloning of CyaB2 (M74S/L75T/M258S/M259T)/CyaB1.....	67
3.4.2.9. Cloning of CyaB2 (M258T)/CyaB1.....	68
3.4.2.10. Cloning of CyaB2 (GAFlinker1)/CyaB1.....	70
3.4.3. Cloning of hPDE2 mutants.....	73
3.4.3.1. Cloning of hPDE2NGAF/CyaB1 α 1-helix mutants	73
3.4.3.2. Cloning of hPDE2NGAF/CyaB1 –connecting helix mutants...	75
3.4.3.3. Cloning of Cloning of the quadruple mutant of hPDE2GAF/CyaB1.....	77
3.4.3.4. Cloning of hPDE2NGAFcr.....	78
3.4.3.5. Cloning of Δ N-hPDE2GAFcr.....	79
3.4.3.6. Cloning of Δ N-hPDE2GAF (L396A/L397A)cr.....	79
3.4.3.7. Cloning of hPDE2NGAF (L396A/L397A)cr.....	80
3.4.3.8. Cloning of Δ N-hPDE2GAF (I230A/L231A/L396A/L397A)cr.	80
3.4.4. Cloning of hPDE5 mutants.....	
3.4.4.1. Cloning of hPDE5NGAF(L152A/L153A)/CyaB1	81
3.4.4.2. Cloning of hPDE5NGAF (L333A/L334A)/CyaB1 and hPDE5NGAF (L152A/L153A/L396A/L397A)/CyaB1.....	83
3.4.4.3. Cloning of hPDE5NGAF and mutants.....	84
3.4.4.4. Cloning of Δ N-hPDE5GAF (L333A/L334A).....	85
3.4.4.5. Cloning of Δ N-hPDE5GAF (L152A/L153A/L333A/L334A)...	85
3.4.5. Cloning of CyaB1 constructs.....	87
3.4.5.1. Displacement of CyaB1 PAS by hPDE5 catalytic linker.....	87
3.4.5.2. Cloning of Constructs IA and IB.....	89
3.4.5.3. Cloning of CyaB1(PAS2)/CyaB1.....	91
3.4.5.4. Cloning of CyaB1 (571+L).....	93
3.4.5.5. Cloning of CyaB1 PAS and CyaB1 PAS/catalytic for crystallization purposes.....	95
3.4.5.6. Cloning of CyaB1 GAFcr for crystallization purposes.....	96

3.4.5.7. Cloning of CyaB2 PAS and CyaB2 catalytic domain for crystallization purposes.....	97
3.4.5.8. Cloning of CyaB2 PAS/catalytic domain for crystallization purposes.....	98
4. Results.....	99
4.1. The effect of the N-terminal domain on signaling in the PDE2 GAF tandem/CyaB1 chimera.....	99
4.1.1. Biochemical characterization of hPDE2NGAF/CyaB1 chimera ...	99
4.1.1.1. Expression and purification of hPDE2NGAF /CyaB1 chimera.	100
4.1.1.2. Protein dependence	101
4.1.1.3. Dose response study of hPDE2NGAF/CyaB1 Chimera.....	101
4.1.1.4. Time dependence.....	102
4.1.1.5. Temperature dependence.....	103
4.1.1.6. pH dependence.....	104
4.1.1.7. ATP kinetics.....	104
4.1.2. Effect of N-terminus on CyaB1 AC activity.....	105
4.1.2.1. Expression and purification of the protein.....	106
4.1.2.2. Protein dependence	106
4.1.2.3. Dose response study.....	107
4.1.2.4. Time dependence.....	107
4.1.2.5. Substrate kinetics.....	108
4.1.2.6. Crystallization of ΔN_{1-227} -hPDE2GAF/CyaB1.....	109
4.1.3. Exchange by hPDE5 N-terminus.....	110
4.1.3.1. Protein dependence	111
4.1.3.2. Dose response study.....	111
4.1.4. Truncation of rat PDE2GAF.CyaB1 N-terminus.....	112
4.2. Role of the connecting helix of the GAF-tandem.....	114
4.2.1. CyaB2 GAF tandem.....	114
4.2.1.1. Biochemical characterization of CyaB2 GAF/CyaB1 AC chimera.....	114
4.2.1.2. Role of the connecting helix length.....	115
4.2.1.2.1. Shortening of the connecting helix.....	116
4.2.1.2.2. Elongation of the connecting helix.....	118
4.2.1.2.3. Exchange of the connecting helix.....	120
4.2.1.3. Crystallization of CyaB2 ($\Delta R253$ -A255) and CyaB2 (256+NAA).....	122

4.2.1.3.1. CyaB2GAF (Δ R253-A255).....	122
4.2.1.3.2. CyaB2GAF (256 + NAA)cr	125
4.2.1.4.Mutation of GAFa α – helices.....	126
4.2.1.4.1. α 1-helix.....	126
4.2.1.4.2. α 2-helix.....	128
4.2.1.5.Mutation of connecting helix of CyaB2 GAF.....	130
4.2.1.6.Dimerization study and gel filtration.....	135
4.2.1.7.Crystallization of CyaB2 PAS (444-568), catalytic (569-860 and PAS/catalytic (444-860) domains.....	136
4.2.2. hPDE2 GAF tandem.....	137
4.2.2.1.Mutation of GAFa α 1– helix.....	137
4.2.2.2.Mutation of the connecting helix of hPDE2NGAF/CyaB1.....	140
4.2.2.3.Quadruple mutation of both helices.....	142
4.2.2.4.Crystallization of hPDE2GAF \pm N-terminus.....	144
4.2.2.4.1. hPDE2NGAFcr.....	144
4.2.2.4.2. Δ N-hPDE2 GAF	145
4.2.2.5.Glutaraldehyde dimerization and gel filtration of hPDE2GAF and mutants	146
4.2.3. hPDE5 GAF tandem.....	150
4.2.3.1.hPDE5/CyaB1 mutants.....	151
4.2.3.2.Dimerization by Glutaraldehyde and gel filtration of hPDE5 and mutants.....	154
4.3. Signal transduction through the PAS domain of CyaB1.....	159
4.3.1. Exchange of CyaB1 PAS domain by the PDE5 linker.....	159
4.3.1.1.Control (truncated catalytic domains).....	160
4.3.1.2.Category A	164
4.3.1.3.Category B.....	165
4.3.2. Exchange of CyaB1 PAS domain by CyaB2 PAS domain.....	167
4.3.3. Insertion of tetradekapeptide linker between PAS and catalytic domains of CyaB1.....	170
4.3.4. Crystallization trials of the CyaB1 domains.....	172
4.3.4.1. Crystallization of CyaB1 GAF domain.....	172
4.3.4.2.Crystallization of CyaB1 PAS domain.....	175
4.3.4.3.Crystallization of Catalytic and PAS/catalytic domains of CyaB1.....	179

5. Discussion.....	183
5.1. Biochemical characterization of hPDE2NGAF/CyaB1 chimera.....	183
5.1.1. hPDE2NGAF/CyaB1 chimera had a 5-fold stimulation upon binding of cGMP	183
5.2. Role of the N-terminal domain on the activity and regulation of PDE2/CyaB1 chimera.....	185
5.2.1. Effect of the hPDE2 N-terminus.....	185
5.2.2. Effect of hPDE5 N-terminus on the regulation and activity of hPDE2/CyaB1 AC chimera.....	186
5.2.3. The CyaB1 N-terminus reduced the fold stimulation by cGMP of rat PDE2 GAF.....	186
5.3. Role of the connecting helix in the signal transduction.....	187
5.3.1. Shortening and elongation of the connecting helix of CyaB2GAF disturb dimerization and signaling.....	187
5.3.2. The effect of CyaB1 connecting helix on the signaling of CyaB2 GAF.....	189
5.3.3. The role of the two hydrophobic residues (ML) in $\alpha 1$ and $\alpha 2$ helices of CyaB2 GAF.....	189
5.3.4. The role of two methionines in the connecting helix on dimerization and signaling.....	191
5.3.5. Mutation of two hydrophobic aa residues in the $\alpha 1$ -helix and another in the connecting helix disturbed the dimerization of hPDE2 and hPDE5 GAF domain.....	192
5.4. Signal transduction through CyaB1 PAS domain.....	194
5.4.1. Is it determined by the binding of a divalent cation to the PAS domain?.....	194
5.4.2. CyaB1 catalytic domain utilizes only one ATP catalytic core depends on the truncation.....	195
5.4.3. The linker of hPDE5 can transduce the signal between GAF and catalytic domains of CyaB1 but with less efficiency.....	197
5.4.4. Exchange of the PAS domain by that of CyaB2 is still able to transduce the signal but with less efficiency.....	199
5.4.5. The insertion of a flexible linker between the catalytic linker and the catalytic domain of CyaB1 completely destroyed signaling to the catalytic domain.....	199

Content

5.4.6. Crystallization of CyaB1 PAS domain.....	200
5.4.7. Discovering of metal ligand for the CayB1 PAS.....	201
5.4.8. Importance of this work.....	201
5.4.9. Open questions and outlook.....	201
6. Conclusion.....	203
7. Appendix.....	205
8. References.....	225

List of constructs

1. hPDE2 constructs

Construct	Description
1. hPDE2NGAF/CyaB1	hPDE2 ₁₋₅₅₈ -CyaB1 ₃₈₆₋₈₅₉
2. ΔN-hPDE2GAF/CyaB1	hPDE2 ₂₂₈₋₅₅₈ -CyaB1 ₃₈₆₋₈₅₉
3. hPDE5N-PDE2GAF/CyaB1	hPDE5 ₁₋₁₅₀ -hPDE2 ₂₂₈₋₅₅₈ -CyaB1 ₃₈₆₋₈₅₉
4. ΔN-rPDE2GAF/CyaB1	rPDE2 ₂₀₇₋₅₄₆ -CyaB1 ₃₈₆₋₈₅₉
5. hPDE2 (I230S)/CyaB1	hPDE2 ₁₋₅₅₈ (I230S)-CyaB1 ₃₈₆₋₈₅₉
6. hPDE2 (L231S)/CyaB1	hPDE2 ₁₋₅₅₈ (L231S)-CyaB1 ₃₈₆₋₈₅₉
7. hPDE2 (C393S)/CyaB1	hPDE2 ₁₋₅₅₈ (C393S)-CyaB1 ₃₈₆₋₈₅₉
8. hPDE2 (L396A/L397A)/CyaB1	hPDE2 ₁₋₅₅₈ (L396A/L397A)-CyaB1 ₃₈₆₋₈₅₉
9. hPDE2 (C393S/L396A/L397A)/CyaB1	hPDE2 ₁₋₅₅₈ (C393S/L396A/L397A)-CyaB1 ₃₈₆₋₈₅₉
10. ΔN-hPDE2 (I230A/L231A/L396A/L397A)/CyaB1	hPDE2 ₂₂₈₋₅₅₈ (I230A/L231A/L396A/L397A)/CyaB1 ₃₈₆₋₈₅₉
11. hPDE2NGAFcr	hPDE2 ₁₋₅₆₂ for crystallization
12. ΔN-hPDE2cr	hPDE2 ₂₂₈₋₅₆₂ for crystallization
13. hPDE2NGAF (L396A/L397A)	hPDE2 ₁₋₅₆₂ (L396A/L397A)
14. ΔN-hPDE2GAF (L396A/L397A)	hPDE2 ₂₂₈₋₅₆₂ (L396A/L397A)
15. ΔN-hPDE2GAF (I230A/L231A/L396A/L397A)	hPDE2GAF ₂₂₈₋₅₆₂ (I230A/L231A/L396A/L397A)

2. CyaB2 constructs

Construct	Description
1. CyaB2(ΔR253)/CyaB1	CyaB2 ₁₋₂₅₂ -CyaB2 ₂₅₄₋₄₄₁ -CyaB1 ₃₈₆₋₈₅₉
2. CyaB2(ΔR253-A254)/CyaB1	CyaB2 ₁₋₂₅₂ -CyaB2 ₂₅₅₋₄₄₁ -CyaB1 ₃₈₆₋₈₅₉
3. CyaB2(ΔR253-A255)/CyaB1	CyaB2 ₁₋₂₅₂ -CyaB2 ₂₅₆₋₄₄₁ -CyaB1 ₃₈₆₋₈₅₉
4. CyaB2(ΔR253-A256)/CyaB1	CyaB2 ₁₋₂₅₂ -CyaB2 ₂₅₇₋₄₄₁ -CyaB1 ₃₈₆₋₈₅₉
5. CyaB2(256+NAA)/CyaB1	CyaB2 ₁₋₂₅₆ -NAA-CyaB2 ₂₅₇₋₄₄₁ -CyaB1 ₃₈₆₋₈₅₉
6. CyaB2(256+NAAI)/CyaB1	CyaB2 ₁₋₂₅₆ -NAAI-CyaB2 ₂₅₇₋₄₄₁ -CyaB1 ₃₈₆₋₈₅₉
7. CyaB2(M74G/L75G)/CyaB1	CyaB2 ₁₋₄₄₁ (M74G/L75G)-CyaB1 ₃₈₆₋₈₅₉
8. CyaB2(M74S/L75T)/CyaB1	CyaB2 ₁₋₄₄₁ (M74S/L75T)-CyaB1 ₃₈₆₋₈₅₉
9. CyaB2(M87S)/CyaB1	CyaB2 ₁₋₄₄₁ (M87S)-CyaB1 ₃₈₆₋₈₅₉
10. CyaB2(L88S)/CyaB1	CyaB2 ₁₋₄₄₁ (L88S)-CyaB1 ₃₈₆₋₈₅₉
11. CyaB2(M87A/L88S)/CyaB1	CyaB2 ₁₋₄₄₁ (M87A/L88S)-CyaB1 ₃₈₆₋₈₅₉
12. CyaB2(M258T)/CyaB1	CyaB2 ₁₋₄₄₁ (M258T)-CyaB1 ₃₈₆₋₈₅₉

List of constructs

13. CyaB2(M258L/M259L)/CyaB1	CyaB2 ₁₋₄₄₁ (M258L/M259L)-CyaB1 ₃₈₆₋₈₅₉
14. CyaB2(M258G/M259G)/CyaB1	CyaB2 ₁₋₄₄₁ (M258G/M259G)-CyaB1 ₃₈₆₋₈₅₉
15. CyaB2(M258A/M259A)/CyaB1	CyaB2 ₁₋₄₄₁ (M258A/M259A)-CyaB1 ₃₈₆₋₈₅₉
16. CyaB2(M258S/M259T)/CyaB1	CyaB2 ₁₋₄₄₁ (M258S/M259T)-CyaB1 ₃₈₆₋₈₅₉
17. CyaB2(M74S/L75T/M258S/M259T)/CyaB1	CyaB2 ₁₋₄₄₁ (M74S/L75T/M258S/M259T)-CyaB1 ₃₈₆₋₈₅₉
18. CyaB2(GAFlinker1)/CyaB1	CyaB2 ₁₋₂₃₀ -CyaB1 ₁₉₇₋₂₂₉ -CyaB2 ₂₆₄₋₄₄₁ -CyaB1 ₃₈₆₋₈₅₉
19. CyaB2 ((Δ R253-A255)cr	CyaB2 ₅₈₋₂₅₂ -CyaB2 ₂₅₆₋₄₄₅ for crystallization
20. CyaB2(256+NAA)cr	CyaB2 ₅₈₋₂₅₆ -NAA-CyaB2 ₂₅₇₋₄₄₅ for crystallization
21. CyaB2(M258L/M259L)	CyaB2 ₅₈₋₄₄₅ (M258L/M259L)
22. CyaB2 (M258S/M259T)	CyaB2 ₅₈₋₄₄₅ (M258S/M259T)
23. CyaB2PAS/Cat	CyaB2 ₄₄₄₋₈₆₀ for crystallization
24. CyaB2PAS	CyaB2 ₄₄₄₋₅₆₈ for crystallization
25. CyaB2Catalytic	CyaB2 ₅₆₉₋₈₆₀ for crystallization

3. hPDE5 constructs

Construct	Description
1. hPDE5(L152A/L153A)/CyaB1	hPDE5 ₁₋₅₁₃ (L152A/L153A)-CyaB1 ₃₈₆₋₈₅₉
2. hPDE5(L333A/L334A)/CyaB1	hPDE5 ₁₋₅₁₃ (L333A/L334A)-CyaB1 ₃₈₆₋₈₅₉
3. hPDE5(L152A/L153A/L333A/L334A)/CyaB1	hPDE5 ₁₋₅₁₃ (L152A/L153A/L333A/L334A)-CyaB1 ₃₈₆₋₈₅₉
4. hPDE5NGAF	hPDE5 ₁₋₅₁₇
5. hPDE5(L152A/L153A)	hPDE5 ₁₋₅₁₇ (L152A/L153A)
6. hPDE5(L333A/L334A)	hPDE5 ₁₋₅₁₇ (L333A/L334A)
7. hPDE5(L152A/L153A/L333A/L334)	hPDE5 ₁₋₅₁₇ (L152A/L153A/L333A/L334A)
8. Δ N-hPDE5cr (from Ana Banjac)	hPDE5 ₁₃₆₋₅₁₇
9. Δ N-hPDE5(L333A/L334A)	hPDE5 ₁₃₆₋₅₁₇ (L333A/L334A)
10. Δ N-hPDE5(L152A/L153A/L333A/L334A)	hPDE5 ₁₃₆₋₅₁₇ (L152A/L153A/L333A/L334A)

4. CyaB1 constructs

Construct	Description
1. Construct IA	CyaB1 ₁₋₃₈₇ -hPDE5 ₅₁₃₋₅₃₇ -CyaB1 ₅₉₅₋₈₅₉
2. Construct IIA	CyaB1 ₁₋₃₈₇ -hPDE5 ₅₁₃₋₅₃₇ -CyaB1 ₅₈₉₋₈₅₉
3. Construct IIIA	CyaB1 ₁₋₃₈₇ -hPDE5 ₅₁₃₋₅₃₇ -CyaB1 ₅₇₂₋₈₅₉
4. Construct IVA	CyaB1 ₁₋₃₈₇ -hPDE5 ₅₁₃₋₅₃₇ -CyaB1 ₅₆₀₋₈₅₉

List of constructs

5. Construct IB	CyaB1 ₁₋₃₈₇ -hPDE5 ₅₁₃₋₅₄₈ -CyaB1 ₅₉₅₋₈₅₉
6. Construct IIB	CyaB1 ₁₋₃₈₇ -hPDE5 ₅₁₃₋₅₄₈ -CyaB1 ₅₈₉₋₈₅₉
7. Construct IIIB	CyaB1 ₁₋₃₈₇ -hPDE5 ₅₁₃₋₅₄₈ -CyaB1 ₅₇₂₋₈₅₉
8. Construct IVB	CyaB1 ₁₋₃₈₇ -hPDE5 ₅₁₃₋₅₄₈ -CyaB1 ₅₆₀₋₈₅₉
9. Construct I (from T.Kanacher)	CyaB1 ₅₉₅₋₈₅₉
10. Construct II (from J.Linder)	CyaB1 ₅₈₉₋₈₅₉
11. Construct III (from J.Linder)	CyaB1 ₅₇₂₋₈₅₉
12. Construct IV (from J.Linder)	CyaB1 ₅₆₀₋₈₅₉
13. CyaB1GAF (from A.Schultz)	CyaB1 ₄₂₋₃₈₉
14. CyaB1PAS	CyaB1 ₃₈₇₋₅₇₁
15. CyaB1PAS/catalytic	CyaB1 ₃₈₇₋₈₅₉
16. CyaB1(PAS2)/CyaB1	CyaB1 ₁₋₃₈₇ -CyaB2 ₄₄₄₋₅₇₀ -CyaB1 ₅₇₀₋₈₅₉
17. CyaB1(571 + L)	CyaB1 ₁₋₅₇₁ -TRAAGGPPAAGGLE-CyaB1 ₅₇₂₋₈₅₉

Abbreviations

Abb.	Illustration
AA/Bis	Acrylamide/ Bisacrylamide (37.5:1)
Amp	Ampicillin
AC	Adenylyl cyclase
aa	amino acid
bp	base pair
bPDE2	Bovine phosphodiesterase 2
BSA	Bovine serum albumine
cpm	counts per minute
CyaB1/CyaB2	adenylate cyclases CyaB1/CyaB2 from <i>Anabaena</i> sp. PCC 7120
CyaB1 AC	Catalytic domain of CyaB1 enzyme
dNTP	deoxy nucleoside triphosphate
ddNTP	dideoxy nucleoside triphosphate (for sequencing)
EtBr	Ethidium bromide
ESRF	European Synchrotron Radiation Facility
HEPES	4-(2-hydroxyethyl)-1-piperazineethanesulfonic acid
hPDE2	human phosphodiesterase 2
IPTG	Isopropyl thiogalactoside
LB- medium	Luria-Bertani culture medium for bacteria
MCS	Multiple cloning site
MES	2-(N-Morpholino) ethanesulphonic acid
Min	Minute
Ni ⁺² -NTA agarose	Nickel-nitrilotriacetic acid Agarose
ORF	open reading frame

Abbreviations

PAGE	Polyacrylamide gel electrophoresis
PDE's	Phosphodiesterase (s)
PEG	Polyethylene Glycol
rPDE2	rat phosphodiesterase 2
rpm	revolution per minute
RT	room temperature
Sec	Second
SMBDs	small molecules binding domain
TBS	Tris buffered saline
TEMED	N,N,N',N'-trimethylethylene diamine
Tris	2-amino-2-hydroxymethyl-propane-1,3-diol
WT	Wild type
X-Gal	5-bromo-4-chloro-3-indolyl- β -D- Galactopyranoside

Abbreviation for aa residues

1 letter code	3-letters code	Full name
A	Ala	Alanine
C	Cys	Cysteine
D	Asp	Aspartic acid
E	Glu	Glutamic acid
F	Phe	Phenylalanine
G	Gly	Glycine
H	His	Histidine
I	Ile	Isoleucine
K	Lys	Lysine
L	Leu	Leucine
M	Met	Methionine
N	Asn	Asparagine
P	Pro	Proline
Q	Gln	Glutamine
R	Arg	Arginine
S	Ser	Serine
T	Thr	Threonine
V	Val	Valine
W	Trp	Tryptophane
Y	Tyr	Tyrosine
X		Any residue
aa		Amino acid

Abbreviation of bases

- A: Adenine
- T: Thymine
- G: Guanine
- C: Cytosine

1 Introduction

Signal transduction

Living organisms usually adapt themselves to continuous changes of the environment. The control of biological function occurs at the systematic, cellular and molecular level. Cells in the pluricellular organisms do not respond only to exterior inputs, but to substances produced by other cells of the same organism.

The availability of complete genome sequences of organisms representing each of the three divisions of cellular life (bacteria, archaea and eukaryota) has provided unprecedented opportunities for comparative analysis of the relative significance of different regulatory processes in these organisms. Regulatory mechanisms can be classified into partially overlapping broad categories in the basis of the sites and targets of their action. One of these categories is signal transduction (signaling) whereby an extracellular or intracellular stimulus leads to a cascade of molecular interactions that affects one or more cellular functions resulting in a response to the initial signal [1].

From the time of their identification by Rall and Sutherland in 1958 [2-4], the cyclic nucleotide second messengers, cAMP and cGMP, were considered to be key molecules for transducing the action of extracellular signals such as hormones, neurotransmitters, and light into the most diverse cell functions, thus playing an important role in a wide array of physiological processes that include vision, cell growth and division, memory, and immune responses [5-7]. Cellular activation of adenylate and guanylate cyclases, respectively, results in the cyclization of ATP and GTP to 3'-5' cyclic adenosine monophosphate (cAMP) and 3'-5' cyclic guanosine monophosphate (cGMP) respectively. Each of them activates in addition to other enzymes, protein kinases, the protein kinase activated by cAMP (PKA) and the protein kinase activated by cGMP. Activated PKA and PKG are able to phosphorylate a number of cellular effector proteins (for example ion channels, G-protein-coupled receptors, structural proteins). It is possible in this way for the second messengers to control a wide variety of physiological processes in a wide variety of organs. However, the cyclic nucleotides are also able to act directly on effector molecules. Thus, it is known, for example, that cGMP can act directly on ion channels and thus can influence the cellular ion concentration. The phosphodiesterases (PDEs) are a control mechanism for controlling the activity of cAMP and cGMP. PDEs hydrolyse the cyclic monophosphates to monophosphates AMP and GMP (Fig.1.1) [8, 9].

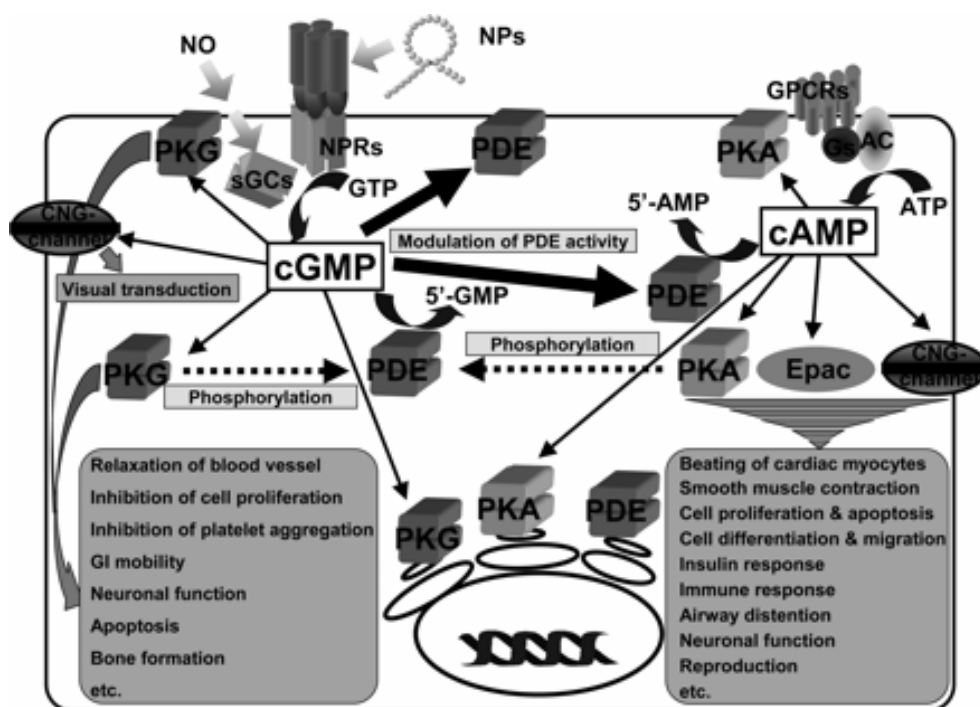


Fig.1.1: cyclic nucleotide signaling and regulation. Localization of fundamental molecules involved in cAMP and cGMP signalling is illustrated. Effector molecules of cAMP and cGMP are indicated by arrows from each cyclic nucleotide. Phosphorylation of PDEs by PKA and PKG is demonstrated by dotted arrows. Modulation by PDE activity by cGMP is shown by thick arrow. Cellular and physiological outputs of cyclic nucleotide signaling are shown in gray-coloured boxes. NPs indicate natriuretic peptides; NO, nitric oxide; NPRs, natriuretic peptide receptors; sGCs, soluble guanylyl cyclases; AC, adenylyl cyclases; Gs, GTP-binding protein α subunit; GPCRs, G protein-coupled receptors; Epac, exchange protein directly activated by cAMP; CNG-channel, cyclic nucleotide-gated channel. Image taken from [9].

Until recently, it has been difficult to understand how these simple, small, second messenger molecules could provide both the specificity of action and the diversity of function necessary for such regulation [10].

1.1 Small molecule binding domains (SMBD)

The ability to sense small molecules is the key for every life form and provides information about the extracellular environment, monitors intracellular physiological status, or establishes cell-cell communication. Sensory signaling proteins are often modular in nature with distinct domains for ligand sensing and for output signals. A number of these domains are abundant in bacteria and animals [11].

SMBDs are compact globular domains distinct from the catalytic domains of the respective enzymes, whose principal biochemical role is to exert a regulatory effect and/or to transmit signal by binding a small molecule. This can include small molecule-mediated regulation of

transcription (kinases), signal transduction (PDEs and phosphatases) and transport (membrane associated ABC ATPases) [1, 12]

Most of the SMBD are relatively small domains, often ~ 100 amino acid residues in length, and in general, their sequences do not share high similarities as those of enzymatic domains. More than 21 SMBD were identified in the database for example: PAS (**P**ER, **A**RNT, **S**IM), GAF (**c**GMP-PDE, **A**denylyl cyclase, **F**hlA), ACT (**A**spartokinase, **C**horismate mutase, **T**yrA), CBS (**C**ystothionine **β** -Synthase), cNMPBD (**c**yclic **N**ucleotide **M**ono**P**hosphate **B**inding **D**omain), HAMP domain (**H**istidine kinases, **A**denylyl cyclases, **M**ethyl-accepting chemotaxis protein and **P**hosphatases) and many other domains. Several SMBD were found to be fused to enzymatic domains involved in metabolic reactions which suggests the regulation of the catalytic activity through small molecule binding [1].

1.1.1 GAF Domains

The GAF domain is one of the largest families of small molecule binding regulatory domains [13]. Although ligand binding was documented for only few predicted GAFs, ligand binding GAF domains have been shown to bind formate, aromatic compounds (e.g. tetrapyrrole and photopigments) and cyclic nucleotides. GAF domains are found in many different proteins in nearly all phyla, including histidine kinases, phosphotransferases, ATPases, cyclases and phosphodiesterases. The acronym GAF is derived from mammalian **c**GMP-activated PDEs, *Anabaena* Adenylyl cyclases, and *E.coli* Formate hydrogen lyase transcription activator (FhlA), enzymes where they were initially recognized [14, 15]. GAF domains have been shown to be associated with gene regulation in bacteria, light-detection and signalling pathways in plants and cyanobacterial phytochromes, ethylene detection and signalling in plants, nitrogen fixation in bacteria, feed forward control of cyanobacterial ACs by cAMP binding and the two component sensor histidine kinase in viruses, bacteria and plants [14, 16]. Figure 1.2 shows the abundance of GAF domains in different phyla.



Fig.1.2: Domain structures of mammalian GAF and PAS domain-containing phosphodiesterases and other representative GAF domain proteins. Image is taken from ref. [17].

The PDE superfamily is the only group of mammalian proteins known to have GAFs; all isoforms of five families (PDEs 2, 5, 6, 10 and 11) contain a tandem GAF (a and b), and in PDEs 2, 5, 6, and 11, at least one GAF forms an allosteric site for cGMP binding while the GAF domain of PDE10 forms an allosteric binding site for cAMP [13, 18, 19]. In addition to cyclic nucleotide binding, GAF domains of mammalian PDEs are involved in protein-protein interactions that provide for homologous and heterologous dimerization of PDE catalytic monomer as well as for binding of PDE6 catalytic monomers with specific members of the family of inhibitory proteins known as $P\gamma$ [20]. The dimerization in PDEs may be important for regulation, enzyme stability, subcellular localization, or other features. The importance of GAF domains and cGMP allosteric interactions in the PDEs is illustrated by the H258D mutation in the GAFa domain of human PDE6B, which causes the autosomal dominant

congenital stationary night blindness [21]. In addition, recessive mutations in hPDE6B gene that cause truncations in the gene product result in retinitis pigmentosa [22].

Up to date, four GAF domains have been structurally elucidated. The yeast GAF domain, YKG9, resolved at 1.9 Å, was the first GAF domain crystal structure to be elucidated and was found to form a homodimer with no ligand binding [17]. Another two are cyclic nucleotide binding-GAF tandems. Mouse PDE2 GAF tandem, resolved at 2.9 Å, is a parallel dimer with cGMP molecule bound to the GAF b subdomain of each monomer. The tandem GAF domain of the *CyaB2* AC, resolved at 1.9 Å, which is an antiparallel dimer with four cAMP molecules bound to each subdomain, GAF a and b, of both monomers [23, 24]. The last GAF crystal structure was an *E.coli* fRMsR (methionine-R-sulfoxide reductase), which was resolved at 2.1 Å and considered to represent a GAF domain with enzymatic activity [25].

Even among cGMP-binding PDEs the functions of the respective GAFs are not conserved. Many questions remain unclear regarding the structure-function relationships within the regulatory domain of these PDEs, the role of GAFs a and b in function and physical parameters that provide for cGMP binding and regulation of function by post-translational modifications such as phosphorylation [15].

The presence of the GAF domains in almost half of the mammalian PDEs families makes them particularly attractive therapeutic targets for manipulation of cAMP and cGMP signalling [13].

1.1.2 PAS Domains

The PAS domain is one of the regulatory modules that can be found in proteins in all kingdoms of life (archaea, bacteria and eukarya) [14, 26-28]. The PAS module was first identified in the *Drosophilla* clock protein PER, and the basic helix-loop-helix containing transcription factor ARNT (aryl hydrocarbon receptor nuclear translocator) in mammals and SIM (single minded protein) in insects [29], and it is considered one of the important signaling modules that monitors changes in light, redox potential, oxygen, small ligands, or the overall energy level of a cell [26, 30-32], in addition to their role in mediating protein-protein interactions [1].

These domains are sometimes referred to as LOV domains (Light, Oxygen or Voltage domains). Unlike many other sensory domains, PAS domains are located in the cytoplasm [26] and are found in serine/threonine kinases [33], histidine kinases [34], photoreceptors and chemoreceptors for taxis and tropism [35], cyclic nucleotide phosphodiesterase [36], circadian

clock proteins [37, 38], voltage activated ion channels [39], as well as regulators of responses to hypoxia [40] and embryological development of the central nervous system [29]. Most PAS domains bind cofactors or ligands, which are required for the detection of sensory input signals [31].

PAS domains convert various input stimuli into signals that propagate to downstream components by altering intra- or intermolecular protein-protein interactions. The mechanisms whereby PAS domains transmit the input signal into the effector domain are of great current interest but are poorly understood [41].

The specificity in sensing arises from cofactors that are associated with PAS domains: *p*-hydroxycinnamic acid in the bacterial photoactive yellow protein, PYP [42]; a heme in the bacterial oxygen sensor FixL [43]; and flavin adenine dinucleotide (FAD) in a bacterial redox potential sensor NifL [44]. A plant photoreceptor, NPH1 that also senses redox potential has a flavin mononucleotide (FMN) cofactor in its PAS domain [45].

The PAS domain superfamily is highly diverse in sequence and in length but is suggested to share the common conformational flexibility and the basic three dimensional (3D) structure, consisting of a PAS core motif, helical connector and a PAC motif [30, 46].

Similar to the GAF domain, mutations in the PAS domain were also found to cause inherited diseases. A mutation in the HERG PAS domain (T65P) of K⁺ channel in the heart causes congenital long QT syndrome which manifests itself by a prolonged QT interval on the electrocardiogram and by a propensity for tachyarrhythmias causing syncope and sudden death [47].

1.2 Phosphodiesterases

Phosphodiesterases split the phosphodiester bond and generate the mononucleotides. PDEs are classified by their primary structure similarities into three classes [48]:

- The class I domain: all share a C-terminal catalytic domain of 250 aa's with the invariant motif H(X)3H(X)25-35D/E that forms the two metal ion binding sites in the active centre [49]. This class includes all mammalian PDEs, as well as several genes identified in *Drosophila*, *Caenorhabditis* and yeast.
- The class II domain: shares the signature sequence HXHLDH in its catalytic domain which may be part of a metal ion binding site. Class II is comprised of a few enzymes from *Saccharomyces cerevesae* (PDE gene 1 product), *Dictyostelium discoideum*,

Introduction

Schizosaccharomyces pombe, *Candida albicans* and a periplasmic PDE from *Vibrio fischeri*.

- Class III PDE domain: cpdA gene of *E.coli* [48].

Twenty-one genes encoding PDEs have been identified in the human genome [50, 51], and corresponding proteins have been characterized in terms of their physicochemical properties and regulatory properties [6, 7]. Based in their sequence relatedness, kinetics, modes of regulation and pharmacological properties, the class I mammalian PDEs can be further subdivided into 11 families (PDE1 – PDE11)[52]. The different PDEs of the same family are functionally related despite the fact that their amino acid sequences show considerable divergence. Functional analyses and amino acid sequence comparisons of various PDEs indicate that all PDEs are multidomain proteins with different domains functioning in catalysis and regulation of activity [53]. Table 1.1 shows the different characteristics of different PDEs.

PDEs affect the cellular levels of cyclic nucleotides. Inhibiting these enzymes is an attractive strategy in the development of smooth-muscle relaxants and drugs to treat inflammatory diseases, asthma, chronic obstructive pulmonary disease, depression and many other diseases. The first selective inhibitor was PDE5-inhibitor, ViagraTM (Sildenafil), which was marketed for the treatment of male erectile dysfunction and later for pulmonary hypertension. This was followed by developing more selective PDE5-inhibitors and other PDE inhibitors [54-56].

Because all PDEs share a high degree of sequence similarity in their catalytic domain, the selectivity profile of all inhibitors at least partially overlap [10]. At the time that PDE4 inhibitors cause nausea and emesis, possibly by inhibiting PDE4D in the brain, sildenafil and related PDE5 inhibitors exhibit cross-reactivity with PDE6 and PDE11, which is thought to be responsible for side effects such as blue-tinged vision and back and muscle pain. Information about the binding mode of PDE inhibitors will therefore be crucial for the design of drugs that target these enzymes in a more selective manner [57].

Table 1.1: Biochemical characteristics of human PDE families modified according to [9, 58]:

Gene Family	Substrate	Localisation		Inhibitors
		Tissue	Intracellular	
hPDE1 A/B C	cGMP>cAMP cGMP=cAMP	Brain, smooth muscles, heart ,testis	cytosolic	Vinpocetine, ICOS, SCH51866
hPDE2A	cGMP=cAMP	Adrenal cortex, brain, heart	PDE2A1 is cytosolic while PDE2A2 and A3 are membrane- bound	EHNA, BDP, BAY 60-7550, IC933
hPDE3 A/B	cGMP<cAMP	Heart, smooth muscle, adipose tissue, platelets	A membrane bound or cytosolic but B is membrane bound	Cilostamide, Milrinone, Trequinsin, Cilastazol, OPC-33540
hPDE4 A/B/C/D	cAMP	Ubiquitous (immune system, olfactory system, Brain, testis, lung and other tissues)	PDE4A5 is membrane bound but other splices are predominantly cytosolic	Rolipram, Ruflumilast, Cilomilast, Ro 20-1724, AWD 12-281, V-11294A, SCH351591
hPDE5A	cGMP	Smooth muscle, platelets, cerebellum	cytosolic	Zaprinast, Sildenafil, Vardenafil, Tadalafil, DA-8159
hPDE6 A/B/C	cGMP	Retina	cytosolic	-
hPDE7 A/B	cAMP	Skeletal muscle, immune cells, brain	cytosolic	BRL 50481, IC242
hPDE8 A/B	cAMP	Immune cells, liver, kidney, testis, thyroid	Cytosolic and particulate	-
hPDE9A	cGMP	Brain, kidney	cytosolic	BAY 73-6691
hPDE10A	cAMP>cGMP	Brain, testis	A1 and A3 are cytosolic but A2 is particulate	-
hPDE11A	cGMP=cAMP	Prostate, testis, skeletal muscle	cytosolic	-

1.2.1 PDE regulatory domain

The PDE N-terminal domains determine several properties such as regulation of enzyme activity by posttranslational modifications (e.g. phosphorylation by PKA, PKB, ERK2, CaMK and PKG), and binding of other messenger molecules (e.g. cGMP, cAMP, Ca⁺², calmodulin, and phosphatidic acid) or by specifying the subcellular localization of the enzymes by protein-protein interactions and membrane insertion [59, 60].

PDE1 family, two tandem Ca⁺²/Calmodulin domains are present N-terminally. The binding of both Ca⁺² and calmodulin is required for full activation of the enzyme which varies from 3-10 fold depending on the source, tissue and enzyme preparation [10].

Introduction

In PDE2, 5, 6, 10, and 11 families, two tandem GAF domains in the regulatory domain were found to bind cyclic nucleotide which activates the catalytic domain and enhance dimerization. Phosphorylation sites were identified in PDE1, 2, 3, 4, 5, 6, 10 and 11 which differ in their effect on the catalytic domain [61-64].

A membrane divergent N-terminal region with its membrane associated domain and a hydrophilic catalytic domain were identified in PDE3. Studies of different truncated PDE3 forms revealed that the N-terminal was not required for maintaining full catalytic activity and sensitivity to PDE3 specific inhibitors, although it may be important for localization [65]. cGMP was found to have an inhibitory effect on PDE3, but the mechanism of inhibition was not due to binding to the regulatory domain as the GAF domain, rather by competition with cAMP at the catalytic site [10].

In the PDE4 N-terminus, two tandem UCR (Upstream Conserved Region) domain and one phosphorylation site are regulating the catalytic domain. Different splice variants are expressed by PDE4 genes which are distinguished by long forms and short forms. Long forms possess both UCR1 and UCR2. The UCR tandem has been shown to be responsible for the dimerization of the enzyme. In addition, phosphorylation of serine in UCR1 of PDE4 long forms causes the activation of the enzyme by 60-250%[58].

At the time a PKA pseudosubstrate site is present in the N terminus of PDE7A subfamily, PDE8 contains REC and PAS domains in its N-terminal portion. REC domain functions as a receiver of signals from the sensor component in 2-component signal transduction systems in lower organisms. PAS domain is involved in the binding of small ligands and protein-protein interaction. However, regulation of PDE8 via REC or PAS domain is unknown. Lastly, there is no report on the regulation of PDE9A activity or the presence of endogenous PDE9A activity in either tissue or cell extracts [9]. Binding of a ligand or phosphorylation in these N-terminal domains causes a change in the conformation of the catalytic domain with an increase in V_{max} or decrease in K_m toward the cyclic nucleotide substrate and often modifies interaction with inhibitors. The changes in conformation of the catalytic domain that follow modification at the N-terminus are unknown but may provide a window of opportunity for new drug design [62]. Figure 1.3 shows the different N-termini of the 11 PDE families with phosphorylation sites.

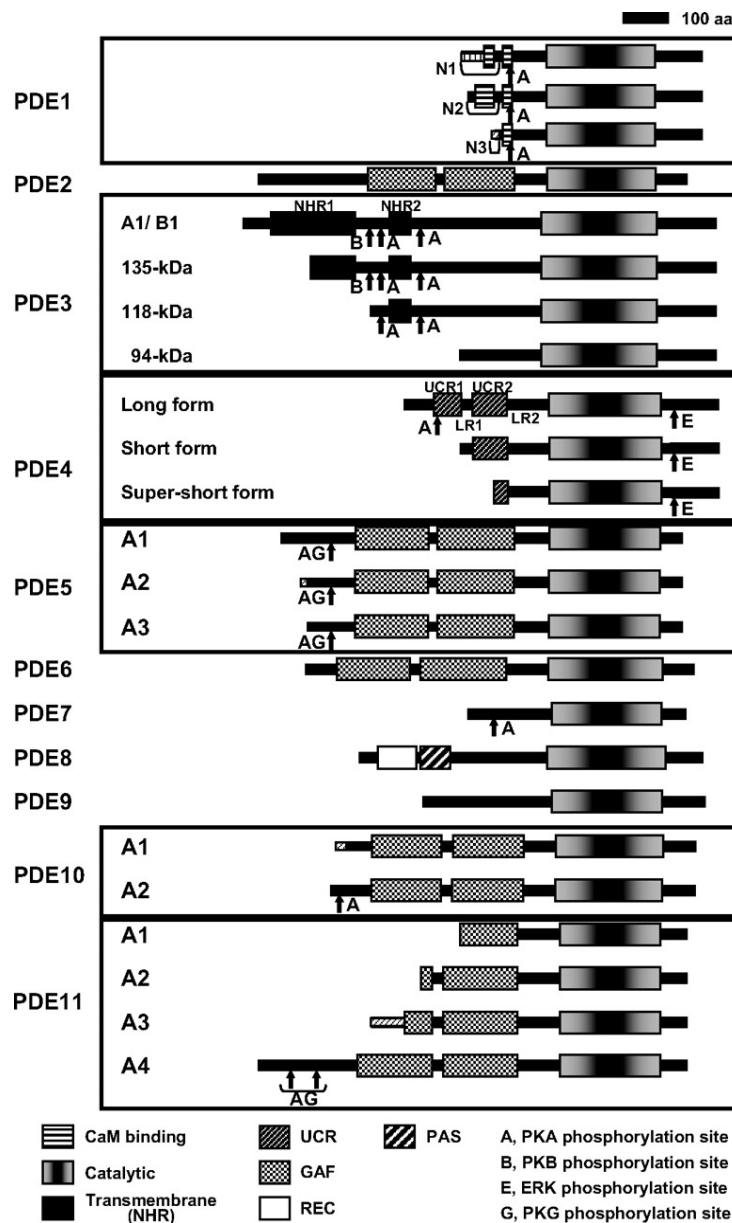


Figure 1.3: Schematic representation of the eleven human PDE families. Representative members that constitute the 11 human PDE families are shown here. Each PDE protein is indicated by a thick line. protein regions are represented by rectangles with patterns. N-terminal variation of PDE1A variants carrying N1, N2, and N3 sequences are boxed. Splice variants of PDE5, PDE10, and PDE11 families are also shown in boxes. The 3 isoforms in the PDE4 family are illustrated and boxed. PDE3 enzymes produced by alternative translation initiation are boxed. Reported phosphorylation sites are indicated with arrows. ERK phosphorylation site in PDE4A variants is absent. image taken from [9].

1.2.2 PDE catalytic domain:

Although PDE families contain a variable N-terminal regulatory domain, they share a similar C-terminal catalytic domain. Within each family, sequence similarity in the catalytic domain is high (typically 75% or greater) while the catalytic domain similarity between families is generally of 20–45% [66]. Crystal structures have been reported for the catalytic domains of eight PDE families in the unliganded form, in complex with products or inhibitors: PDE1B

Introduction

[67], PDE2A [53], PDE3B [68], PDE4B/4D [69-71], PDE5A [72], PDE7A [73], PDE9A [74] and PDE10A2 [75]. The catalytic domain of PDE4 and probably all other class I PDEs are composed of 16 alpha helices consisting of three subdomains that define a deep pocket where the substrate binds. The presence of three subdomains likely facilitates the ability for conformational changes to occur within the catalytic domain, which may account for different apparent conformations detected by substrate or inhibitor binding. Beside the substrate in the catalytic pocket, two metals were observed to bind, a tightly bound Zn^{+2} is coordinated by histidine and aspartate residues and another less tightly bound Mg^{+2} which is considered to be important for catalysis [62].

The PDEs have different substrate specificities: Some are cAMP selective hydrolases (PDE 4, 7 and 8), others are cGMP selective hydrolases (PDE 5, 6 and 9) and the rest can hydrolyse both cAMP and cGMP (PDE1, 2, 3, 10 and 11). Selectivity in this case is commonly defined as high substrate preference at physiological concentration [52, 53]. However, how the catalytic pocket of the PDE families selectively recognizes cAMP and cGMP is still not clear. On the basis of the crystal structure of PDE4-cAMP and PDE5-cGMP, a glutamate switch mechanism was proposed for the substrate specificity. However, this mechanism has been challenged by mutagenesis experiments. Experiments of the Q817A mutation in PDE5A1 reduced cGMP affinity by 60-fold but didn't significantly impact cAMP binding [76]. In addition, in dual substrate specific PDE2 and PDE10 crystal structures, presence of hydrogen bond between the invariant glutamine and a scaffolding tyrosine will block free rotation of glutamine side chain and prohibit gain of two hydrogen bonds with cAMP or cGMP. Moreover, in the structure of PDE10A2, the Gln726 forms two hydrogen bonds with cAMP but one with cGMP. A structural model shows that Gln726 will retain one hydrogen bond with cGMP even after switching the side chain conformation of the invariant glutamine. In conclusion, the glutamine appears to be important for substrate affinity but less critical for differentiation of substrate. In general, the substrate specificity is determined by multiple elements and individual PDE families have characteristic mechanisms and this can be due to the variation in the amino acids and the shape/size of nucleotide binding pocket [75, 77].

Although the crystal structures of many PDE catalytic domains were solved, no high resolution structure of any PDE enzyme has been reported. Little is known about the molecular details of signal transduction from the regulatory domain to the catalytic domain [58].

1.3 Class III Adenylyl cyclases

Adenylyl cyclases are responsible of production of cAMP from ATP in both eukaryotic and prokaryotic cells. Class III adenylyl cyclases are universal. They are found in metazoa, protozoa, fungi, eubacteria, some archaebacteria and certain green algae. However, neither class III ACs nor any other type of ACs has ever been conclusively identified in higher plants. Class III class is subdivided into another four subclasses (a-d). In mammals, ACs function as pseudoheterodimer with a single catalytic pocket. In bacteria and protozoa, ACs are homodimers with two catalytic pockets [78].

Six canonical amino acids have been identified in ACs, which serve three principal functions in catalysis. Two aspartate residues coordinate two metal cofactors (Mg^{+2} or Mn^{+2}), a lysine and an aspartate pair are responsible for selecting ATP over GTP as substrate and an arginine and asparagine couple stabilizes the transition state [78].

CyaB1, is a class III adenylate cyclase in which the above amino acid residues correspond to D606 and D650 for coordination of the metal cofactor, K646, T721 for adenine binding and N728, R 732 for the stabilization of the transition state [79]. To ascertain that these amino acids are in agreement with canonical class III catalytic cleft, different mutants have been generated. The mutation of T721A lowered the AC activity but did not relax the substrate specificity for ATP as GTP was not accepted as substrate [79, 80].

1.4 *Cyanobacterium anabaena* sp. Strain 7120 adenylyl cyclases, CyaB1 and CyaB2

Cyanobacteria are a diverse group of prokaryotes known as blue green algae. They are either unicellular or filamentous, and perform plant-type oxygen evolving photosynthesis. They are known to inhabit a variety of sea and fresh water habitats [81]. In 2001, the entire genome of filamentous heterocyst-forming, N_2 -fixing cyanobacterium, *Anabaena* sp. PCC 7120 (*Anabaena*), was determined [82]. Later, domain analysis revealed that the *anabaena* genome encodes a large number of signal transducing proteins in which the number of signaling domains in single protein is extremely large compared with other bacteria. In the total genome, 87 GAF domains were detected in 62 putative proteins, while 143 PAS domains were detected in 61 proteins [30].

Introduction

More than ten adenylate cyclase genes have been annotated in cyanobacteria. The deduced proteins have structurally related catalytic domains in their carboxyl terminal regions and characteristically diverse domains upstream of the catalytic domains [83](see fig. 1.4).

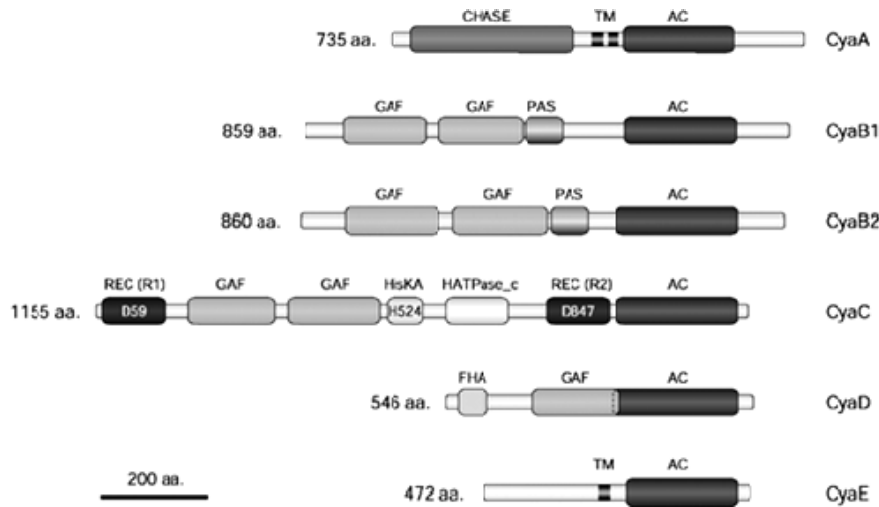


Fig. 1.4: Domain structure of six adenylate cyclases of *Anabaena* sp. PCC 7120 identified by complementation cloning, including CyaB1 and CyaB2. PAS and GAF are mentioned before, HisKA: dimerization and phosphoacceptor domain of Histidine kinases; HATPase_c: ATPase domains of Histidine kinase; REC: response regulator receiver domain; CHASE: predicted to be ligand binding domain; TM: transmembrane domain. Image taken from [81].

Among these enzymes, the deduced products of CyaB1 and CyaB2 genes have two distinct domains in the amino-terminal half, a GAF domain (GAFa and GAFb), and a PAS domain in addition to a C-terminal catalytic domain [83]. The GAF domains show significant similarity to cGMP binding tandem GAF domain of the mammalian cyclic nucleotide phosphodiesterases (PDEs) and have a regulatory action on the catalytic domain. In CyaB1, the binding of cAMP to the GAFb domain increases the V_{max} of the AC activity 27-fold, thus functioning as an autoactivating switch and a feed forward mechanism. In CyaB2, the molecular mechanism of activation shows some differences. The crystal structure of CyaB2 GAF tandem revealed an antiparallel dimer with four molecules of cAMP binding to each of the four GAFs. The exchange of the CyaB1 GAF by those of mammalian PDEs and CyaB2 has produced functional chimeras regulated by the new GAF which suggests that the GAF domains do not bind the catalytic domain, but that the signal is transmitted through the intervening PAS domain [84].

CyaB1 and CyaB2 are the first identified directly Na^+ -responsive signalling molecules that function in sodium homeostasis. The knock out of CyaB1 and CyaB2 from Cyanobacteria produced mutant strains that are not able to grow below 0.6M Na^+ . Mutants lacking CyaB1 had defects in Na^+/H^+ antiporter function. The addition of external cAMP has reversed the

inhibitory effect of sodium and improved the survival of the mutated cells at low concentration of NaCl. This effect was assigned to presence of metal binding pockets in the GAF domain [85].

1.5 Aim of work

According to experiments performed by Tobias Kanacher by the exchange of GAF domain of CyaB1 by rat PDE2 GAF domain, the success of this exchange gave the idea to use the CyaB1 PAS/catalytic domain as a reporter to study the function of different parts of the regulatory domain. Because cAMP and cGMP are working concomitantly as allosteric activators and substrates in PDEs, it was beneficial to use the CyaB1 PAS/catalytic domain as a reporter which utilizes ATP as substrate and cAMP or cGMP (depending on the GAF swapped) as an allosteric activator. Chimeras of mammalian GAF domains and the CyaB1 adenylyl cyclase have been prepared and successfully employed as a tool to study GAF tandem domains of mammalian phosphodiesterases with respect to ligand specificity, role of N-terminal regions upstream of the GAF tandem, role of phosphorylation sites and identification of previously unknown ligands.

In the first part of this thesis, the effect of the N-terminus of hPDE2 on the activity of the enzyme has been studied, so different constructs (\pm N-terminus, with hPDE5 N-terminus) have been cloned and assayed for activity and activation. In addition, rPDE2 GAF was also studied (\pm CyaB1 N-terminus).

The second aim of this project was to examine the role of the connecting helix of the GAF tandem domain in the dimerization of the enzyme and hence signal transduction. Three different GAF tandems, two of human phosphodiesterases, PDE2 and PDE5, and one from Cyanobacteria anabaena strain PCC 7120, CyaB2, have been selected for this study. The crystal structure of two of them (mPDE2 and CyaB2) has been solved [23, 24]. Accordingly, the boundaries of the connecting helix and the α 1-helix could be exactly determined. In this study different approaches have been taken. First, the length of this connecting helix which was determined in the two crystal structure to be of thirty three aa's, and as the stimulation factor for CyaB2GAF was much higher than that of PDE2 GAF, CyaB2 was selected for this study. The second part was to study the effect of the hydrophobic region in the middle of this connecting linker and α 1-helix preceding GAF α on the transduction of the signal through the two motifs GAF tandem using site-directed mutation (fig.1.5).

Introduction

```
CyaB1A : FVCLLDFTITAEFQQFLRAIEILIN-NEALEN-----MLEKVLLEAITLKIQQILQAEHTAIFLVDYDK---CQLWSKVPQ-DNGQ : 73
CyaB1B : -----F-YVAARNQRGVTAALLRATQTLGQS-LD-----LEATLQIVMEQARILMQADRSTLFLYRKEM---GELWTKVAA-AADT : 69
CyaB2A : FKQVVTEVEQKIQIVHQTLMLDSHGFEFEN-----ILQEMLQSIITLKTGELLGADRITIFLLDEEK---QELWSIVAA-GEED : 73
CyaB2B : -----F-YIATQKQRAAAAAMMKAVKSLSQSSLD-----LEDTLKRVMDEAKEELMNADRSTLWLIDRDR---HELWTKITQ-DNGS : 70
hPDE2A : ---AEDQKGGAAAYTDRDRK-ILQLCGELYD--LD-----ASSLQKVLQYQLQOQETRASRCLLVSEDN---LQLSCKVIG---DK : 69
hPDE2B : ---F-QKEQKLCRCQALLQVAKNLFTHLDD---SVLLIQQEITFEARNLSNAEICSVFLLDQN---ELVAKVFDGGVVD : 69
hPDE5A : -LTPPRF-DHDEGDQCSR--LLELVKDISSH-LD-----VTALCHKIFLHIHGLISADRYSLFLVCEDESSNDKFLSRLFDVAEGS : 76
hPDE5B : -----Y-ETSLLENKRNVLLDLASLIFEEQQS---LEVTLKKAATIIISFMQVQKCTIFIVDEDCS---DSFSVVFHMECEEL : 72
hPDE6aA : -VDFSNY--HSPSSMEESEIIFDLLRDFQEN-LQ---TEKCIENVMKCLCFLLQADRMSLFMYRTRNG-IAELATRLFNHVKDA : 76
hPDE6aB : -----SY--LHNCETRRGQILLWSGSKVFEELTD---IERQFHKALYTVRAFLLNCDRYSVGLLDMTKQ---KEFFDVVWPVLMGEV : 72
hPDE10A : ---VSRY---QDTNMQGVVYELN---SYIEQRLDLTGGDNQLLYELSSIIKIATKADGFALYFLGECN---NSLCIFTPPGIKEG : 73
hPDE10B : -----CRGLAKQTELNDFLLDVSKTIFYDNIVA---IDSLEHIMIIYAKNLVNADRCAFLQVDHKN---KELYSDFDIGEEK : 71
hPDE11A : -PTAIDY-KCHLKKHNERQFFLELVKDISND-LD---LTSLSYKILIFVCLMVDADRCSLFLVEGAAGKKTIVSKFFDVHAGT : 78
hPDE11B : -----F-AASRKEYERSRALLEVVNDLFEETD---LEKIVKIKIMHRAQTLLKCEKRSVLLLEDIESPVVKFTKSFELMSPKC : 74

CyaB1A : KF-----LEIR-----TPITVGIPIGHVASTGQYLNISETHATP---LFSPLE---RQMGY : 118
CyaB1B : TQL-----IEIR-----IPANRGI VGYVASTGDALNIS-DAYK DPR--FDPITD---RKTGY : 115
CyaB2A : RS-----LEIR-----IPADKGLIAGEVATFKQVNVIPDFYHDPDRSIFAQKQE---KITGY : 121
CyaB2B : TK-----ELR-----VPIGKGFAGI VASGQKLNIPFDLYDHPDSATAKQID---QNGY : 117
hPDE2A : VLG-----EEVS---FPL-TGCLGQVVEDKKSITQLK-DLTSED---VQQLQ---SMLGC : 112
hPDE2B : D-----ESYIEIR-----IPADQGLIAGHVATGQILNIP-DAYAHPL--FYRGVD---DSTGF : 115
hPDE5A : TLEEVSN---NCRIR-----LEWNKGI VGHVAAALGEPLNIK-DAYEDPR--FNAEVD---QITGY : 126
hPDE5B : EKSSDTLTREHDAN-----KINMYAQYVKNITMEPLNIP-DVSKDKR--FPWTIENTGNVNGQ : 127
hPDE6aA : VLEDCLVMPD-QEIV-----FPLDMGI VGHVAHKKIANVP-NTEEDH--FCDFVD---ILTEY : 129
hPDE6aB : PPYSGPRTPDGREINFYKVIDYILHGKEDIKVIPNPPDHWALVSGLPAYVAQNGLICNIM-NAPAEF--FAFQKE-PLDESGW : 153
hPDE10A : KP-----RLIPAG-----PITQGTTVSAYVAKSRKTLIVE-DILGDER--FPRGTG---LESGT : 121
hPDE10B : EGKPVFK--KTKIEIR-----FSIEKGIAGI VARTGEVLNIP-DAYADPR--FNR EVD---LTYGT : 123
hPDE11A : PLLPCSSTENSNEVQ-----VPWKGIGI VGEHGETVNIP-DAYQDRR--FNDEID---KLTGY : 132
hPDE11B : SADAENSFKESMEKSSY-----SDWLINNSTAELVASTGLPVNIS-DAYQDPR--FDAEAD---QISGF : 132

CyaB1A : KINNILCMPVVS-SKQIVAVVQLANKTG-----NIPFNRNDEESFRDFAASIGIILETCQS----- : 174
CyaB1B : LTRNILCLPVFN-SANELIGVTQLINKQ-----QGSFTASDEEFMRAFNIQAGVALENARLFENVLLE-- : 177
CyaB2A : RITYTMLALPLLS-EQGRLVAVVQLLNKLP---YSPDALLAERIDNQGFSADEQLFQEFAPSI RLLLESSRS----- : 191
CyaB2B : RTCSLLCMPVFN-GDQELIGVTQLVNNKKTGEFFPPYNPETWPIAPECQFASFDNRNDEEFMEAFNIQAGVALQNAQLFATVKQEQ : 201
hPDE2A : ELQAMLCVPIVSRATQVVALACAFNKLE-----GDLFIDEDEHVIQHCFFHYTSTVLTSTLA : 169
hPDE2B : RTRNILCFPIKN-ENQEVIGVAELVNKIN-----GPWFSEKDEDLATAFSTVCGISIAHSLLYKKVNEAQY : 180
hPDE5A : KTQSILCMPIKN-HREEVGVQAQAINKKS---NGGFTTEKDEKDFAAFLAFCGI VLNHAQL----- : 184
hPDE5B : CIRSELLCTPIKNKGNKVKI GVCQLVNMKEEN-----TG-KVKPFNRNDEQFLEAFVIFCGLGIQNTQMYEAVRAMA : 198
hPDE6aA : KTKNILLASPIMN--GKDVVAITIMAVNKVD-----GSHFTIKRDEITLLKYLNFANLIMKWYHL : 184
hPDE6aB : MIKNVLSMPIVNNK-EIIVGVATIFYNRKDG-----KPFDEMDETLMESLTQFLGWSVLNPDTYESMNKLEN : 218
hPDE10A : RIQSVLCLPIVIT-AIGDLIGILELY-RHWG---KEAFCLSHQEVATANLAWASVAIHQVQV : 177
hPDE10B : TTRNILCMPIVS-RGS-VIGVVQMVNKLIS-----GSAFSKTIDENNFKMFVFCALALHCANMYHRIRHSEC : 187
hPDE11A : KTKSLLCMPIRS-SDGEIIGVAQAINKIP-----EGAPFTEDEKVMQMYLPFCGIAISNAQL : 189
hPDE11B : HIRSVLCPVPIWNSN-HQIIGVAQVLRIDG-----KPFDDADQRLFEAFVIFCGLGINNTIMYDQVKKSWA : 197
```

Fig.1.5: Alignment prepared by ClustalW method for human PDE GAF domains and cyanobacterial, CyaB1 and CyaB2, GAF domains. h is for human, a and b are for GAFa and GAFb. Red: 100% similarity, Blue: 60-90% similarity and Black: < 60% similarity.

And third, I will try to explore the mechanism by which the signal transduced through the PAS domain of CyaB1 (from GAF domain to the catalytic domain). A recent mechanism suggested that GAF domain activation may be accomplished by movement of rigid domains by a fixed angle and distance and hence, the PAS domain has no role in signalling, an experiment in which the GAF domain was directly swapped in front of the catalytic domain has shown loss of the activation (J.Linder, personal communication). This was performed by the exchange of CyaB1 PAS by first hPDE5 catalytic linker and second by the PAS domain of CyaB2. Then, a flexible linker (14 aa's in length) was inserted between the PAS and catalytic domain of CyaB1, and lastly I tried to crystallize different PAS domains of CyaB1 and CyaB2 either alone or attached to their catalytic domain.

2 Materials and equipments

2.1 Chemicals and materials

Art Robbins Instruments, California (USA): 96 well Intelli-plate polished shelf crystallization plates

AGS, Heidelberg: restriction endonucleases with 10x reaction buffer

American National Can, Chicago (USA): Parafilm "M" Laboratory film

AppliChem, Darmstadt: Acrylamide 4K-solution (37.5:1) 30%, HEPES, IPTG

Applied biosystems, California (USA): BigDye Terminator cycle sequencing kit version 3.1

Applegene, Heidelberg: Taq DNA-polymerase with 10x reaction buffer

ASID BONZ GmbH, Herrenberg: ProLine Latex surgical gloves

Axygen Scientific, Union City (USA): PCR tubes PCR-02-R

Becton Dickinson (BD), Basel (Schweiz): Falcon tubes 15 and 50 ml, 10 ml-disposable syringes

BIO-RAD, München: BIO-RAD Protein-Assay dye reagent

Biozym Diagnostik, Hess. Oldendorf: Sequagel XR, Sequagel Complete Buffer Reagent, Chill-out 14 liquid Wax

Dianova, Hamburg: Secondary goat antimouse IgG-F_c horseradish peroxidase conjugated antibodies

Emerald BioStructures, Bainbridge Island, Washington (USA): Wizard I and II reagent kits for protein crystallization

Fluka, Basel: cAMP, glucose, glutaraldehyde (25% in water), PEG 1000, sodium dodecyl sulphate (SDS)

GE Health Care, Freiburg (2,8-³H)- cAMP (ammonium salt), ECL Plus western Blotting detection system, hyperfilm ECL, formamide, thermosequenase fluorescent labeled primer cycle sequencing kit

Fortuna, Wertheim: Pasteur pipettes

Griener Labortechnik, Nürtingen: Sterile Petri dishes

Hampton Research, California (USA): Crystal screenTM, Crystal screen 2 and crystal screen lite reagent kits for protein crystallization screening, VDX 24-well polystyrene pre-greased crystallization plates, 22 mm siliconized cover slides, 100% PEG 400, PEG 3350, PEG 8000

Hartmann Analytik, Braunschweig: (α -³²P)-ATP

ICN Biomedicals, Eschwege: Ethidium bromide tablets

Materials and equipments

Kimberly-Clark Roswell (USA): *Safeskin Satin Plus-Latex-* gloves, *Kimtech^{science}* Precision wipes

Macherey-Nagel, Düren: Nucleotrap kit, *Porablot* PDVF- blotting membrane (2µm pore size)

Merck, Darmstadt: Acetic acid 100%, Aluminium oxide 90% active, ammonium sulphate, calcium chloride, chloroform, disodium hydrogen phosphate, DMSO, ethanol, imidazole, glucose, glycerol 87%, magnesium chloride hexahydrate, 2-mercaptoethanol, methanol, sodium acetate, sodium chloride, sodium hydroxide, sodium pyrophosphate

MWG-Biotech, Ebersberg: Oligonucleotides (PCR and sequencing primers)

New England Biolabs, Schwalbach/Taunus: BSA for molecular biology, restriction endonucleases, T4-Polynucleotide kinase and 10x kinase buffer

Novagen R&D systems, Wiesbaden: pET16b- Expression vector, *E. coli BL21 (DE3)-[pREP4]* cells

Pall Corporation, Michigan (USA): NANOSEP 10K OMEGA centrifugal devices.

Peqlab, Erlangen: PeqGold Protein Marker, dNTPs

Perkin Elmer, Boston (USA): Ultima Gold XR-LSC- scintillator, super polyethylene vials, 20 ml

Promega, Madison (USA): *Pfu* DNA-polymerase enzyme with 10x buffer, *Wizard Plus SV* Plasmid Purification Kit (Minipreps)

Qiagen, Hilden: Ni-NTA Agarose, pQE30, pQE60 and pQE82 - expression vectors, purified mouse monoclonal *RGS-His₄* antibody and *Tetra-His* antibody, *Taq*-DNA- polymerase

Roche (Boehringer), Mannheim: alkaline phosphatase, ATP, Combithek[®] Protein standards for chromatography, *Complete-EDTA-free* protease inhibitor tablets, dNTPs, λ-DNA, Restriction endonucleases, Klenow-polymerase with 10x buffer, Rapid DNA ligation Kit

Roth, Karlsruhe: Aluminium foil, agarose, ampicillin, brilliant blue G250 and R250 (Coomassie), glacial acetic acid, glycine, isopropanol, kanamycin, LB-Agar, LB-broth powder

Sartorius, Göttingen: Sterile Nalgene syringe filter (0.22 µm), HAWP filter (0.45 µm) Vivaspin 500 µl and 2 ml 10k protein concentrator

Schleicher & Schuell, Dassel: Whatmann Paper 3MM

Serva, Heidelberg: Visking dialysis tubing 8/32 (diameter: 6 mm) and 27/32 (diameter: 21 mm), Glass wool

Sigma-Aldrich: Ethanol, APS, bromophenol blue, BSA, cAMP, cGMP, Corning Spin-X Centrifugation filters (0.2 µm), Dowex 50WX4-400, EDTA, Glycerol 99%, IPTG, LB-agar,

Materials and equipments

LB-broth, monothioglycerol, MOPS, sodium citrate, TEMED, tetracycline, tris, tween 20, ponceau S, X-gal

SLG, LP Italiana, Milan (Italy): 10 and 25 ml disposable pipettes

Stratagene, Heidelberg: *pBluescript II SK (-)* cloning vector, *E.coli XL 1- Blue* cells

TPP, Transadingen (Switzerland): Falcon tubes 15 and 50 ml

Vetter, Entringen: Eppicups, white, yellow and blue tips

Whatman International Ltd. Maidstone (UK): *Whatman 3 MM* paper.

2.2 Equipments

Bender & Hobein, Zurich: Vortex *Genie 2TM*

Berthold, Wildbad: Hand –Fuss Monitor *LB 1043 B*, Hand Monitor *LB 1210 B*

Biometra, Göttingen: *TRIO-* thermoblock thermocycler with *Trio* heated lid

Biorad, München: Blotting apparatus *Trans-Blot SD Semi Dry Transfer Cell*

Branson, Danbury, Connecticut (USA): Sonifier *B-12*, Ultrasound bath *Bransonic B12*

Bühler, Tübingen: *KL-15* and *KL- 2* shakers

Carl Zeiss, Göttingen: Microscope *Axioskope 40/40 FL* with fixed polarisator, Lambda plate, *Canon powershot G2* high quality digital camera with 4.0 Mpixel, CDD sensor and 3x optical zoom

Eberhard-Karls-Universität, Tübingen: Gel electrophoresis chambers, combs and moulds for agarose gel

Eppendorf, Hamburg: BioPhotometer, Multipipette, Pipettes, Table centrifuges *5414*, *5415*, *5402*, Thermomixer *5436*, Thermostat *5320*, Thermomixer *Compact*

Förbel, Lindau: Consort *microcomputer electrophoresis power supply E411*

GE Health Care, Freiburg: *ÄKTA* FPLC Instrument, chromatography column *Supradex 200 HR 10/30*, Liquid scintillation counter *Rackbeta 1209* (LKB Wallac), *Hoefler Mighty small SE245* gel casting apparatus, *Mighty small II E250* chamber, Electrophoresis power supply *EPS 301*

Gilson, Middleton (USA): Pipettes

Heraeus, Osterode: Megafuge *1.0 R (BS 4402/A)*

Hirschmann Laborgeräte, Eberstadt: *Pipetus-Reddot* electronic pipette

H.Saur Laborbedarf, Reutlingen: Vacuum centrifuge type BA-VC.300H

Infors AG, Bottmingen (Switzerland): *Unitron* incubator

Kontron-Hermle, Gosheim: *Centrikon H401 & ZK401*, Rotors *A6.14 (SS34)* and *A8.24* (GSA)

KSG Sterilisatoren, Olching: Sterilisor *KSG 40.2.1*

LTF Labortechnik, Wasserburg: Videoprinter *Mitsubishi Video Copy Processor P91* with *Sony CCD video Camera Modul XC- ST500E*, thermopapers *K65HM*, Software *BioCapt Version 99.01s*

Metrohm, Herisau (Switzerland): pH- Meter *E 512 and 605*

Mettler-Tolido, Steinbach: Balance *Mettler PL 200*, pH-electrode *inlab 423*

Millipore, Eschborn: *MilliQ UF Plus* apparatus

MWG-Biotech, Ebersberg: LI-COR DNA Sequencer *model 4000*, BaseImagIR version 4.0 software

Promega, Madison (USA): Vac-Man (vacuum for Wizard plus SV Plasmid Purification Kit), wizard minicolumns

Sartorius, Göttingen: Balance *BP 2100 S*, Analytical balance *Handy*

SLM-AMINCO Instruments, Urbana (USA): French Press *FA-078-E1*

WTC Binder, Tuttlingen: Incubators

2.3 Bacterial strains

Table 2.1: The bacterial strains used in cloning, their Supplier and characteristics:

Strain	Supplier	Genotype	characteristics
<i>E. coli XL1 Blue</i>	Stratagene (Heidelberg)	<i>recA1 endA1 gyrA96 thi-1 hsdR17 supE44 relA1 lac [F' proAB lacIqZΔM15 Tn10 (Tetr)]</i>	Cloning cells (Tetracycline resistant)
<i>E. coli DH5α</i>	Invitrogen (Karlsruhe)	<i>F⁻, Φ 80dlacZΔM15, Δ(lacZYA- argF)U169, deoR, recA1, endA1, hsdR17(rK⁻, mK⁺), phoA, supE44, λ⁻, thi-1, gyrA96, relA1</i>	Cloning cells (No antibiotic)
<i>E.coli BL21 (DE3) [pREP4]</i>	Novagene (Wiesbaden)	<i>F⁻, ompT, hsdS_β(r_β-m_β-), dcm, gal, (DE3) tonA</i>	Expression cells (Kanamycin resistant)

2.4 Plasmids

Table 2.2: Plasmids, their supplier and characteristics.

Plasmid	Size (kb)	Supplier	Characteristics
pBluescript II SK (-)	2.961	Stratagene (Heidelberg)	Cloning and transcription vector, <i>lacZa</i> , Amp ^R
pQE30	3.462	Qiagene (Hilden)	Expression vector, Amp ^R , 6xHis-tag (N)
pQE60	3.431	Qiagene (Hilden)	Expression vector, Amp ^R , 6xHis-tag (C)
pQE82	4.752	Qiagene (Hilden)	Expression vector, Amp ^R , 6xHis-tag (N)
pET16b-pQE30 MCS*	5.634	Novagene (Wiesbaden)	Expression vector, Amp ^R , 6xHis-tag (N)

* pET16b was from Novagene and modified by the insertion of the MCS of pQE30 by A.Schultz.

2.5 Oligonucleotides

Restriction sites are UNDERLINED, mutations are in **BOLD** and inserted bases are in *bold italic small letters*

s = sense primer as = antisense primer o = orientation

Stop codon = (between parenthesis) ... = deleted bases

Restriction sites

2.5.1 Sequencing primers

Table 2.3: Sequencing primers, their annealing temperatures and positions.

Name	o	T _a (°C)	Sequence (5' → 3')	Position	Comment
T3	as	56	AAT TAA CCC TCA CTA AAG GG	772-791	pBluescript II SK (-)
T7	s	56	TAA TAC GAC TCA CTA TAG GG	626-645 5320-5249	pBluescript II SK (-), pET16/pQE30 MCS
R-800-pET MCS pQE30	as	56	ACC CCT CAA GAC CCG TTT AGA	5423-5443	pET16b / MCS pQE30
U-pQE-IR	s	54	GAA TTC ATT AAA GAG GAG AAA	88-108	pQE30, pQE60 and pQE82
R-pQE-IR	as	54	CAT TAC TGG ATC TAT CAA CAG G	212-233	pQE30, pQE60 and pQE82
U-IR-800 CyaB1-PAS2	s	56	GCT TGT CAG ATG CTG TAA TTT C	1190-1211	CyaB1 holoenzyme
R-IR-800 GAFCyaB1	as	56	ACT TTT ATG ATT AGC ATC ACC	1279-1299	CyaB1 holoenzyme
U-IR-800 KatCyaB1	s	56	GAT GCC TTA ATG GTT GGT G	1768-1786	CyaB1 holoenzyme
U-IR-800 CyaB2GAF	s	56	TCG ATA TTT GCC CAA AAA CAA	484-504	CyaB2 holoenzyme
U-IR-800 hPDE2GAF	s	56	GAG AAG CAT ACC CTG GTC	541-558	hPDE2 holoenzyme
U-IR-800 PDE5GAF	s	56	CAT GAT GAA GGG GAC CAG TGC T	427-448	hPDE5 holoenzyme

2.5.2 Cloning primers

2.5.2.1 CyaB1 holoenzyme

Table 2.4: Cloning primers of CyaB1 holoenzyme

#	Name	o	position	Sequence (5' → 3')	comment
1	CyaB1GAFlnk spe s	s	489-606	AAA <u>ACT AGT</u> <i>gca gat gag caa ttg</i> <i>ttt caa gaa</i> TTT GCT GCT TCT ATT GGG	SpeI
2	CyaB12GAFlnkXba as	as	670-687	AAA <u>TCT AGA</u> <i>tcc aga cta ctt tgg</i> <i>ctc aga</i> GAT TGA GTA GCG CGT AAA AG	XbaI
3	PASCyaB1s-Bam	s	1162-1182	AAA <u>GGA TCC</u> AAA CAA TAT CAA AAA GAC ATT	BamHI
4	PASCyaB1as-Sma	as	1696-1713	AAA <u>CCC GGG</u> (CTA) AGT AGT TTT GAG GCG CTT	SmaI
5	KatCyaB1s-Afl	s	1708-1725	AAA <u>CTT AAG</u> ACT ACT ATG TAT CGC TAC	AflII
6	KatCyaB1as-Kpn	as	2563-2580	AAA <u>GGT ACC</u> (CTA) CTT TGT GAA AAT TGT	KpnI
7	PASCyaB2as-Mlu	as	1696-1713	AAA <u>ACG CGT</u> AGT AGT TTT GAG GCG CTT	MluI
8	KatCyaB1s-Xho	s	1714-1731	AAA <u>CTC GAG</u> ATG TAT CGC TAC CTT ACA	XhoI
9	CyaB1GAFcr s	s	124-141	AAA <u>CCA TGG</u> ACT TTA TCA CTG CCG AA	NcoI From Anita
10	CyaB1GAFcr as	as	1144-1167	AAA <u>GGA TCC</u> TTG TTT TTC TAG TAA TAC ATT TTC	BamHI From Anita
11	CyaB1-XhoI A732(neu) as	as	2176-2203	AAA <u>TCT CGA</u> <u>GGG</u> CGG AAC TTA AAT TCA CAC C	XhoI From Anita

2.5.2.2 CyaB2 holoenzyme and mutants

Table 2.5: Cloning primers of CyaB2 holoenzyme

#	Name	o	position	Sequence (5' → 3')	comment
Primers for CyaB2 holoenzyme					
12	CyaB2 N-Bam s	s	1-18	AAA <u>GGA TCC</u> ATG TCA TTG CAA CAG CGT	BamHI From Anita
13	CyaB2GAFB Xho as	as	1306-1323	AAA <u>TCT GAG</u> CTT GAC TGT GGC AAA CAA	Xho I From Anita
14	pasCyaB2s Bam	s	1330-1347	AAA <u>GGA TCC</u> GAG CAA ATG CAA CGG GAT	BamHI
15	pasCyaB2as-Hind	as	1687-1704	AAA <u>AAG CTT</u> (CTA) GCG CTT CTC ATC GCT AAT	HinDIII
16	KatalCyaB2s-Bam	s	1705-1722	AAA <u>GGA TCC</u> CTC AAG AGT ACG ATG TAT	BamHI
17	PASCyaB2s-Xho	s	1330-1347	AAA <u>CTC GAG</u> GAG CAA ATG CAA CGG GAT	XhoI
18	CyaB2GAFcr s	s	172-189	AAA <u>CC A TGG</u> TTA CAG AAG TCG AGC AA	NcoI From Anita
19	CyaB2GAFcr as	as	1315-1332	AAA <u>GGA TTC</u> CTC TTG TTG CTT GAC TGT	BamHI From Anita
20	PASCyaB2as-Afl	as	1687-1704	AAA <u>CTT AAG</u> GCG CTT CTC ATC GCT AAT	Afl II
21	CyaB2cat sma as	as	2567-2583	AAA <u>CCC GGG</u> (TCA) CTT CTC CTG AAA CGT	SmaI
Primers where aa's are deleted or inserted					
22	CyaB2GAFlnk Bgl (- R)s	s	733-780	AAA <u>AGA TCT</u> TTT TAT ATA GCG ACG CAA AAA CAA ... GCG GCG GCG	Bgl II
23	CyaB2GAFln(- RA)Bgl	s	733-780	AAA <u>AGA TCT</u> TTT TAT ATA GCG ACG CAA AAA CAA GCG GCG GCG ATG ATG AAG	Bgl II
24	CyaB2GAFlnk- RAABgl	s	733-780	AAA <u>AGA TCT</u> TTT TAT ATA GCG ACG CAA AAA CAA GCG GCG ATG ATG AAG	Bgl II

Materials and equipments

25	CyaB2GAFlnk -RAAABgls	s	733-780	AAA <u>AGA TCT</u> TTT TAT ATA GCG ACG CAA AAA CAA GCG ATG ATG AAG GCG GTA AAG	Bgl II
26	CyaB2GAFlnk +NAABgls	s	733-783	AAA <u>AGA TCT</u> TTT TAT ATA GCG ACG CAA AAA CAA AGG GCG GCG GCG <i>aac gca gca</i> GCG ATG ATG AAG GCG	Bgl II
27	CyaB2GAFlnk +NAAI	s	733-783	AAA <u>AGA TCT</u> TTT TAT ATA GCG ACG CAA AAA CAA AGG GCG GCG GCG <i>aac gca gca att</i> GCG ATG ATG AAG GCG	Bgl II
28	CyaB2GAFlnk Bgl as	as	709-726	AAA <u>AGA TCT</u> TGA CGA CTC CAA AAT CAA	Bgl II
29	CyaB2GAF spe as	as	646-660	AAA <u>ACT AGT</u> AAA ACC TTG ATT ATC	Spe I
30	CyaB2-XbaI (s)	s	813-837	AAA TCT AGA AGA TAC CCT CAA ACG GGT A	XbaI From Sandra
31	CyaB2-RA as	as	739-774	CAT CGC CGC CGC TTG TTT TTG CGT CGC TAT	Fusion PCR From Anita
32	CyaB2-RA s	s	745-780	ACG CAA AAA CAA GCG GCG GCG ATG ATG AAG	Fusion PCR From Anita
Primers for CyaB2 mutants					
33	CyaB2GAFA M74Ss	s	250-276	AAA <u>CTG CAG</u> GAG AGC TTG CAG TCA ATT ACC	PstI
34	CyaB2GAFA L75Ss	s	250-276	AAA <u>CTG CAG</u> GAG ATG AGC CAG TCA ATT ACC	PstI
35	CyaB2GAFA ML75ASs	s	250-279	AAA <u>CTG CAG</u> GAG GCA AGC CAG TCA ATT ACC TTA	PstI
36	CyaB2N-ter Pst as	as	235-255	AAA <u>CTG CAG</u> GAT ATT TTC AAA CCC	PstI
37	CyaB2GAFB Bgl	s	733-768	AAA <u>AGA TCT</u> TTT TAT ATA GCG ACG CAA AAA CAA AGG GCG GCG GCG	BglIII

Materials and equipments

38	CyaB2 MM258LL Bgl s	s	733-780	AAA <u>AGA TCT</u> TTT TAT ATA GCG ACG CAA AAA CAA AGG GCG GCG GCG GCG CTG CTG AAG GCG GTA AAG	BglIII
39	CyaB2 MM258AA Bgl s	s	733-780	AAA <u>AGA TCT</u> TTT TAT ATA GCG ACG CAA AAA CAA AGG GCG GCG GCG GCG GCG GCG AAG GCG GTA AAG	BglIII
40	CyaB2 MM258GG Bgl s	s	733-780	AAA <u>AGA TCT</u> TTT TAT ATA GCG ACG CAA AAA CAA AGG GCG GCG GCG GCG GGG GGG AAG GCG GTA AAG	BglIII
41	CyaB2 MM258ST Bgl s	s	733-780	AAA <u>AGA TCT</u> TTT TAT ATA GCG ACG CAA AAA CAA AGG GCG GCG GCG GCG TCG ACG AAG GCG GTA AAG	BglIII
42	CyaB2GAFA sfu s	s	238-261	AAA <u>TTC GAA</u> AAT ATC CTG CAA GAG ATG	SfuI
43	CyaB2 ML74GG sfu as	as	208-243	AAA <u>TTC GAA</u> CCC GTG AGA ATC CCC CCC TGA CAG GGT TTG	SfuI
44	CyaB2ML74ST sfu as	as	208-243	AAA <u>TTC GAA</u> CCC GTG AGA ATC CGT GGA TGA CAG GGT TTG	SfuI

2.5.2.3 hPDE5 GAF domain

Table 2.6: Cloning primers of hPDE5

#	Name	o	Position	Sequence (5' → 3')	Comment
45	hPDE5N-ter Bam s	s	1-18	AAA <u>GGA TCC</u> ATG GAG CGG GCC GGC CCC	BamHI
46	hPDE5N-ter Bgl I s	s	1-18	AAA <u>AGA TCT</u> ATG GAG CGG GCC GGC CCC	BglIII From J.Weber
47	hPDE5N-ter Xba as	as	430-450	AAA <u>TCT AGA</u> GCA CTG GTC CCC TTC ATC	XbaI

Materials and equipments

48	PDE5 5' Xho	s	1537-1554	AAA <u>CTC GAG</u> AGA GCC ATG GCC AAG CAA	XhoI
49	hPDE5-I-as1	as	1558-1581	AAA <u>AGA TCT</u> TGT TTC TTC CTC TGC TGC TGA AGC	BglII
50	hPDE5-I-as2	as	1594-1614	AAA <u>AGA TCT</u> CAC CAC AGC AGC CGC TAA CGA	BglII
51	hPDE5LL152AA s	s	444-468	GTG CTC AAG AGC CGC GGA ATT AGT G	Fusion PCR
52	hPDE5LL152AA as	as	444-468	CAC TAA TTC CGC GGC TCT TGA GCA C	Fusion PCR
53	hPDE5LL333AA as	as	985-1043	AAA <u>TCT AGA</u> GAT TGT TGT TCT TCA AAA ATT AAA CTA GCA AGG TCA GCC GCC ACC TGA TTT CT	Xba I
54	PDE5 XbaI (as)	as	1020-1037	AAA <u>TCT AGA</u> GAT TGT TGT TCT TCA AAA	XbaI From Sandra
55	hPDE5 SphI	s	407-423	AAA <u>GCA TGC</u> TAA CCC CTC CAA GGT TT	SphI From Ana

2.5.2.4 rPDE2 GAF domain

Table 2.7: Cloning primers of rat PDE2

#	Name	o	Position	Sequence (5' → 3')	Comment
56	PDE2N-ter Bam s	s	1-18	AAA <u>GGA TCC</u> ATG GTC CTG GTG TTG CAC	BamHI
57	PDE2N-term.stu as	s	547-564	AAA <u>AGG CCT</u> GCG CTG CTG CAG GGC CTG	StuI
58	PDE2 GAF. Stu s	s	571-600	AAA <u>AGG CCT</u> GAA GCT GTT CAG AAC ACC TCA GCA GAT CCC	StuI
59	PDE2GAF Xba s	s	646-663 (r) 682-702 (h)	AAA <u>TCT AGA</u> AAG ATC CTG CAA CTG TGT	XbaI
60	PDE2GAF Bam s	s	619-636	AAA <u>GGA TCC</u> GAG AAG GGA TAC ACC GCC	BamHI
61	Mouse XhoI as	as	1616-1638	AAA <u>CTC GAG</u> ATT CAC CTT TTT GTA TAG GAG AG	XhoI From Tobias

2.5.2.5 hPDE2 GAF domain

Table 2.8: Cloning primers of hPDE2

#	Name	o	Position	Sequence (5' → 3')	Comment
62	hPDE2N-terBam s	s	1-18	AAA <u>GGA TCC</u> ATG GGG CAG GCA TGC GGC	BamHI
63	hPDE2GAF Sma as	as	755-776	AAA <u>CCC GGG</u> TCT CCT GCT GCA GGT	SmaI
64	hPDE2GAF Sma s	s	770-790	AAA <u>CCC GGG</u> CAT CCC GCT GCT GCC	SmaI
65	hPDE2GAF Bam s	s	682-699	AAA <u>GGA TCC</u> CGC AAG ATC CTC CAA CTG	BamHI
66	hPDE2GAF Hind as	as	1669-1686	AAA <u>AAG CTT</u> (TCA) ATA CTG AGC CTC ATT CAC	HinDIII
67	hPDE2GAFA s	s	694-717	AAA <u>CAA TTG</u> TGC GGG GAA CTC TAC GAC	MfeI
68	hPDE2N-ter L231S as	as	676-699	AAA <u>CAA TTG</u> GCT GAT CTT GCG GTC GCG	MfeI
69	hPDE2N-ter I230S as	as	676-699	AAA <u>CAA TTG</u> GAG GCT CTT GCG GTC GCG	MfeI
70	hPDE2GAFA afl as	as	1147-1170	AAA <u>CTT AAG</u> TTT CTG TTC CTT CTG GAA	AflII
71	hPDE2CS/LL396AA s	s	1165-1203	AAA <u>CTT AAG</u> TGT GAG TCC CAG GCT GCT GCC CAA GTG GCA AAG	AflII
72	hPDE2C393S s	s	1165-1185	AAA <u>CTT AAG</u> TGT GAG TCC CAG GCT CTT CTC	AflII
73	hPDE2 LL396AA s	s	1165-1203	AAA <u>CTT AAG</u> TGT GAG TGC CAG GCT GCT GCC CAA GTG GCA AAG	AflII
74	hPDE2(-N) IL230AA BamHI	s	682-708	AAA <u>GGA TCC</u> CGC AAG GCC GCC CAA CTG TGC GGG GAA	BamHI

2.6 Buffers and solutions

MilliQ water was used; pH values were adjusted at RT, unless indicated otherwise.

2.6.1 Molecular biology

All solutions and buffers for molecular biology methods were either sterile-filtered (0.22 μ m) or autoclaved for 20 min at 121°C (1bar)

2.6.1.1 Solutions for DNA treatment:

TAE

40 mM Tris/Acetate pH 8.0
1 mM EDTA

TE buffer

10 mM Tris/HCl pH 7.5
1 mM Na₂EDTA

10x Klenow buffer

200 mM Tris/HCl pH 7.5
60 mM MgCl₂
10 mM Dithiothreitol

10x TBE buffer (LI-COR)

1.34 M Tris/HCl pH 8.3
440 mM Boric acid
25 mM Na₂EDTA

4x Loading sample buffer (BX)

0.05 % Bromophenol blue
0.05 % Xylenecyanol
50 % Glycerol

dNTP's

25 mM of each dNTP

10x dephosphorylation buffer

500 mM Tris/HCl pH 8.5
1 mM Na₂EDTA

10x-CM buffer

100 mM CaCl₂
100 mM MgCl₂

2.6.1.2 Solutions for Bacterial culture media

LB-Agar plates

35g/l LB Agar

LB-medium

20g/l LB broth

Antibiotic stock solutions

100 mg/ml Ampicillin in water
50 mg/ml Kanamycin in water
5 mg/ml Tetracycline in ethanol

LB-antibiotic-Agar plates

100 μ g Ampicillin/ml LB Agar and/or
50 μ g Kanamycin/mL LB Agar

2.6.1.3 Solutions for blue/white selection

IPTG

0.1M IPTG in water

X-GAL

20 mg/ml in DMF

2.6.2 Protein chemistry

2.6.2.1 Protein Purification with Ni^{+2} -NTA- Agarose

The pH was adjusted at 4°C and all solutions were kept at 4°C.

Pellet washing buffer

50 mM Tris/HCl pH 8.0
1 mM EDTA

Washing buffer A

50 mM Tris/HCl pH 8.5
400 mM NaCl
2 mM $MgCl_2$
7.5 mM imidazole, pH 8.5
20% Glycerol

Washing buffer C

50 mM Tris/HCl pH 8.5
10 mM NaCl
2 mM $MgCl_2$
25 mM imidazole, pH 8.5
20% Glycerol

Dialysis buffer 1

50 mM Tris/HCl pH 8.5
10 mM NaCl
2 mM $MgCl_2$
35 % Glycerol

Cell lysis buffer

50 mM Tris/HCl pH 8.5

0.02 % α -monothioglycerol

Washing buffer B

50 mM Tris/HCl pH 8.5
400 mM NaCl
2 mM $MgCl_2$
15 mM imidazole, pH 8.5
20 % Glycerol

Elution buffer 1

50 mM Tris/HCl pH 8.5
10 mM NaCl
2 mM $MgCl_2$
300 mM imidazole, pH 8.5
20 % Glycerol

DNase buffer

10 mM Tris/HCl pH 7.5
10% Glycerol
2 mg/ml DNase

2.6.2.2 SDS-Polyacrylamide gel electrophoresis

Resolving gel buffer

1.5 M Tris/HCl pH 8.8
0.4 % SDS

10x electrophoresis buffer

250 mM Tris
1.92 M Glycine
1 % SDS

4x sample buffer

130 mM Tris/HCl pH 6.8
10 % SDS
20 % Glycerol
10 % β -mercaptoethanol
0.06 % Bromophenol blue

Stacking gel buffer

500 mM Tris/HCl pH 6.8
0.4 % SDS

Coomassie staining solution (see)

0.2 % Brilliant blue G-250
45% ethanol
10 % Acetic acid

Bleaching solution for SDS-PAGE gel

10 % Acetic acid
30 % Ethanol

APS solution

10% APS in water

2.6.2.3 Western Blot

TBS buffer (Tris Buffered Saline)

20 mM Tris/HCl pH 7.5
150 mM NaCl

TBS-T

0.1 % Tween 20 in TBS buffer

Towbin- Blot buffer

25 mM Tris/HCl
192 mM Glycine
20 % Methanol

Secondary antibody

Goat anti-mouse polyclonal antibodies conjugated with horseradish peroxidase diluted 1: 5000 in M-TBS-T

Ponceau S staining solution

0.1 % (w/v) Ponceau S
5 % Acetic acid

M-TBS-T

5 % Milk powder in TBS-T buffer

Primary antibody:

RGS-His4-antibody
0.04-0.2 µg/ml in M-TBS-T

His4- antibodies

0.1 µg/ml M-TBS-T

2.6.2.4 Cyclase Enzyme test

ATP Stock Solution

5 mM ATP pH 7.5 (adjusted with Tris)

10x AC Start solution

750 µM ATP with
1500-2500 kBq (α -³²P)-ATP/ml solution
A concentration of 0.1 and 1 mM have been used in the substrate kinetics

AC Stop buffer

3 mM cAMP/NaOH pH 7.5
3 mM ATP
1.5 % SDS

2x AC-Cocktail

100 mM Tris/HCl pH 7.5
20 mM MgCl₂
43% Glycerol

Different buffers of the same concentration substituted Tris/HCl in pH dependence studies.

cAMP or cGMP Stock solution

40 mM cNMP pH 7.5 (adjusted by Tris)

cNMP (for allosteric activation)

serial dilution from the above stocks have been prepared and used in the assay (volume of 10 µl)

³H-cAMP (internal standard)

20 mM cAMP
10-20 kBq/ml of [2,8-³H-cAMP] (NH₄⁺)
pH was adjusted to 7.5 by Tris solution

2.6.2.5 *Dimerization buffers*

The proteins for dimerization studies should be free of Tris, therefore, new solutions for protein purification were prepared, in addition to the dimerization solution which was used for the reaction

Washing buffer D

50 mM phosphate buffer pH 7.4
400 mM NaCl
2 mM MgCl₂
7.5 mM imidazole, pH 8.0
20% Glycerol

Washing buffer E

50 mM phosphate buffer pH 7.4
400 mM NaCl
2 mM MgCl₂
15 mM imidazole, pH 8.0
20 % Glycerol

Washing buffer F

50 mM phosphate buffer pH 7.4
10 mM NaCl
2 mM MgCl₂
25 mM imidazole, pH 8.0
20% Glycerol

Elution buffer 2

50 mM phosphate buffer pH 7.4
10 mM NaCl
2 mM MgCl₂
300 mM imidazole, pH 8.0
20 % Glycerol

Crosslinking buffer

50 mM Phosphate buffer pH 7.4
10 mM NaCl
22% Glycerol

2.6.2.6 *Other solutions*

Crystallization buffer

10 % Glycerol
10 mM Tris/HCl pH 7.5
1 mM MgCl₂
0.05% thioglycerol

For the crystallization of CyaB1 PAS domain, the above crystallization buffer but with 20% glycerol was used

FPLC buffer

50 mM Tris/HCl pH 7.5
200 mM NaCl
2 mM MgCl₂
20% Glycerol

3 Methods

3.1 Bioinformatics and Databases

Since 1977, DNA sequences of thousands of organisms have been decoded and stored in Databases [86-88]. A comparison of genes within a species or between different species can show similarities between protein functions.

In this work, different databases have been employed to determine the domain-organization and domain boundaries of different enzymes, gene and protein sequences, in addition to exploring other proteins that contain similar domains and show the identity and similarity with our query. These databases include:

1. SMART search: (<http://smart.embl-heidelberg.de>)
2. BLAST search: (<http://www.ncbi.nlm.nih.gov/blast>)
3. Pfam search: (www.sanger.ac.uk/software/pfam/search)
4. Expasy PROSITE: (<http://Expasy.org>)
5. Cyanobacteria database: (<http://bacteria.kazusa.or.jp/cyano/>)

DNA STAR and GeneDoc (programs for handling of DNA and protein sequences) were used. RasTop was employed to evaluate the crystal structures of proteins.

3.2 Molecular biology methods

3.2.1 Polymerase Chain Reaction (PCR)

The PCR reactions were run in 50 μ l with a thermocycler with heatable lids. The samples contained 1-5 ng of DNA to be amplified, 200 μ M dNTP, 0.5 μ M of each primer, 1 U *Taq*-DNA-Polymerase or 2 U of *pfu*-polymerase enzyme in addition to 1 x of corresponding reaction buffer (2 mM $MgSO_4$ was already included). The temperature program is shown in table 3.1:

Table 3.1: The temperature program used for PCR

		<i>Taq</i> - polymerase	
Phase		Temp.	time
Denaturation		95°C	5 min
25-30 cycles	Denaturation	95°C	1 min
	Primer annealing	T _a	1 min
	Extension	72°C	1 min/ kb
Fill up		72°C	5 min
		4°C	pause

The annealing temperature was calculated with the formula:

$$T_a (^{\circ}\text{C}) = 2 \times (\text{AT}) + 4 \times (\text{GC})$$

AT and GC represent the number of A + T and G + C respectively in the primer sequence. The lower annealing temperature was used in cases where the annealing temperatures of the two primers were different.

When there is no possibility for silent introduction of restriction sites, the fusion cloning was used. In a fusion PCR, two separate PCR reactions are performed; the antisense primer of PCR1 and the sense primer of PCR2 have a short region of overlapping homology (~ 10 bp) at their ends. At the end of the reaction, the product of PCR1 and PCR2 are gel-purified and used as template for a third reaction which fuses the two linear DNA fragments in one fragment as follows:

In a 0.5 ml PCR tube, 100 ng of each of the two PCR products was mixed with 5 μl *pfu*-polymerase buffer containing MgSO_4 , 0.2 mM of dNTP mixture and 0.5 μM of the 5'- primer of the first PCR and the 3'- primer of the second PCR. Water was added to a final volume of 49 μl and the PCR mixture was heated to 95°C before 1 μl of *pfu*-polymerase is added and the program was continued. A pre-run of 5 cycles at lower temperature (8°C below the calculated T_a) was performed followed by 25 cycles at 6°C higher temperature.

At the end of the reaction 10 μL of the PCR product is run on the agarose gel, the band of the correct size is excised from the gel and purified using *NucleoTrap*[®] DNA purification kit. The ends of DNA fragments produced by taq polymerase were blunted and phosphorylated, while those produced by pfu polymerase were phosphorylated directly without prior Klenow digestion.

3.2.2 Isolation of DNA by Agarose gel electrophoresis:

Agarose was dissolved in TAE-buffer by heating in a microwave. The solution was poured into a mould in which a well-forming comb was fitted and left to congeal, the agarose concentration was chosen according to the expected size (bp) of the DNA fragments:

≥ 2000 bp	0.8 - 1 %
500-2000 bp	1 - 1.8 %
≤ 500 bp	2 %

TAE buffer was used for electrophoresis, agarose gels were placed horizontally in an electrophoresis apparatus, the DNA samples were mixed with loading sample buffer (BX), and electrophoresis was performed at 80-100 V for 45-60 min at room temperature.

The size markers EcoRI/Hind III-digested λ -DNA (λ Marker) and MspI/SspI digested pBluescript II SK (-)-Vector (π Marker) were coelectrophoresed with DNA samples.

Table 3.2: DNA size markers used in agarose gel.

λ Marker (bp)	π Marker (bp)
21226	489
5184	404
4973	312
4277	270
3530	242/241
2027	215
1904	190
1584	157
1330	147
983	110
831	67
564	57
125	34
	26

For DNA detection, the gel was emerged in an ethidium bromide bath (0.01 mg/ml) for 2 min, run for another 10 min, DNA bands were visualized by UV-light and photographed. Long exposure of the DNA to UV light can damage the DNA and should be avoided. In some cases, the bands were excised and purified for further reactions.

3.2.3 Purification of DNA fragments from agarose gel

3.2.3.1 Use of DNA purification kit

Upon running a PCR product or restriction digestion by agarose gel electrophoresis, the desired band was excised from the agarose gel using a scalpel, and purified by Nucleotrap DNA purification kit according to the manufacturer's protocol. The purified DNA was eluted using 25- 50 μ l water and stored at 4°C or -20°C. In the case of DNA with sticky ends, storage at -20°C should be avoided due to the damage of the sticky ends caused by freezing.

3.2.3.2 Use of squeeze-freeze method

For simple, quick, and safe handling of small amounts of DNA (less than 1 microgram) or small fragments of DNA (80-100 bp), the squeeze-freeze method [89] was carried out. After electrophoresis, bands of interest are cut out of the gel. A hand-made filtration assembly was prepared by cutting the upper part of an eppendorf tube; make a small hole in the lower part and covering the hole by small piece of glass wool. The gel slices were put over the glass wool, another empty eppendorf tube was put below, the whole set was put into a small box to avoid the fall of ice into the opened tube and frozen at -80°C for 30 min, thawed and centrifuged through the filtration assembly (14000 rpm, 10 min) whereby the DNA-containing buffer was squeezed out. To concentrate the DNA solution and exchange the TAE buffer by water, further purification by ethanol precipitation was performed (see section 3.2.11.3).

3.2.4 Generation of blunt ends:

After PCR using *Taq polymerase* or restriction digestion, the DNA fragment was blunted using the Klenow fragment of the DNA polymerase I. Maximally 500 ng DNA, 1 μ l of 10x Klenow buffer and 0.8 μ l of Klenow polymerase (1U/ μ l) in a 10 μ l reaction volume were mixed. The reaction mixture was incubated for 10 min at 37°C. Then, 1 μ l of dNTP (20 mM) was added and the incubation continued for another 28 min. The Klenow enzyme was inactivated by heating the sample at 70°C for 10 min.

3.2.5 5'-Phosphorylation of PCR products:

In order to ligate the PCR product into the EcoRV-restricted pBluescript, the DNA should be phosphorylated. The 10 μ l Klenow-treated DNA solution is cooled for 5 min in ice, mixed with 2.5 μ l of ATP (1.7 mM), 1 μ l of T4 polynucleotide kinase (10U), and 1.5 μ l of T4-PNK buffer (1X) in 15 μ l were incubated at 37°C for 1 hr. At the end of the reaction, the content

was mixed with 400 μ l of NT2 solution of Nucleotrap[®] kit and the DNA purification was continued accordingly (section 3.2.3.1)

3.2.6 Dephosphorylation of plasmid vectors:

To avoid religation of digested-vectors without insert, the 5'-phosphate was removed using alkaline phosphatase. 500 ng DNA, 1U/pmol of enzyme and 1X dephosphorylation buffer were mixed in 20 μ l and incubated at 37°C for 1 hr. The compatibility of alkaline phosphatase with all buffer systems allowed the dephosphorylation directly after restriction digestion of the plasmid without the need to change or modify the buffer system.

3.2.7 Photometric determination of the DNA concentration:

Using a 1 cm quartz cuvette, the content of the double-stranded DNA was measured at 260 nm. An OD of 1 corresponds to 50 μ g/ml for double stranded DNA. The ratio OD₂₆₀/OD₂₈₀ was calculated to estimate purity. A ratio of > 1.8 was desirable.

3.2.8 Ligation of the DNA fragment:

DNA fragments were ligated to each other using the Rapid Ligation Kit according to the instructions of the manufacturer. The molar ratio of vector to insert should be 1:3 which was estimated from the bands of agarose gel.

3.2.9 Transformation of the recombinant DNA

3.2.9.1 Preparation of the competent cells:

E.coli competent cells were prepared by CaCl₂ method [90]. Small quantity of cells from glycerol stock was inoculated into 5 ml LB medium containing 10 μ g/ml tetracycline in case of *XL1* cells and 50 μ g/ml of kanamycin in case of *BL21* and grown at 37°C and 210 rpm overnight. In the morning, the preculture was transferred into 200 ml of fresh LB-medium (without antibiotic for *XL1* and with kanamycin for *BL21*) and incubated to an OD of 0.2-0.4. Then the cells were cooled in ice for 15 min, centrifuged (2000 x g, 4°C, 10 min). The pellets were combined during careful suspension in 50 ml of sterile cold 0.1M CaCl₂ solution, cooled in ice for another 20 min and centrifuged as before. The pellets were suspended in 10 ml of 0.1 M of CaCl₂/ 20% glycerol solution, cooled in ice for 3-5 hrs, portioned in Eppendorf cups as 100 μ l portions and stored at -80°C. Competent cells can not be defrosted more than once.

3.2.9.2 Transformation of DNA-plasmid into competent cells

The DNA ligation reaction (21µl from a rapid ligation kit protocol) was added to 100 µl-competent cells, mixed gently and incubated in ice for 20-30 min, cells were then heat-pulsed at 42°C for 60 sec. and incubated in ice for another 10-20 min. 500 µl of LB-broth (without antibiotic) were added and cells were incubated at 37°C for 1 hr at 210 rpm. 100-200 µl of the mixture were spread over preheated LB/Amp or LB/Amp/Kan agar plates. Plates were incubated in an inverted position (to prevent water condensation) for 12-16 hrs at 37°C.

To retransform an already purified plasmid, 1 µl of the purified miniprep was added to competent cells, incubated in ice for 5-10 min, heat shocked at 42°C for 50 sec, incubated again in ice for 2 min, 200 µl LB medium is added, left at room temperature for 10 min and 100 µl is plated on agar plate (with the suitable antibiotic) or all was added to 5 ml-LB test tube and incubated at 37°C for overnight.

3.2.10 White-blue colony screen

If the transformation was made with a PCR product ligated in pBluescript then a blue-white screen is performed. X-gal is used to indicate whether a bacterium expresses the beta galactosidase enzyme which is encoded by the *LacZ* gene. X-gal is cleaved by β-galactosidase yielding galactose and 5-bromo-4-chloro-3-hydroxyindole which is oxidized to 5,5'-dibromo-4,4'-dichloro-indigo, an insoluble blue dye. Thus, when 40 µl of X-gal (2%) and 40 µl of 0.1M IPTG, an inducer of β-galactosidase, are spread over an agar plate, colonies which have a functional *lacZ* gene can easily be distinguished by blue colour, while those carrying the recombinant DNA in the *lacZ* gene form white colonies.

3.2.11 Isolation of DNA

3.2.11.1 Isolation and purification of DNA from bacterial cultures (minipreps):

Plasmid DNA was isolated from bacterial cultures using miniprep kits. The standard protocol of the wizard Plus Minipreps DNA Purification system (PROMEGA) was carried out using 5 ml of overnight bacterial culture. The DNA was eluted with 50-60 µl of sterile water. The purified plasmid could be stored at 4°C or -20°C.

3.2.11.2 Phenol/chloroform extraction

If the *BL21 (DE3) [pREP4] E.coli* cells were used for cloning, DNAses destabilize the DNA and further purification of minipreps by phenol/chloroform is advisable. The purified DNA was mixed with half its volume of phenol and the mixture is vortexed for 1 min and

centrifuged (1 min, 13600 rpm, RT). The upper aqueous layer was transferred carefully to new Eppendorf cup, extracted by chloroform (a volume equal to that of phenol) twice, vortexed and centrifuged. The chloroform layer was discarded and the aqueous phase was further purified by ethanol precipitation.

3.2.11.3 Ethanol precipitation

To concentrate DNA or change buffer, an ethanol precipitation was carried out. The volume of DNA solution was measured by pipette and precipitated by addition of $0.375 * V_{DNA}$ and $2.5 * V_{DNA}$ of cold 95% ethanol, mix well, incubate at 4°C for 30 min and pellet the DNA by centrifugation at 14000 x g for 20 min at 4°C. A subsequent wash with half the volume of 70% ethanol, followed by brief centrifugation (14000 rpm, 10 min, 4°C) was performed to remove residual salt and moisture. The ethanol is left to dry, the DNA is dissolved in 60 µl water, heated at 42°C and vortexed.

3.2.12 Enzymatic digestion:

In 10 µl volume, 400-600 ng of DNA was incubated with 1U of restriction enzyme in the respective buffer, 5 µg of BSA was added to stabilize some enzymes. The DNA-enzyme mixture was incubated at the recommended temperature for a minimum of 1hr and a maximum of overnight. In the case of simultaneous digestion with 2 or more enzymes, the most compatible buffer was used. If no compatible buffer is available, the digestion is performed for each enzyme alone with its buffer and *Nucleotrap*[®] purification between the two digestions was carried out. The digest was analysed by electrophoresis to visualize the fragments pattern and to test for complete digestion. The bands were excised and purified when ligation to another DNA is required.

3.2.13 DNA sequencing

3.2.13.1 Chain terminating sequencing:

DNA fidelity was ascertained by sequencing using the thermo sequenase Fluorescent labelled primer cycle sequencing kit (GE Health care) [91]. 8-10 µl (~130 ng/Kb) plasmid-DNA were mixed with 2 µl (2-3 µM) fluorescent labelled primers, 3% DMSO and then the volume was completed to 18 µl with water. 4 µl of these mixtures were mixed each with 2µl of the reaction mixture (see manufacturer's protocol), covered with a drop of chill out wax and then run in a thermocycler according to the following program:

Table 3.3: Temperature program used for Li-Cor sequencing reaction

Methods

Phase	Temperature	Time	Cycles
Denaturation	95°C	2 min	
Denaturation	95°C	20 s	30
Primer annealing	T _a	20 s	
Extension	70°C	20 s	
Filling-up	4°C	∞	

Annealing temperatures were according to table 2.3 (section 2.5.1).

After completion, samples were mixed with 6 µl stop buffer and 1 µl samples were loaded on 6% polyacrylamide gel. Electrophoresis was performed with TBE buffer at 50 W (1500 V, 37 mA, 50°C) using Li-Cor DNA sequencer Model 4000.

3.2.13.2 Capillary DNA sequencing:

For the last constructs, the Capillary DNA sequencing was used [92, 93]. The concentration of the DNA and OD280/260 were measured. In a small eppendorf tube, 4 µl of the diluted sequencing kit are pipetted to the bottom of the tube, 1.2 µl of a suitable nonlabeled primer (20 pmol/µl) are pipetted to the side followed by pipetting 5 µl of purified DNA (100 ng/µl) at the lid of the eppendorf tube. The eppendorf tube is closed and centrifuged for a short time and PCR reaction is carried out using the program in table 3.4

Table 3.4: Temperature program used for capillary sequencing reaction

Phase	Temperature	Time	Cycles
Denaturation	96°C	1 min	
Denaturation	96°C	10 s	25
Primer annealing	50°C	5 s	
Extension	60°C	4 min	
Filling-up	4°C	∞	

After completion, DNA was precipitated using 40µl of isopropanol, left at RT for 10 min, and centrifuged at 13000 rpm for 30 min, and the isopropanol layer was removed and discarded. The DNA was washed by 150 µl of 80% ethanol, centrifuged (13000 rpm, 5 min), ethanol is discarded and DNA pellets are dried in a speed Vac. Eppendorf tubes are kept at 4°C until applied to the robot. Before loading to the capillary electrophoresis, DNA pellets are

dissolved in 15 μ l of HiDi buffer (High-Divalent-cation: 368 mM NaCl, 10 mM KCl, 13.8 mM CaCl₂, 101 mM MgCl₂, and 10 mM HEPES pH 7.6), left at RT for 15 min vortexed and centrifuged. Samples were automatically loaded by the capillary sequencing robot.

3.2.14 Glycerol stocks:

For long term storage of the recombinant DNA, 1 ml of the overnight bacterial culture (with cDNA) was centrifuged (2 min, 13600 x g, RT) the pellet was suspended carefully in 750 μ l of a mixture of LB-broth/glycerol (4:1) and stored at -80°C.

3.3 Protein Chemistry

3.3.1 Preculture:

E.coli strain BL-21 (DE3) [pREP4] (Kan^R) was used for expression. DNA in expression vectors pQE30, pQE82 or pET-pQE30 MCS was transformed into BL21 (DE3) [pREP4] cells and a glycerol stock was prepared. The preculture was prepared by inoculating 10 ml of LB-broth containing 100 μ g/ml ampicillin and 25 μ g/ml kanamycin with a small amount of the glycerol stock using a sterile tip and the preculture was incubated for overnight at 37°C and 210 rpm.

3.3.2 Expression:

The 5-10 ml of the overnight preculture were inoculated and grown in 200 ml LB-broth containing 100 μ g/ml Ampicillin and 25 μ g/ml Kanamycin at 30°C, 210 rpm to A₆₀₀ of 0.5-0.6 (approx. after 1.5-2.5 hrs). The protein expression was induced by 300 μ M IPTG (21- 27°C, 210 rpm). Constructs which consist of three or more distinct domains were induced by 30-50 μ M IPTG (16-19°C, 210 rpm, overnight). 10 mM MgCl₂ was added wherever CyaB1 catalytic domain is within the construct.

Initially, two hours after induction, 1 ml of culture is centrifuged at 13,000 rpm for 2 min, washed by 1ml cell wash buffer and centrifuged again. Pellets are resuspended in 100 μ l of cell lysis buffer, destroyed by sonification (3 times for 5 sec, level 4) in ice and centrifuged (14,000 rpm, 15 min, 4°C). 15 μ l of the supernatant was mixed with 5 μ l of SDS 4x sample buffer, heated for 95°C for 5 min and loaded on SDS-PAGE while pellets were suspended in 50 μ l of water, 20 μ l were mixed with 20 μ l of 4x sample buffer, heated to 95°C for 5 min, centrifuged shortly and 5 μ l was loaded. The supernatant and pellets of enzyme were run concomitantly with empty pQE30 expressed under the same expression conditions.

3.3.3 Cell harvesting and washing

After 4-6 hrs for one or 2 domain constructs and 16-20 hrs in larger constructs, cells were harvested (15 min, 5000 x g, 4°C), the supernatant was discarded, the pellet was resuspended in 40 ml of cold cell wash buffer, transferred into 50 ml-Falcon tubes, centrifuged (15 min, 5500 × g, 4°C), flash-frozen in liquid N₂ or/and stored at – 80°C.

3.3.4 Purification of soluble proteins from E.coli:

Frozen pellets were thawed on ice (10-15 min), suspended in 20 ml of cell lysis buffer, passed twice through the French Press (1000 psi) and the homogenate was centrifuged (30 min, 18000 x g, 4°C). The supernatant was mixed with 250 mM NaCl and 15 mM imidazole end concentrations, 110-350 µl Ni⁺²-NTA agarose was mixed with 5 ml cell lysis buffer, 300 µl NaCl (5M), 75 µl imidazole (1M), 25 µl MgCl₂ (2M). The mixture was added to the supernatant and slowly rocked for 1.5-3 hrs in ice. Samples were then centrifuged (5 min, 2500 x g, 4°C). The supernatant was discarded, and Ni⁺²-NTA resin was poured into 10 ml syringe with a Wizard mini-column attached, washed by 2 ml of each washing buffer A, B, C and the protein was eluted by 400-600 µl elution buffer 1.

3.3.5 Protein dialysis

To remove imidazole and change buffer, samples of 600 µl-6 ml were dialyzed (VISKING Dialysis Tubing, MWCO 12000-14000) for 14-16 hrs at 4°C against either the dialysis buffer, dimerization buffer or the crystallization buffer and the protein was used immediately or kept at -20°C in the corresponding buffer.

3.3.6 Bio-Rad Protein determination:

The Bio-Rad protein assay according to Bradford was used [94].

3.3.7 Sample concentration:

For crystallization experiments, protein concentration was required. Two types of concentrators were used. Samples were concentrated by ultrafiltration using the *NANOSEP 10K (Omega membrane)* centrifugal devices MWCO 10000 using an *eppendorf* centrifuge (11,000 x g, 4°C, 5-30 min) or by *Vivaspin 10k* concentrator using *Heraeus Megafuge 1.0 R* centrifuge (4300 x g, 4°C, 5-15 min) until the desirable protein concentration was achieved. In *NANOSEP* concentrators, the protein was recovered from the filter with pipette. For *Vivaspin*, the protein was obtained by the centrifuging the concentrator in an inverted position

Methods

for 1 min to get the protein into the lid. Both devices were kept at 4°C with 0.5 ml of crystallization buffer for repeated use.

3.3.8 SDS-PAGE:

SDS-PAGE according to Laemmli is probably the worlds most widely used biochemical method. [95]. Two 80×60×6mm (L×W×T) minigels were casted according to the proteins molecular weights to be run as determined in table 3.5.

Table 3.5: The components of resolving and stacking gels, used in preparation of two SDS-PAGE minigels.

Resolving Gel (pH 8.8)	7.5%	10%	12.5%	15%	Stacking gel (pH 6.8)	4.5%
Resolving gel buffer	3 ml	3 ml	3 ml	3 ml	Stacking gel buffer	1 ml
H ₂ O	6 ml	5 ml	4 ml	3 ml	H ₂ O	2.4 ml
Acrylamide/Bisacrylamide 37.5:1 (30%)	3 ml	4 ml	5 ml	6 ml	Acrylamide/Bisacrylamide 37.5:1	0.6 ml
TEMED	10 µl	10 µl	10 µl	10 µl	TEMED	10 µl
APS 10 %	80 µl	80 µl	80 µl	80 µl	APS 10 %	40 µl

Mighty small II vertical electrophoresis apparatus from *HOEFER* was used. A volume equivalent to 2-4 µg of protein samples was mixed with 5 µl of 4x- sample buffer, heated for 95°C for 5 min and loaded on the gel. 10 µl PeqGold protein size marker (table 3.6) was run simultaneously: 20mA, 200V, 1 hr, stained with coomassie blue for 30 min with gentle agitation, decolourised for 20-25 min and washed with water until bands are clearly detected.

Tabl 3.6: PeqGold marker for protein size determination contains 1 µg of each protein.

PeqGold Marker	Mw (kDa)
Lysozyme	14.4
β-Lactoglobulin	18.4
RE Bsp981	25
Lactate dehydrogenase	35
Ovalbumin	45
Bovine serum albumin	66
β -galactosidase	116

3.3.9 Western Blot

The semi-Dry electrophoretic transfer of sample proteins to membranes for immunoblotting occurs after protein separation by SDS-PAGE [96]. Care must be taken when working with PVDF (*polyvinylidene fluoride*) membranes, forceps is used and membranes are handled by their edges so as not to damage the surface. The blot membrane (6×8cm) was successively soaked in methanol (to improve its wettability) for 10 min, wetted in water for another 10 min and then transferred to towbin buffer together with the gel and six pieces of Whatman 3MM papers (7.5×9.5cm) for a third 10 min interval. The following sandwich set-up was built up for the electric transfer:

- Three soaked Whatman 3 MM papers were layed on the anode plate.
- the blot membrane was layed over them, the gel was spread evenly over the membrane using glass rod to remove air bubbles and finally three soaked Whatman papers were layed again on the side of the cathode plate. Excess buffer was wiped off using a tissue paper before the lid is being fixed.

Protein transfer was carried out for 2.5-3 hr at 20V and 2.5 mA/cm². The gel was stained in Coomassie Brilliant blue to check transfer efficiency.

The membrane was stained in Ponceau S for about 5 min, then it was decolourized with deionized water until the protein bands were clear enough for the marker bands to be marked with a pencil (note: Ponceau S is preferred over coomassie because it has better water solubility and so can be easily washed from the membrane). To prevent the non-specific binding of the antibodies, the membrane was blocked with M-TBS-T buffer for at least 1 hr at RT or overnight at 4°C and excess milk was washed with TBS-T buffer (2 x 10 sec, 2 x 5 min). It was then incubated with the primary antibody (mouse monoclonal RGS-His4 antibody 1:2000, or Tetra His antibody 1:1000 diluted in M-TBS) for 1 hr. After washing by TBS-T (1x 15 min, 2 x 5 min), the membrane was shaken with the secondary antibody (goat anti-mouse IgG-F_c horseradish peroxidase conjugated antibodies 1:5000 diluted in M-TBS) for 1hr and then washed as above with TBS-T.

The chemilumescient reaction with the *ECL Plus* Western Blotting Detection Kit (GE Health Care) was carried out according to the manufacturer's instructions. After their exposure to the detection reaction, the bands were detected by exposing the membrane to *hyperfilm ECL* (exposure time from 3 sec to 5 min). The films were developed using a *Konica* medical film processor.

3.3.10 Adenylyl cyclase enzyme Assay:

[α - ^{32}P]-ATP was used as a substrate and cyclic [^{32}P] AMP was isolated using a two-column technique (Dowex 50 and neutral alumina) to separate the cAMP product from ATP substrate [97]. [2,8- ^3H] cAMP was used as internal standard to monitor yield.

A standard test 100 μl contained. In 1.5 ml eppendorf tube 40 μl of protein sample including substances like BSA, cGMP and cAMP was mixed with 50 μl of AC test cocktail, 10 μl of (α - ^{32}P)-ATP (750 μM , 150-250 kBq) was added to start the reaction and the tubes were incubated in shaking heating block (37°C, 1000 rpm) unless indicated otherwise. The final concentrations were: 50 mM Tris/HCl buffer pH 7.5, 22% glycerol, 10 mM MgCl_2 , 0.25 $\mu\text{g}/\mu\text{l}$, 75 μM ATP (15-25 kBq). The reaction was stopped by addition of 150 μl of stop buffer. 10 μl of [2, 8- ^3H]-cAMP were added as internal standard followed by 750 μl of water and the mixture was poured on a dowex column (9 \times 1 cm glass column with 1.2 g Dowex 50), after washing with 3 ml water, the samples were eluted with 5 ml water onto Al_2O_3 columns (10 \times 0.5 cm plastic column with 1 g active neutral Al_2O_3 90). Samples were eluted with 4.5 ml 0.1 M Tris/HCl pH 7.5, mixed with 4 ml of Ultima Gold XR Scintillator solution and counted.

Dowex columns were regenerated with 1 \times 5 ml 2M HCl, 1 \times 10 ml water and 1 \times 5 ml water, while Al_2O_3 columns with 2 \times 5 ml 0.1 M Tris/HCl pH 7.5.

Specific activity (A) (pmol/mg/min) was calculated with the following formula

$$A = \frac{\text{Substrate } (\mu\text{M}) \times 100 \mu\text{l}}{\text{time (min)}} \times \frac{1000}{\text{protein } (\mu\text{g})} \times \frac{\text{cpm } [^3\text{H}]_{\text{total}}}{\text{cpm } [^3\text{H}]_{\text{sample}} - 3\% [^{32}\text{P}]_{\text{sample}}} \times \frac{\text{cpm } [^{32}\text{P}]_{\text{sample}} - \text{cpm } [^{32}\text{P}]_{\text{blank}}}{\text{cpm } [^{32}\text{P}]_{\text{total}}}$$

3% of the phosphorous counts were subtracted from the tritium value for each sample because of the spill over of ^{32}P into the tritium channel. Activities lower than double background (in cpm) were considered zero.

In CyaB1 and CyaB2 GAF-containing constructs, cAMP is a product of AC assay and may cause allosteric activation, so such constructs were assayed for 4 min and with a concentration of protein that gives an activity of 300-400 cpm. Constructs which are not activated by cAMP were assayed for 10 min.

The average and the standard error of 4-6 samples were calculated and the activity or specific activity was plotted against the variable parameter.

3.3.11 Crystallization

The x-ray crystallography is used for structure elucidation.

3.3.11.1 Hanging drop vapour diffusion method:

In the hanging drop vapour diffusion method (fig 3.1) the protein/precipitant solution is equilibrated in a closed container with a larger reservoir, where the precipitant concentration is in the appropriate range to produce crystals.

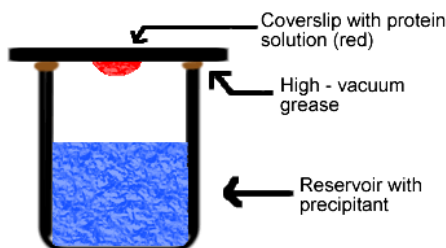


Figure 3.1: Principle of the hanging drop vapour diffusion method where the hanging drop was prepared on a siliconized slide cover by mixing the protein sample and the precipitant (1:1), the slide cover is inverted then over a well (reservoir) containing 500 μ l of the precipitant.

500 μ l of precipitant solution is filled into each well of a VDX crystallization plate containing 24 wells (Hampton research). 1.0 μ l of precipitant is mixed with 1.0 μ l of protein solution (3-21 mg/ml) on a siliconized coverslip (Hampton Research). The coverslip containing the drop hanging up-side down was sealed with grease over the well. For initial crystallization conditions, crystallization screens Wizard I and II (Emerald Biostructures), Crystal Screen I, II, and lite (Hampton Research) were used. The plates were kept at 12°C or 16°C and examined under a polarization microscope every day for the first week and then once a week. Conditions containing crystals were optimized by individually devised screens around the initial condition by altering buffer, precipitant, and additive concentrations and identities, as well as altering the temperature of crystallization (20°C, 12°C and 4°C) and protein concentration.

3.3.11.2 Sitting-drop vapour diffusion method

For the crystallization of Δ N-hPDE2GAF, the sitting drop vapour diffusion experiments were carried out at the department of Biochemistry, University of Tübingen using a *Tecan Freedom Evo 150* crystallization robot. In this method, a 96-well microplate was used; each well contains a raised plastic platform with a depression standing on several legs for carrying out the sitting drop inside the well [98] (see fig.3.2).

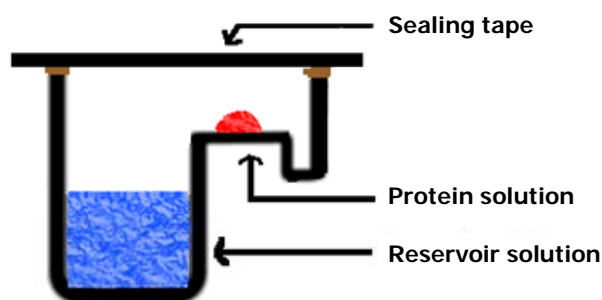


Fig.3.2: Principle of sitting drop vapour diffusion method.

The concentrated protein solution was filtered at 4°C, 10000 rpm using Corning Spin-X Centrifugation filters (0.2 µm) to remove any particles or cell debris before being used in the robot. Each plate is arranged in an 8 x 12 array. Each array location has a reservoir well and two sample wells-each of different size. The maximum fill volume of each reservoir well is 140 µl, with 4 µl and 10 µl for the two sample wells.

75 µl of precipitant solution is filled into each well of an Intelli-microplate containing 96 wells (Art Robbins Instruments). The robot was programmed to mix 300 nl of precipitant with 300 nl of protein solution (12 mg/ml) on the sample well located on the raised platform of each well. Two drops were pipetted in the platform of each well, the protein in the presence and in the absence of 2 mM cGMP, providing an economic method to crystallize proteins. The plates were sealed by a sealing tape, stored at 4 and 20°C and screened for crystals every week. Four kits from Hampton were used, Crystal screen I, II (at 20°C), lite and PEG/Ion kits (at 4 and 20°C).

3.3.12 Size exclusion chromatography (Gel Filtration)

Buffers have been prepared using milliQ water, filtered through 0.2 µm microfilter, and degassed. 200 µl of 1-2 mg/ml protein were applied to a Supradex 200 HR 10/30 column previously washed by twice its volume of FPLC-buffer (50 mM Tris/HCl pH 7.5, 200 mM NaCl, 2 mM MgCl₂, 20% glycerol). The protein was detected by UV detector at 280nm. The flow rate was 0.4mL/min (see table 3.7).

Table 3.7: chromatography conditions and column dimensions:

Column type	Supradex 200 HR 30/10
Column volume	23.562ml
Column dimensions	30 cm length × 1 cm diameter
Elution	30 ml of FPLC buffer
Start of fractionation	7ml
Fraction Volume	0.5ml

Methods

The protein containing fractions (monomer and dimer) were collected and analysed by SDS-PAGE or western blot. The column was calibrated by different proteins (Combithek, Roche, Mannheim) (table 3.8)

Table 3.8: Calibration proteins used in the chromatography and their sizes

protein	Size (kDa)
Ferritin	450
Aldolase	158
Phos b	96
Bovine serum albumin	68
Ovalbumin	45
Cytochrome C	12.5

The sizes of calibrated proteins were plotted against their retention volume in a logarithmic scale (fig.3.3) and the equation obtained from the straight line was used to calculate the sizes of the different proteins.

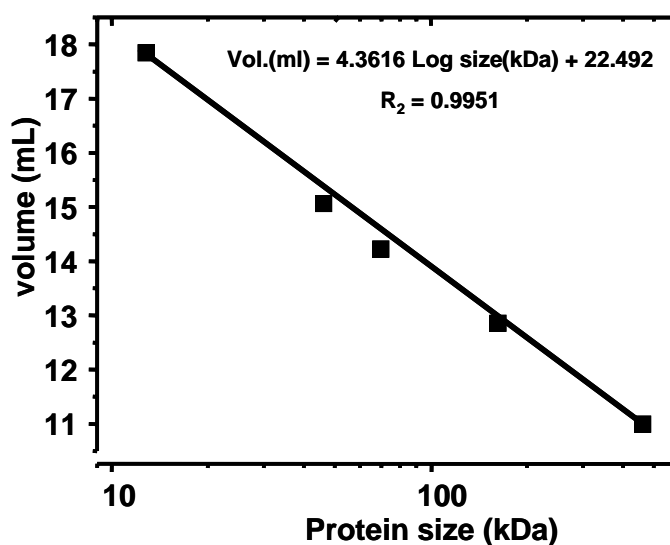


Fig.3.3: Calibration curve of the gel filtration chromatography column. The column used was a 1 x 30-cm S-200 HR column. Flow was maintained using a peristaltic pump at a constant output of 0.4 ml/min. The selective permeation range was standardized using known commercial protein standards (Combithek, Roche, Mannheim): Ferritin (450 kDa), Aldolase (158 kDa), Bovine serum albumin (68 kDa), Ovalbumin (45 kDa), and Cytochrome C (12.5 kDa).

3.3.13 Dimerization studies:

Glutaraldehyde is a bifunctional cross-linking reagent capable of reacting with amino acid side chains, particularly with the lysine NH₂ group, to form *Schiff* bases [99]. The ability of proteins to form dimers was assessed by chemical crosslinking using glutaraldehyde 25% (Fluka) as described previously by Ramesh and Nagaraja [100].

3.4 Cloning:

The key used in the drawing of the cloning procedures was as in fig.3.4

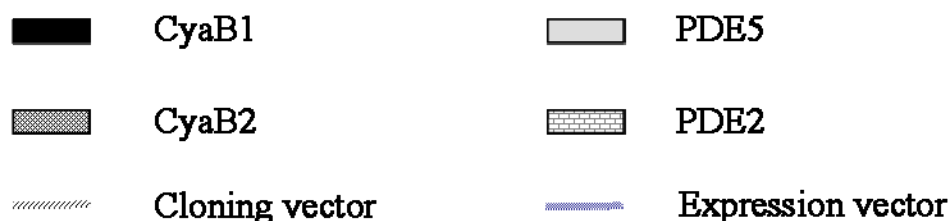


Fig.3.4: a key indicates the colour used for the representation of each enzyme DNA. Each 1 cm represents 200 bp

All PCR products were amplified by Taq DNA-polymerase, treated by Klenow, phosphorylated, inserted into EcoRV-digested dephosphorylated pBSKII(-) and sequenced and the correct clones were selected for further digestions and ligations.

The end clones are determined by a box and whether it has N-terminal or C-terminal His-tag was also indicated. Most to the constructs were cloned in *E.coli XL1* or *DH5α* and sometimes in *E.coli BL21 (DE3) [pREP4]* and the end clones were transformed into *E.coli BL21(DE3) [pREP4]* for expression.

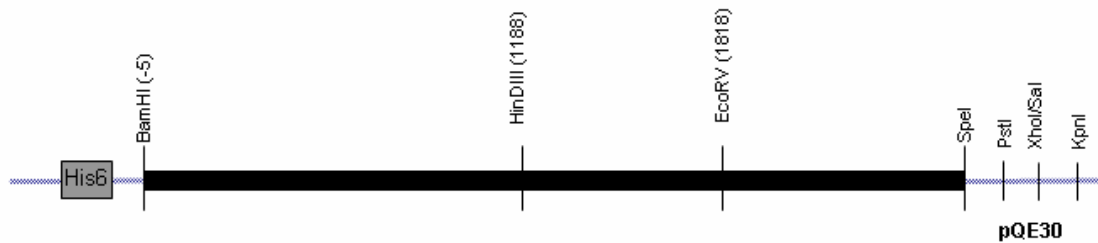
The DNAs of the following enzymes were already available in the Laboratory and were used as provided or used as templates to clone other constructs. The original DNA of CyaB1 was provided as a gift from prof. Ohmori, Tokyo, Japan while that of hPDE2A3 in Paqpaq was provided by ALTANA pharmaceuticals, Konstanz, Germany. CyaB1 in pQE30 and pBluescript, hPDE5NGAF/CyaB1 chimera in pET-MCS-pQE30 and CyaB2NGAF/CyaB1 in pQE30 were obtained from S.Bruder. CyaB1 holoenzyme with different cutting sites and modified pBluescript (pBSKII (-)) was obtained from A.Schultz. CyaB2 holoenzyme and truncated CyaB1 catalytic domains were obtained from J.Linder. hPDE5 holoenzyme was obtained from J.Weber and ΔN-hPDE5GAF was obtained from A.Banjac.

Some of the construct were cloned by A.Schultz and J.Linder (mentioned wherever necessary)

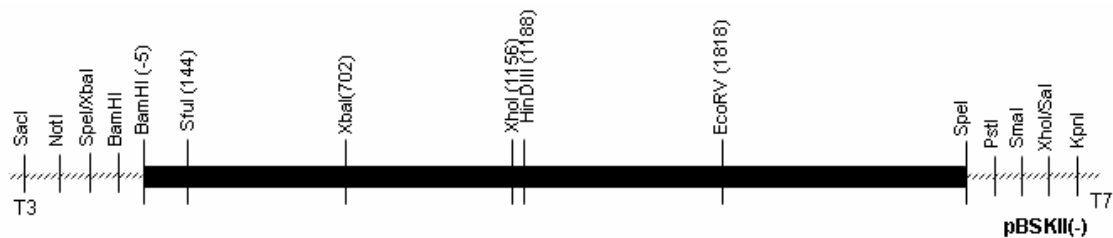
Methods

The starting clones which were used either as templates or used as they are for comparison purposes:

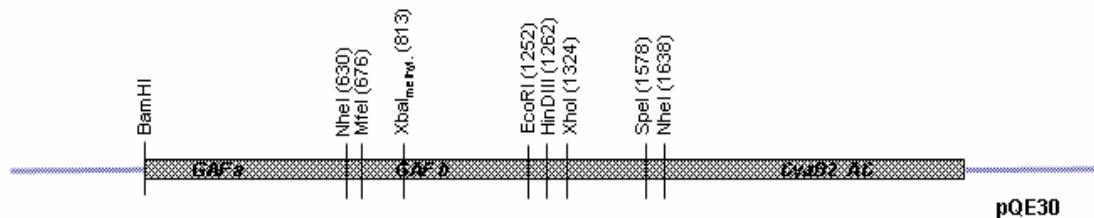
1. CyaB1 holoenzyme in *pQE30* (from S.Bruder)



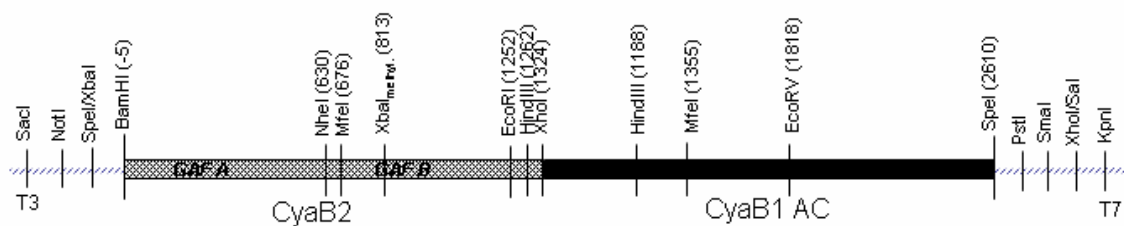
2. CyaB1 holoenzyme with SfuI site in *pBSKII (-)* (from A. Schultz)



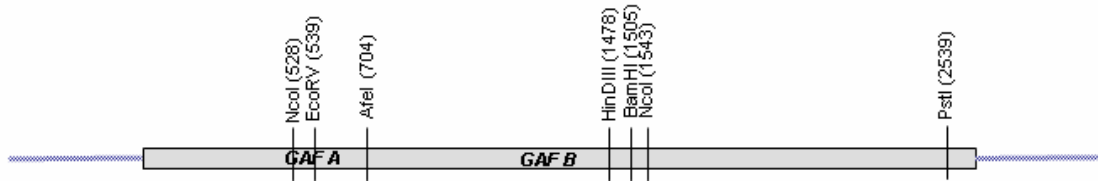
3. CyaB2 holoenzyme in *pQE30* (from J.Linder)



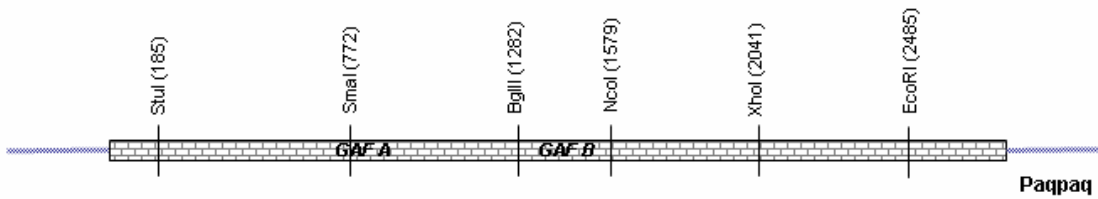
4. CyaB2NGAF/CyaB1 chimera in *pBSKII (-)* or in *pQE30* (from S.Bruder)



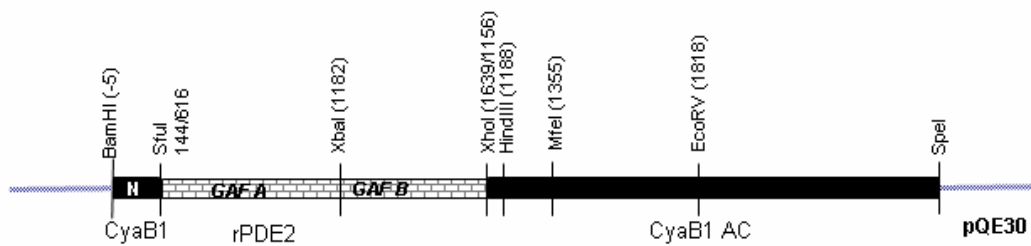
5. hPDE5 holoenzyme in *pcDNA3-Ziocin* vector (from J.Weber)



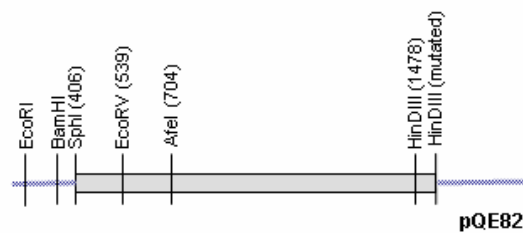
6. hPDE2 holoenzyme in *Paqpaq* vector (from ALTANA pharmaceuticals)



7. CyaB1N-rPDE2GAF/CyaB1 in *pQE30* (from T.Kanacher)

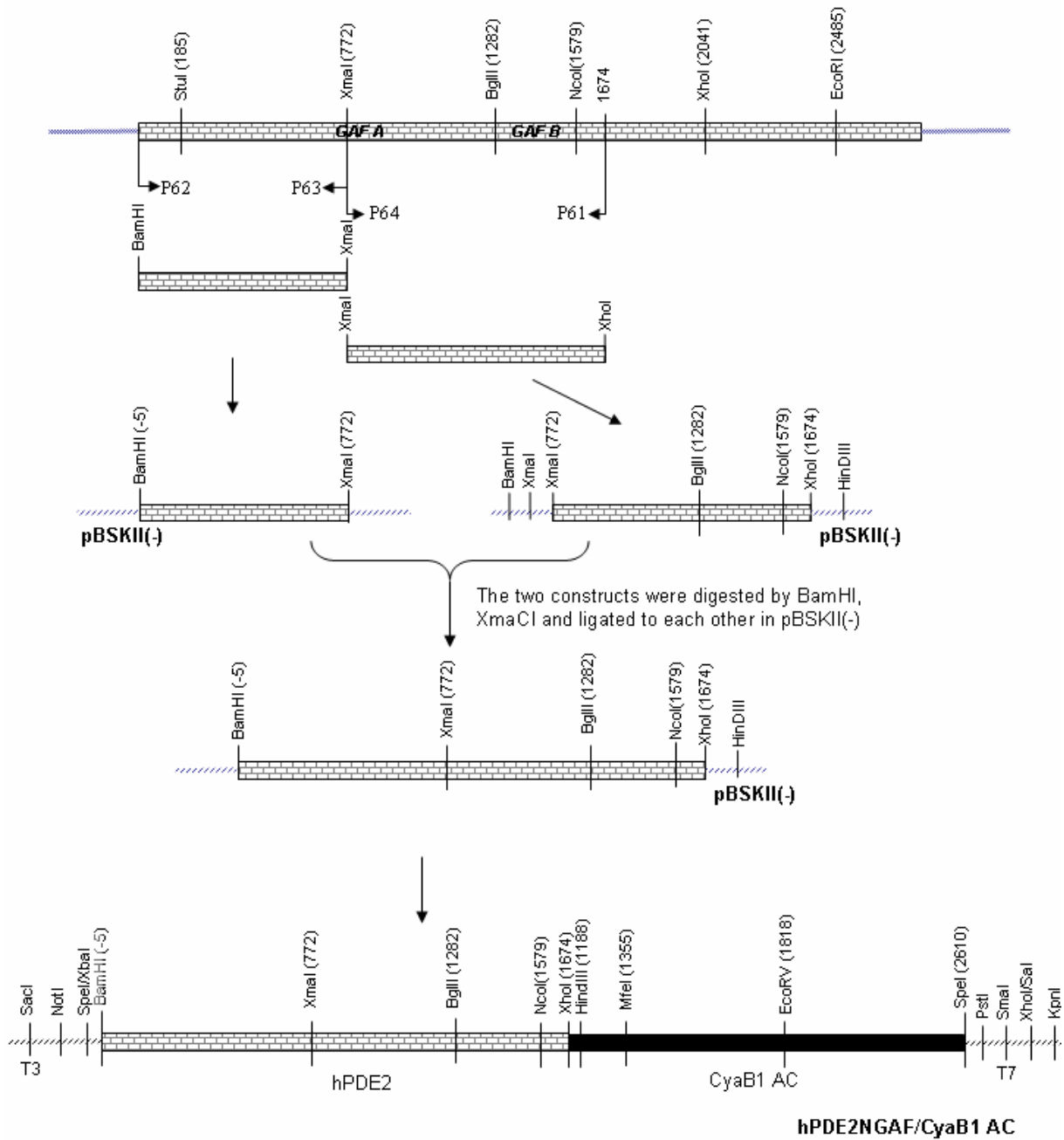


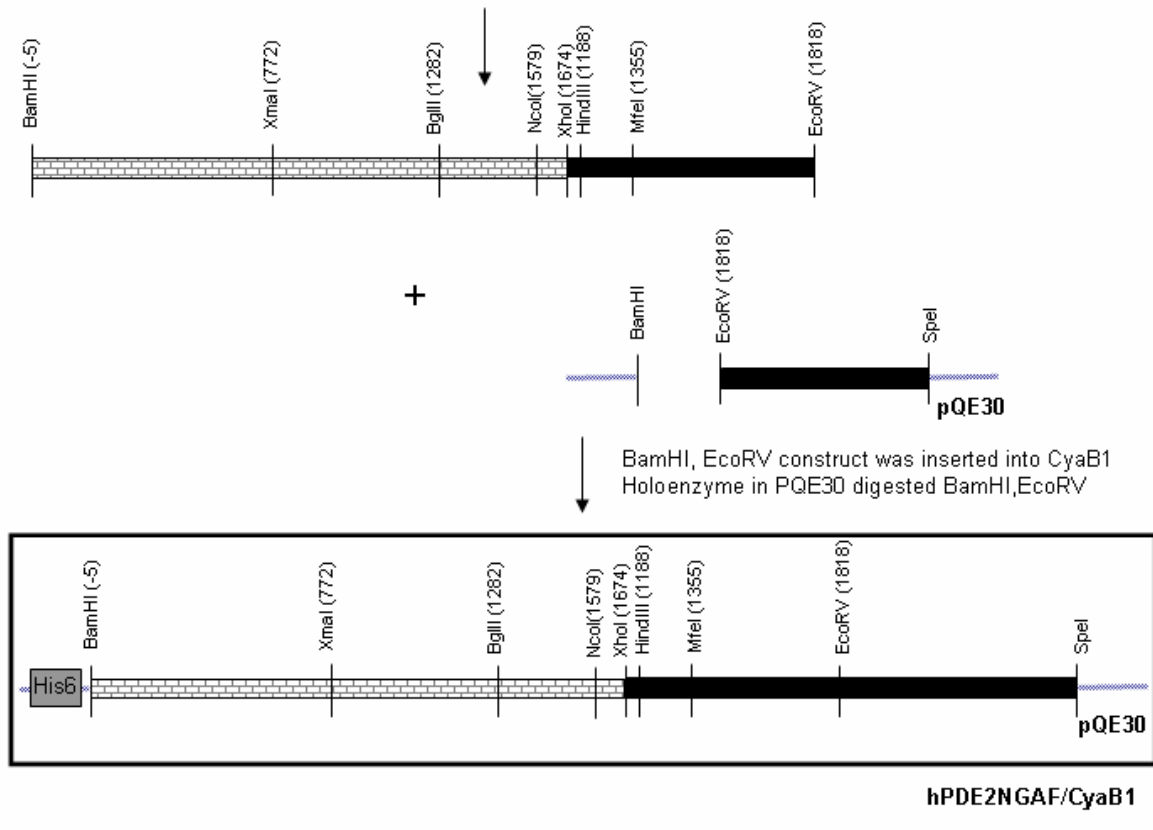
8. ΔN-hPDE5 GAFcr on *pQE82* (from A.Banjac).



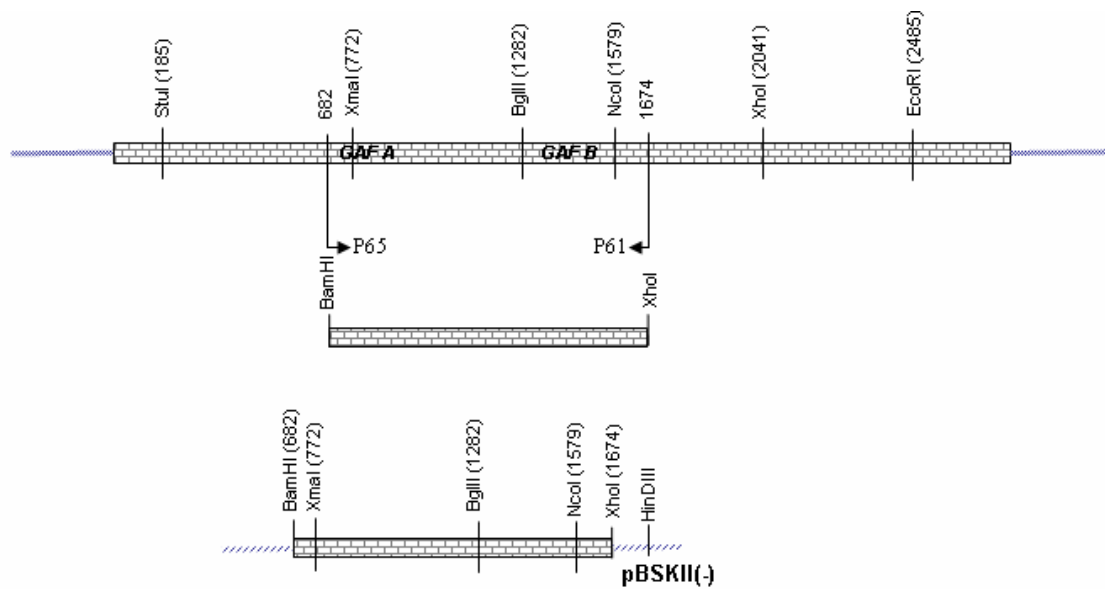
3.4.1 Cloning of hPDE2 constructs

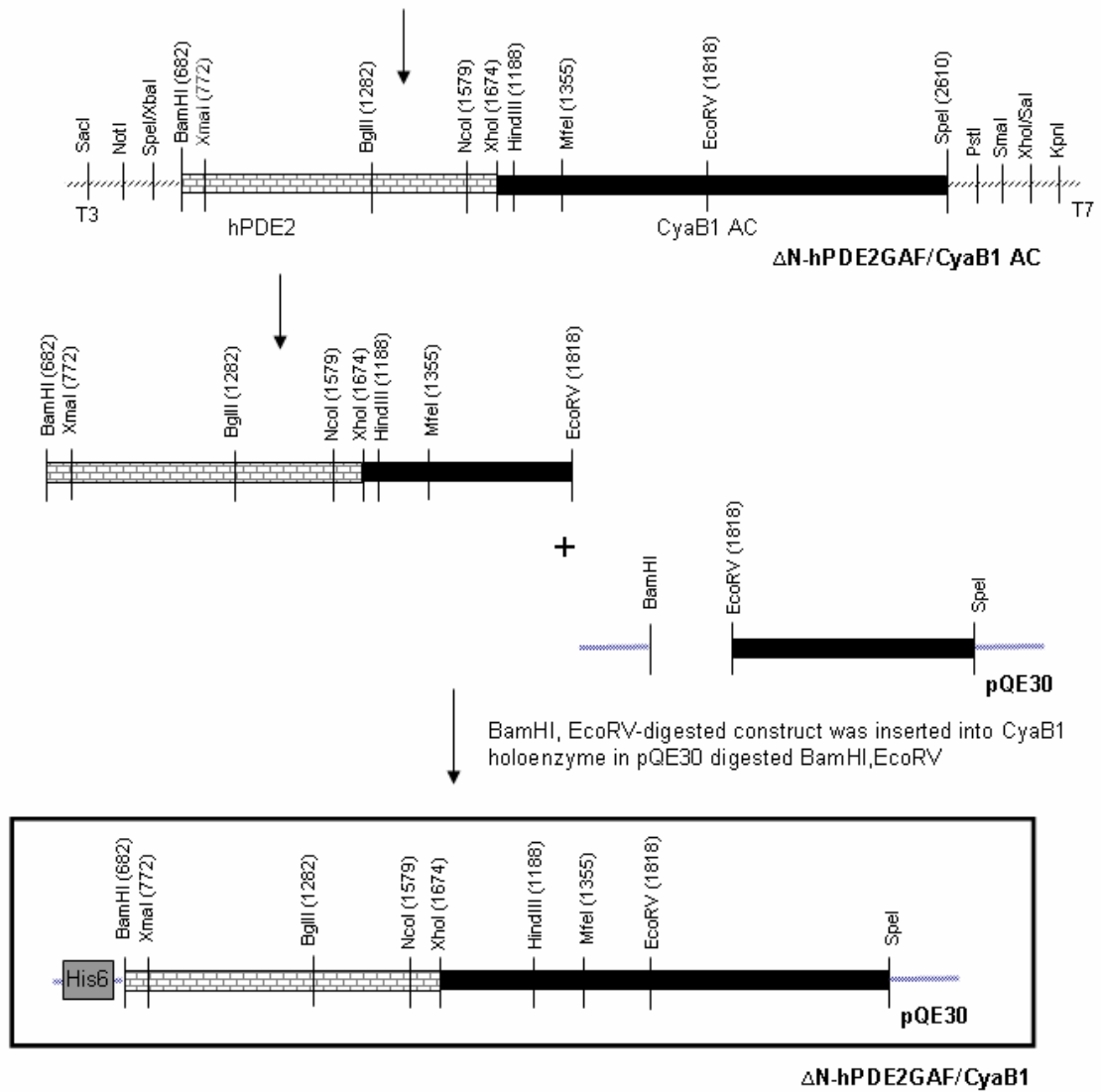
3.4.1.1 Cloning of hPDE2NGAF/CyaB1 chimera



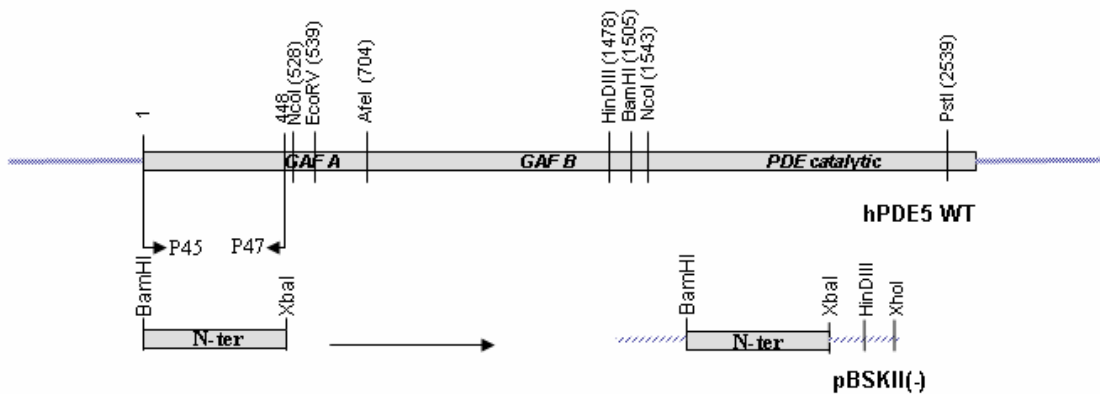


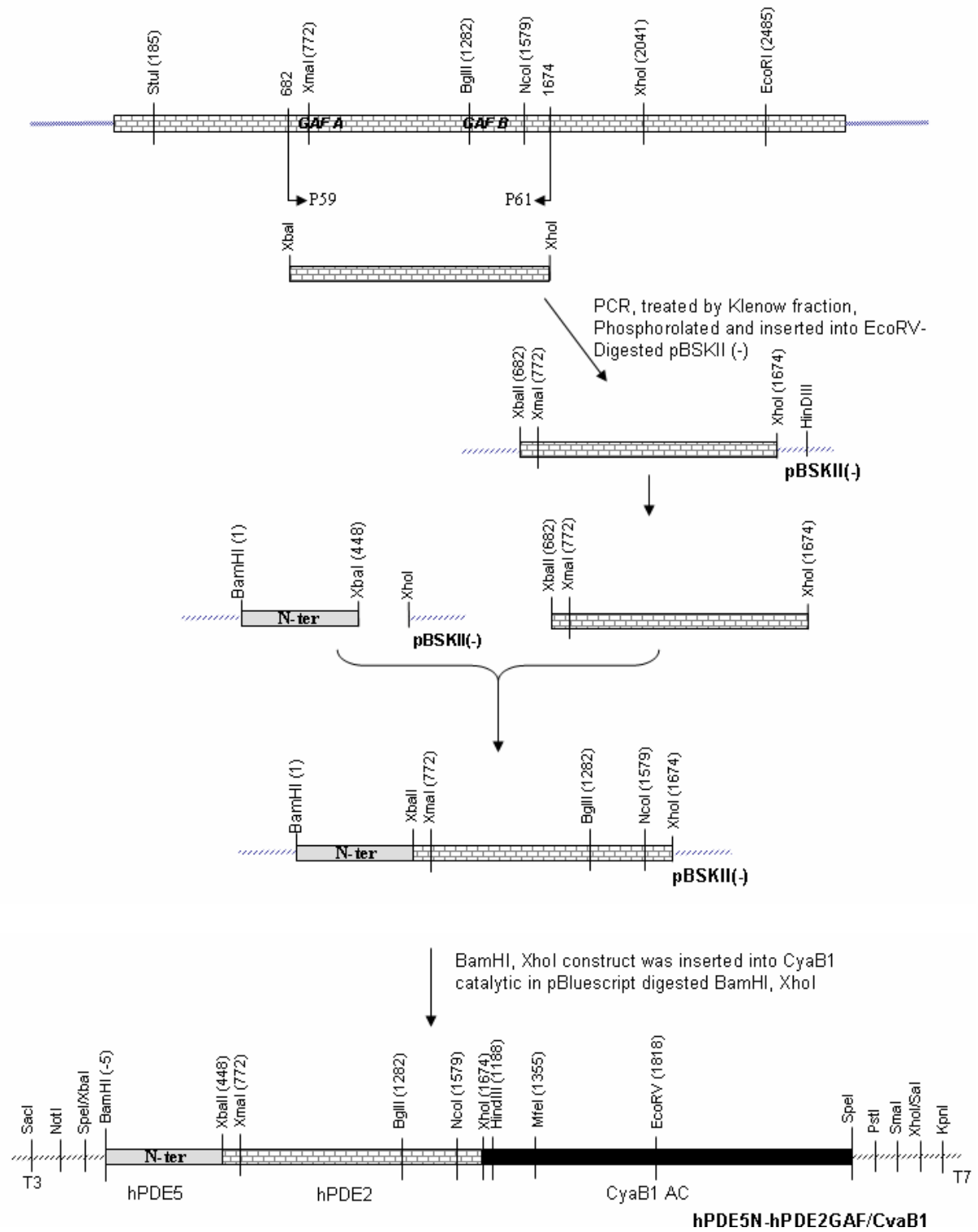
3.4.1.2 Cloning of ΔN-hPDE2GAF/CyaB1 chimera

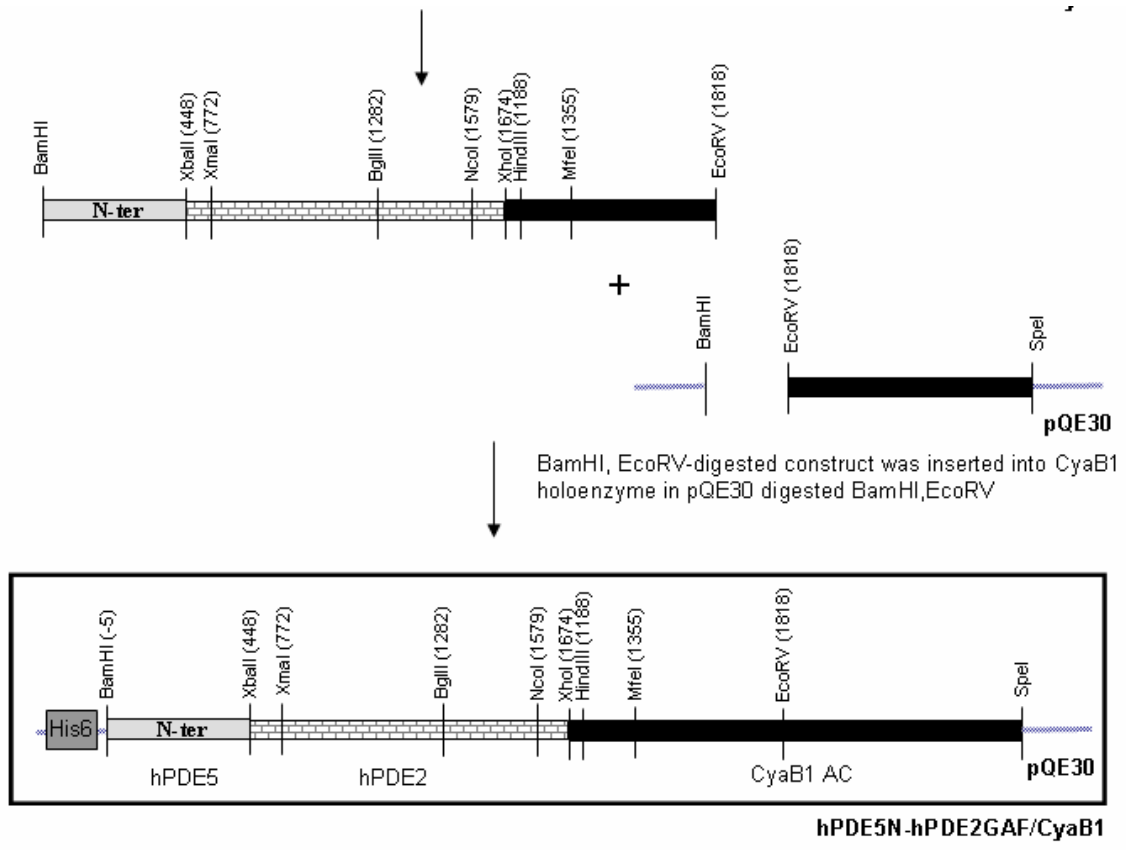




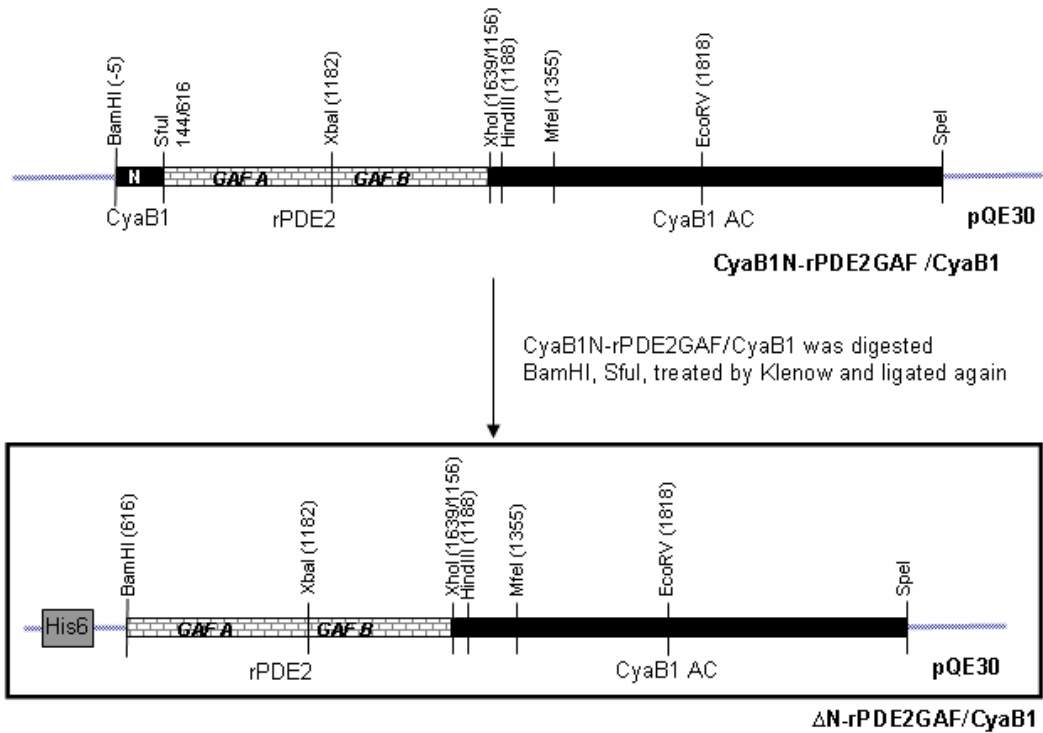
3.4.1.3 Cloning of hpPDE5N-hpPDE2GAF/CyaB1 chimera





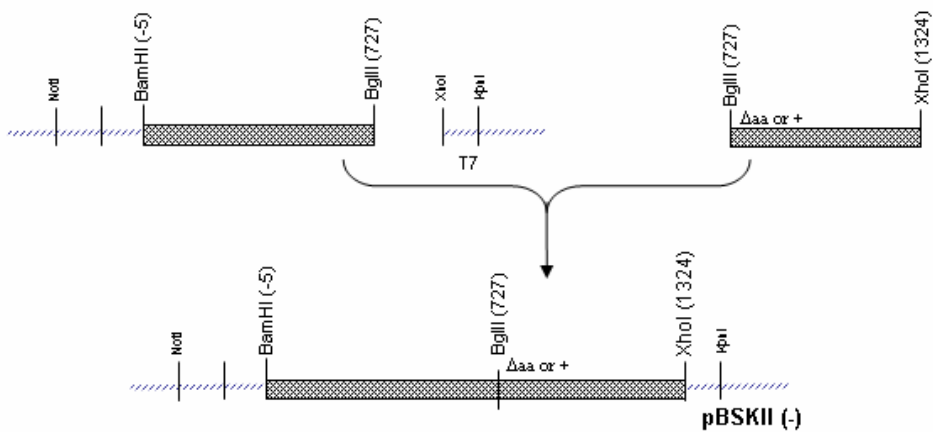
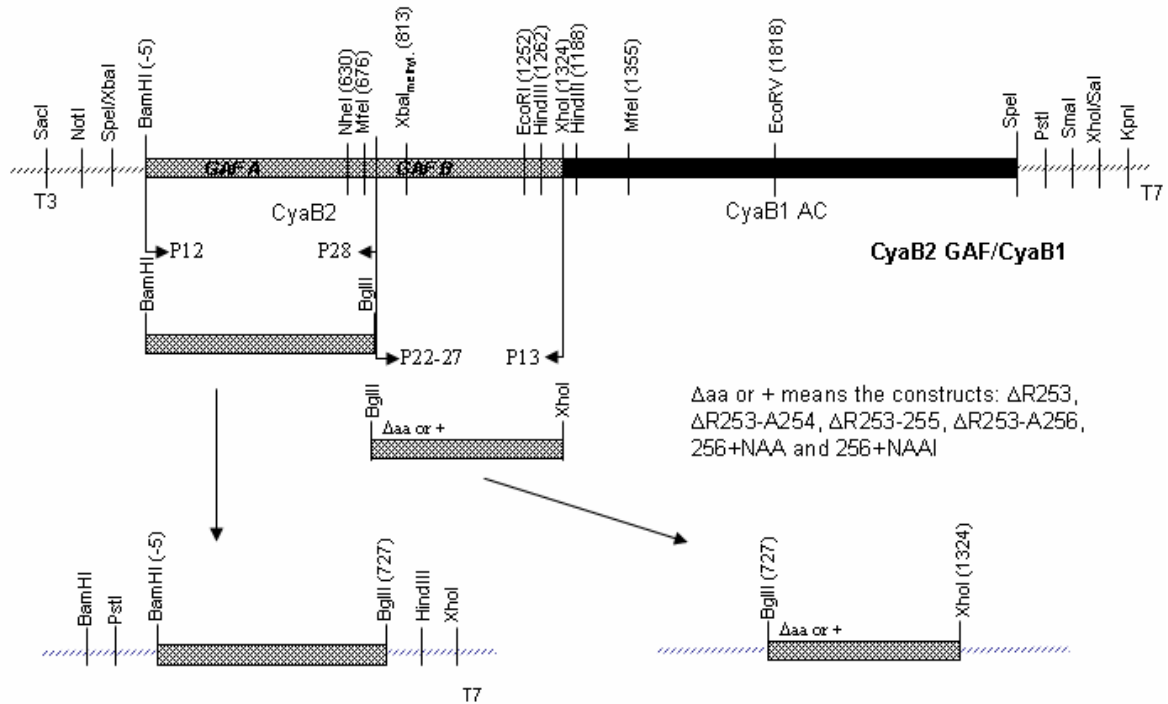


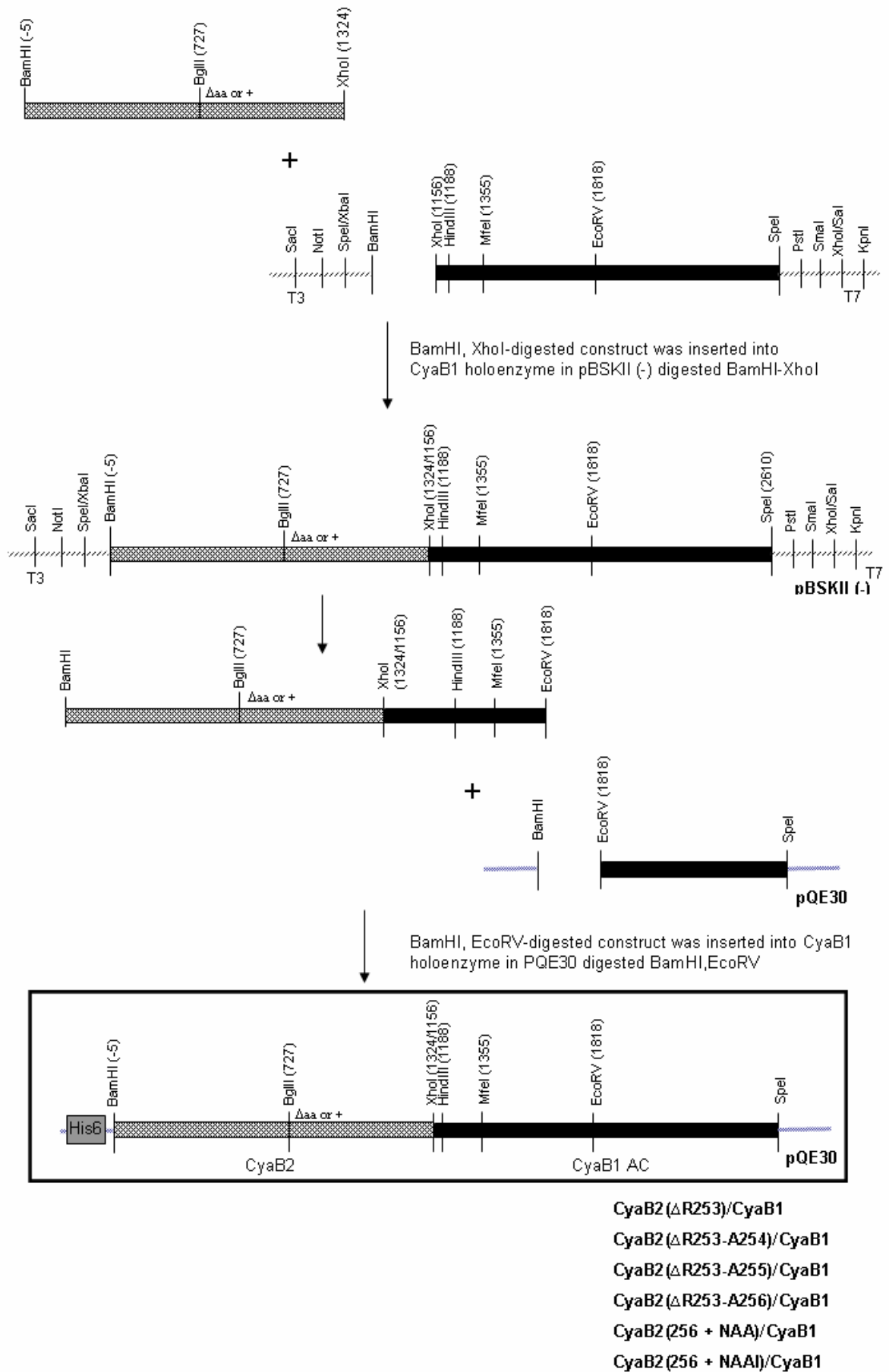
3.4.1.4 Cloning of Δ N-rPDE2GAF/CyaB1



3.4.2 Cloning of CyaB2 constructs and mutants

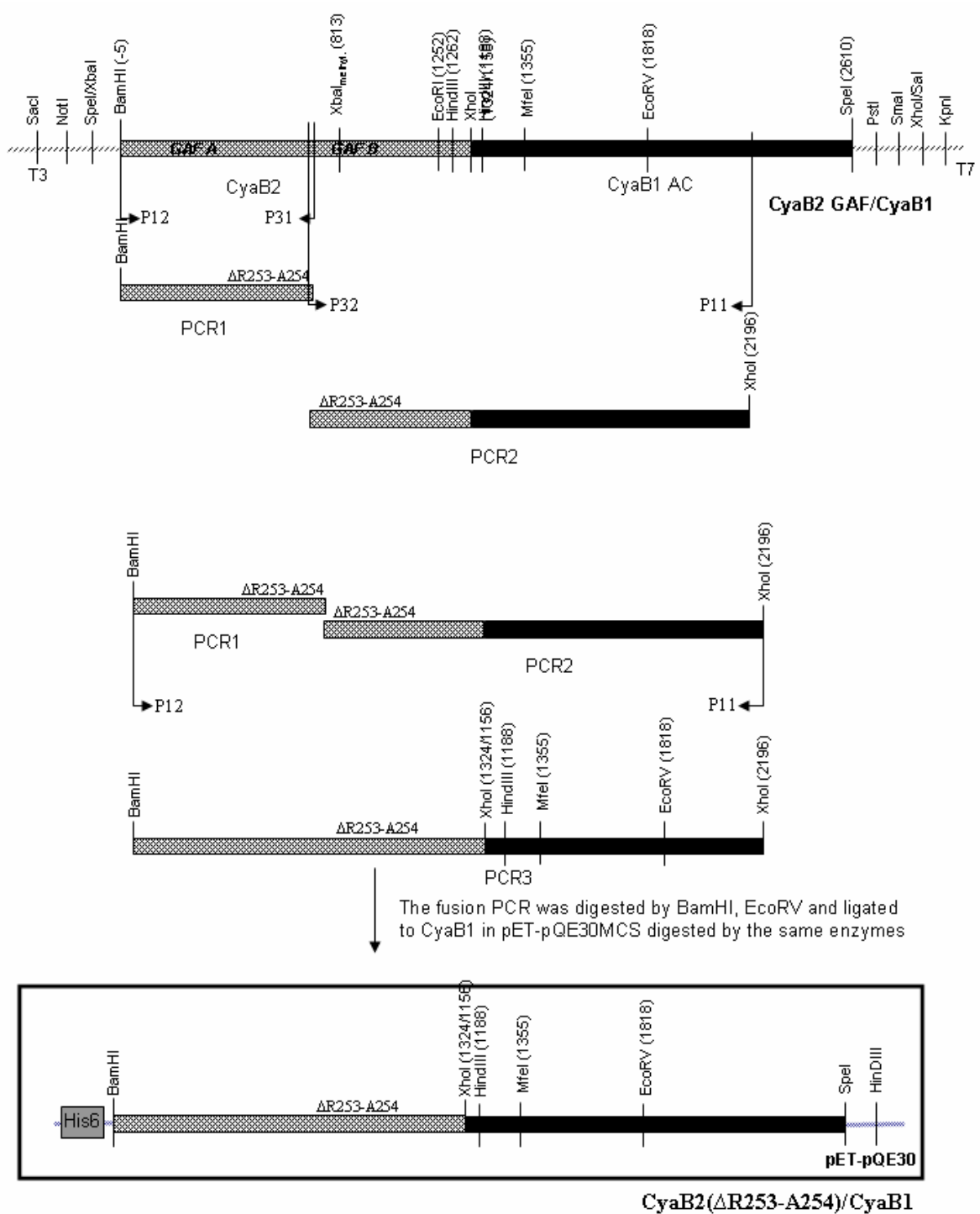
3.4.2.1 Cloning of (Δ aa or + aa)/CyaB1



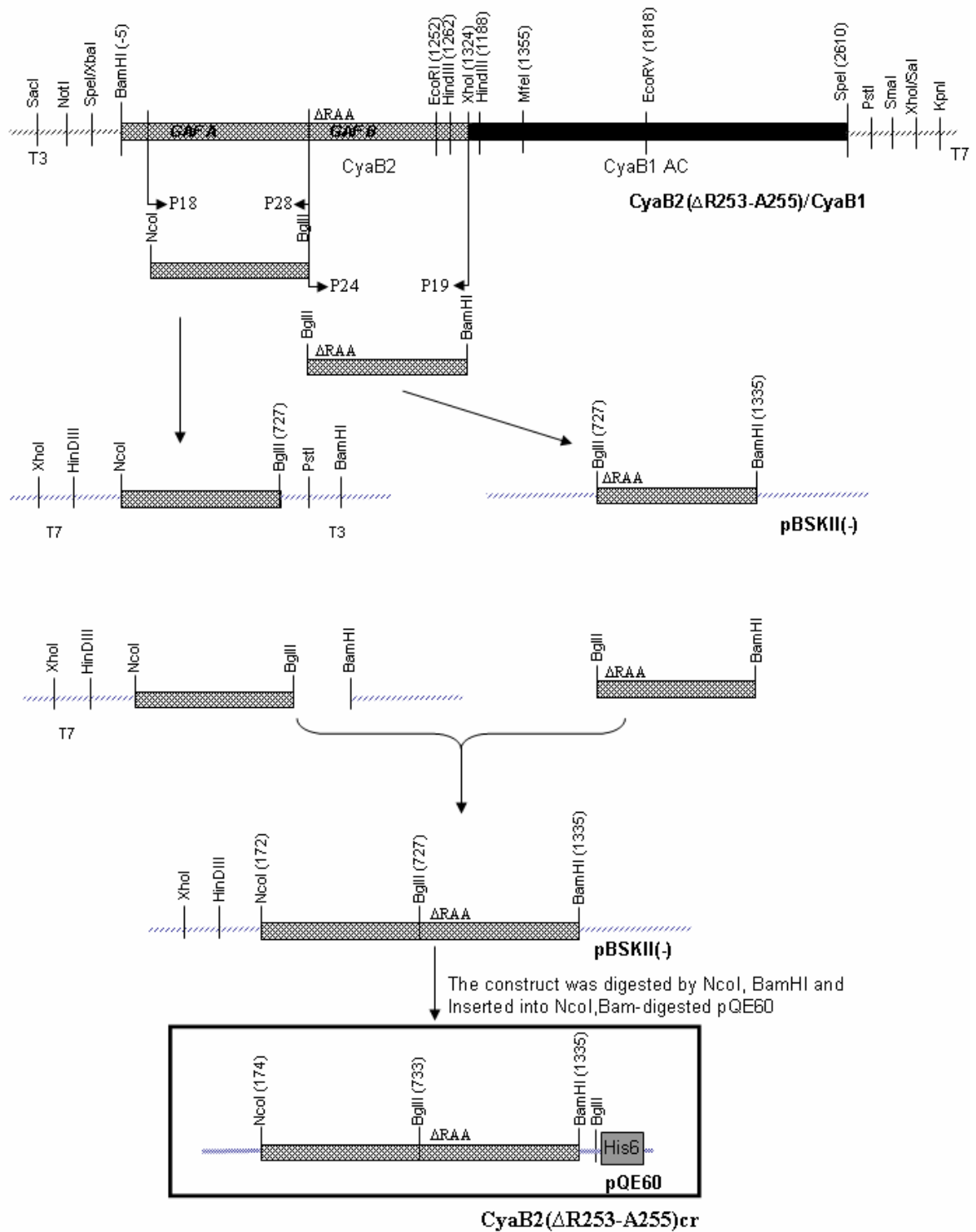


3.4.2.2 Cloning of CyaB2 (Δ R253-A254)/CyaB1

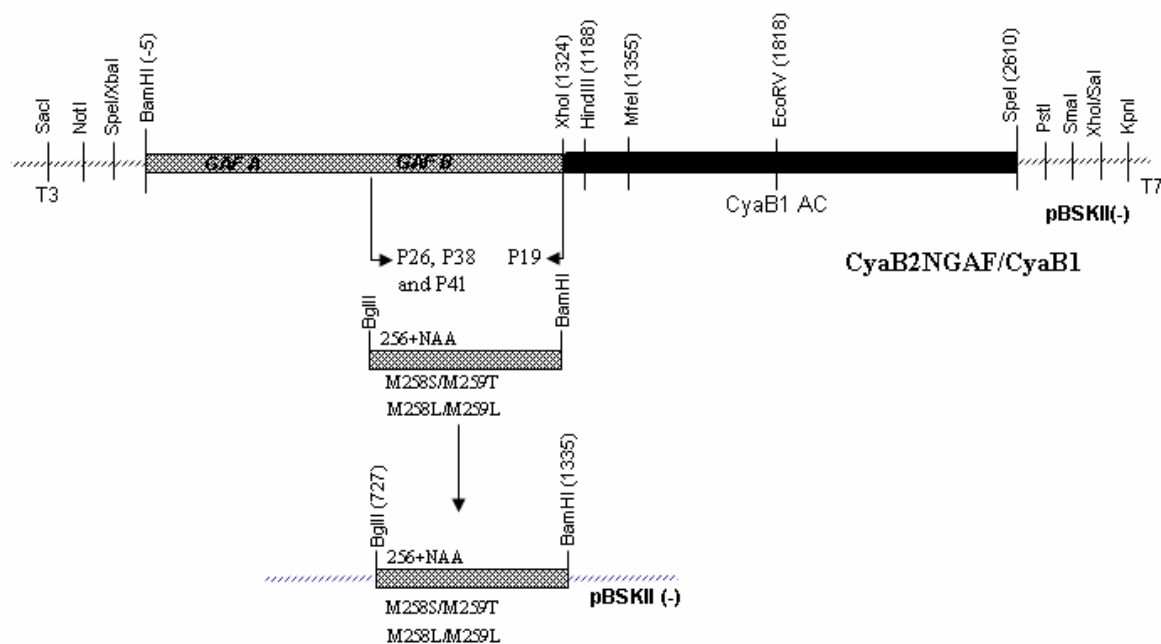
The cloning of this construct was repeated by A.Schultz due to the presence of non-silent mutation in the one prepared above.



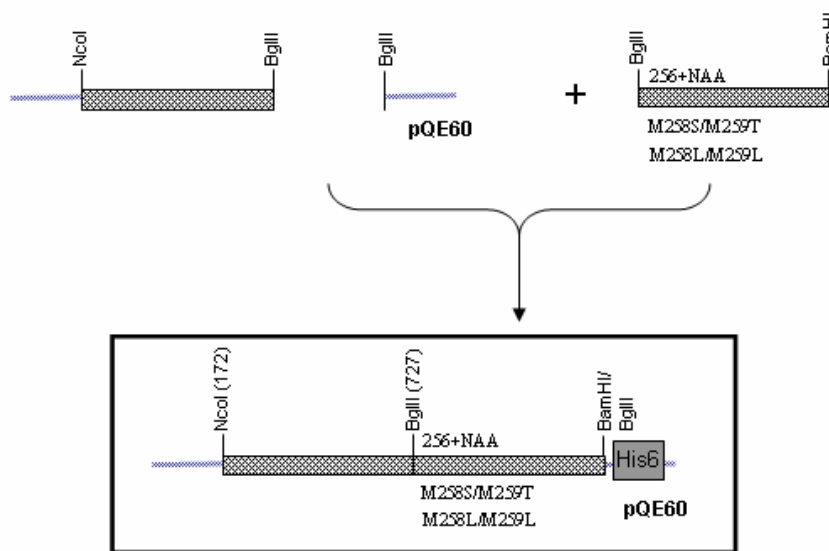
3.4.2.3 Cloning of CyaB2 (Δ R253-A255) GAFcr for crystallization



3.4.2.4 Cloning of CyaB2 (256 + NAA)cr, CyaB2 (M258L/M259L)GAF and CyaB2 (M258S/M259T)GAF

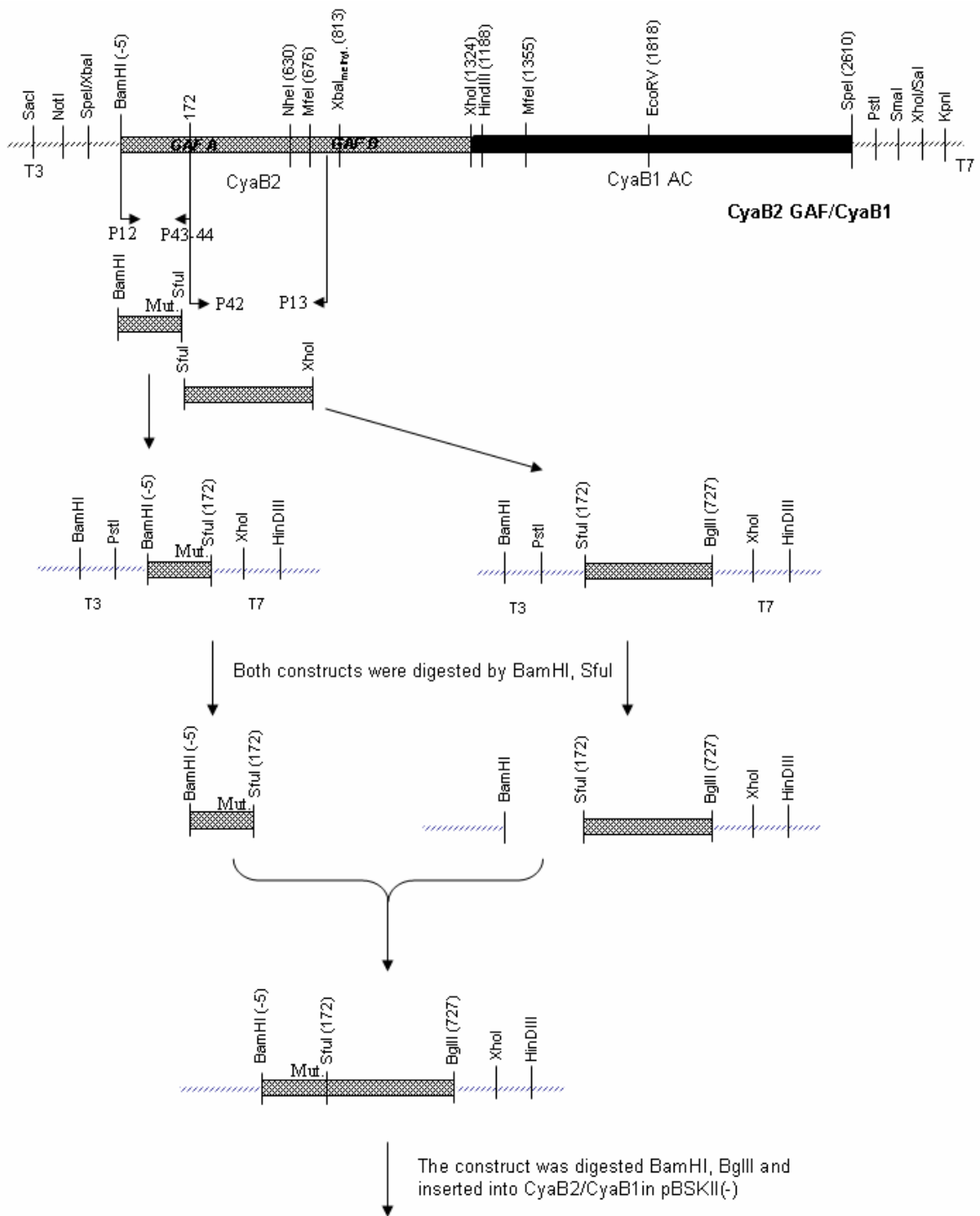


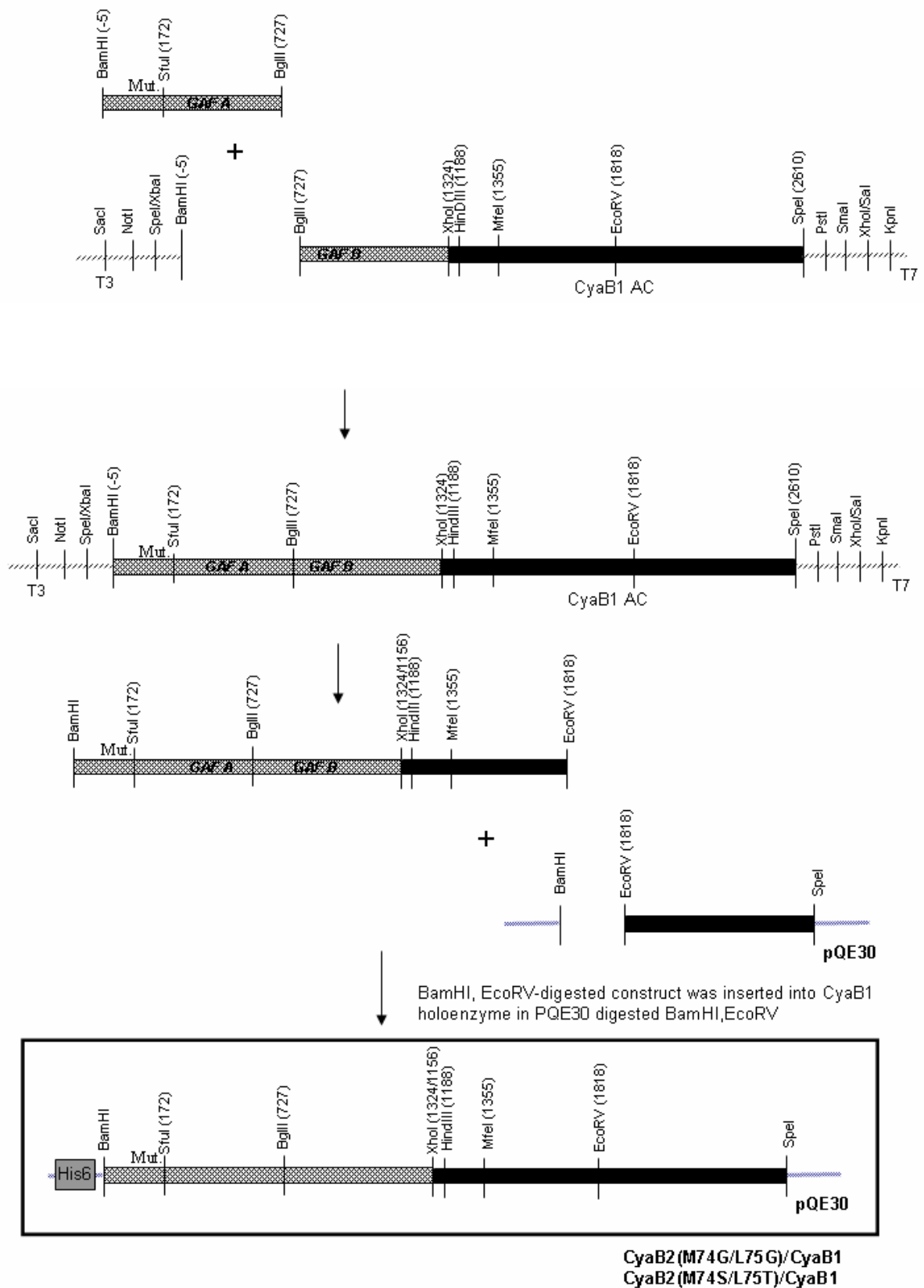
The constructs were digested by BglII, BamHI and inserted into CyaB2(Δ RAA)-pQE60 digested by BglII



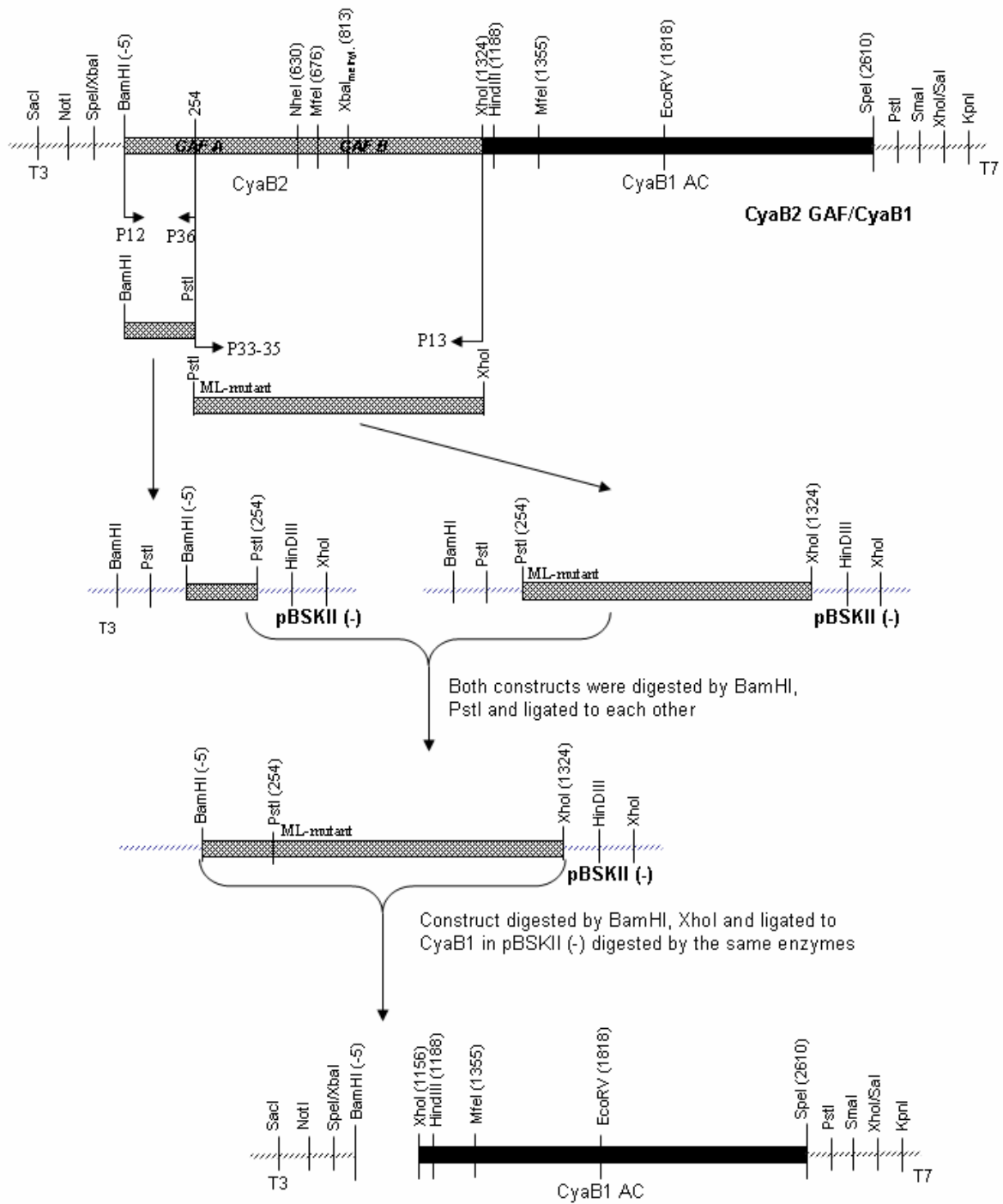
CyaB2(256+ NAA)cr
 CyaB2(M258L/M259L)
 CyaB2(M258S/M259T)

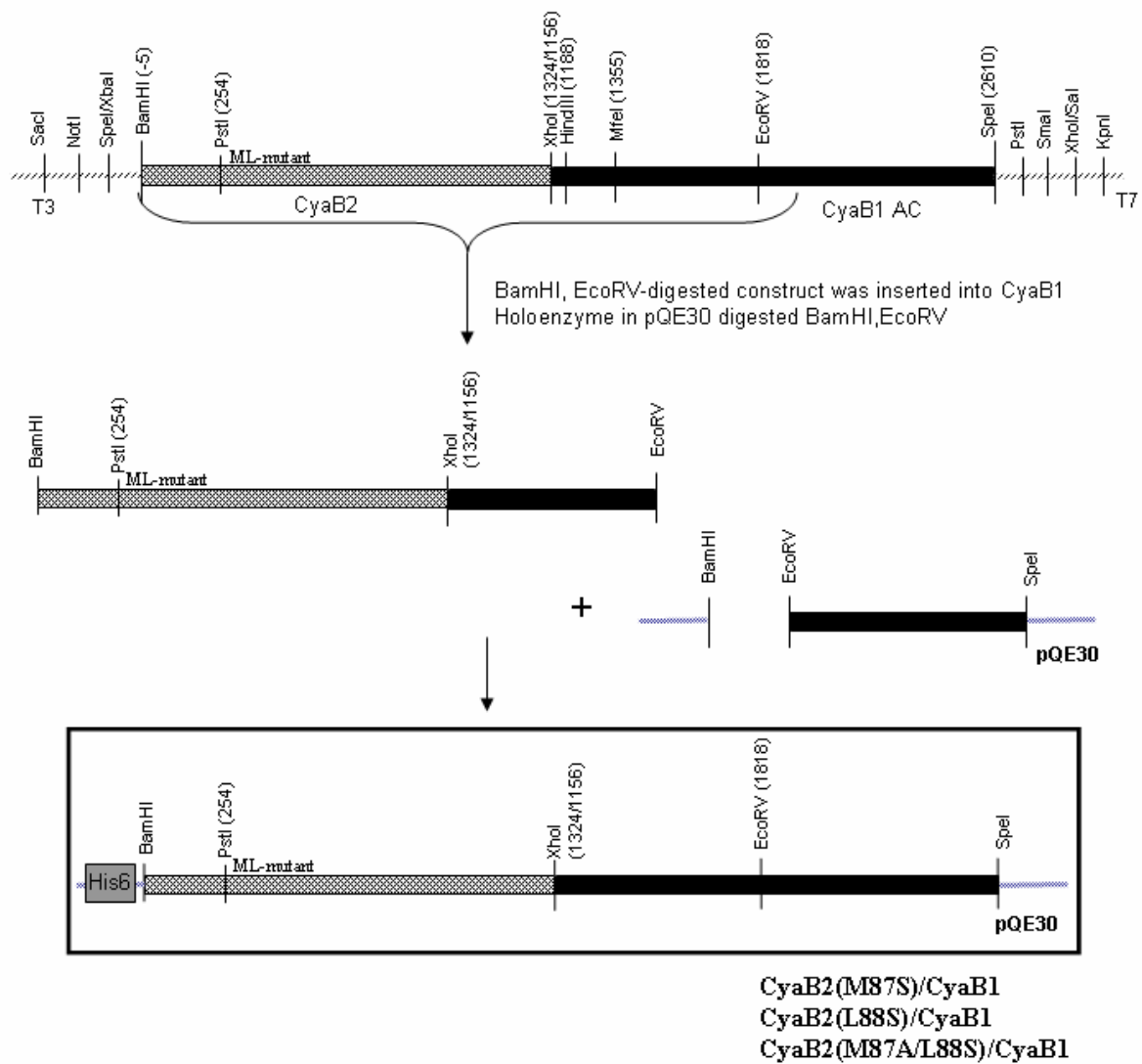
3.4.2.5 Cloning of CyaB2 (M74G/L75G)/CyaB1 and CyaB2 (M74S/L75T)/CyaB1



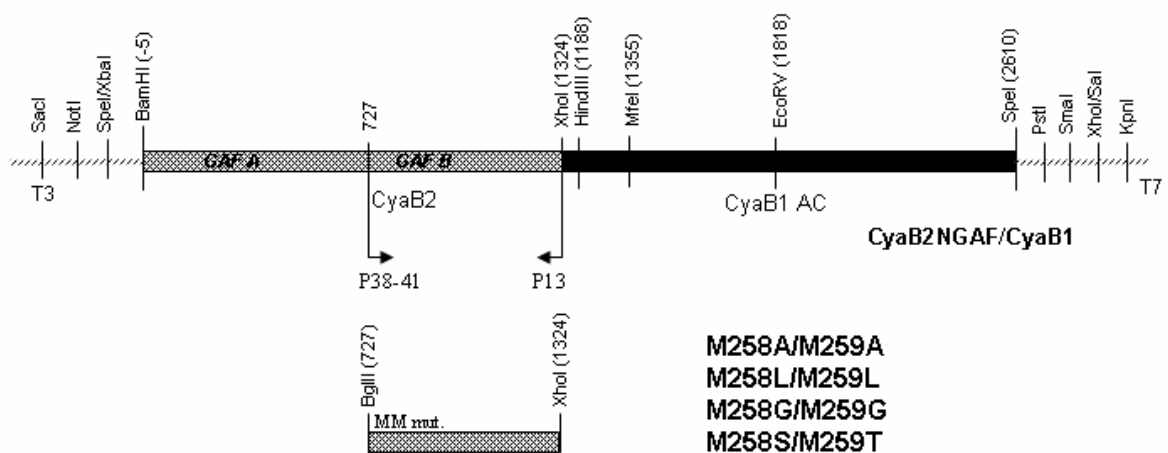


3.4.2.6 Cloning of CyaB2 $\alpha 2$ -mutants (CyaB2 (M87S)/CyaB1, CyaB2 (L88S)/CyaB1 and CyaB2(M87A/L88S)/CyaB1)





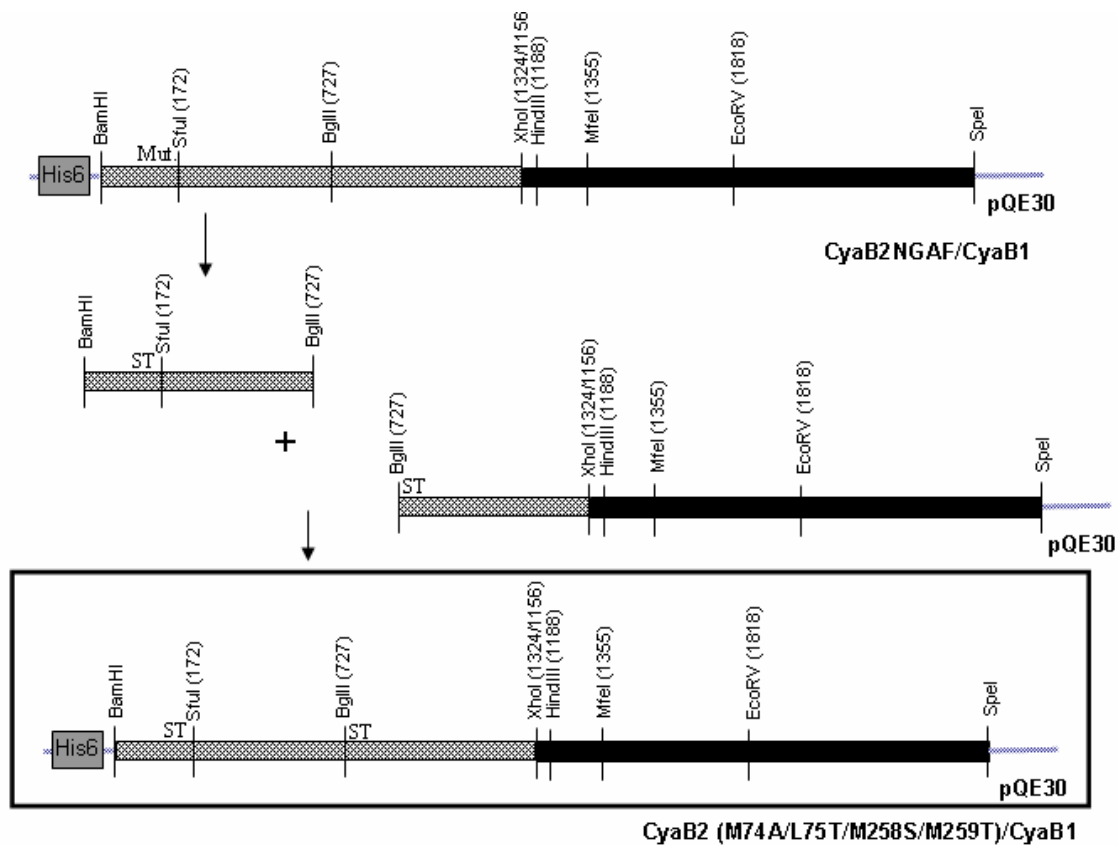
3.4.2.7 Cloning of CyaB2 connecting helix-mutants (CyaB2 (M258A/M259A)/CyaB1, CyaB2 (M258L/M259L)/CyaB1, CyaB2 (M258G/M259G)/CyaB1 and CyaB2 (M258S/M259T)/CyaB1



Methods

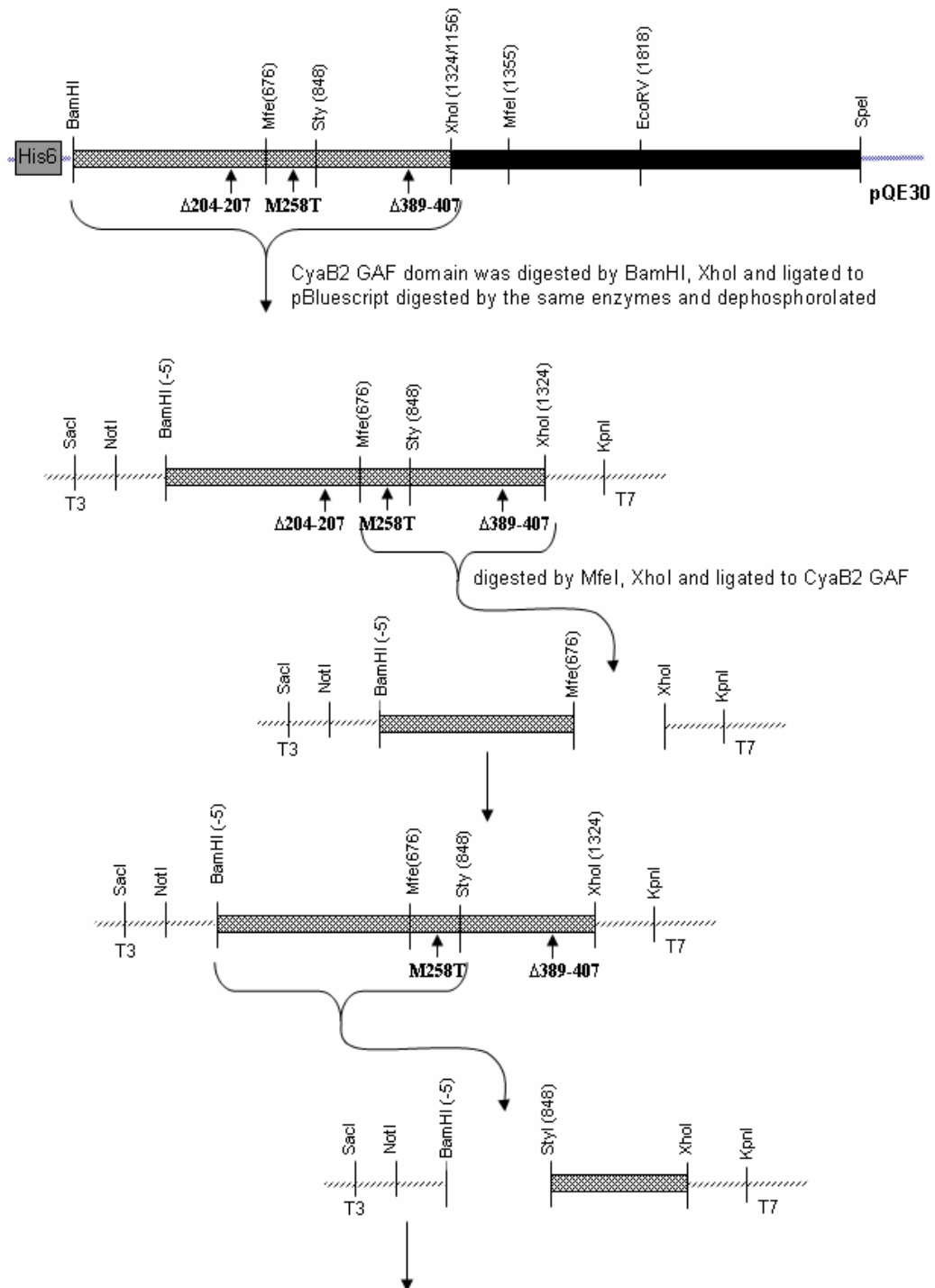
The procedure was continued according to the same way of the shortened and elongated mutants in section 3.4.2.1

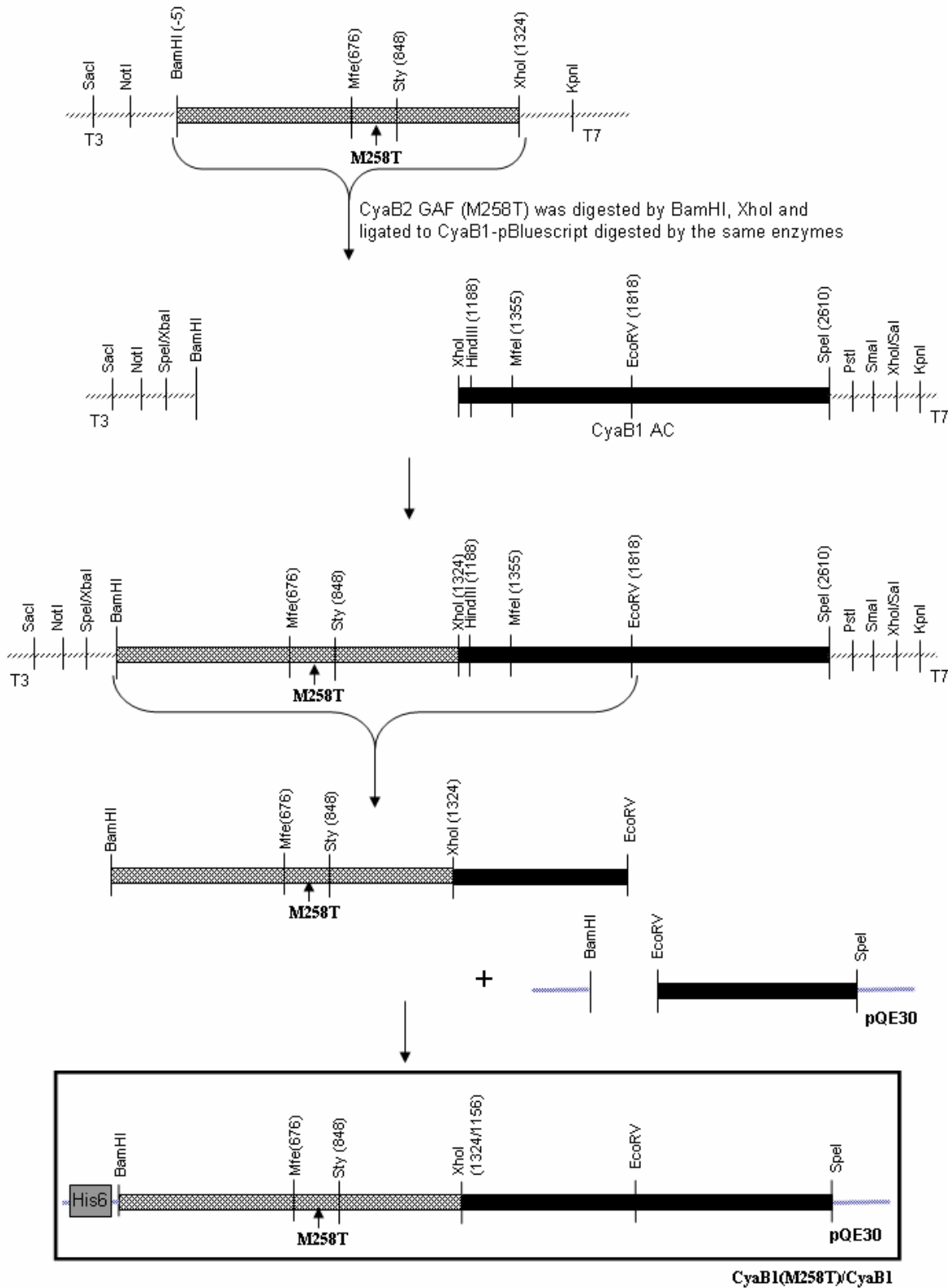
3.4.2.8 Cloning of CyaB2 (M74S/L75T/M258S/M259T)/CyaB1



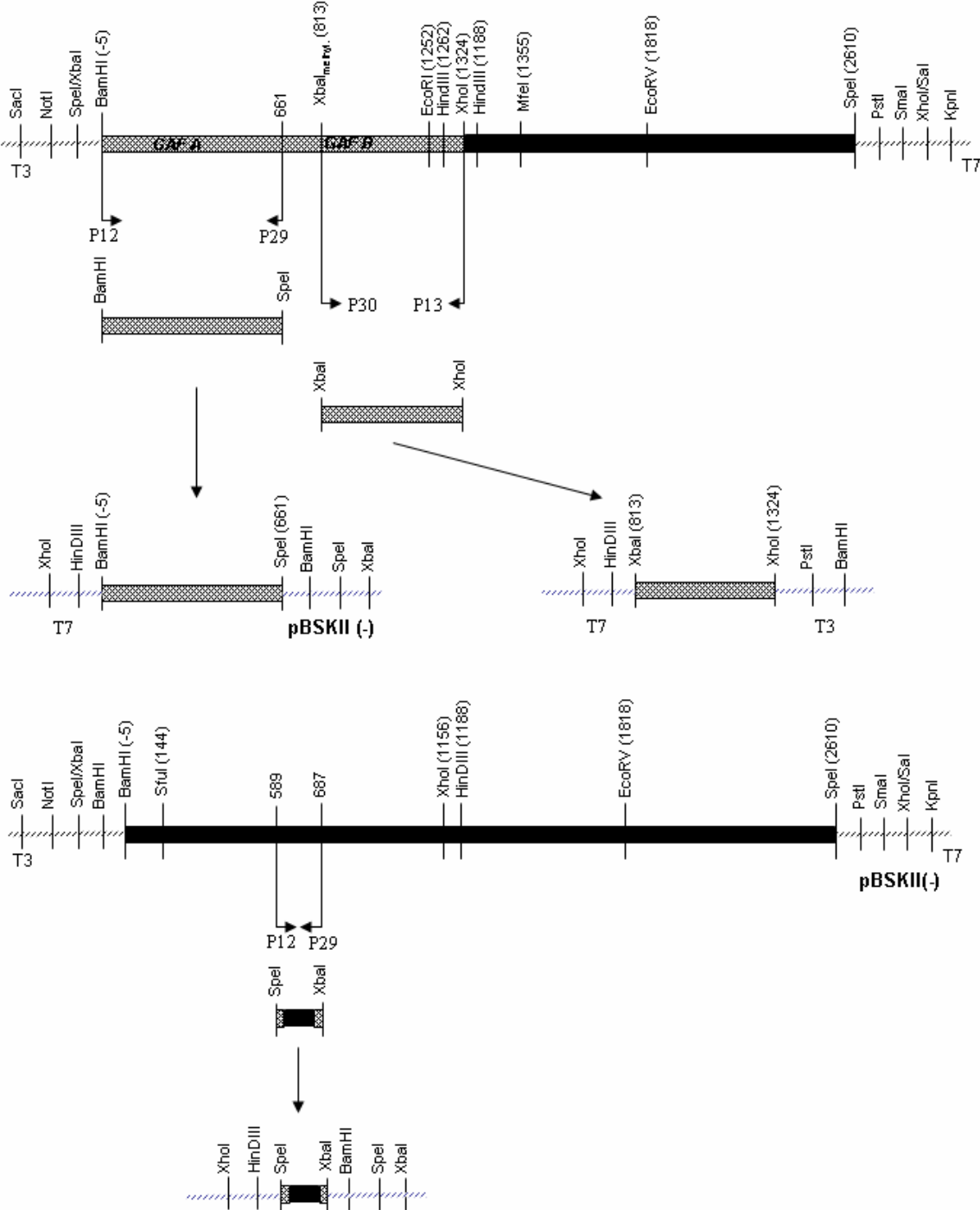
3.4.2.9 Cloning of CyaB2 (M258T)/CyaB1

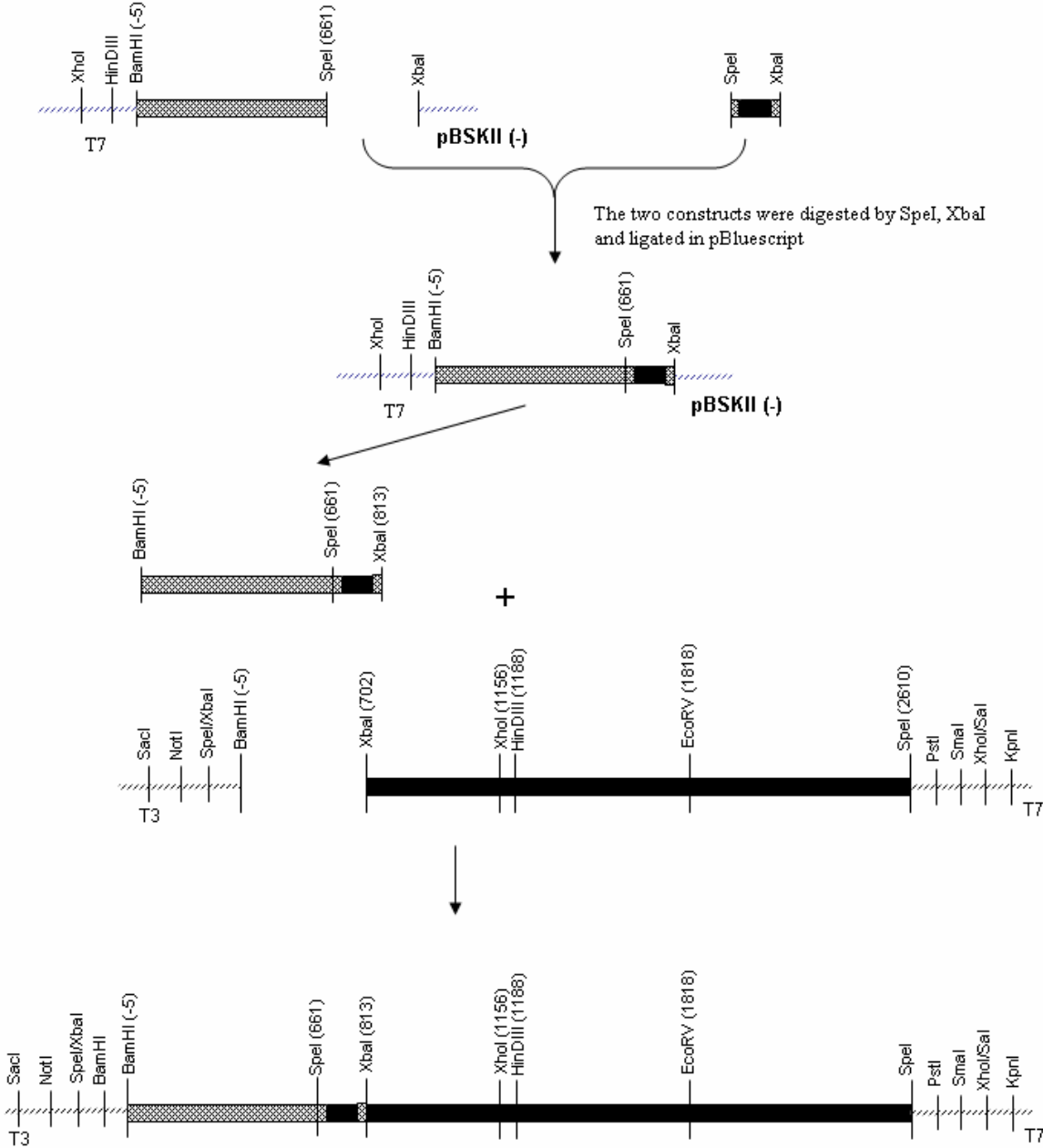
The original construct was obtained from A.Schultz and was modified to obtain a single mutation

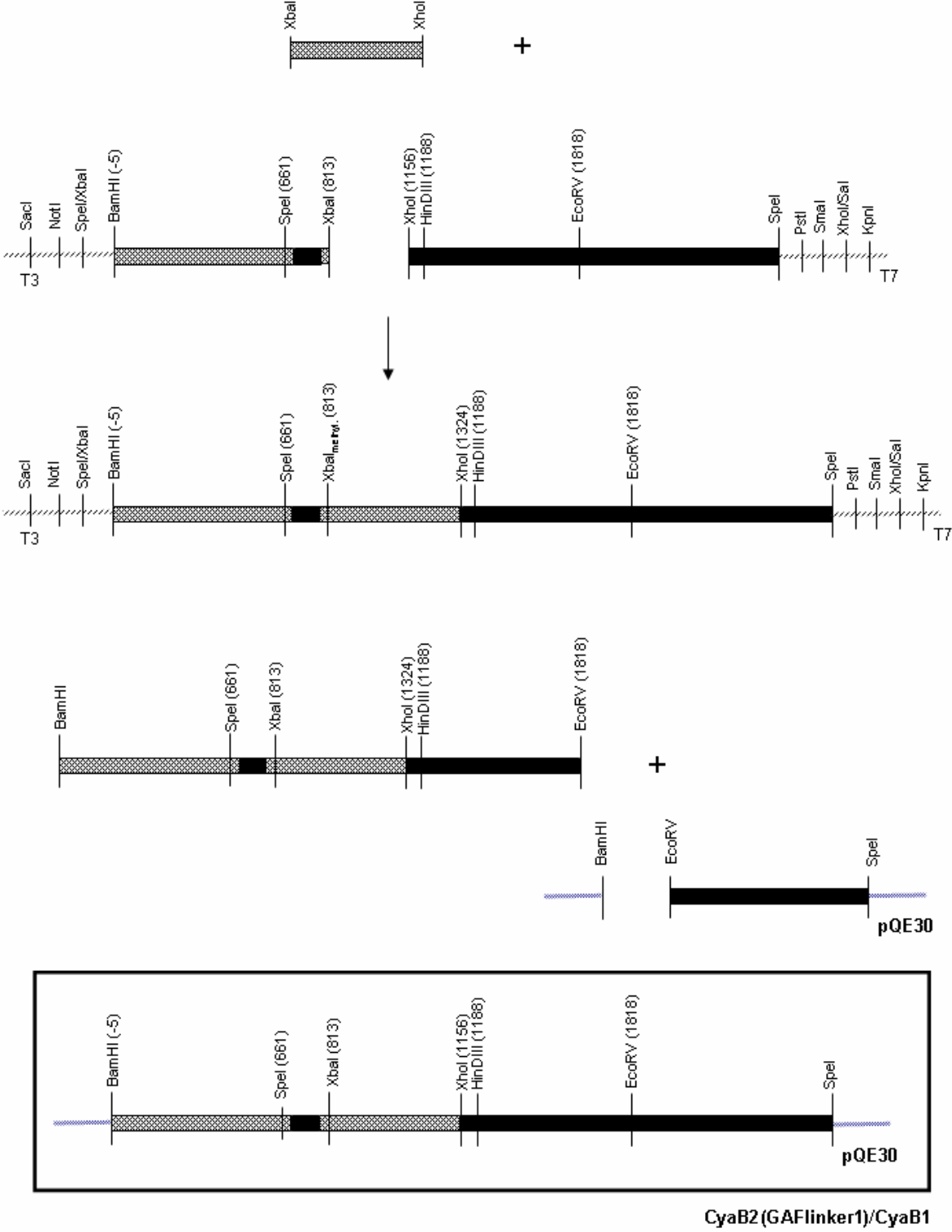




3.4.2.10 Cloning of CyaB2 (GAFlinker1)/CyaB1

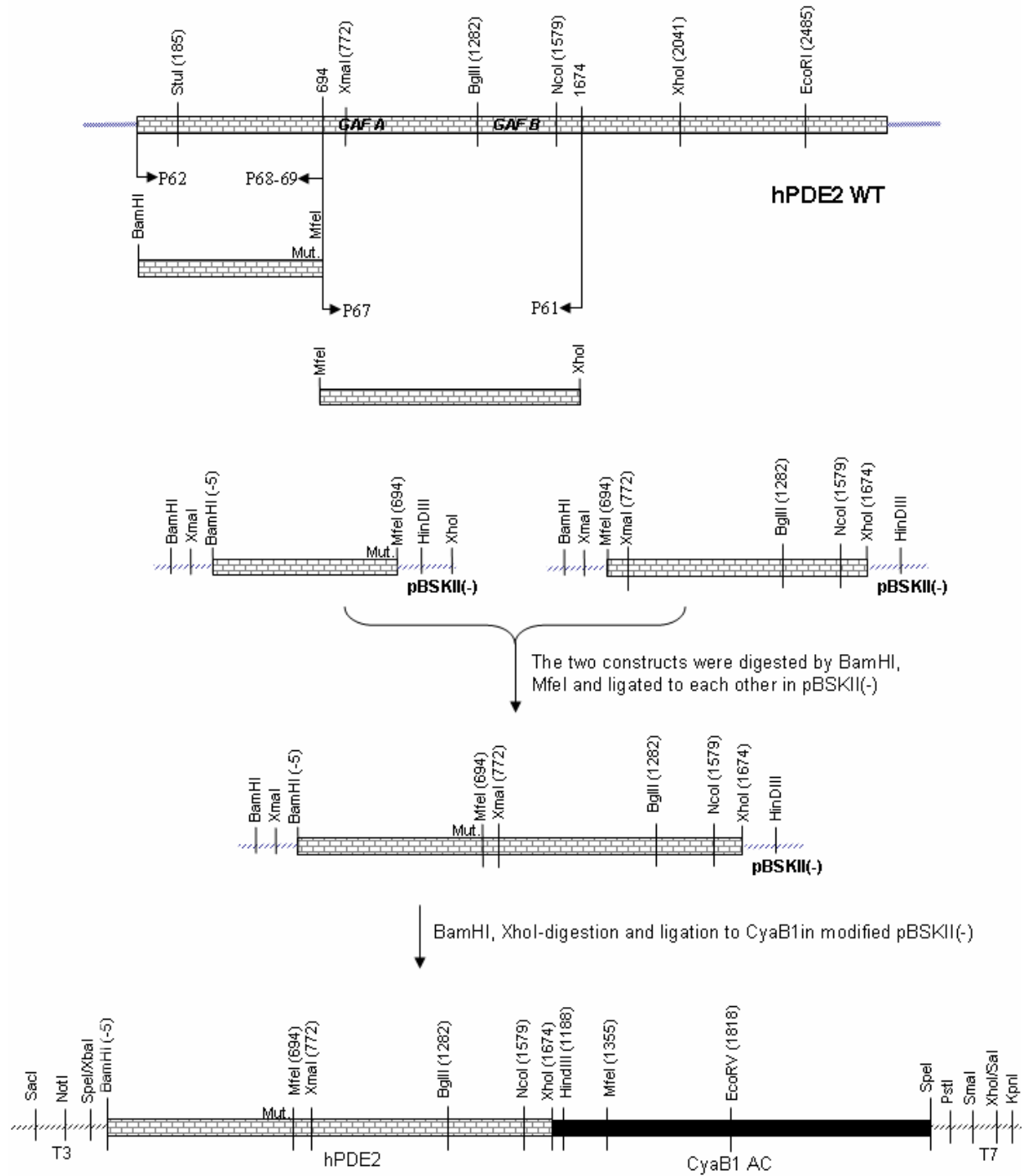




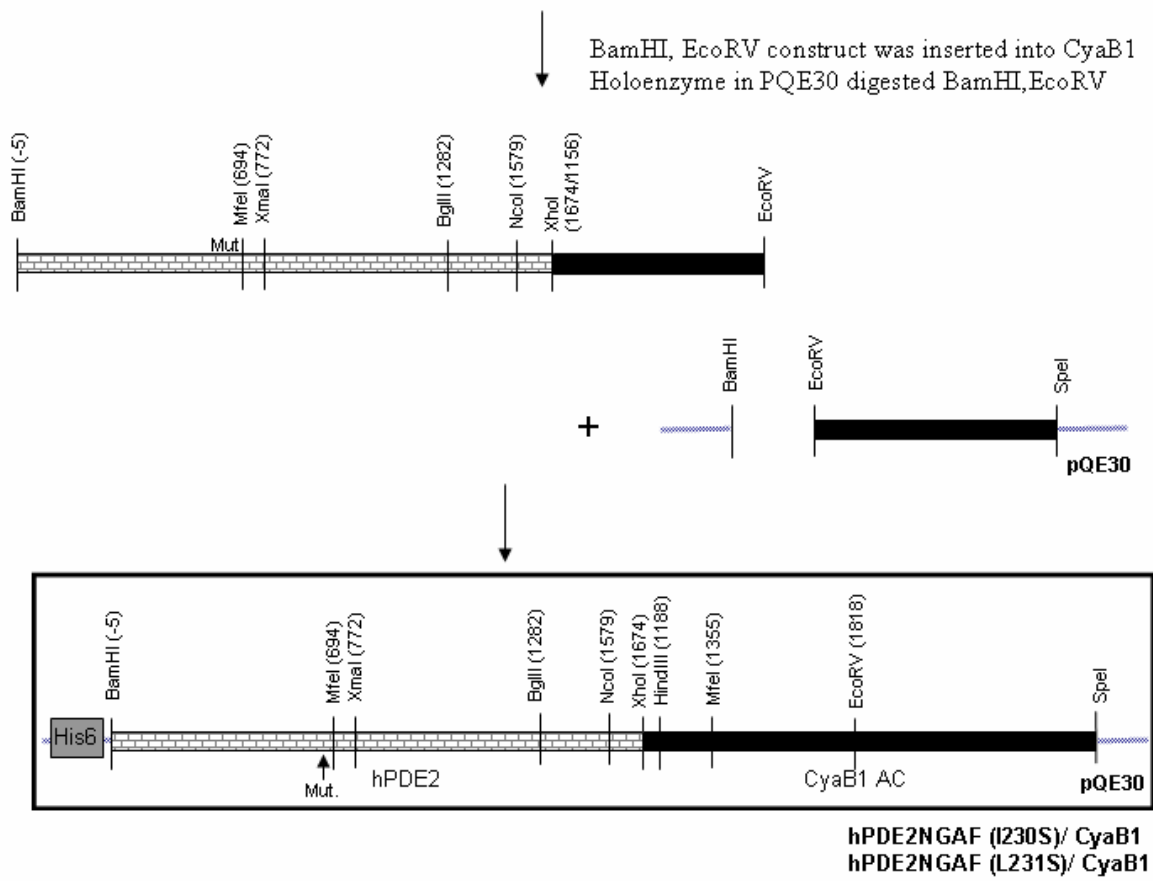


3.4.3 Cloning of hPDE2 mutants

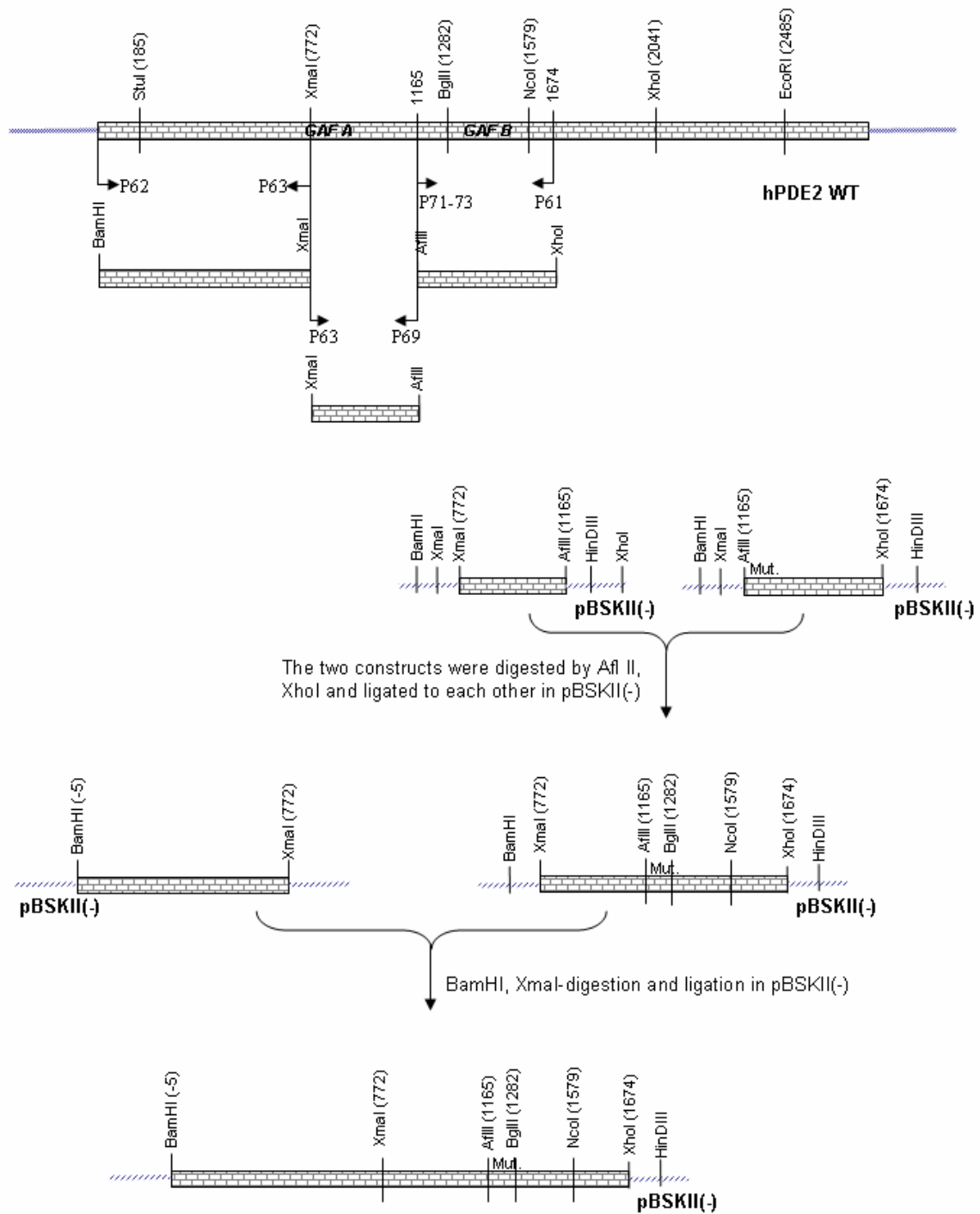
3.4.3.1 Cloning of hPDE2NGAF/CyaB1 α 1-helix mutants

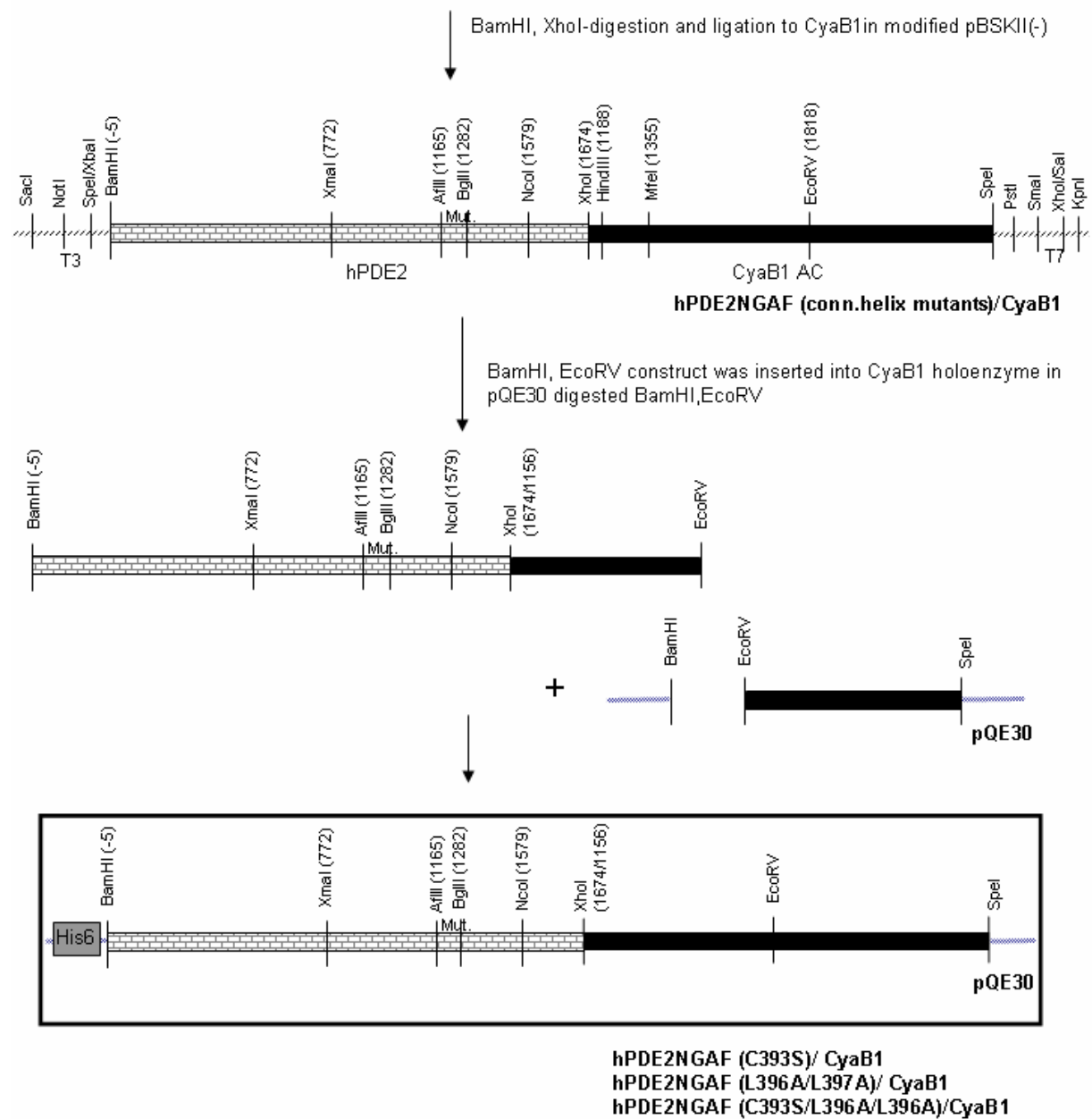


Methods



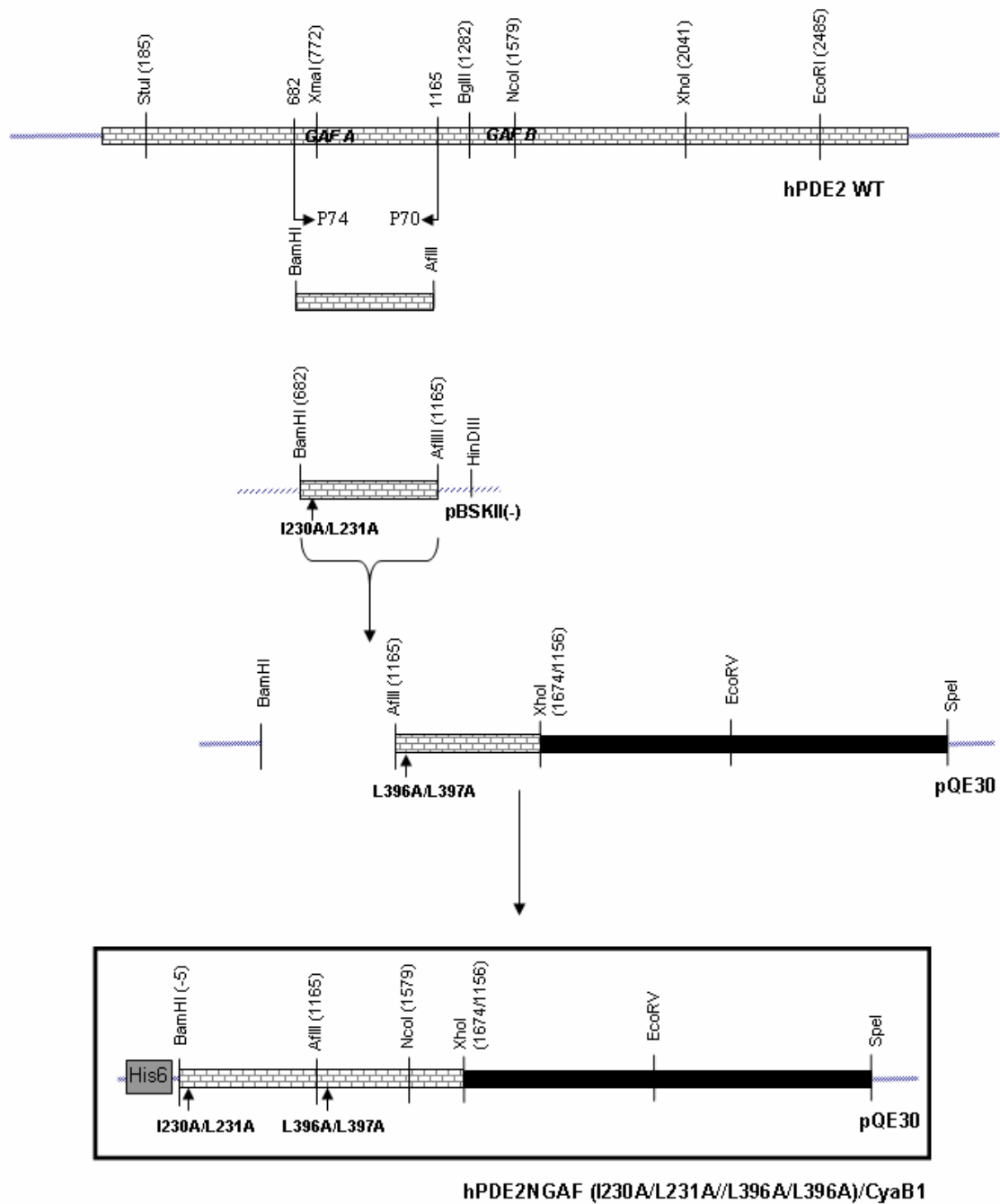
3.4.3.2 Cloning of hPDE2NGAF/CyaB1 –connecting helix mutants



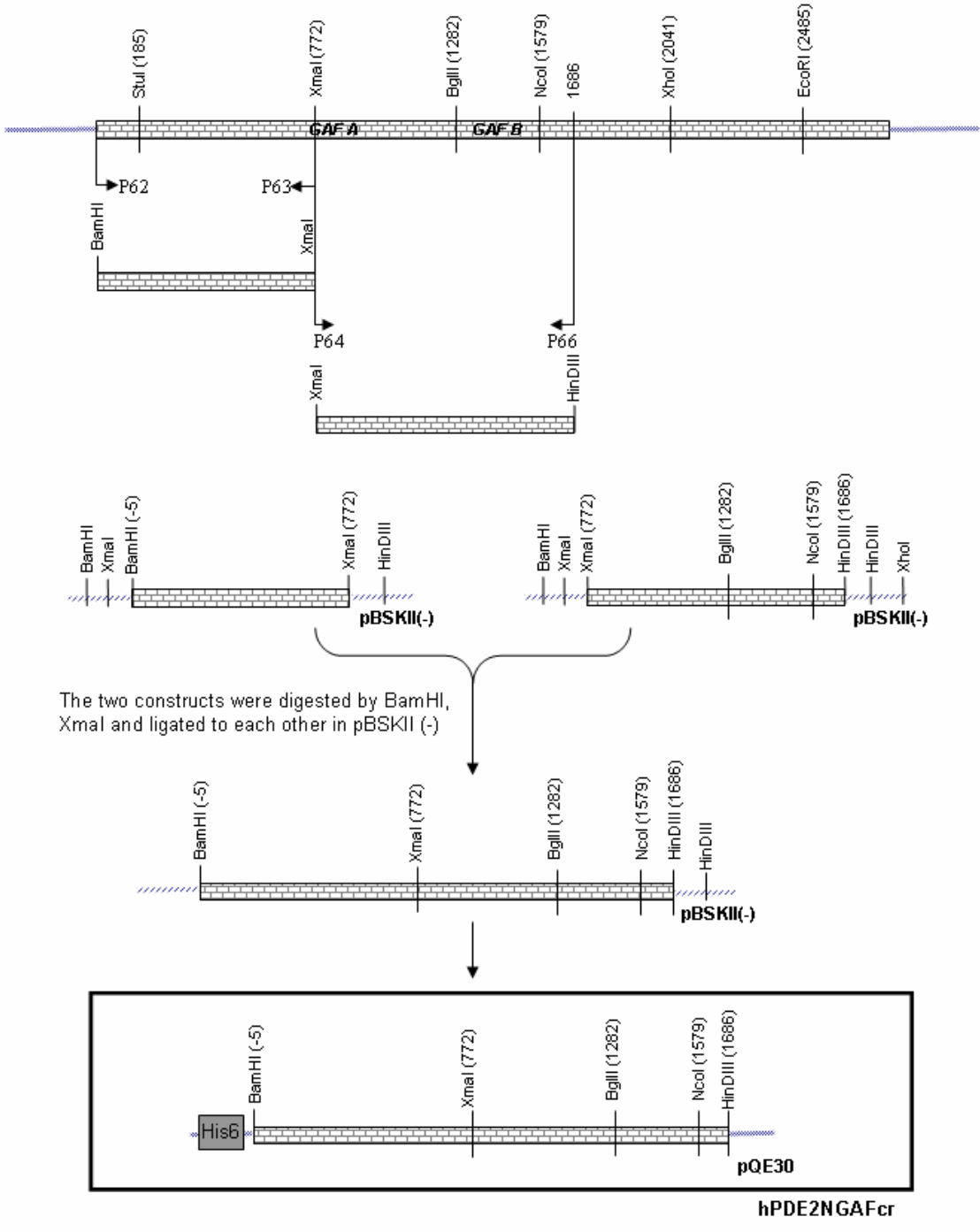


3.4.3.3 Cloning of the quadruple mutant of hPDE2GAF/CyaB1

Δ N-hPDE2GAF(I230A/L231A/L396A/L397A)/CyaB1

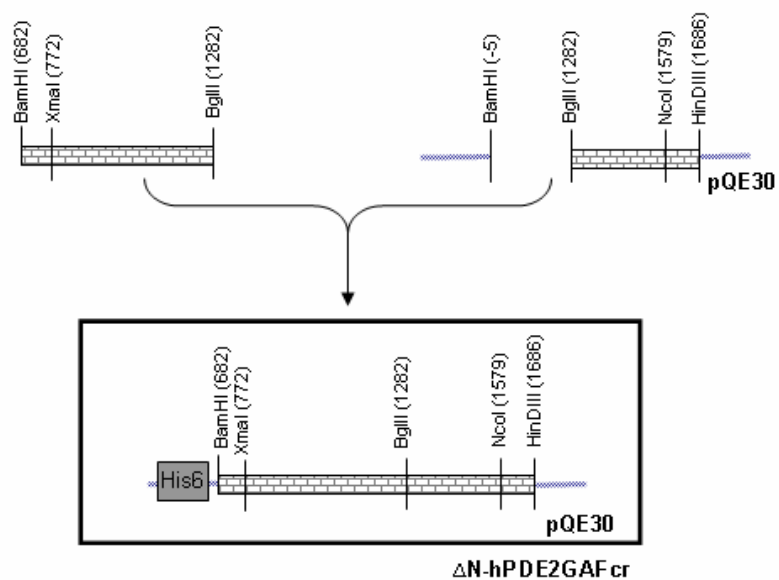


3.4.3.4 Cloning of hPDE2NGAFcr

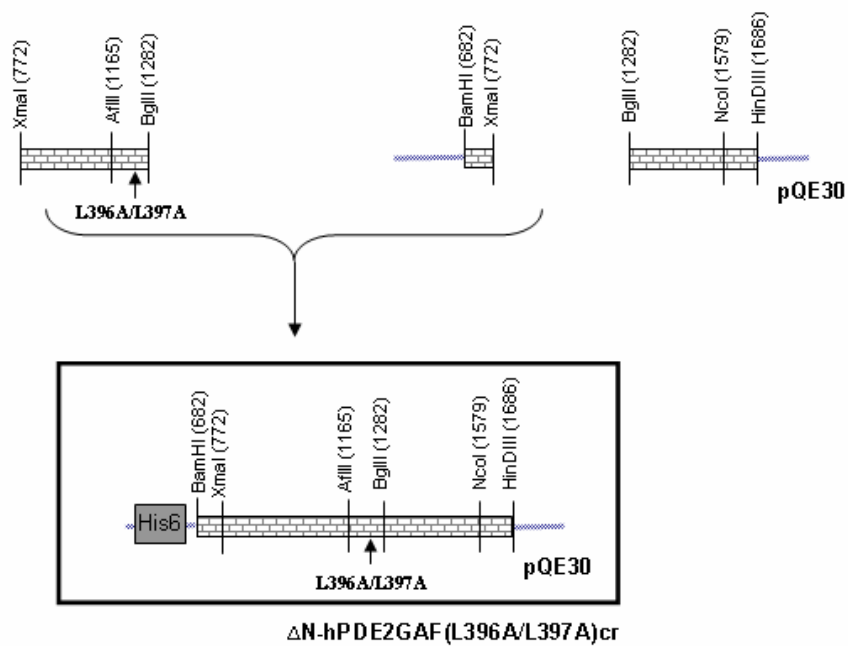


3.4.3.5 Cloning of Δ N-hPDE2GAFcr

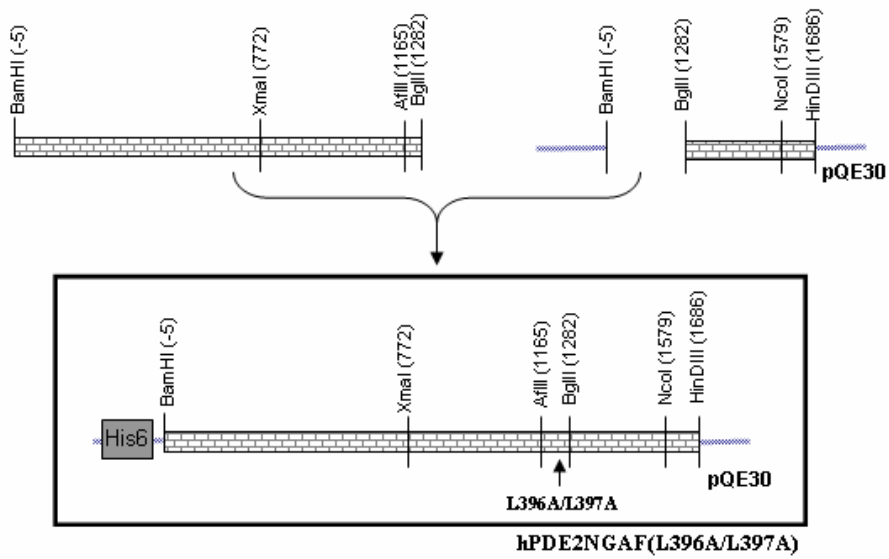
The first segment of Δ N-hPDE2GAF/CyaB1, digested by BamHI, Bgl II and ligated to each other in pQE30



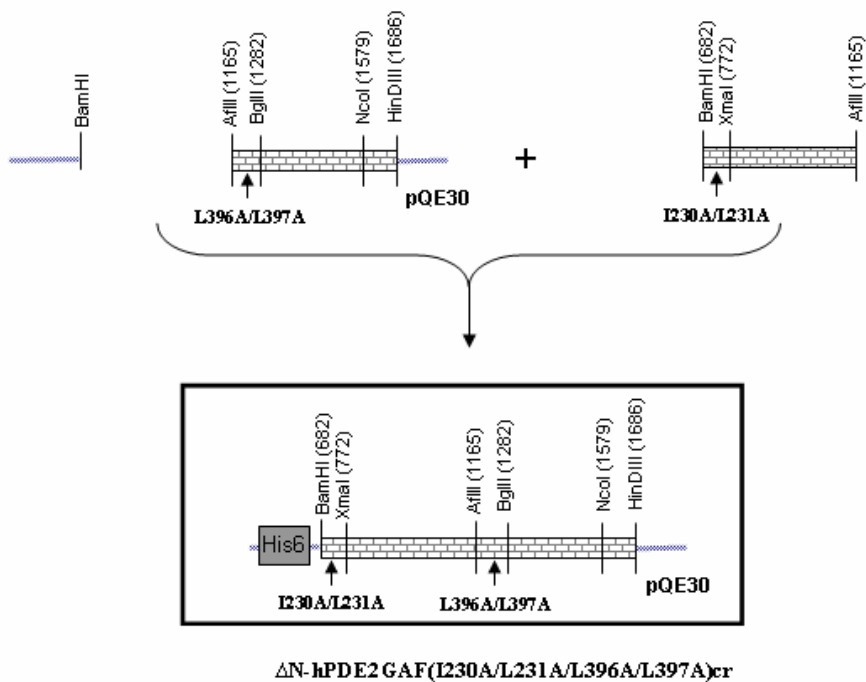
3.4.3.6 Cloning of Δ N-hPDE2GAF (L396A/L397A)cr



3.4.3.7 Cloning of hPDE2NGAF (L396A/L397A)cr

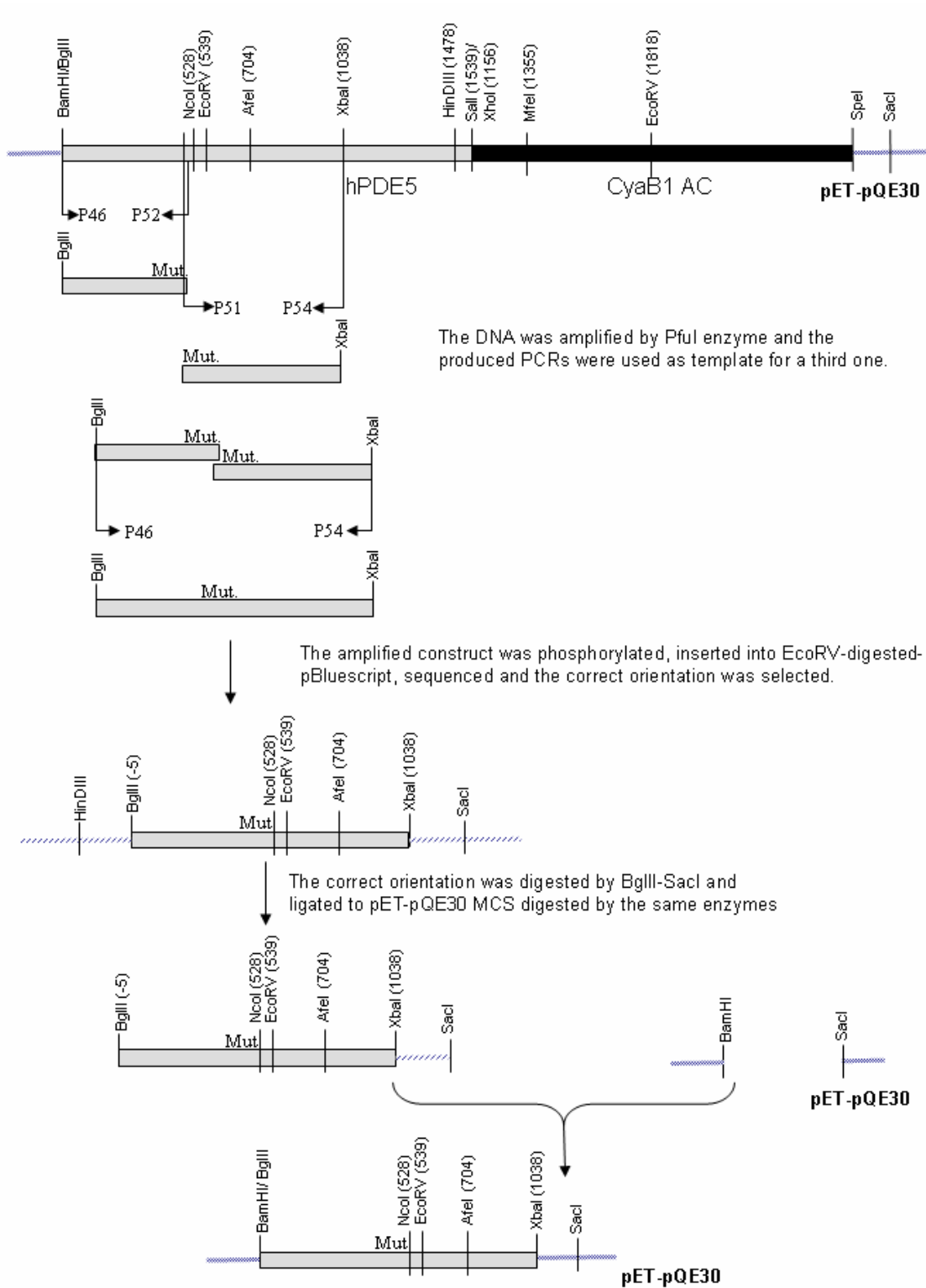


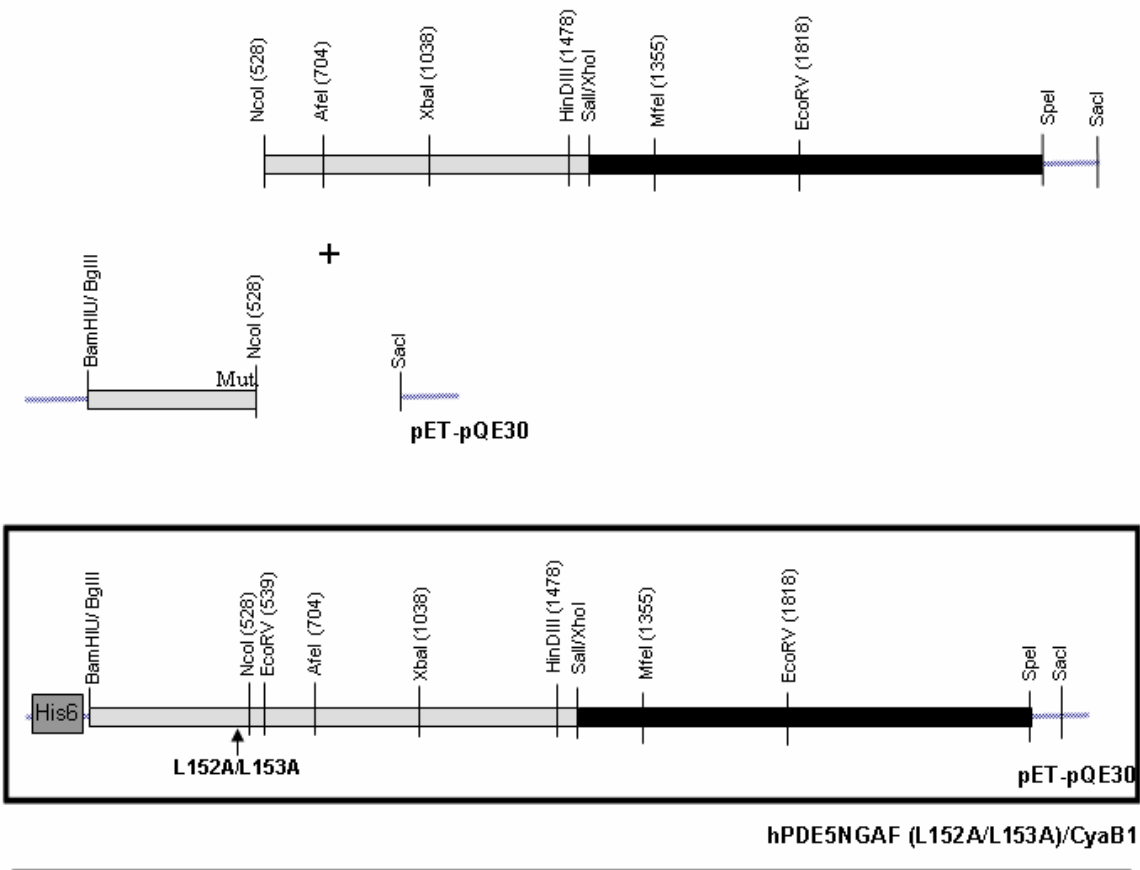
3.4.3.8 Cloning of ΔN-hPDE2GAF (I230A/L231A/L396A/L397A)cr



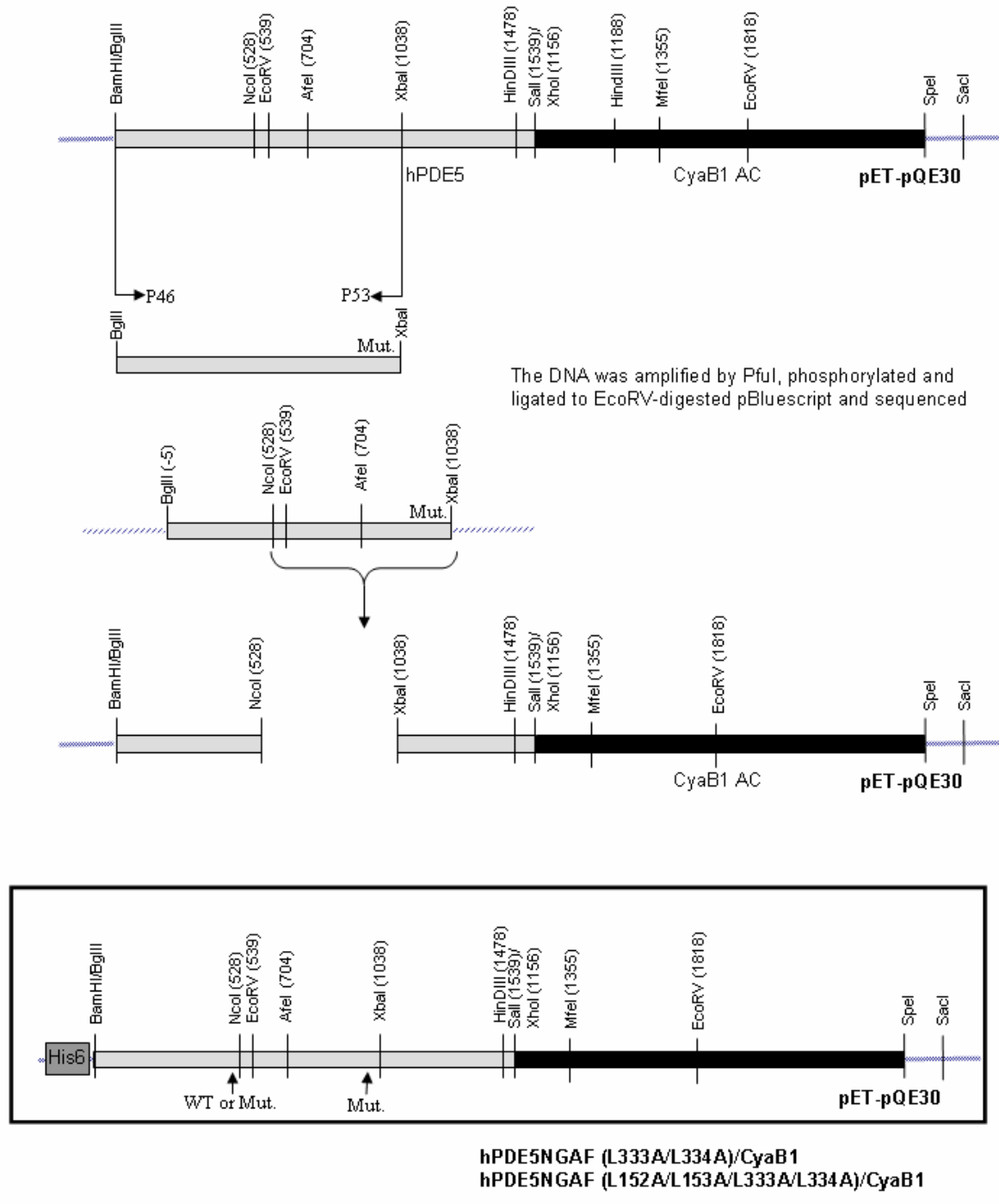
3.4.4 Cloning of hPDE5 mutants

3.4.4.1 Cloning of hPDE5NGAF (L152A/L153A)/CyaB1

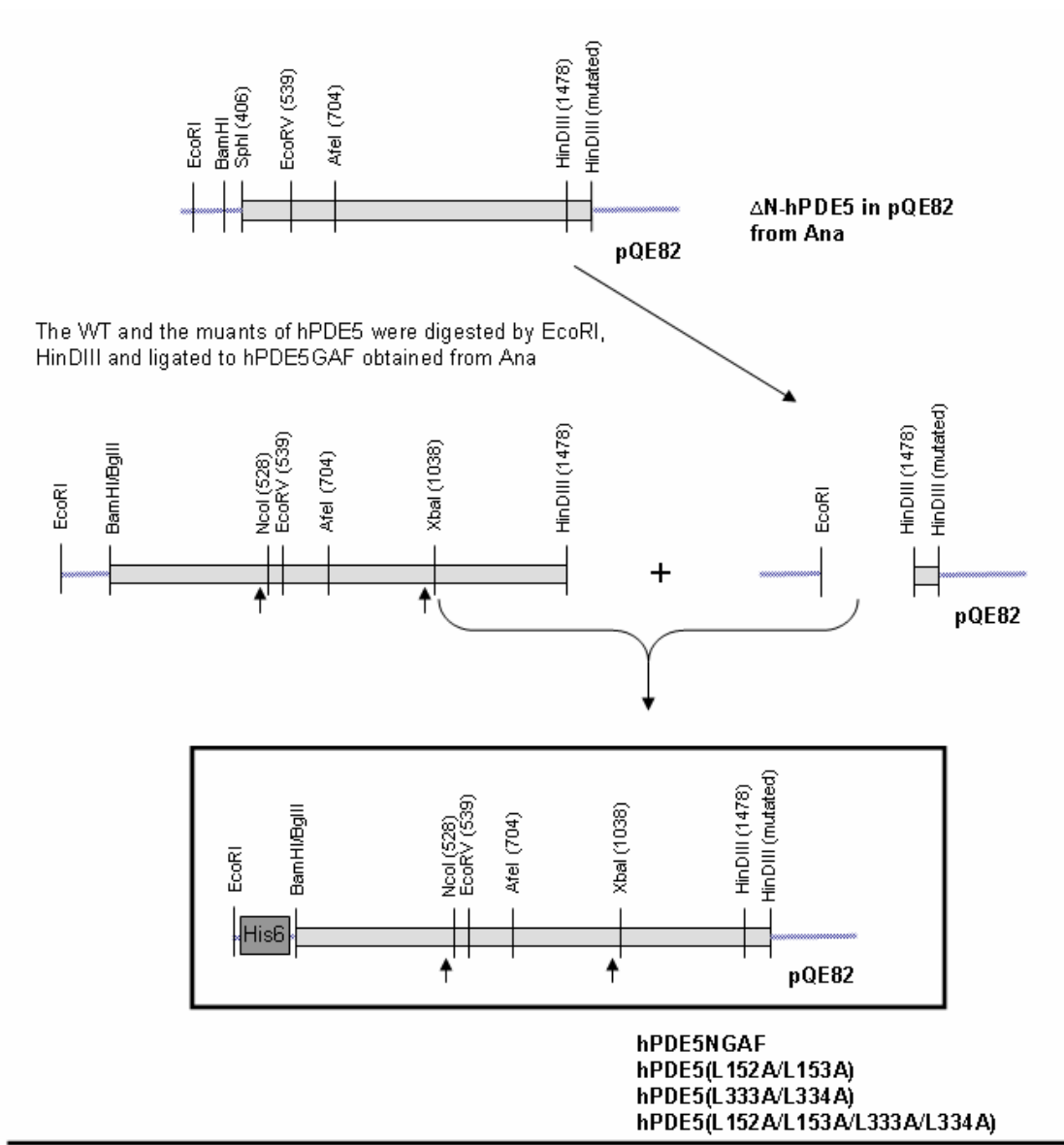




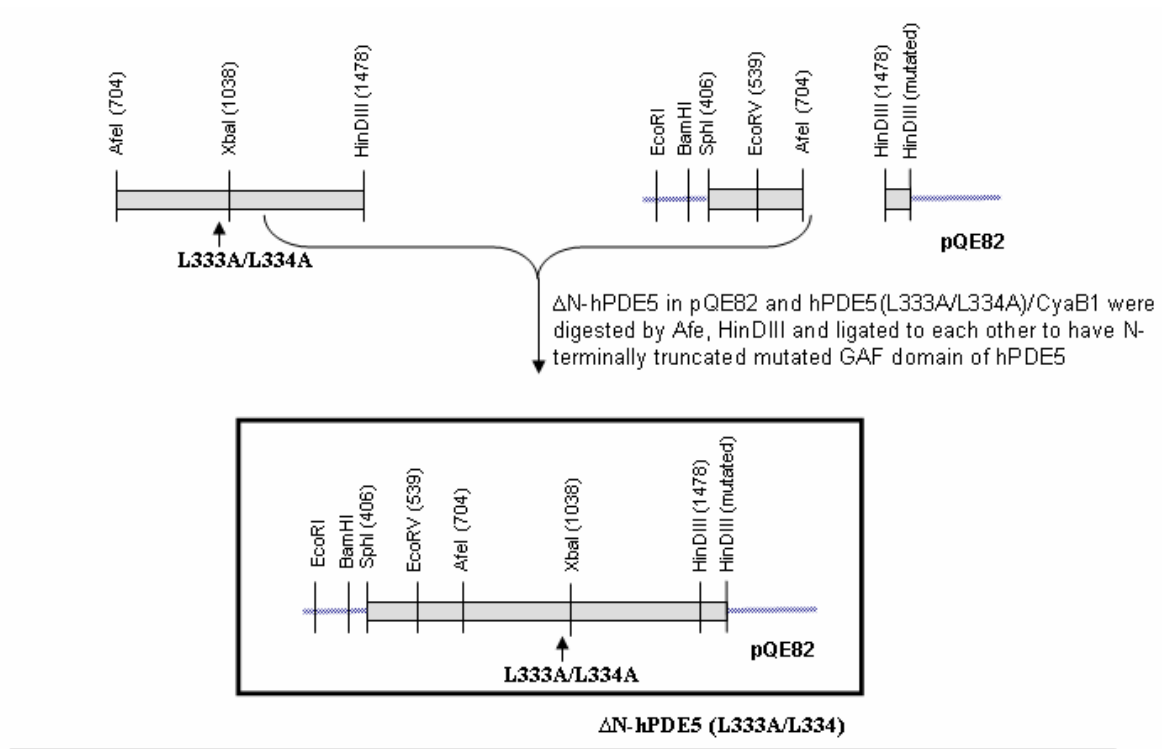
3.4.4.2 Cloning of hPDE5NGAF (L333A/L334A)/CyaB1 and hPDE5NGAF (L152A/L153A/L333A/L334A)/CyaB1



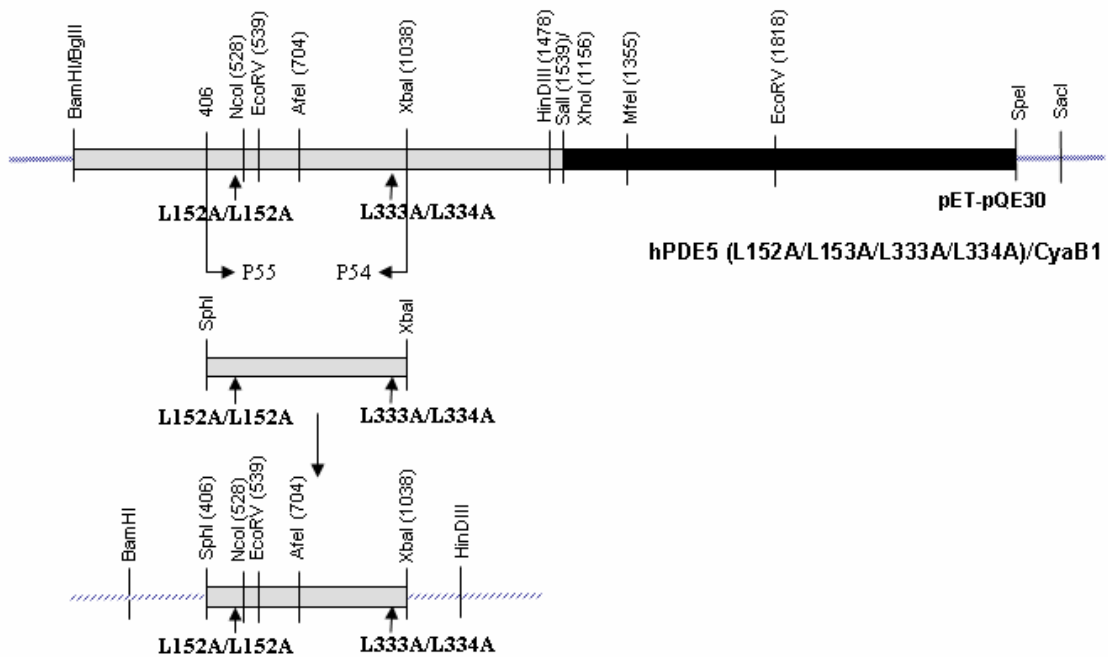
3.4.4.3 Cloning of hPDE5NGAF and mutants

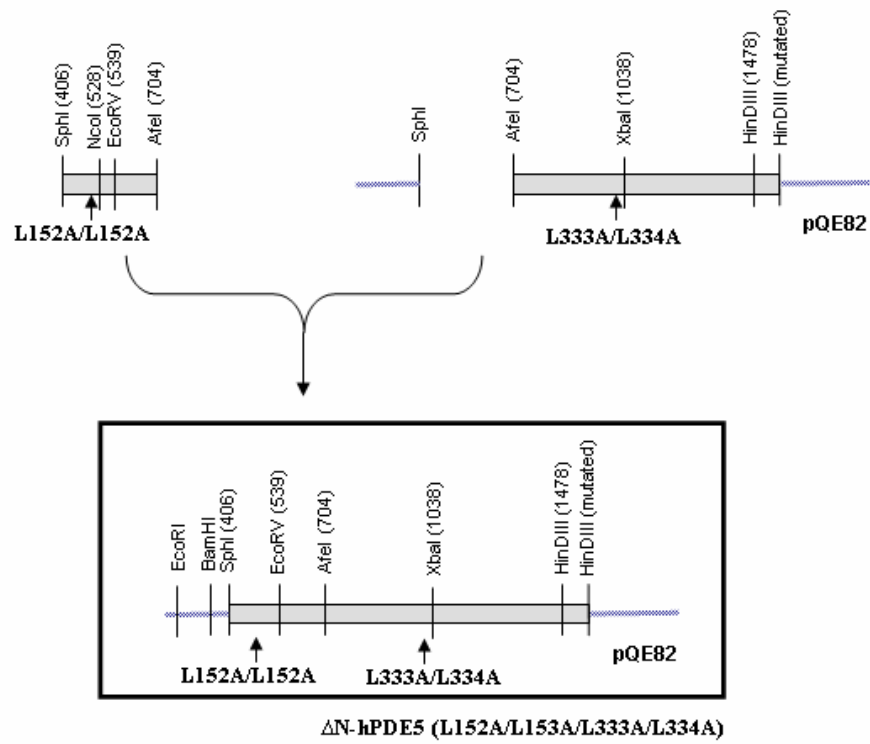


3.4.4.4 Cloning of Δ N-hPDE5GAF (L333A/L334A)



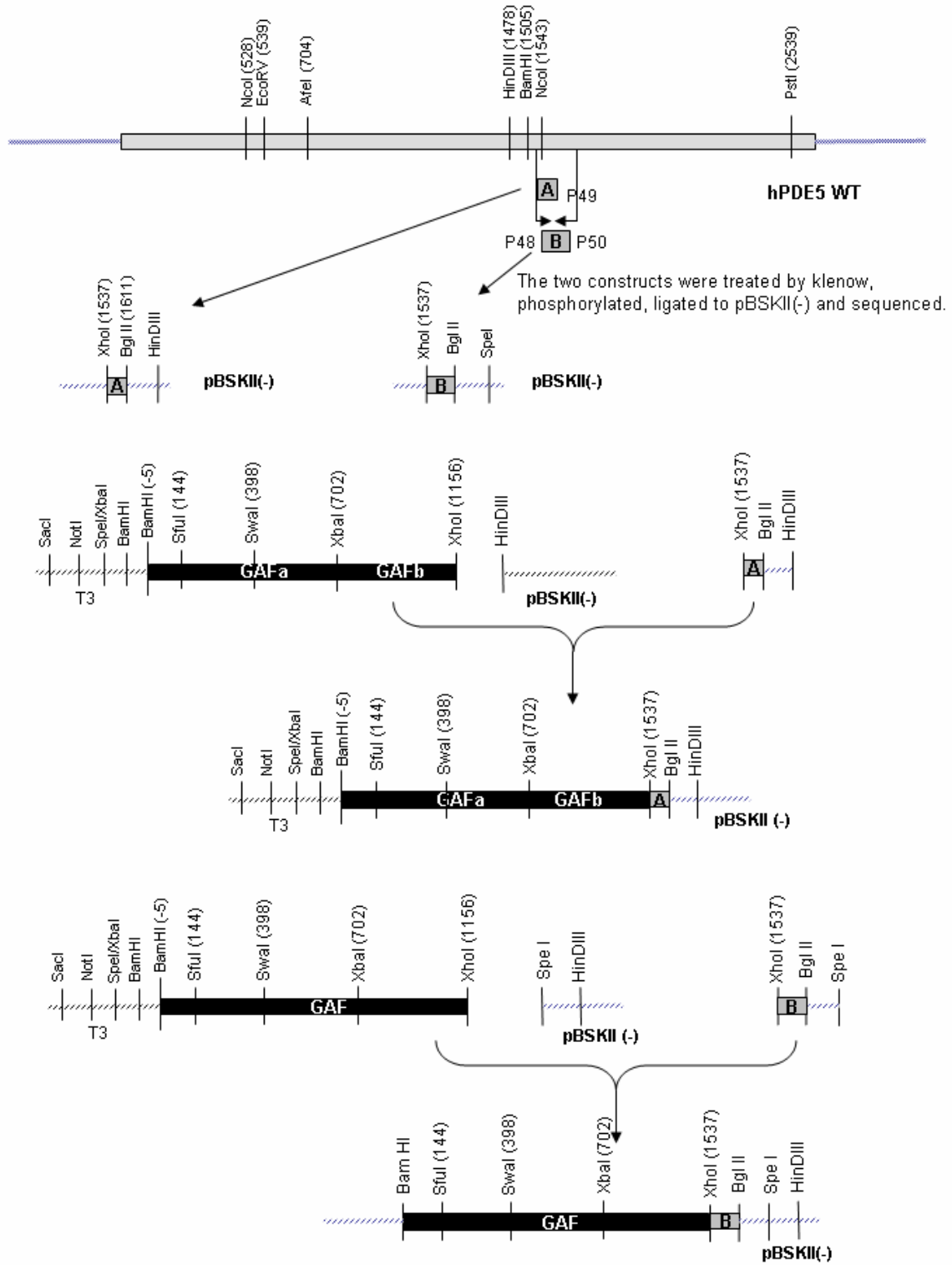
3.4.4.5 Cloning of Δ N-hPDE5GAF (L152A/L153A/L333A/L334A)





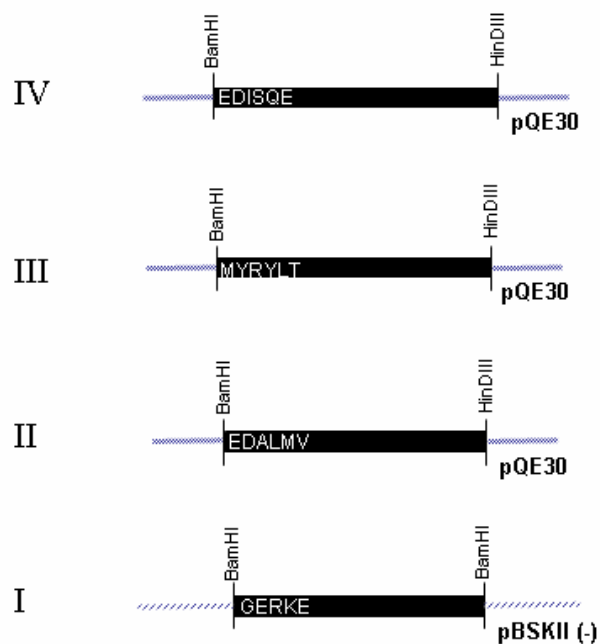
3.4.5 Cloning of CyaB1 constructs

3.4.5.1 Displacement of CyaB1 PAS by hPDE5 catalytic linker

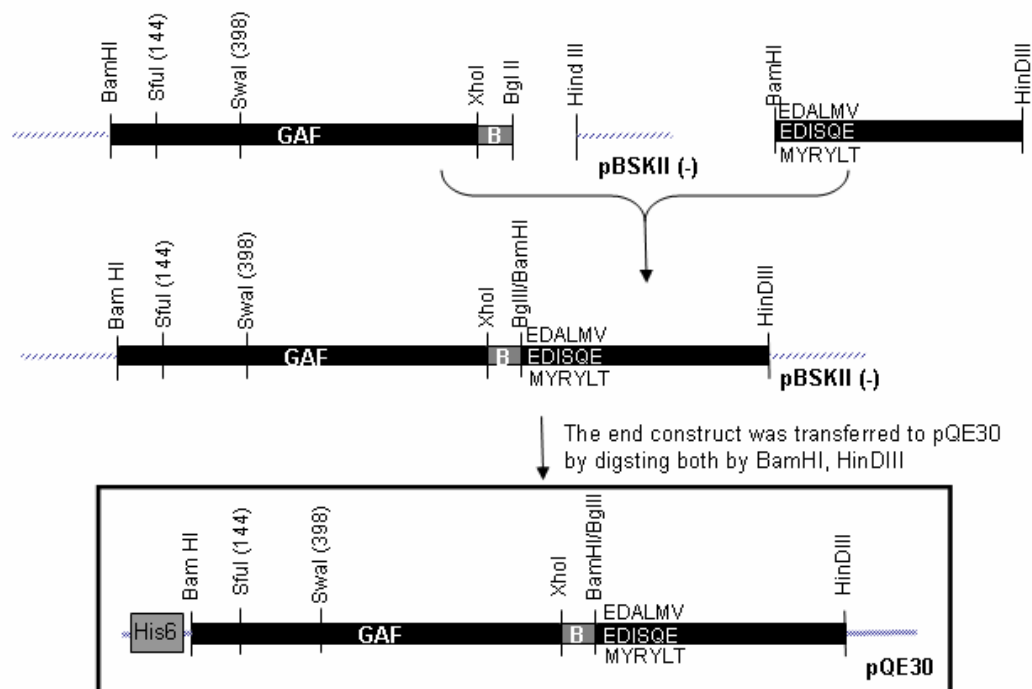


Methods

Different lengths of N-terminally truncated CyaB1 catalytic domain were obtained from Dr. Linder and ligated to these two constructs

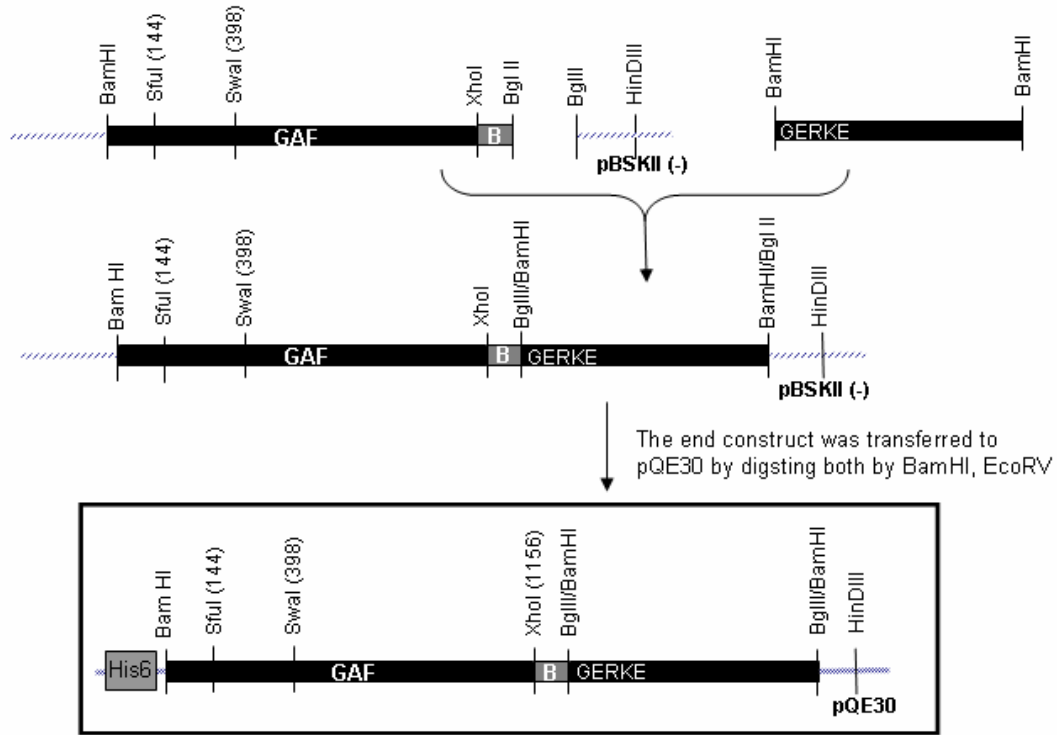


The catalytic domain constructs (I-III) were digested by BamHI, HindIII

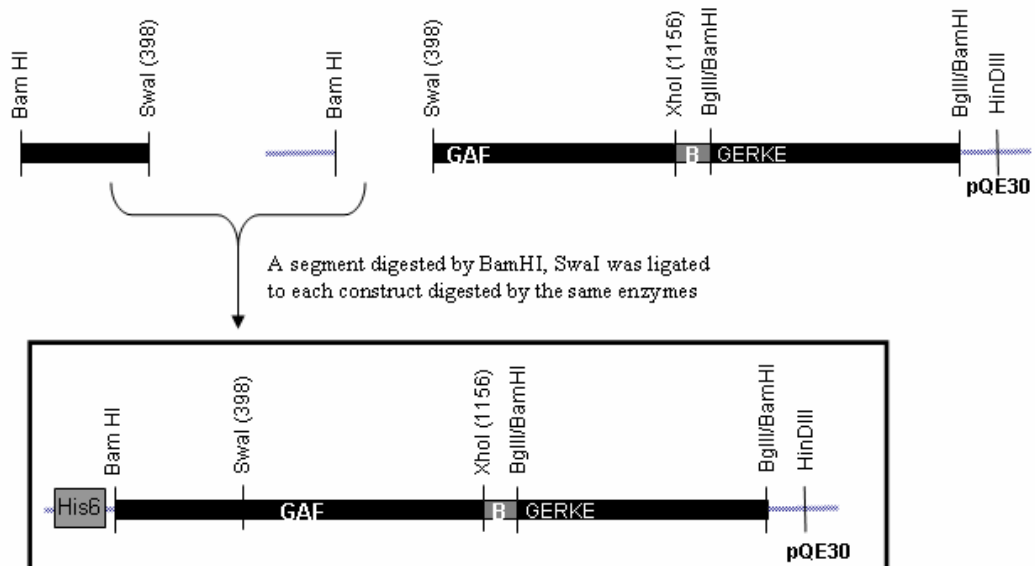


3.4.5.2 Cloning of Constructs IA and IB

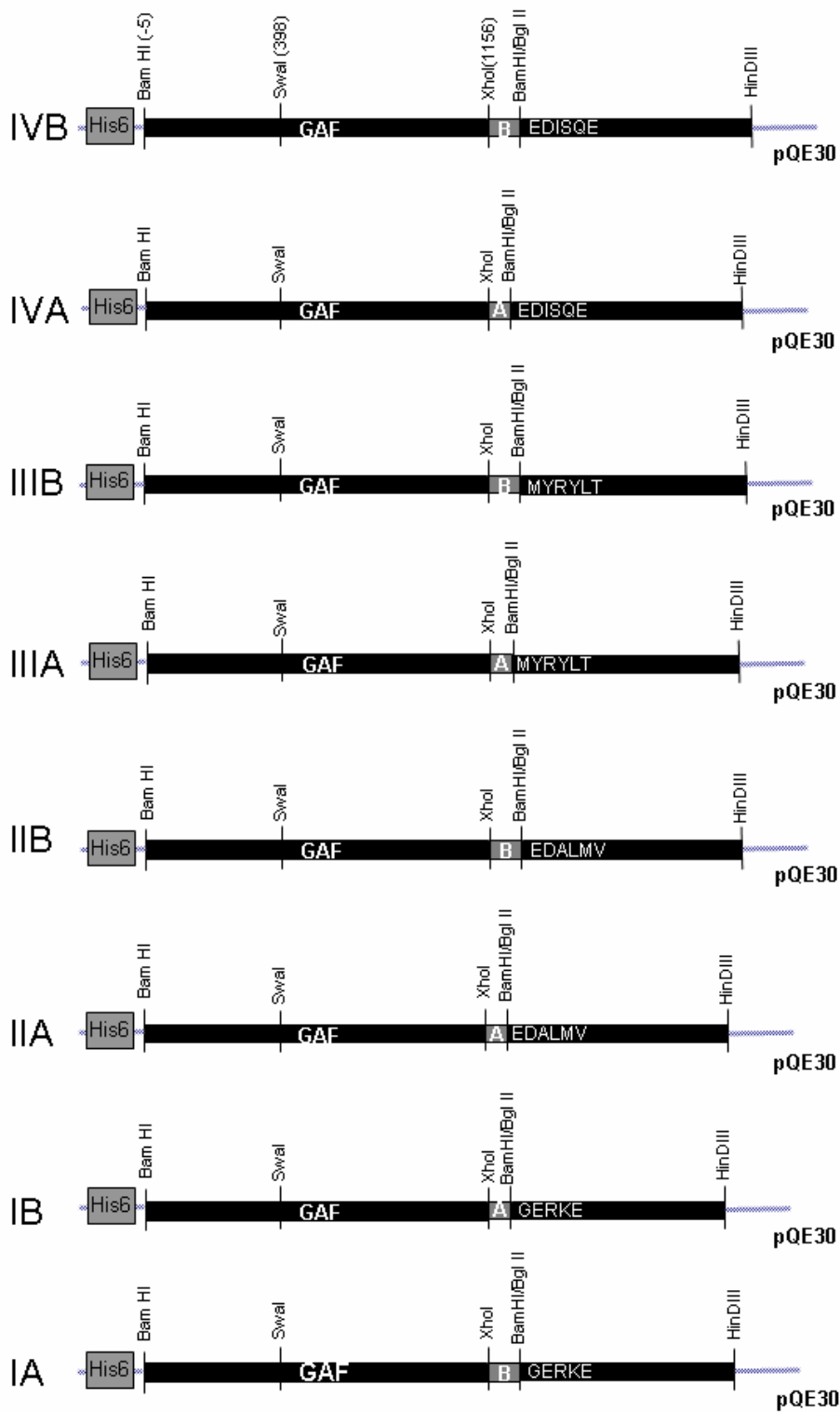
The fourth construct had two BamHI sites at both sides so it was digested by BamHI and ligated to the GAF-Linker digested by BglII



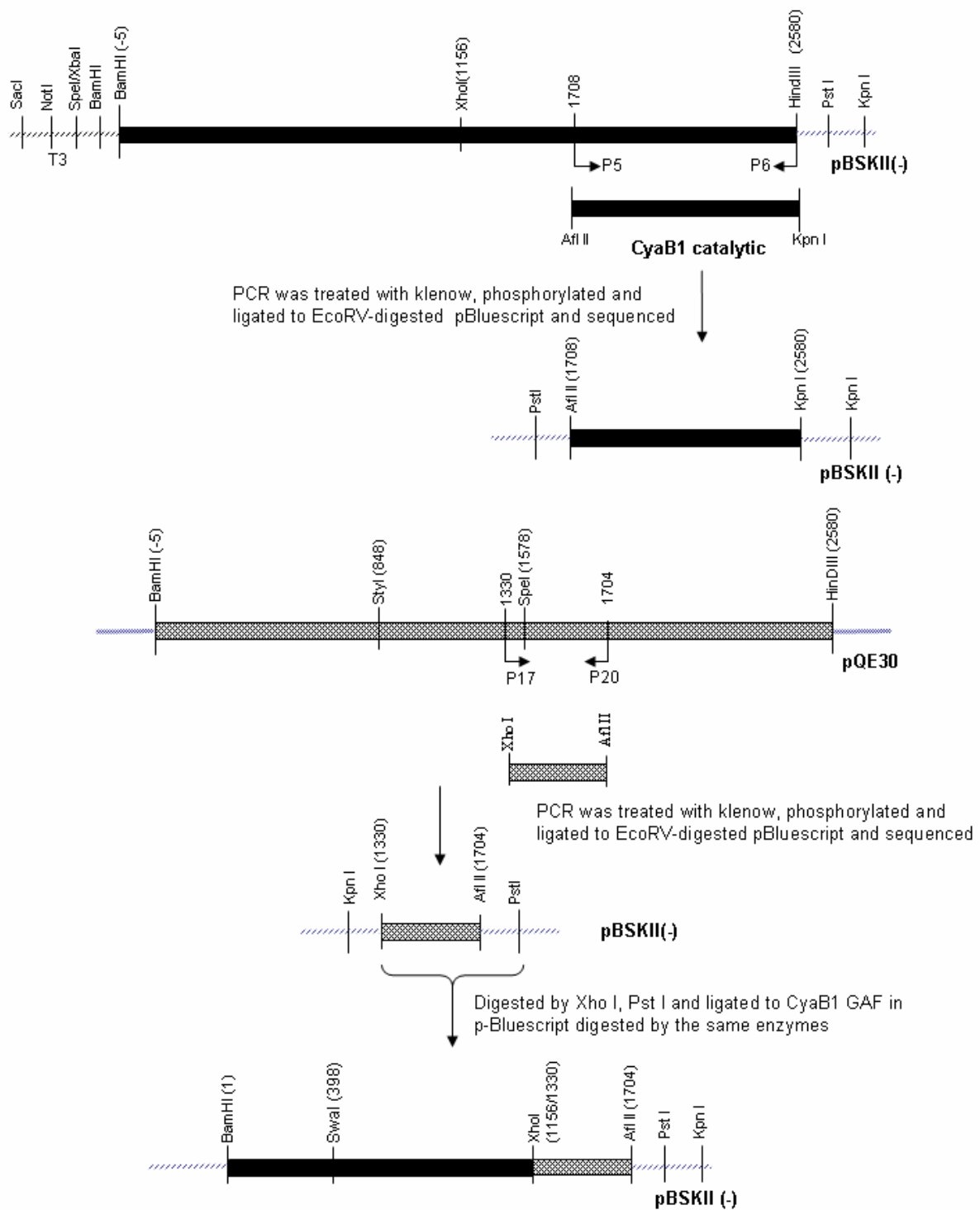
Then I found that the Sfu I site inserted in the GAF domain does not produce a silent mutation but Q49E so I had to correct this mutation for the 8 constructs.

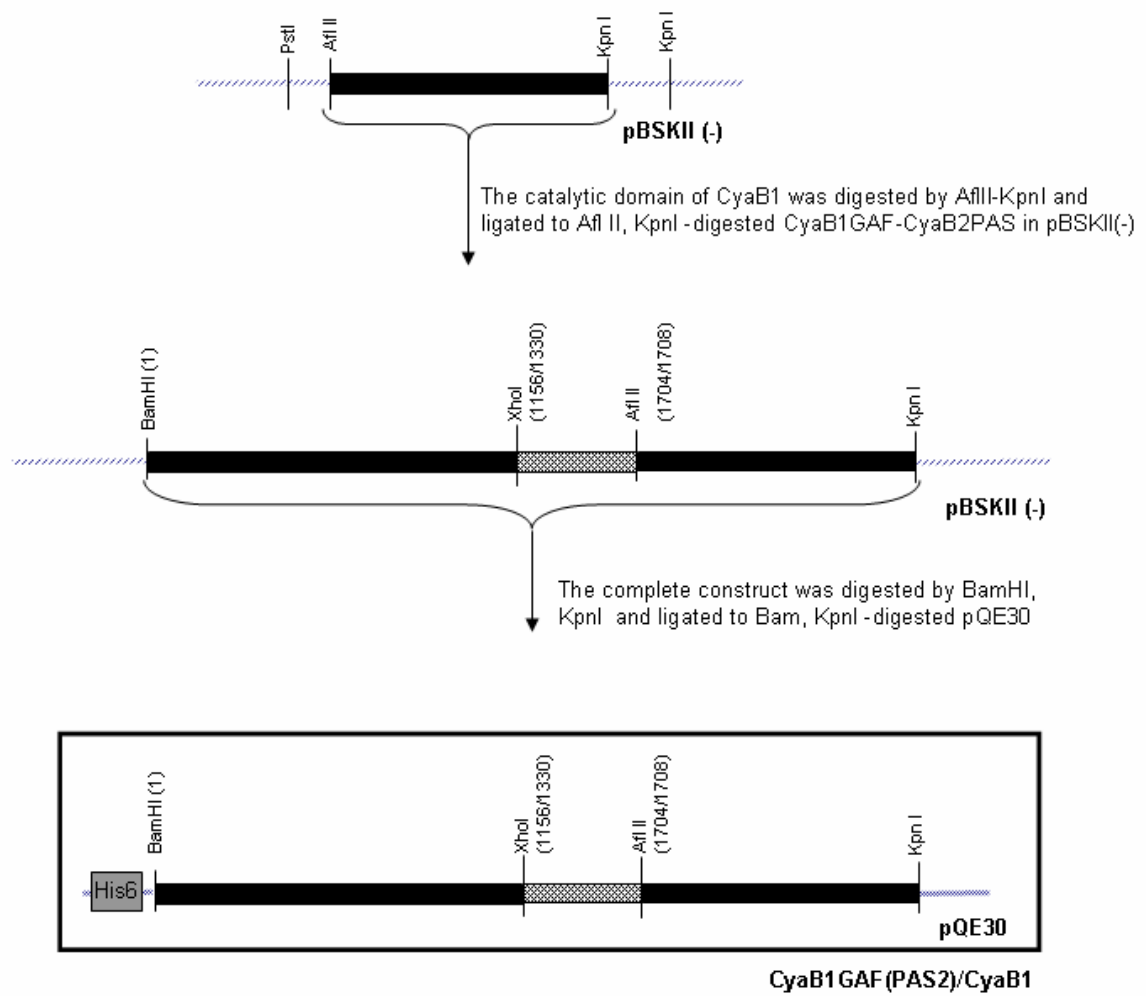


According to the same cloning procedure, 8 different constructs were obtained



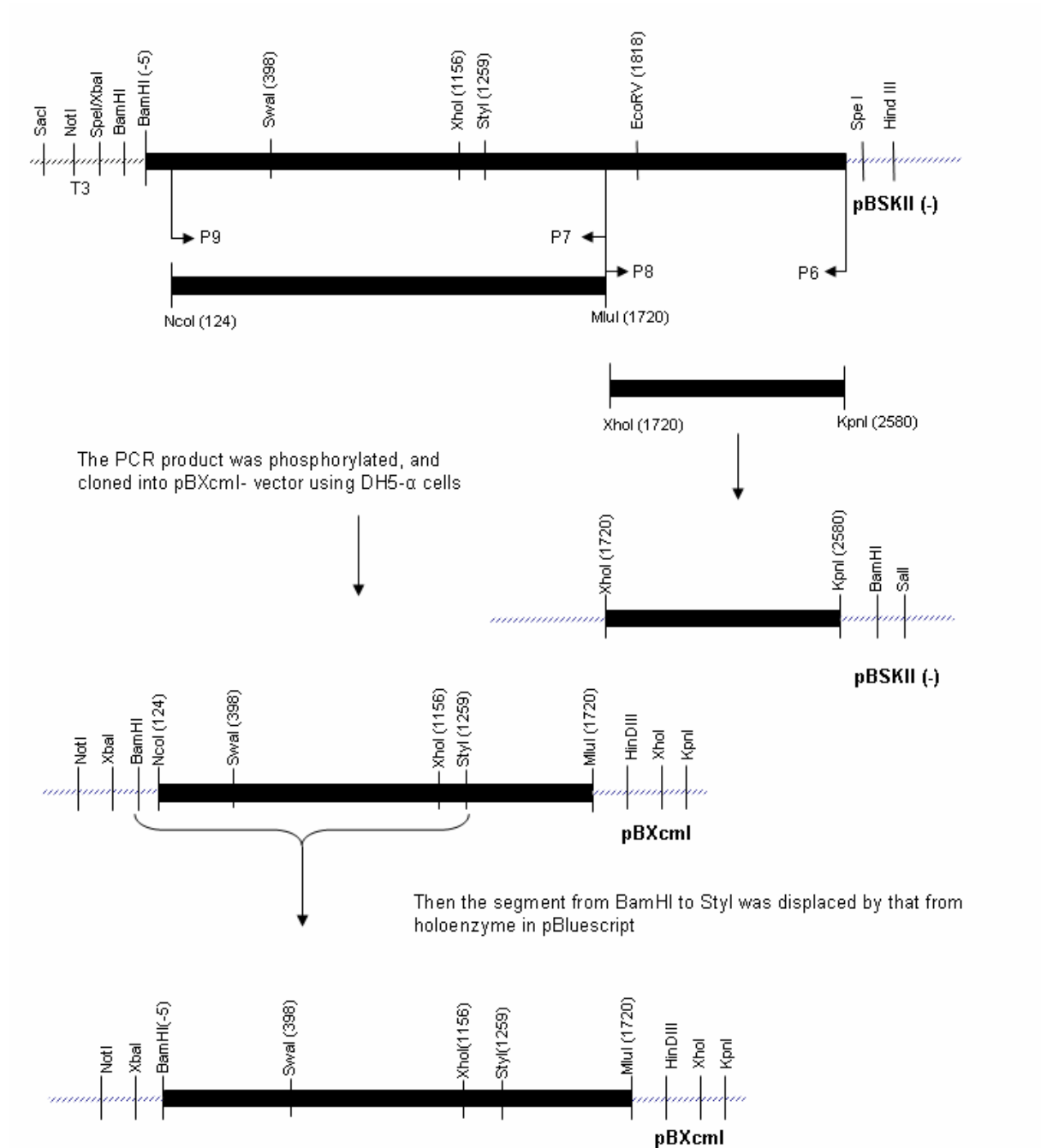
3.4.5.3 Cloning of CyaB1 (PAS2)/CyaB1

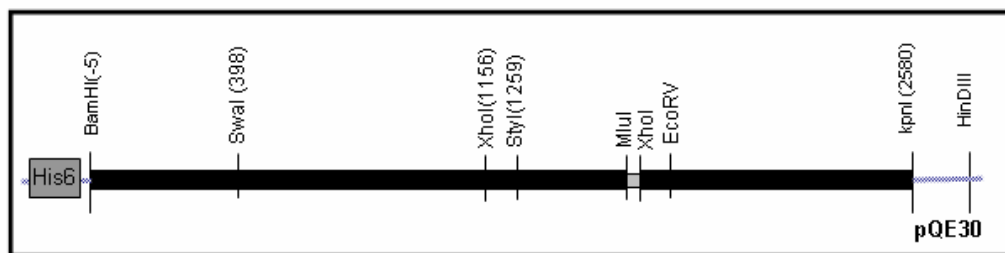
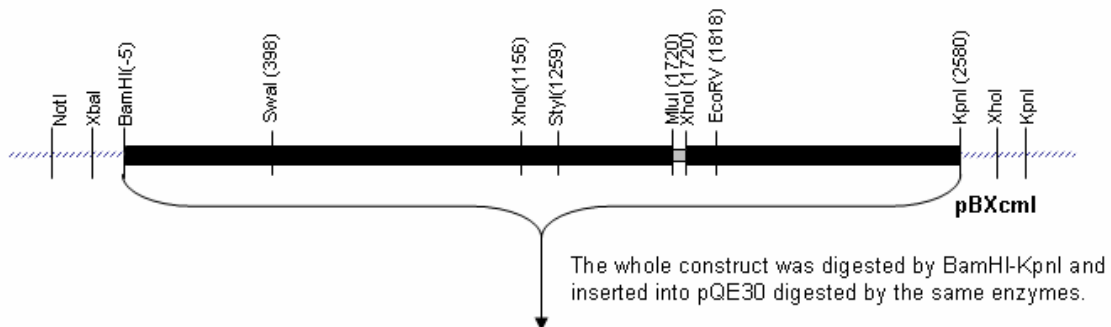
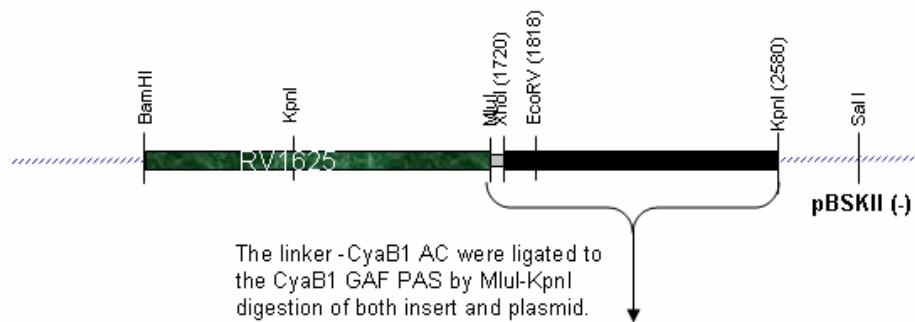
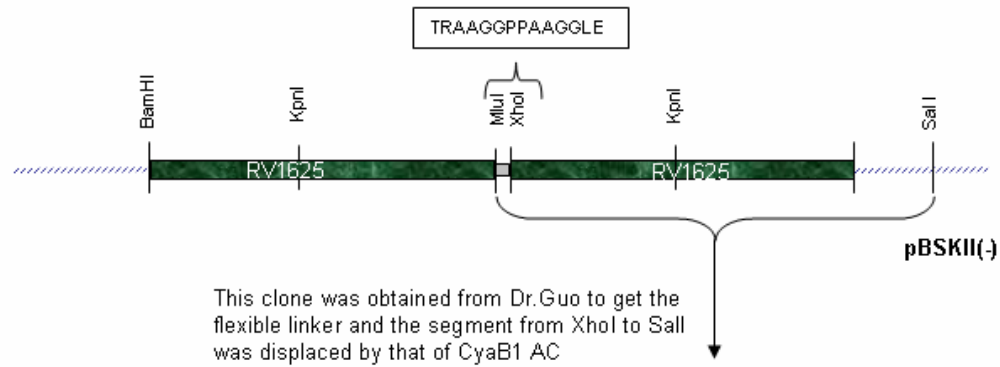




3.4.5.4 Cloning of CyaB1 (571+L)

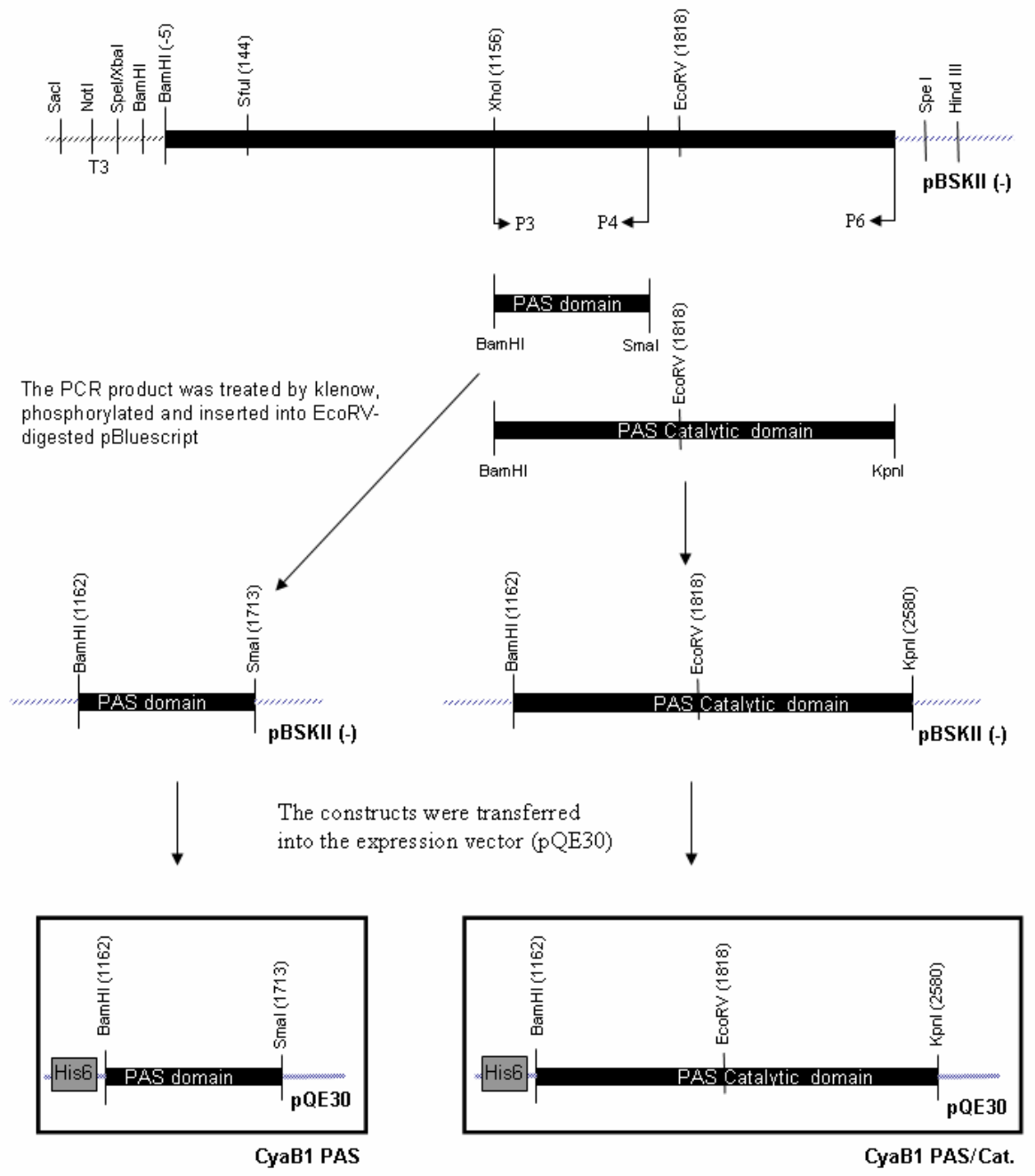
This construct was cloned by A.Schultz



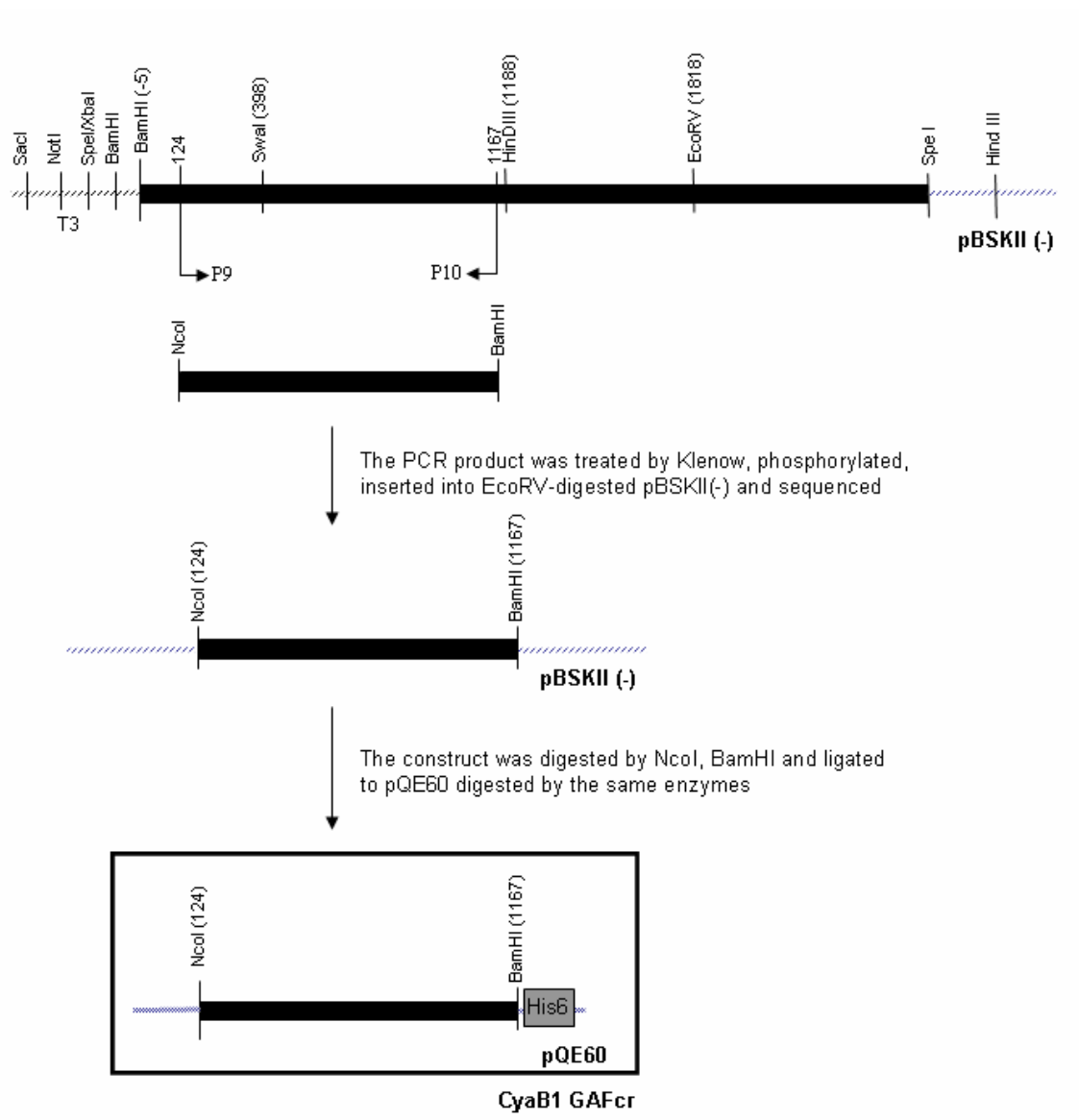


CyaB1(571 + L)

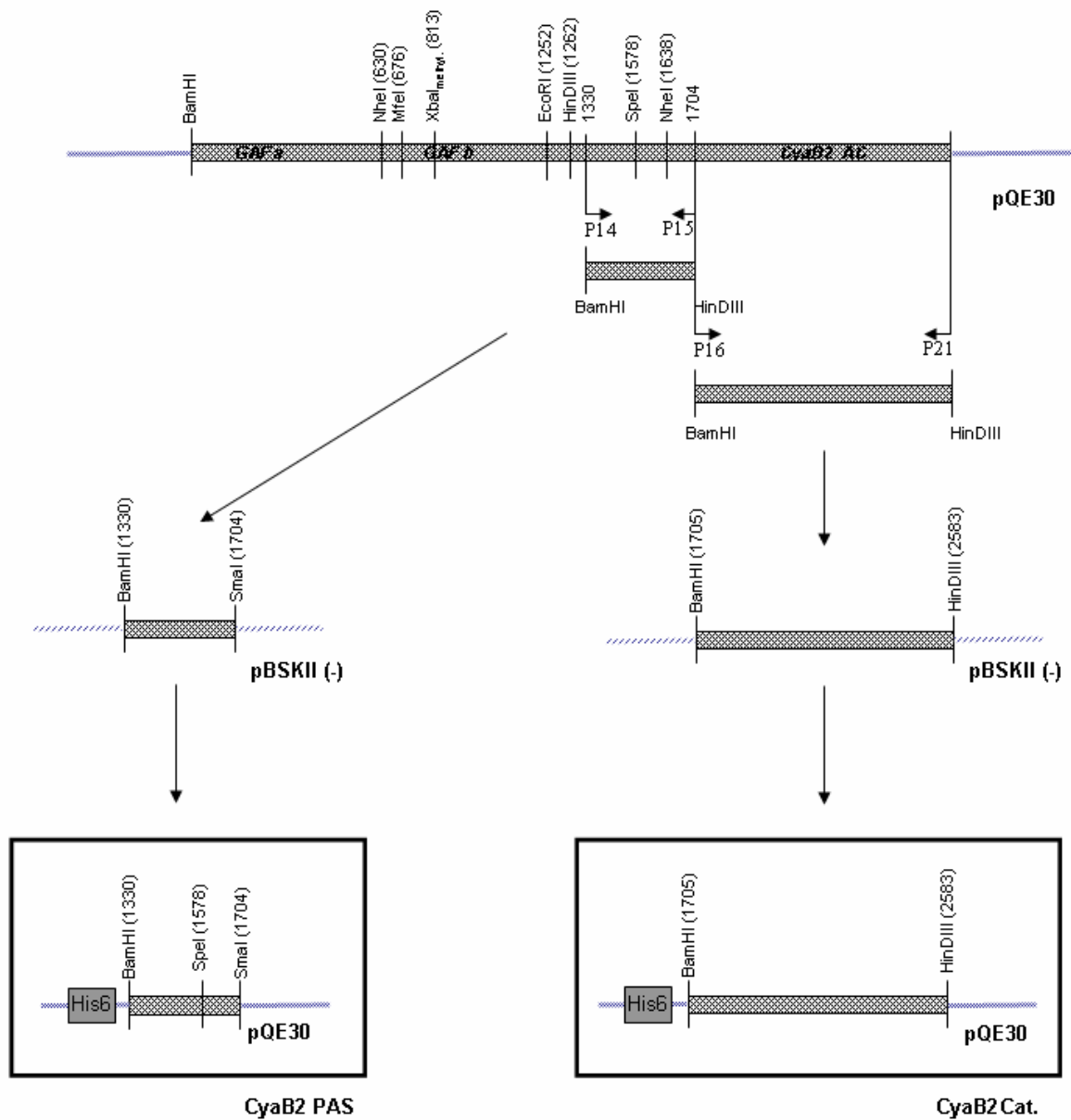
3.4.5.5 Cloning of CyaB1 PAS and CyaB1 PAS/catalytic for crystallization purposes



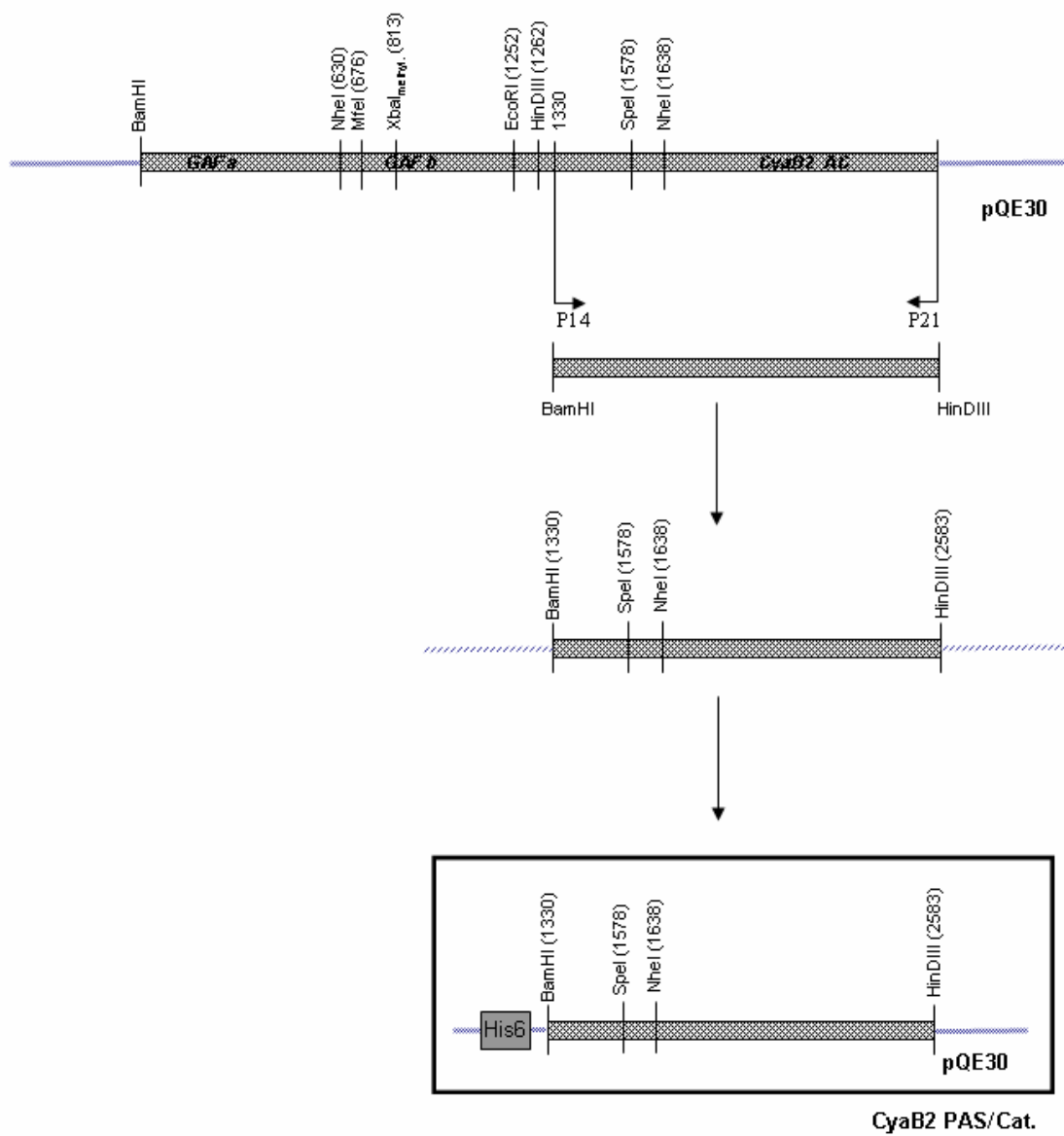
3.4.5.6 Cloning of CyaB1 GAFcr for crystallization purposes



3.4.5.7 Cloning of CyaB2 PAS and CyaB2 catalytic domain for crystallization purposes



3.4.5.8 Cloning of CyaB2 PAS/catalytic domain for crystallization purposes



4 Results

Using the CyaB1 AC as a reporter, the signal transduction through different domains has been studied. In this study three approaches have been considered:

- ❖ The effect of different N-termini on the signal transduction and regulation of PDE2 GAF
- ❖ The effect of the α 1- helix preceding GAFa and the connecting helix that connects the two GAF motifs
- ❖ The signal transduction through the PAS domain of CyaB1 as this domain is not required for the signal transduction in phosphodiesterases.

4.1 The effect of the N-terminal domain on signaling in the PDE2 GAF tandem/CyaB1 chimera

The PDE2 has a long, proline-rich N-terminal domain consisting of about 220 aa's. This N-terminus may be expected to be a separate domain and to have a function by itself in the regulation of the attached catalytic domain. In this part of work, the effect of two N-termini (hPDE2, hPDE5) on the signal transduction of hPDE2/CyaB1 chimera will be studied. In addition, when the first chimera of rPDE2/CyaB1 was constructed, the N-terminus of CyaB1 was included in the construct and again the effect of removal of this N-terminus will be studied.

4.1.1 Biochemical characterization of hPDE2NGAF/CyaB1 chimera

The domain organization of hPDE2NGAF/CyaB1 is shown in figure 4.1. The N-terminus starts at M1–G220, followed by two GAF tandems, GAFa (A221-H368) and GAFb (N402-N558) connected by a 33 aa-linker (C369-K401). Those are located in front of CyaB1 AC (L386-K859).

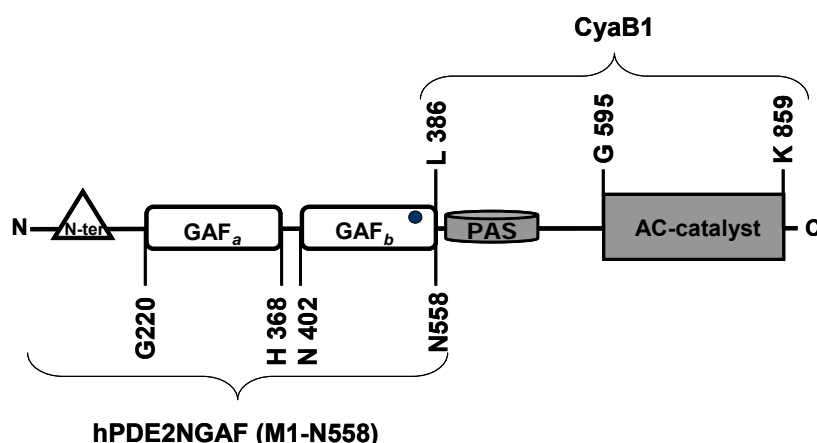


Fig. 4.1: Domain organization of the hPDE2NGAF/CyaB1 chimera, the boundaries of the N-terminus, GAF domain of hPDE2 were determined according the crystal structure of mouse PDE2. CyaB1 was used as before [80]. The domains related to hPDE2 are colourless while those of CyaB1 are grey. The grey circle in the GAFb indicates the allosteric binding site of cGMP.

4.1.1.1 Expression and purification of hPDE2NGAF /CyaB1 chimera

The expressed protein has a calculated MW of 116.2 kDa (including the hexahistidine-tag) and an isoelectric point of 5.17.

The hPD2NGAF/CyaB1 chimera was cloned into pQE30, transformed into *BL21 (DE3) [pREP4] E.coli* and expressed for 16-18 hours with 30 μ M of IPTG and 10 mM of $MgCl_2$ at 16°C. Cells were lysed twice by French Press and purified by adsorption to 200 μ l Ni^{+2} -NTA agarose for 2 hr. Figure 4.2 shows higher amount of the protein localized in pellet. 200 ml of cell culture yielded 120 μ g of protein. The enzyme was dialyzed overnight against dialysis buffer and the fresh protein was assayed. When required it was stored at -20°C. Storage longer than a month decreased both basal activity and fold stimulation.

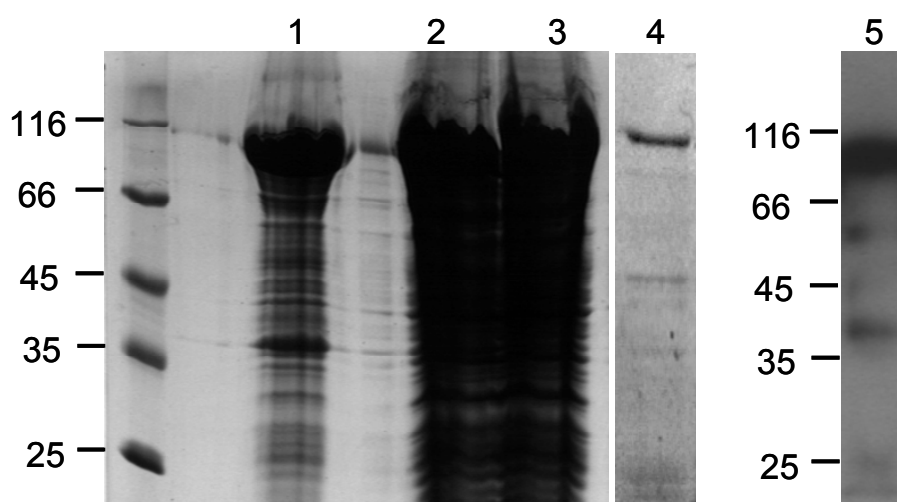


Fig. 4.2: SDS-PAGE (12.5%) and Western blot of hPDE2NGAF/CyaB1 chimera. (1) Cell Pellet, (2) Supernatant after lysis, (3) Supernatant after Ni-NTA binding, (4) Purified protein (2 μ g), (5) Western blot (0.3 μ g).

4.1.1.2 Protein dependence

The protein dependence \pm 100 μ M cGMP used 9 nM to 880 nM protein. Figure 4.3 shows dimerization achieved at low concentration.

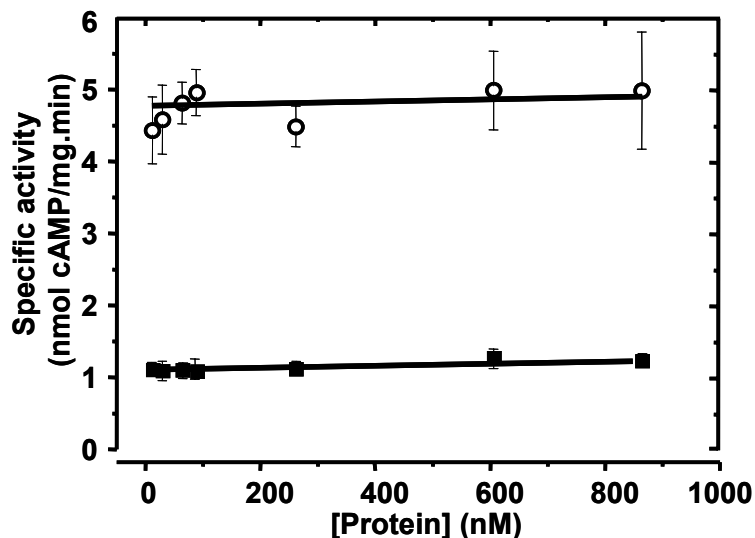


Fig 4.3: Protein dependence curve of hPDE2NGAF/CyaB1 chimera (\blacksquare basal activity, \circ + 100 μ M cGMP). Assay conditions: 10 min, 37 $^{\circ}$ C, 75 μ M Mg $^{+2}$ -ATP, Tris /HCl pH 7.5, n = 6; SEM values are shown as error bars.

4.1.1.3 Dose response study

cGMP dose response curve was established. Basal activity was 1.32 ± 0.1 nmol/mg.min (fig.4.4), stimulation factor was 4.88 ± 0.24 (n = 8), and the EC₅₀ was 9.92 ± 1.04 (n = 8). A concentration of 1 mM cAMP had no effect.

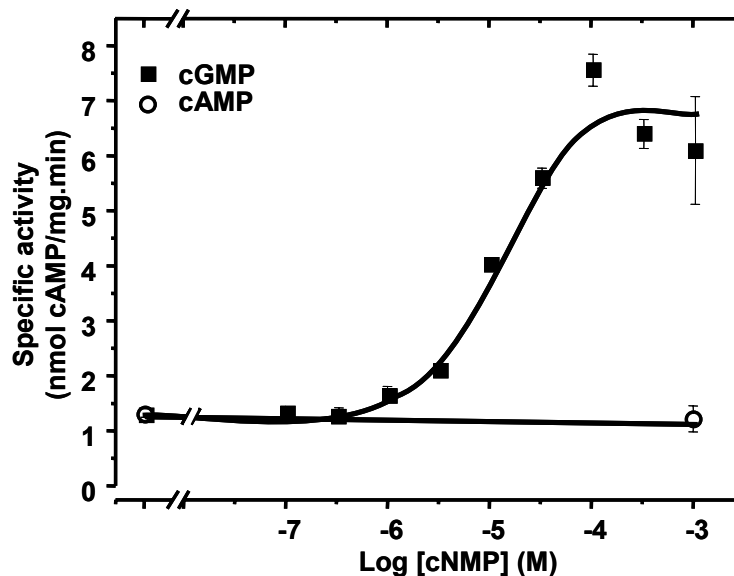


Fig. 4.4: Dose response curve of hPDE2NGAF/CyaB1 chimera. Assay conditions: 4 min, 37 $^{\circ}$ C, 75 μ M ATP, Tris/HCl pH 7.5, 90 nM protein (n = 8).

Results

$\text{Log}(V/V_{\text{max}} - V)$ was plotted against $\text{log}[\text{cGMP}]$ (fig. 4.5). The Hill coefficient was 0.477 ± 0.042 ($R^2 = 0.9754$, $n = 4$); i.e no cooperativity

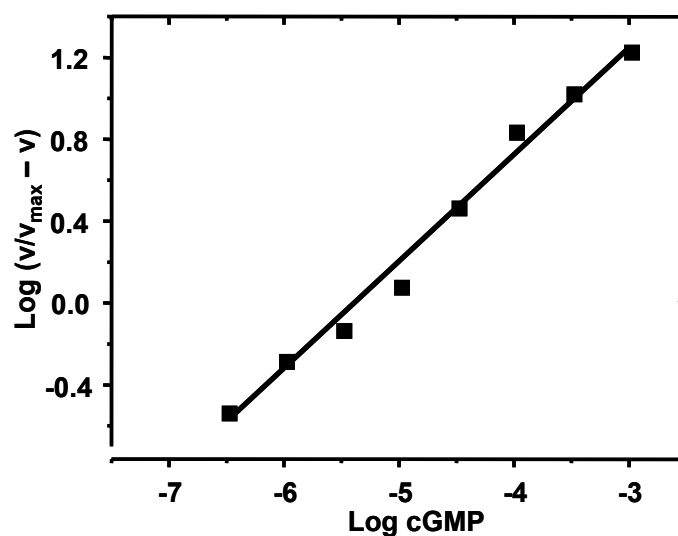


Fig.4.5: Hill plot of hPDE2NGAF/CyaB1 (0.477 ± 0.042 , $R^2 = 0.9754$).

4.1.1.4 Time dependence

90 nM protein was assayed at different time intervals (1-15 min). The reaction was linear (fig. 4.6, A), but plotting the specific activity/ time indicates a slight activation over a period of 1-2 min, possibly due to cGMP-binding to the GAF domain.

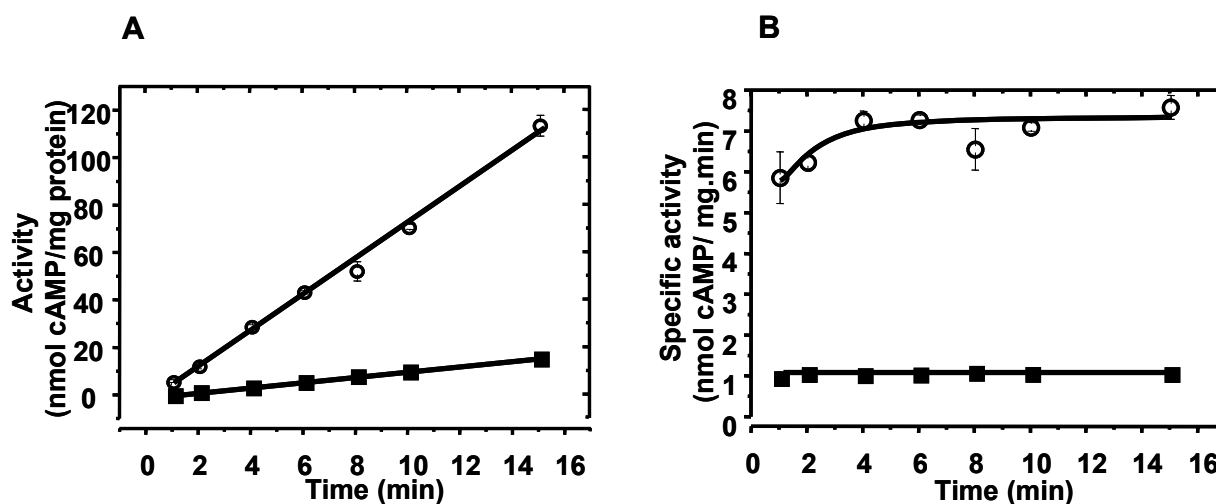


Fig. 4.6: Time dependence of hPDE2NGAF/CyaB1 chimera. (■) Basal activity, (○) +100 μM cGMP). Assay conditions: 75 μM Mg^{+2} -ATP, 37°C, Tris/HCl pH 7.5, 90 nM protein ($n = 4$) (A) Activity against time (B) Specific activity against time.

4.1.1.5 Temperature dependence

The reaction velocity increases with temperature until temperature-induced denaturation of the enzyme. The optimum temperature of the unactivated chimera was 50°C, while that of the cGMP-activated was 55°C (Figure 4.7 A and B).

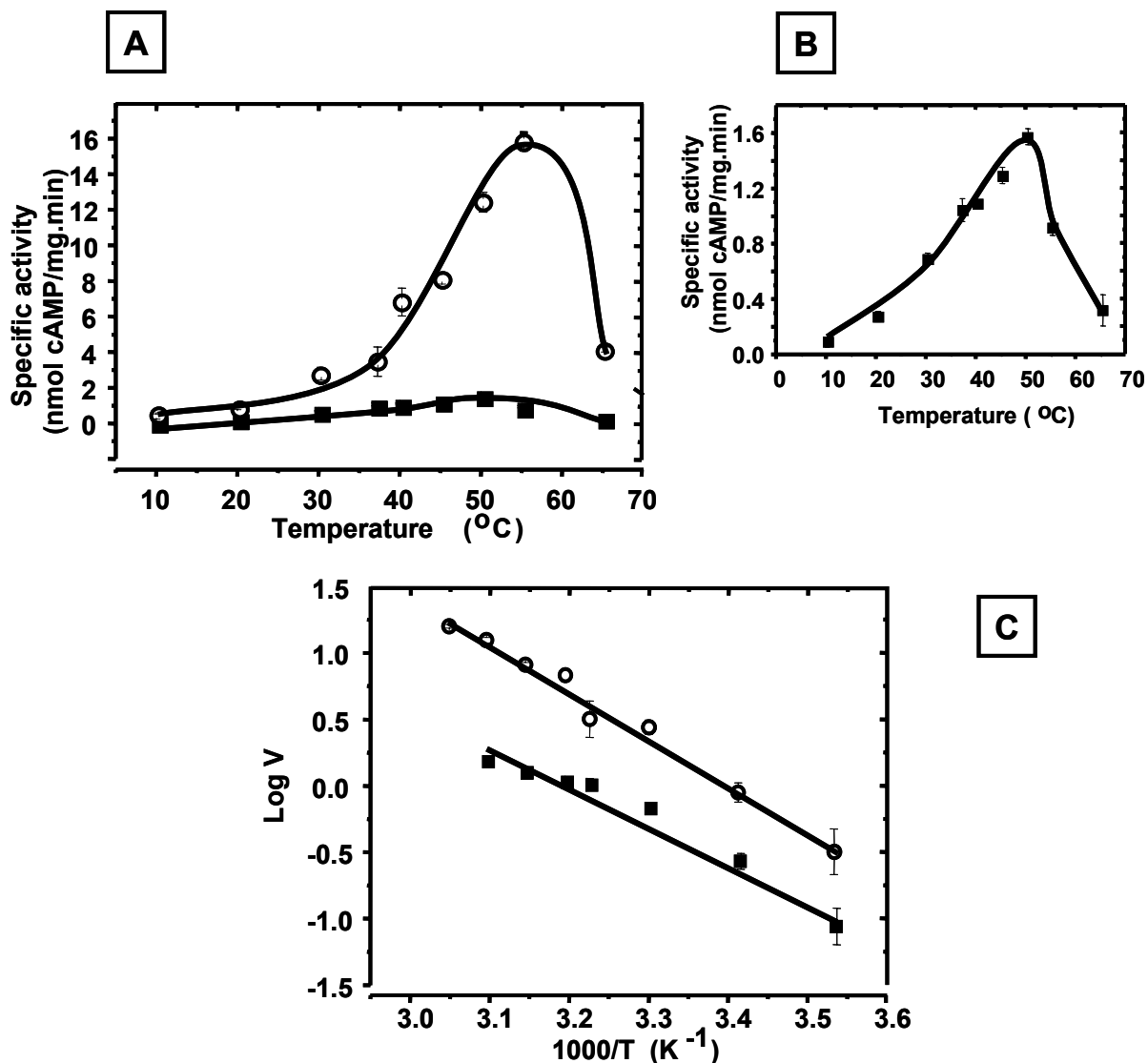


Fig 4.7: Temperature dependence of hPDE2NGAF/CyaB1 chimera. (■) Basal activity, (○) +100 μM cGMP). Assay conditions: 10 min, 75 μM Mg⁺²-ATP, Tris/HCl pH 7.5, 90 nM protein, 10-65°C (n = 4) (A) For both the activated and unactivated (B) For unactivated to show the maximum temperature and (C) Arrhenius plot.

The activation energy (E_a) according to Arrhenius plot was 54 kJ/(mol.K) for the basal activity and 68 kJ/(mol.K) for 100 μM cGMP-activated enzyme. This mirrors the results obtained for CyaB1 holoenzyme which was calculated by T.Kanacher to be 65 kJ/(mol.K) for the activated enzyme but it was lower than the value of the unactivated construct (97 kJ/(mol.K)).

4.1.1.6 pH dependence

The extremes of the pH can lead to denaturation of the enzyme because the structure of the catalytically active protein molecule depends on the ionic character of the amino acid side chains. Different buffer systems and different pH's have been used (see fig.4.8). At pH's lower than isoelectric point of the protein (4.0-5.5), the protein has a negative or zero charge and so the activity was almost zero. The optimum pH was found to be between 7.0-8.5 for the unactivated enzyme and 8.5 for the cGMP-activated construct. Tris/HCl and MOPS/Tris have shown to be the best for the protein AC activity but Tris/HCl was preferred due to its use in all other CyaB1 chimeras and hence, reasonable comparisons can be made. pH optimum for CyaB1 holoenzyme was 7.5 and so Tris/HCl pH 7.5 was used for the assay of all chimeras.

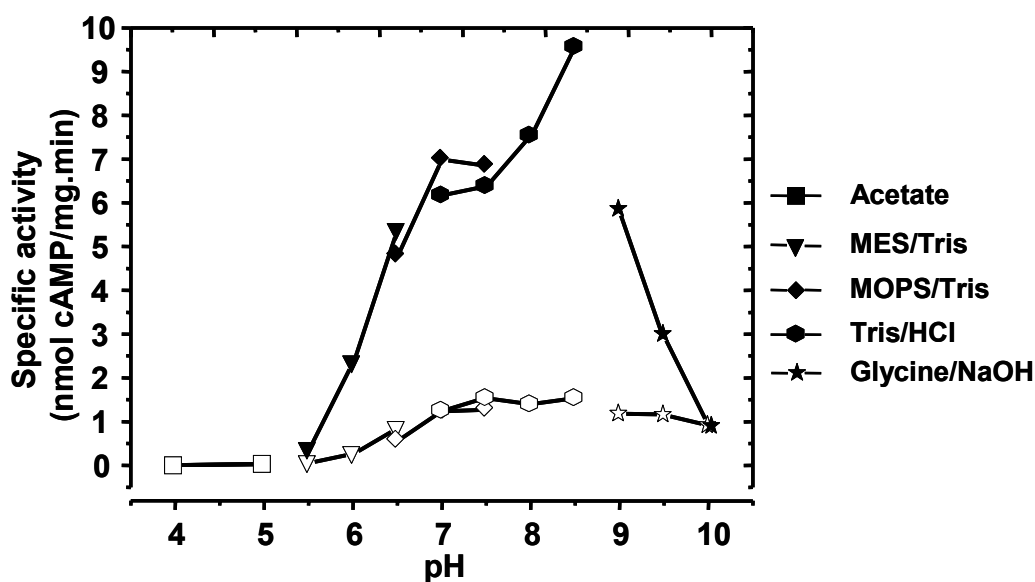


Fig 4.8: pH dependence curve of hPDE2NGAF/CyaB1. Basal activity: empty symbols, 100 μ M cGMP-activated: filled symbols. Assay conditions: 10 min, 75 μ M ATP, 10 mM $MgCl_2$, 37°C, 90 nM protein, pH 4-10 (n = 4)

4.1.1.7 ATP kinetics

The substrate kinetics were tested for hPDE2NGAF/CyaB1 chimera with ATP from 2 to 100 μ M ATP. Michaelis-Menten and Lineweaver-Burke plots show that the unactivated state had a K_m of 16.70 ± 3.88 μ M ATP and a V_{max} of 1.41 ± 0.23 nmol/mg.min while the activated enzyme had a K_m of 5.13 ± 1.92 μ M ATP and a V_{max} 10.52 ± 1.75 (Fig.4.9). Accordingly, the use of an ATP concentration of 75 μ M was meaningful. Compared to CyaB1 holoenzyme values, the K_m was 38 for the unactivated and 24 for the cAMP-activated form [79]. The Hill

Results

coefficient was 0.733 ± 0.037 ($R^2 = 0.9851$) for the unactivated and 0.693 ± 0.13 ($R^2 = 0.985$) for the activated form which shows no cooperativity.

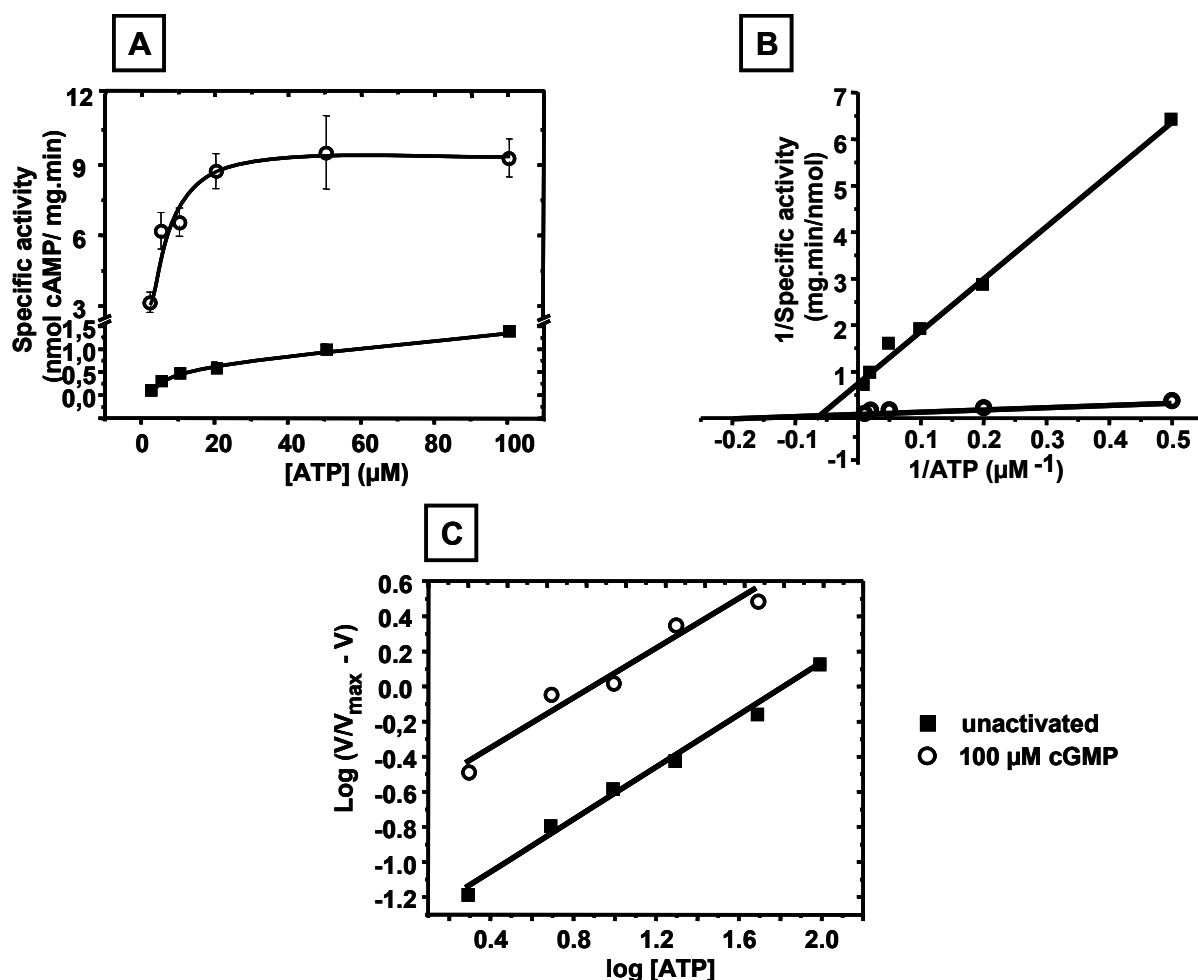


Fig. 4.9: Substrate kinetics of hPDE2NGAF/CyaB1 chimera (A) Michaelis-Menten plot (B) Lineweaver-Burke plot and (C) Hill plot for both activated and unactivated forms of the enzyme. Assay conditions: 4 min, 37°C, 0.1 M Tris/HCl pH 7.5, 130 nM protein and ATP 2-100 μM.

4.1.2 Effect of N-terminus on CyaB1 AC activity

PDE2A2 and PDE2A3 were found to be membrane-bound while PDE2A1 is cytosolic (ref.). To see whether the N-terminal of hPDE2A3 affect AC activity, activation or cGMP affinity, the N-terminus was removed and hPDE2 (228-558)/CyaB1 chimera was generated (Fig.4.10). The boundaries of the GAF domain of human PDE2 were determined by a BLAST Search of the GAF sequence (www.ncbi.nlm.nih.gov/blast).

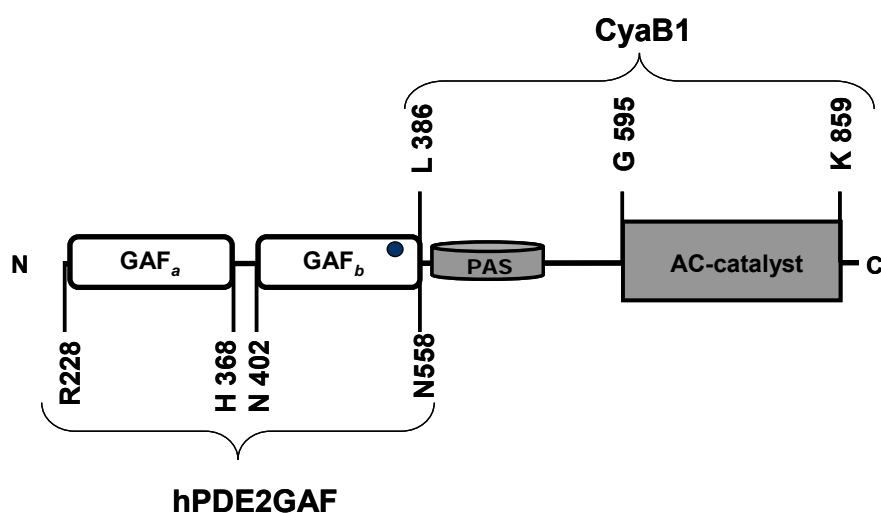


Fig. 4.10: Domain organization of ΔN_{1-227} -hPDE2GAF/CyaB1 showing the amino acid boundaries. Grey circle: allosteric binding site of cGMP.

4.1.2.1 Expression and purification of the protein

The pQE30- ΔN_{1-227} -hPDE2GAF/CyaB1 DNA was transformed into *BL21 (DE3) E.coli* cells. Bacterial cells were grown to OD_{600} of 0.5-0.6 at 30°C and induced by 30 μ M IPTG and 10 mM $MgCl_2$ (overnight at 16°C). The protein was bound to 350 μ l Ni-NTA agarose for 90 min. The eluted His-tagged protein has a calculated MW of 91.86 kDa and >95% purity (Fig.4.11).

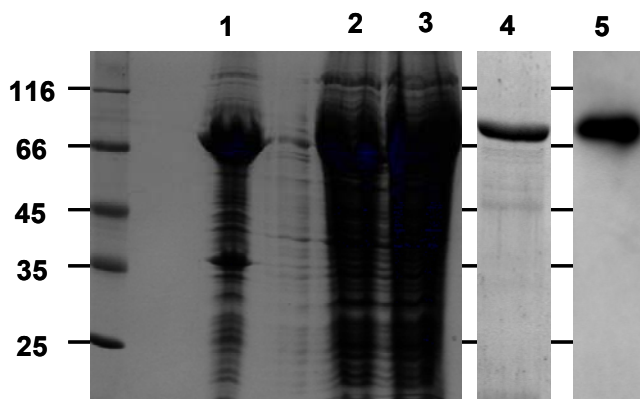


Fig.4.11: SDS PAGE (12.5%) of ΔN_{1-227} -hPDE2GAF/CyaB1 (1) Pellets (2) Supernatant (3) Supernatant after Ni-NTA (4) Purified proteins (2 μ g) (5) Western Blot (0.1 μ g)

4.1.2.2 Protein dependence

The protein dependence was assayed for 11 to 1100 nM (fig.4.12). Specific activity was constant at the low concentrations and declined at higher concentrations which could be due to oligomerization or accumulation of pyrophosphate. The basal activity (12.2 ± 0.8

Results

nmol/mg.min, n = 4) was higher than that of hPDE2NGAF/CyaB1 (1.32 ± 0.08 nmol/mg.min, n = 4).

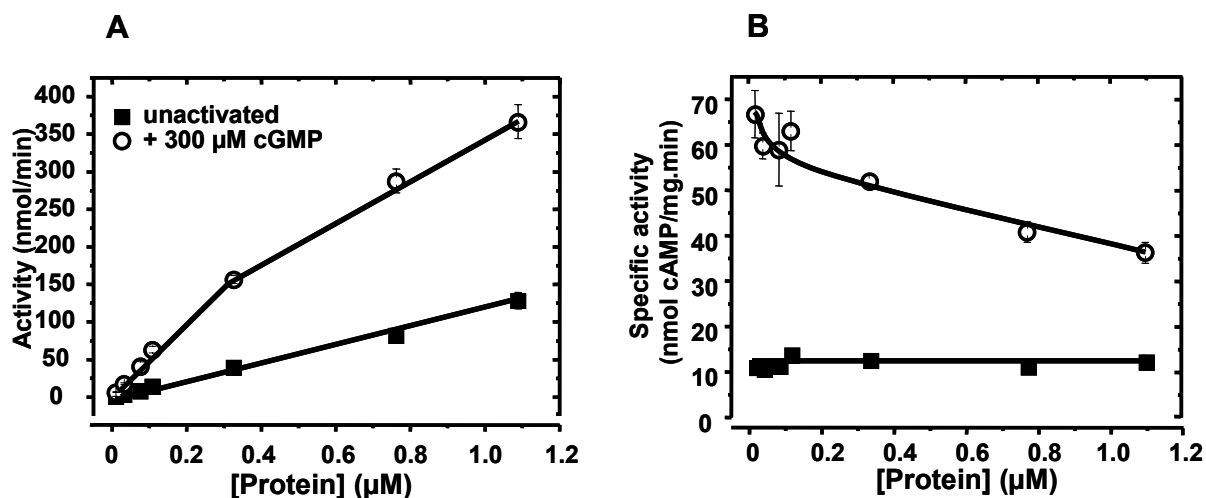


Fig. 4.12: Protein dependence of ΔN_{1-227} -hPDE2GAF/CyaB1. Assay conditions: 4 min, 37°C, 0.1M Tris/HCl pH 7.5, 75 μM Mg^{+2} -ATP (n = 4) (A) Activity against protein concentration (B) Specific activity against protein concentration.

4.1.2.3 Dose response study

The AC activity of the chimera was assayed at increasing concentrations of cGMP. Stimulation factor was 4.2 ± 0.09 , cGMP- EC_{50} of 7.7 ± 0.08 and Hill coefficient of 0.47 ± 0.02 ; i.e identical to the WT chimera.

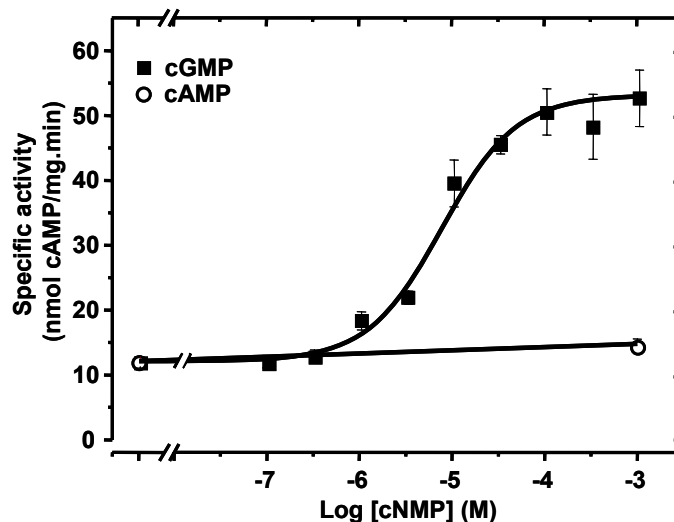


Fig. 4.13: Dose response curve of ΔN_{1-227} -hPDE2GAF/CyaB1. Assay conditions: 10 min, 37°C, 75 μM Mg^{+2} -ATP, Tris/HCl pH 7.5, 55 nM protein (n = 4).

4.1.2.4 Time dependence

The time dependence was linear for both unactivated and activated protein (fig.4.14 A and B).

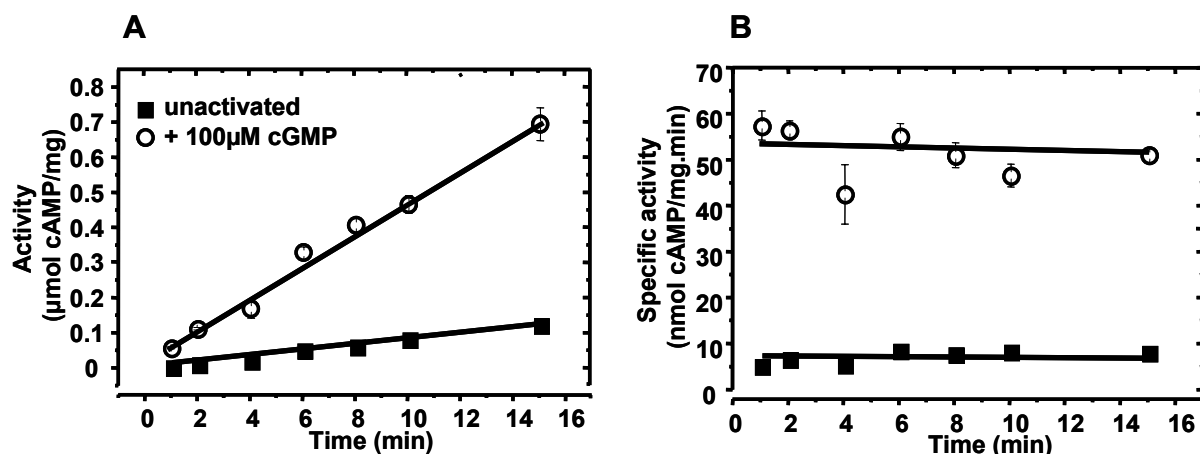


Fig. 4.14: Time dependence of ΔN_{1-227} -hPDE2GAF/CyaB1. Assay condition: 37°C, 75 μM Mg^{+2} -ATP, Tris/HCl pH 7.5, 109 nM protein, 1-15 min (n = 6). **(A)** Activity against time **(B)** Specific activity against time

4.1.2.5 Substrate kinetics

The K_m of ΔN -hPDE2GAF/CyaB1 chimera was 15.65 ± 2.35 (n = 4) as deduced from a Lineweaver-Burke plot. The protein activated by 100 μM cGMP had a K_m of 4.34 ± 0.89 μM (fig.4.15). V_{max} values were 7.31 ± 0.54 and 41.62 ± 3.55 nmol/mg.min for unactivated and cGMP-activated, respectively. The Hill coefficients were 0.85 ± 0.06 ($R^2 = 0.98$) and 0.68 ± 0.02 ($R^2 = 0.98$) for unactivated and activated forms, respectively; indicated no cooperativity.

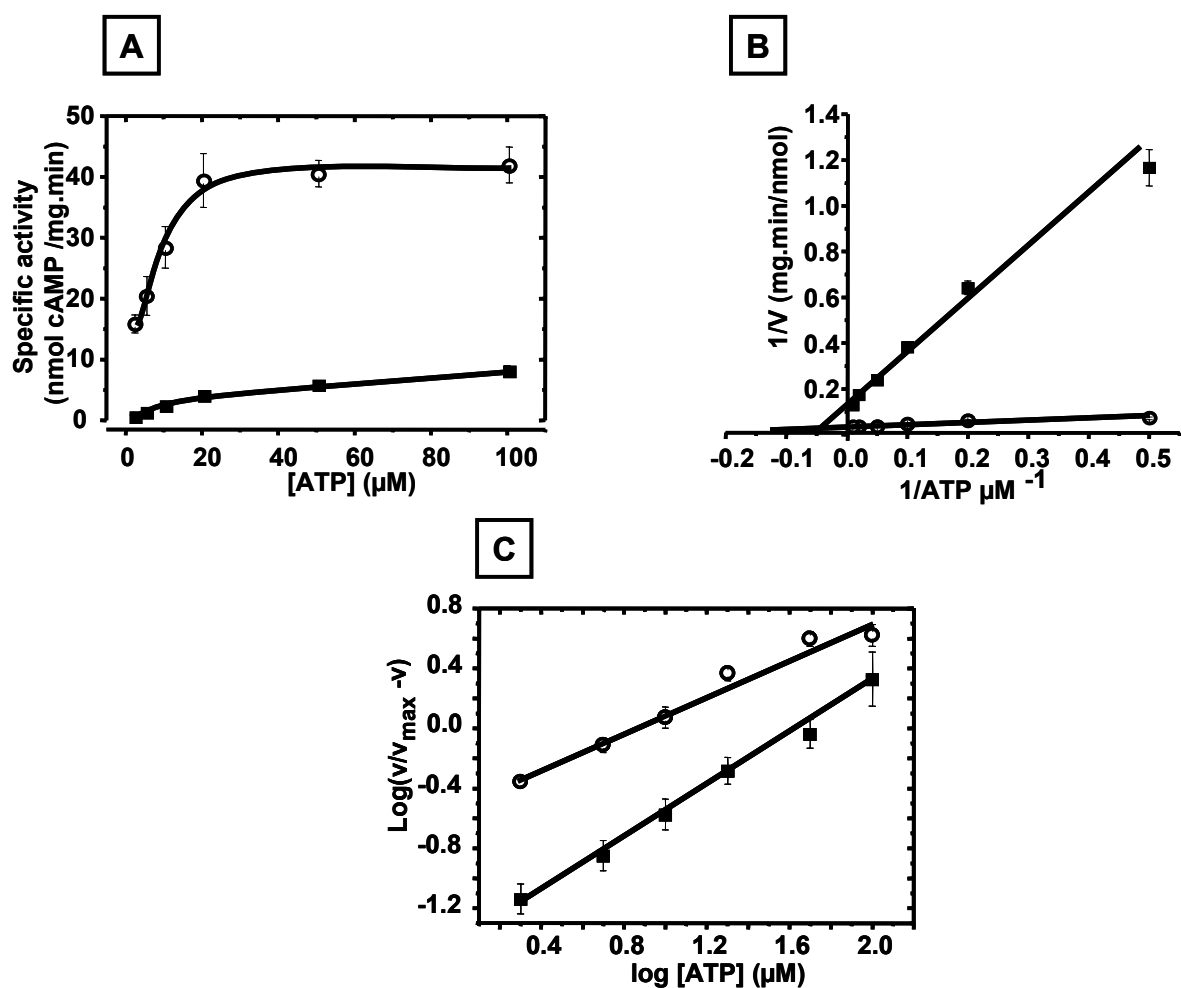


Fig. 4.15: Substrate kinetics of Δ N-hPDE2GAF/CyaB1. (\blacksquare basal activity, \circ + 100 μ M cGMP). Assay conditions: 4 min, 37°C, 0.1M Tris/HCl pH 7.5, 109 nM, 2-100 μ M ATP (n = 4) (A) Michaelis-Menten Plot (B) Lineweaver-Burke plot and (C) Hill Plot.

4.1.2.6 Crystallization of Δ N₁₋₂₂₇-hPDE2GAF/CyaB1

The crystallization of this construct was attempted. The protein was dialysed against crystallization buffer (section 2.6.2.6 with 10% glycerol) and concentrated by ultrafiltration using Nanosep filter (11,000 rpm, 4°C) to 8.2 mg/ml.

Crystal screens I, II and lite (from Hampton) were employed using the hanging drop method. Plates were kept at 16°C and examined one week later. Rosette-like crystals appeared with CS I # 12 (30% isopropanol, 0.1M Na HEPES pH 7.5 and 0.2M MgCl₂) and CS I # 19 (30% isopropanol, 0.1M Tris/HCl pH 8.5 and 0.2M ammonium acetate). Crystallization was reproducible yet efforts to optimize shape and size failed.

4.1.3 Exchange by hPDE5 N-terminus

The N-terminus of the hPDE5 had a regulatory and inhibitory effect on the enzyme (Bruder, 2006). A chimera consisting of hPDE5 N-terminus (M1-S150), hPDE2 GAF (R228-558) and CyaB1 (386-859) was cloned in pQE30 (fig. 4.16), transformed into *BL21 (DE3)[pREP4]* *E.coli* cells and expressed.

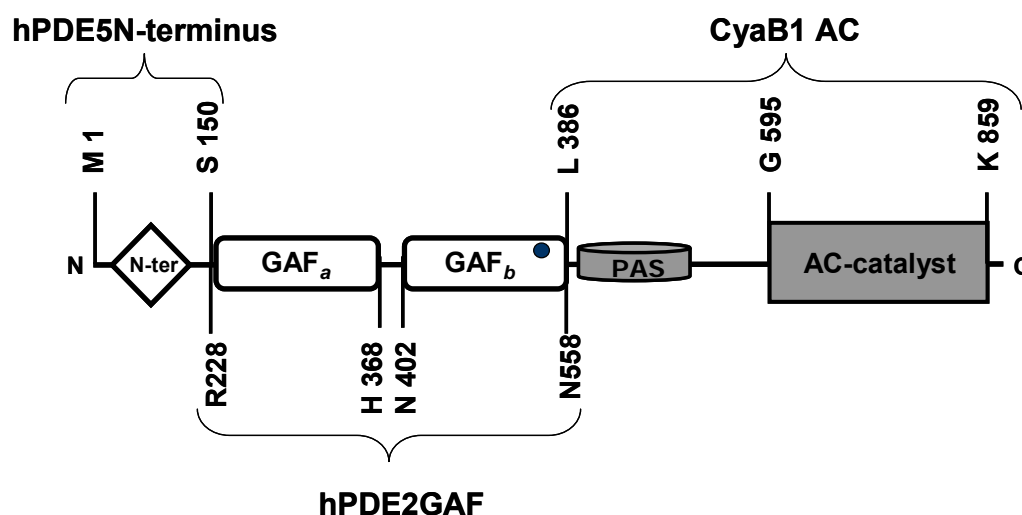


Fig.4.16: Domain organization of hPDE5N-ter-PDE2GAF/CyaB1. The exchanged N-terminus was determined according to an alignment between hPDE5 and rPDE2. Grey circle: allosteric binding site of cGMP.

The protein was purified by binding to 200 μ l of Ni-NTA agarose for 3 hr and eluted by 600 μ l elution buffer. The protein has a calculated MW of 109.2 kDa, an isoelectric point of 5.25. The yield was 150 μ g/200 ml culture (fig.4.17).

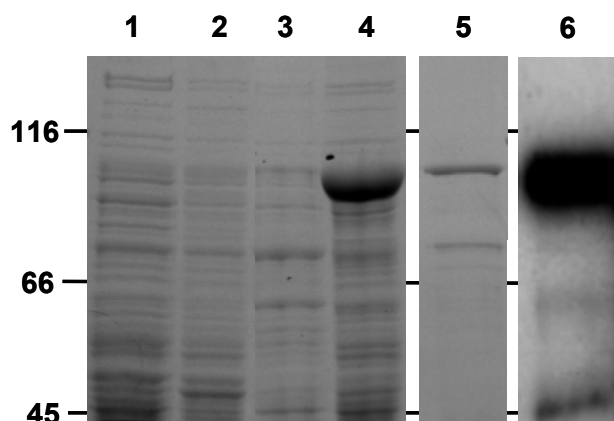


Fig.4.17: SDS-PAGE (7.5%) of hPDE5N-PDE2GAF/CyaB1. (1 and 2) are supernatant and pellet of pQE30 as control (3 and 4) are supernatant and pellet of hPDE5N-PDE2GAF/CyaB1, respectively (5) Purified protein (2 μ g) (6) Western blot (0.3 μ g protein and 12.5% SDS-PAGE)

4.1.3.1 Protein dependence

The protein dependence was linear for both the activated and unactivated enzymes (Fig.4.18).

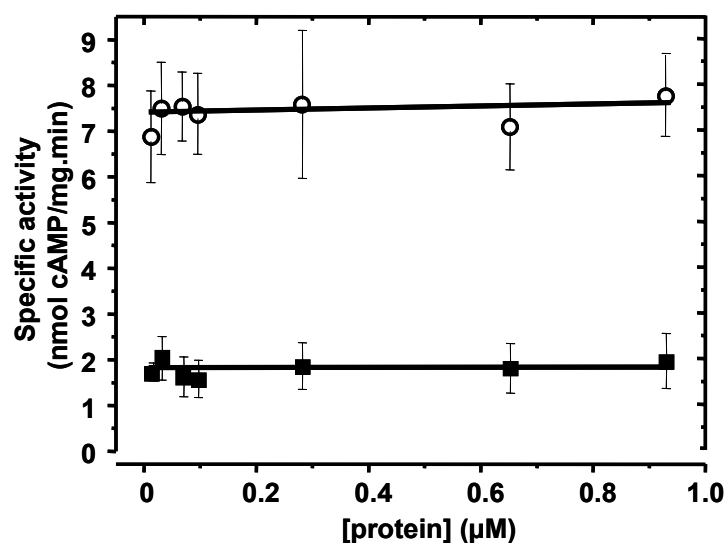


Fig. 4.18: Protein dependence of hPDE5N- hPDE2GAF/CyaB1. (■) unactivated protein (○) +300μM cGMP. Assay conditions: 37°C, 10 min, 75 μM ATP, Tris/HCl pH 7.5 (n = 4).

4.1.3.2 Dose response study

A stimulation factor of 6.44 ± 0.32 and a Hill coefficient of 0.56 ± 0.11 , calculated from the dose response curve of the enzyme (fig.4.19), were consistent with the values obtained for hPDE2NGAF/ CyaB1. The basal activity of 0.67 ± 0.078 and a cGMP-EC₅₀ of 3.67 ± 0.52 were lower for the hPDE5-N-terminally construct than that of the hPDE2 N-terminally chimera.

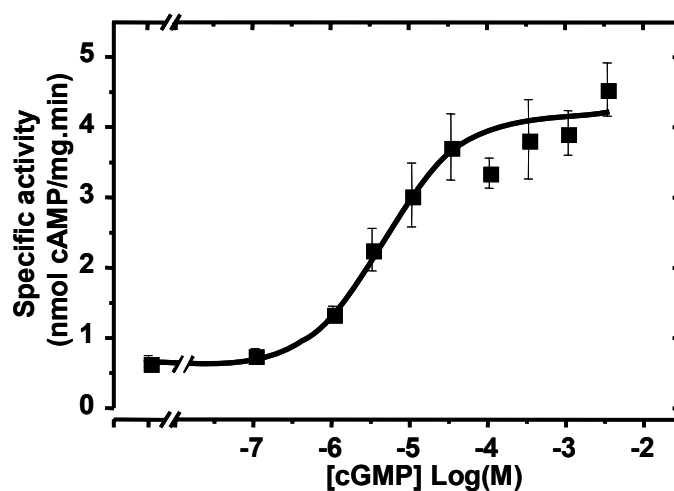


Fig 4.19: Dose response curve of hPDE5N-hPDE2GAF/CyaB1. Assay condition: 37°C, 75 μM Mg⁺²-ATP, 10 min, Tris/HCl pH 7.5, 92 nM Protein concentration (n = 4).

4.1.4 Truncation of rat PDE2GAF.CyaB1 N-terminus

The first successful chimera which has the CyaB1 AC as a reporter was CyaB1N.rPDE2GAF/CyaB1 [80]

I removed the CyaB1 N-terminus and obtained rPDE2GAF (207-546)/CyaB1 which is most similar to hPDE2GAF (228-558)/CyaB1 (fig.4.20)

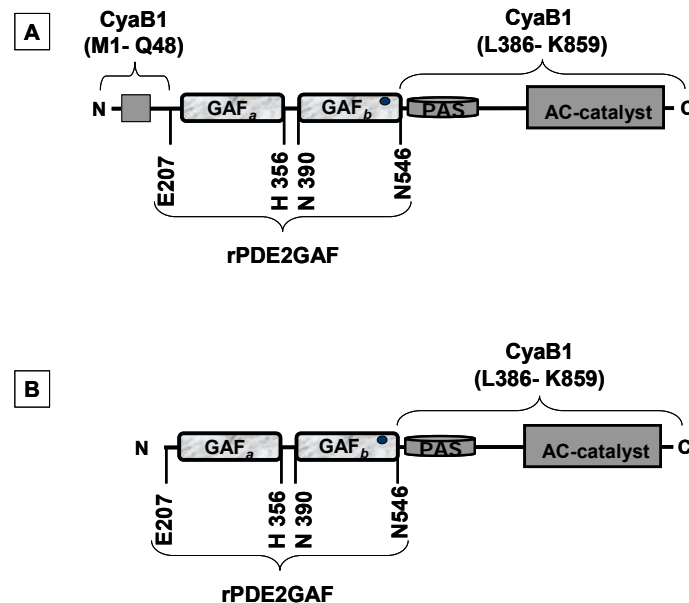


Fig. 4.20: Domain organization of (A) CyaB1N-rPDE2GAF/CyaB1 and (B) rPDE2GAF (207-546)/CyaB1. The grey circles in GAF_b domain indicate the noncatalytic binding site of cGMP.

For CyaB1N.rPDE2/CyaB1, the protein dependence was linear up to 300 nM and then decreased. For ΔN_{1-206} -rPDE2GAF/CyaB1, linearity of the protein dependence was up to 1.1 μ M (see fig.4.21).

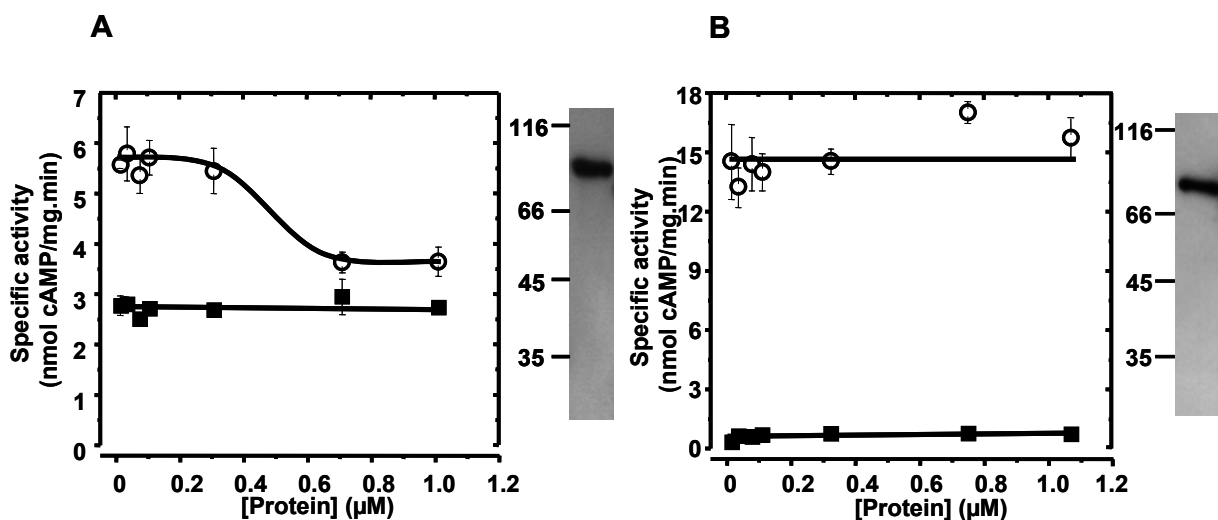


Fig. 4.21: Protein dependence (A) CyaB1N-ter.rPDE2GAF/CyaB1. (Western blot at right, 0.6 μ g) (B) ΔN_{1-206} -rPDE2GAF/CyaB1 (western blot, 0.1 μ g). (■) Basal activity, (○) +100 μ M cGMP. Assay conditions: 10 min, 37°C, 75 μ M Mg⁺²-ATP, 0.1M Tris/HCl pH 7.5 (n = 4)

Results

Dose response curves indicate lower fold stimulation of CyaB1N.rPDE2/CyaB1 (1.90 ± 0.046) compared to the N-terminally truncated construct (21.16 ± 0.538). The cGMP-EC₅₀ values were comparable (11.15 ± 1.84 versus 7.34 ± 0.62 respectively, $n = 4$) and the Hill coefficient of 0.419 ± 0.057 ($R^2 = 0.9803$) and 0.829 ± 0.02 ($R^2 = 0.9870$) for both constructs, respectively, show no cooperativity (fig. 4.22 and table 4.1)

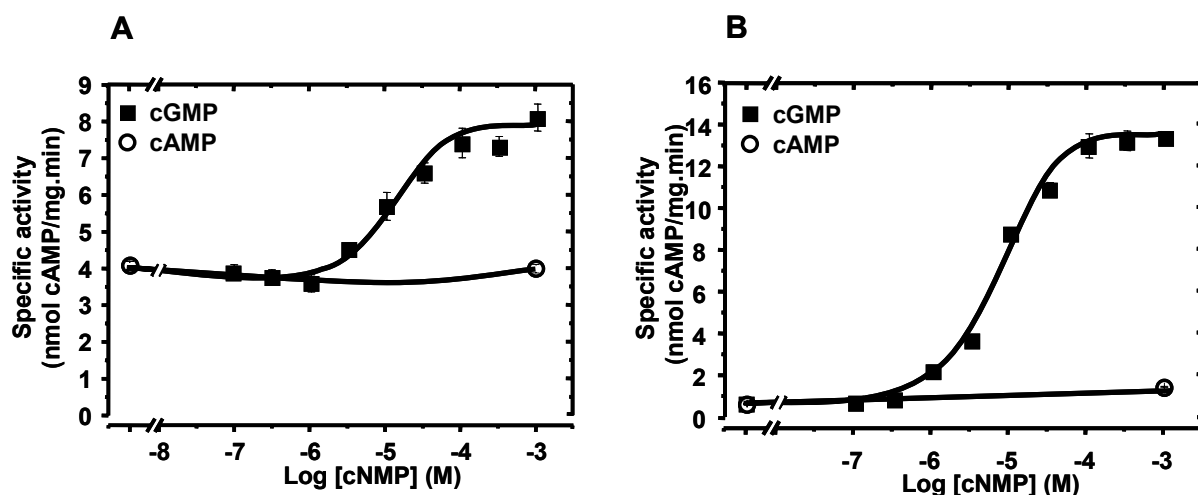


Fig. 4.22: Dose response of rPDE2 chimeras. Assay conditions: 10 min, 37°C, 75μM Mg²⁺-ATP, 0.1M Tris/HCl pH 7.5, 100 nM protein ($n = 4$). (A) CyaB1N-ter.rPDE2GAF/CyaB1 (B) Δ N₁₋₂₀₆-rPDE2GAF/CyaB1

Table 4.1: Summary of kinetic parameters of PDE2GAF/CyaB1 chimera compared to different N-termini inserted in the front of the GAF domain

construct	Basal activity	cGMP-EC ₅₀ (μM)	Stimulation factor (x)	Hill coefficient	figure
hPDE2NGAF/CyaB1	1.32 ± 0.08	9.92 ± 1.04	4.88 ± 0.24	0.477 ± 0.042 ($R^2 = 0.9754$)	4.4
hPDE5N-PDE2GAF/CyaB1	0.67 ± 0.078	3.67 ± 0.52	6.44 ± 0.315	0.56 ± 0.11 ($R^2 = 0.9909$)	4.13
(ΔN ₁₋₂₂₇ -hPDE2GAF/CyaB1	12.2 ± 0.8	7.68 ± 0.072	4.16 ± 0.092	0.469 ± 0.020 ($R^2 = 0.9760$)	4.20
CyaB1N-rPDE2GAF/CyaB1	4.1 ± 0.12	11.2 ± 1.84	1.90 ± 0.046	0.419 ± 0.057 ($R^2 = 0.9803$)	4.23-A
(ΔN ₁₋₂₀₆ -rPDE2GAF/CyaB1	0.63 ± 0.02	7.34 ± 0.62	21.16 ± 0.538	0.829 ± 0.02 ($R^2 = 0.9870$)	4.23-B

4.2 Role of the connecting helix of the GAF-tandem

Three GAF tandems, CyaB2, hPDE2 and hPDE5, have been selected for this study. The crystal structure of two of them has been solved, mouse PDE2 and CyaB2 [23, 24].

4.2.1 CyaB2 GAF tandem

4.2.1.1 Biochemical characterization of CyaB2 GAF/CyaB1 AC chimera

The chimera has been characterized [101]. In this chimera, the CyaB2 GAF (M1- K441) was swapped in front of the AC CyaB1 in pQE30 with an N-terminal His-tag (see fig. 4.23). The protein has a calculated MW of 104.58 kDa and isoelectric point of 5.44.

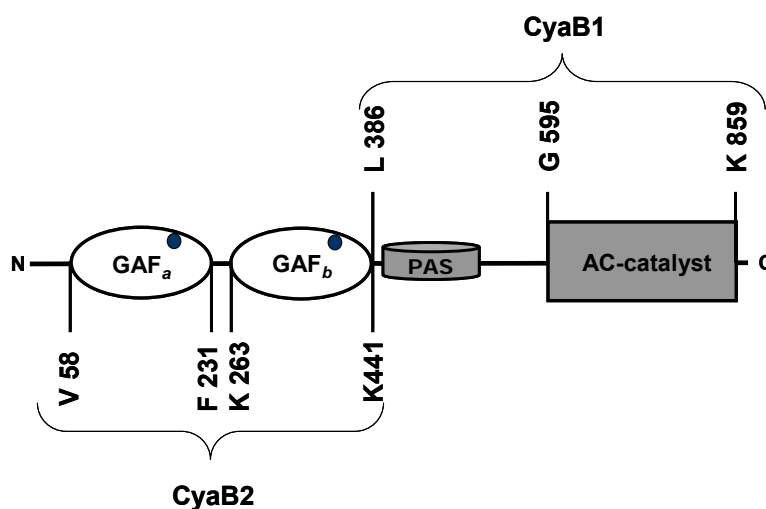


Figure 4.23: Domain organization of CyaB2NGAF/CyaB1 chimera showing the amino acid boundaries of each domain determined by its crystal structure. Circles on the GAF domain indicate binding sites of cAMP to both GAF motifs.

The protein was expressed in *E.coli* BL21(DE3)[pREP4] cells overnight at 19°C, lysed by French Press (twice) and purified by binding to 200 µl of Ni²⁺-NTA Agarose. The eluted protein was dialyzed against dialysis buffer overnight at 4°C to remove imidazole. 0.4 mg of protein was purified from 600 ml culture, and this was stable in 35% glycerol at -20°C (fig.4.24).

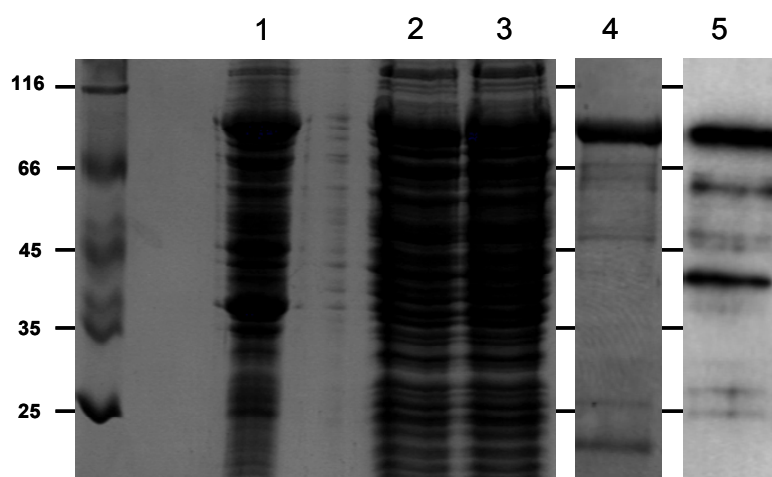


Fig. 4.24: SDS-PAGE (12.5%) of CyaB2NGAF/CyaB1 (1) pellet (2) Supernatant (3) Supernatant after Ni-NTA (4) Purified protein (4 µg) (5) Western blot (0.2 µg)

The protein dependence (fig. 4.25.A) was linear. A slight decrease in activity was observed at high concentration. The dose response curve (fig.4.25.B) shows a large activation by cAMP (747 ± 82 fold; $n = 4$). The EC_{50} for cAMP was 0.53 ± 0.013 µM ($n = 4$). A Hill coefficient of 2.84 ± 0.30 ($R^2 = 0.9231$, $n = 4$) shows positive cooperativity [101].

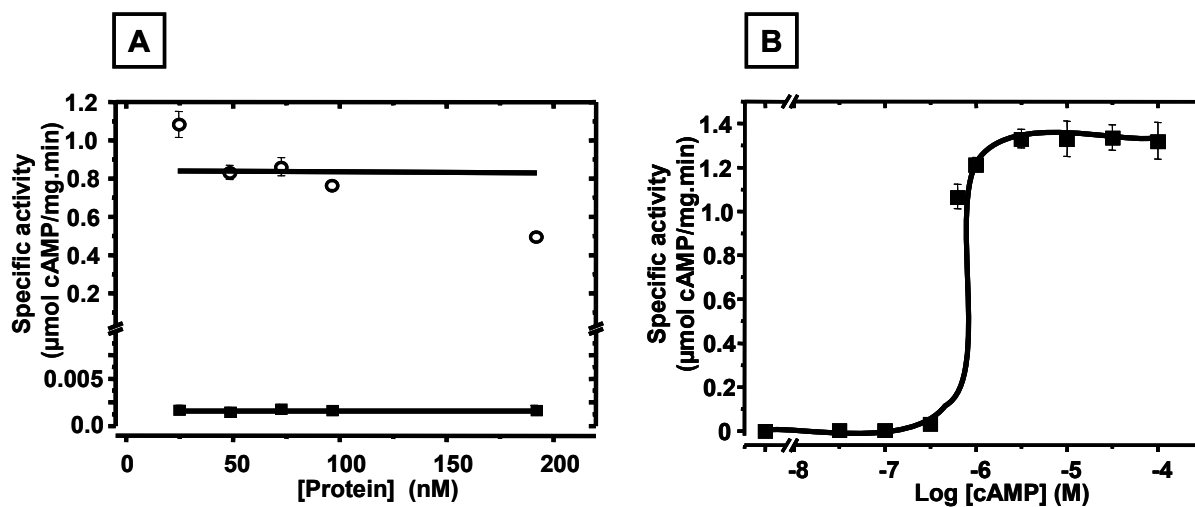


Fig. 4.25: (A) Protein dependence study of CyaB2NGAF/CyaB1 chimera. Assay condition: 37°C, 75 µM ATP, 4 min and Tris/HCl pH 7.5. (■) Unactivated protein (○) +1 mM cAMP (B) cAMP-dose response of CyaB2GAF/CyaB1 chimera. Assay conditions: 37°C, 75 µM ATP, 4 min and 0.1 M Tris/HCl pH 7.5, 20 nM protein ($n = 4$).

4.2.1.2 Role of connecting helix length

According to the crystal structure of CyaB2 GAF (figure 4.26) [17], the boundaries of the GAF connecting helix were between F231-K263. The connecting helix was aligned with the connecting helices of CyaB1 and different PDE-GAF domains. Similarity was poor (fig.4.27). A leucine or isoleucine and two hydrophobic residues (either methionines or leucines) were

the only conserved residues. An accidental mutation of the first methionine of CyaB2 to threonine (M258T) reduced the fold-stimulation by cAMP (unpublished data). Here, I studied the effect of insertion or deletion of aa's or the exchange with the connecting helix from CyaB1 on signal transduction.

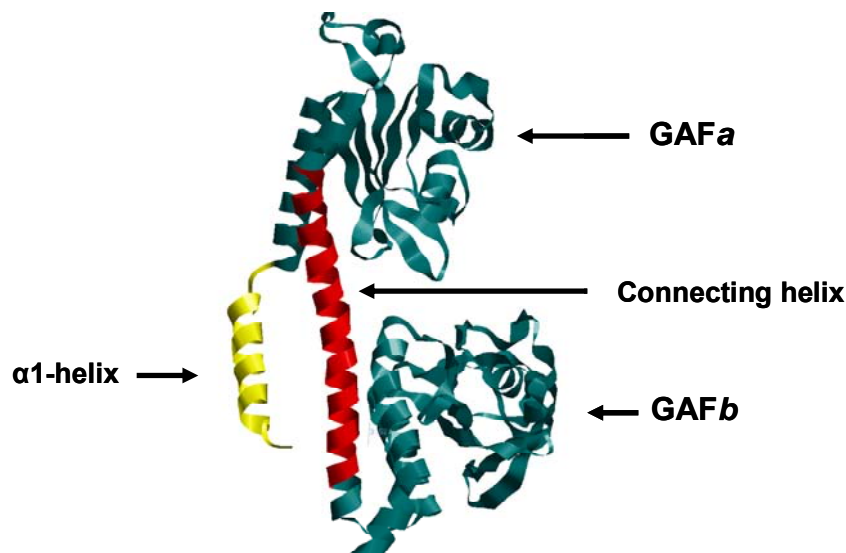


Fig. 4.26: Crystal structure of CyaB2 GAF from [23], showing the GAFa α 1 helix (V58-H78) (yellow) and connecting helix (F231-K263) (red) in addition to GAFa and b (green)

CyaB1	: FAASIGIIL ETCQSFYVAARNQRGVT ALL RATQ	: 229
CyaB2	: FAPSIRLI LESSRSFYIATQKQRAAA AM MKAVK	: 263
hPDE2	: CFHYTSTV LTSTLAFQKEQ KLKCECQ ALLQ VAK	: 401
hPDE5	: YLAFCGIV LHNAQLYETS LLENKRNQV LLDLAS	: 338
hPDE6α	: YLN FVSIILRLHHTSYMYNIESRRSQI LM WSAN	: 248
hPDE10	: NLAWASVA IHQVQVCRGLAKQTELNDFLLD VSK	: 193
hPDE11A4	: YLPFCGIA ISNAQLFAASR KEYERSR ALLE VVN	: 394
mPDE2	: CFHYTGTV LTSTLAFQKEQ KLKCECQ ALLQ VAK	: 377

Figure 4.27: ClustalW alignment of the GAF connecting helices of PDEs, CyaB1 and CyaB2. red: 100% similarity, grey: 80% similarity, blue: 60% similarity residues and Black: <60% similarity.

Due to high affinity toward cAMP and high fold-stimulation, the CyaB2 GAF/CyaB1 chimera was selected for this study. Hence, any change in the affinity or fold-stimulation will be easily observed.

4.2.1.2.1 Shortening of the connecting helix

Each amino acid in an α -helix contributes to 100° of the turn which means that 3.6 amino acids are required to form one turn. To shorten the connecting helix between the two GAF motifs, deletion of up to one turn of the α -helix was suggested. Four constructs have been

Results

cloned, in which 1, 2, 3 or 4 aa's were deleted. RAAA which precede the two conserved hydrophobic amino acids were selected. The three alanines of the RAAA in CyaB2 are not conserved (Fig.4.27).

The four constructs were cloned in pQE30 with N-terminal His-tag, expressed in *BL21 (DE3) [pREP4] E. coli* (30 μ M IPTG, 10 mM MgCl₂ at 18°C, overnight). The proteins were purified by shaking with 350 μ l Ni²⁺-NTA agarose for 90 min. The 104-kDa purified proteins were dialysed overnight against dialysis buffer and assayed. All proteins had good expression and little degradation on the western blot (fig.4.28).

The protein dependence of the four constructs is shown in figure 4.28. Two constructs, (Δ R253)/CyaB1 (curve A) and CyaB2 (Δ R253-A255)/CyaB1 (curve C), have the same profile, a linear increase which levels off. Both constructs reached similar specific activity for both the activated and the unactivated states. In CyaB2 (Δ R253-A254)/CyaB1 (curve B) and CyaB2 (Δ R253-A256)/CyaB1 (curve D), the linearity continued but with different slopes. The specific activities were lower for these two constructs.

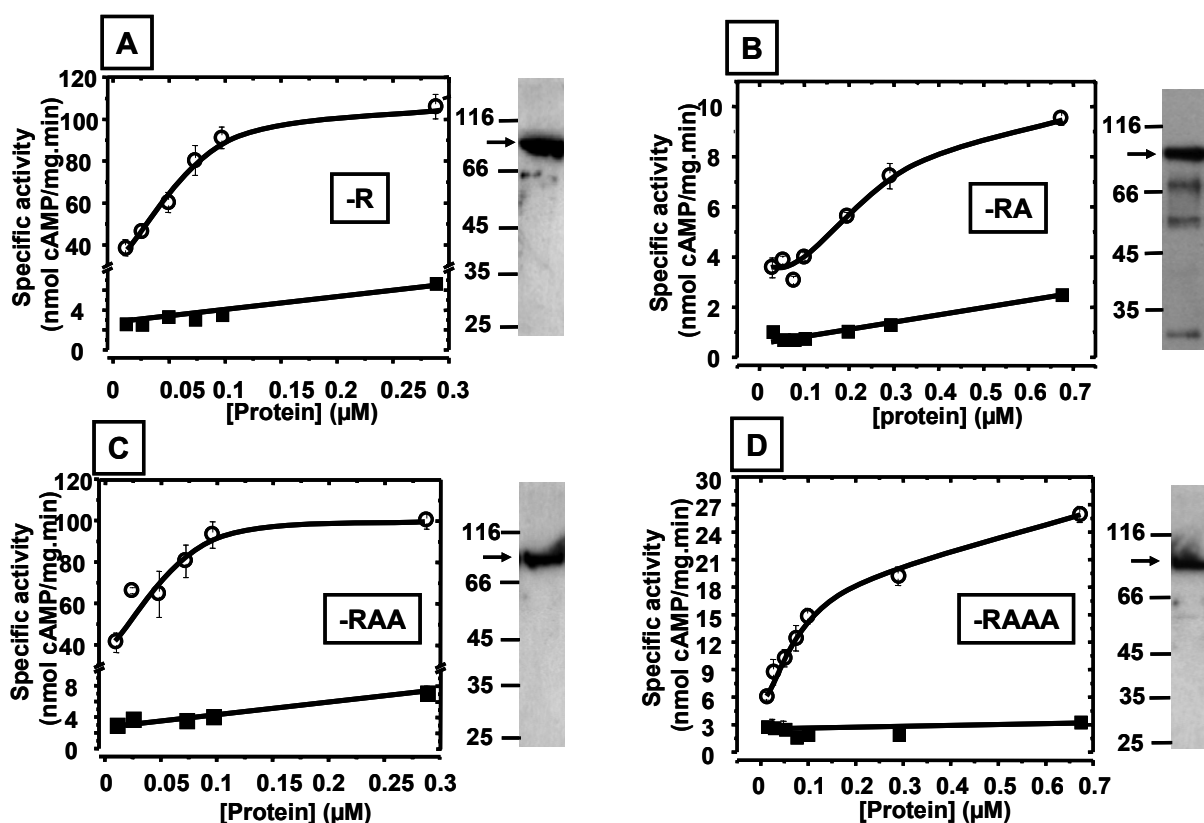


Fig. 4.28: Protein dependence of CyaB2 shortened GAF chimeras. Assay conditions: 4 min, 37°C, 75 μ M ATP, 10 mM MgCl₂, 0.1M Tris/HCl pH 7.5 (n = 4). (■) Unactivated protein (○) +1 mM cAMP (A) CyaB2 (Δ R253)/CyaB1 (B) CyaB2 (Δ R253-A254)/CyaB1 (C) CyaB2 (Δ R253-A255)/CyaB1 (D) CyaB2 (Δ R253-A256)/CyaB1, the Western blot is shown to the right of each curve (0.2 μ g)

Results

Next, cAMP-dose response curves were performed for the four constructs (Figure 4.29). CyaB2 ($\Delta 253$)/CyaB1 has a stimulation factor of 31.1 ± 2.43 , an EC_{50} of 16.3 ± 3.40 and a Hill coefficient of 0.7880 ± 0.040 ($R^2 = 0.9766$) (fig.4.29.A). CyaB2 ($\Delta 253-254$)/CyaB1 has a fold-stimulation of 3.35 ± 0.32 , an EC_{50} of 14.9 ± 1.7 and a Hill coefficient of 0.4577 ± 0.054 ($R^2 = 0.9793$) (Fig.4.29.B). CyaB2 ($\Delta 253-255$)/CyaB1 has a fold-stimulation of 21.4 ± 1.26 , an EC_{50} of 17.9 ± 2.00 and a Hill coefficient of 0.5474 ± 0.034 ($R^2 = 0.9801$) (Fig.4.29.C) and CyaB2 ($\Delta 253-256$)/CyaB1 has a fold-stimulation of 4.88 ± 0.44 , an EC_{50} of 335 ± 1.00 , and a Hill coefficient of 0.262 ± 0.013 ($R^2 = 0.9833$) for (Fig.4.29.D). Basal activities and other parameters are summarized in table 4.2.

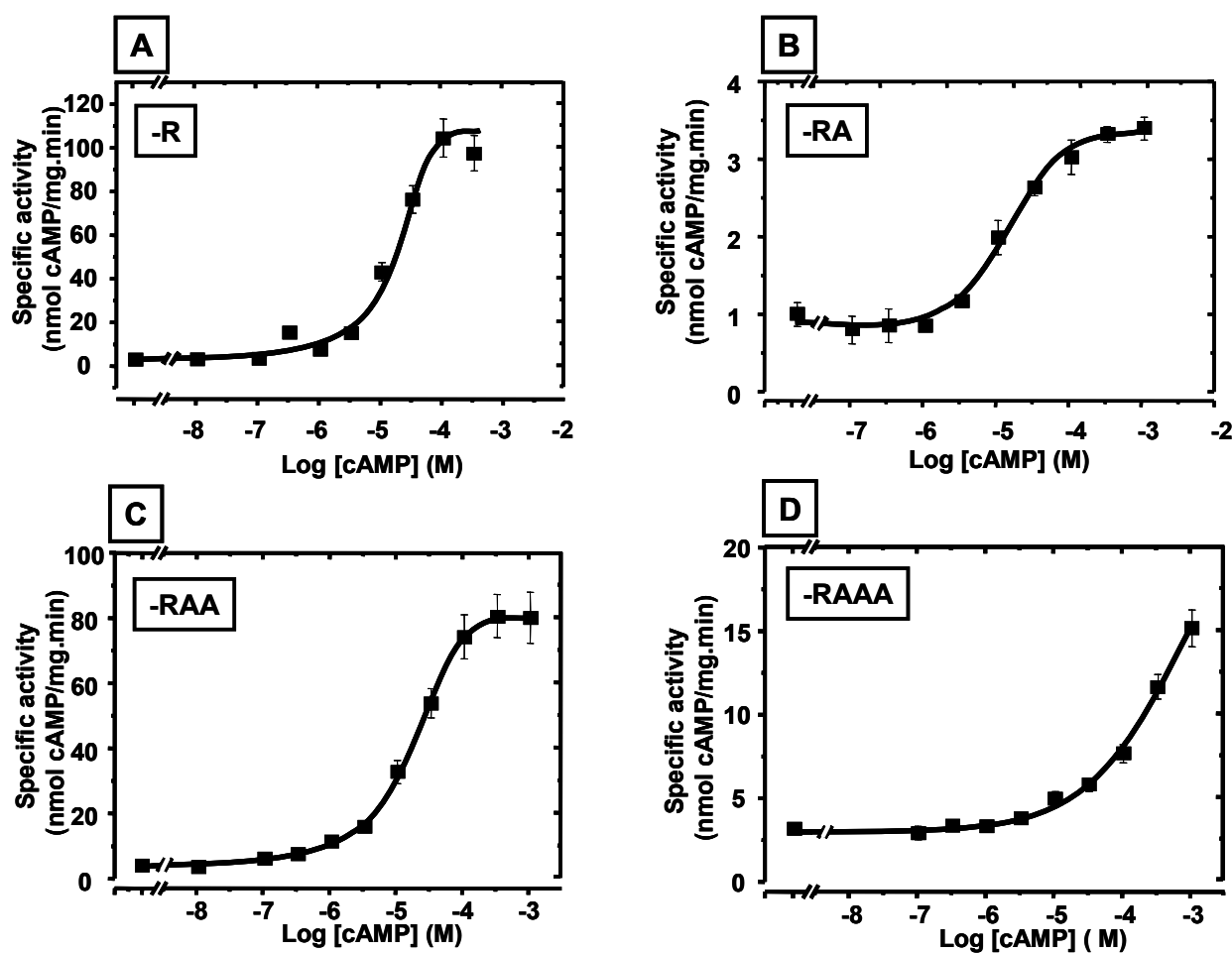


Fig. 4.29: Dose response curve of CyaB2 shortened GAF chimeras (A) CyaB2 ($\Delta R253$)/CyaB1 (B) CyaB2 ($\Delta R253-A254$)/CyaB1 (C) CyaB2 ($\Delta R253-A255$)/CyaB1 (D) CyaB2 ($\Delta R253-A256$)/CyaB1. Assay conditions: 4 min, 37°C, 0.1M Tris/HCl pH 7.5, 75 μ M ATP, 20-50 nM protein (n = 4).

4.2.1.2.2 Elongation of the connecting helix

A flexible sequence (NAAIRS) has been established as an appropriate tool [102, 103]. This motif fits in any molecular structure of the protein without affecting its folding. Here, the connecting helix of CyaB2 GAF is elongated by 3-4 amino acids from the above motif (~1

Results

turn) in the middle of the helix. Two constructs (CyaB2 (256+NAA)/CyaB1 and CyaB2 (256+NAAI)/CyaB1) were generated. They were cloned, expressed and purified as mentioned above (section 4.2.1.2.1). CyaB2 (256+NAA)/CyaB1 was expressed and purified as intact protein while CyaB2 (256+NAAI)/CyaB1 was degraded during purification. Unlike the shortened constructs, both elongated ones had a linear protein dependency (Fig.4.30.A and B). The western blots of both constructs, CyaB2 (256+NAA)/CyaB1 showed a single band with little degradation while CyaB2 (256+NAAI)/CyaB1 showed only two bands of degradation products. Longer exposure of the film had shown a very thin band at the correct size of the protein. In AC assay, the amount of the protein was estimated to be 1% of the measured concentration and according to that the specific activities of protein dependence and dose response assays were calculated.

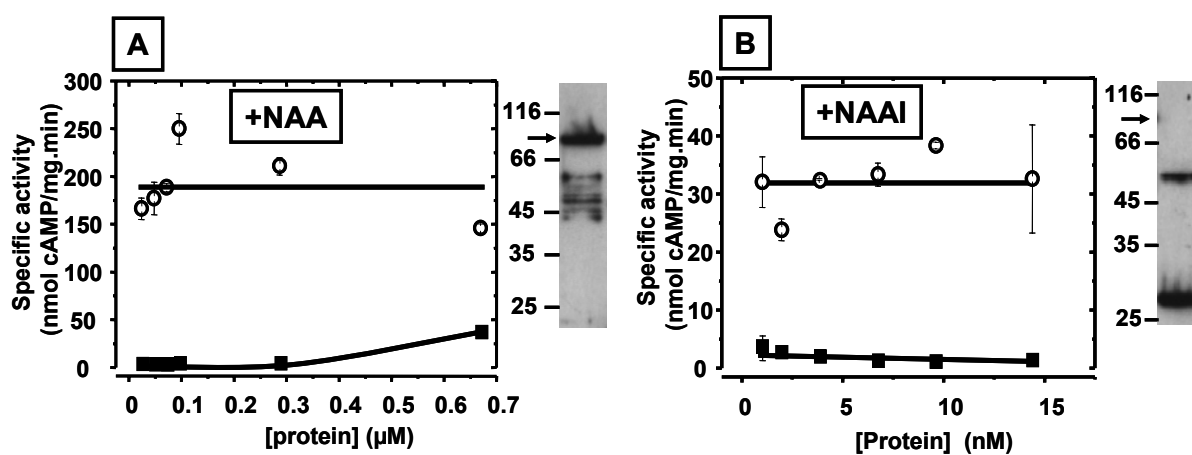


Fig. 4.30: Protein dependence of the elongated constructs. Assay conditions: 4 min, 37°C, 0.1M Tris/HCl pH 7.5, 75 µM ATP (n = 4). **(A)** CyaB2 (256+NAA)/CyaB1 **(B)** CyaB2 (256+NAAI)/CyaB1. Western blots are on the right.

CyaB2 (256+NAA)/CyaB1 (fig.4.31.A) was stimulated 54.1 ± 6.6 fold with an EC_{50} of 10.6 ± 0.28 and a Hill coefficient of 0.8212 ± 0.068 ($R^2 = 0.9833$). CyaB2 (256+NAAI)/CyaB1 curve (figure 4.31.B) shows a fold-stimulation of 42.43 ± 5.01 , an EC_{50} of 8.11 ± 1.10 and Hill coefficient of 0.722 ± 0.051 ($R^2 = 0.9828$) which are similar to the values obtained by CyaB2(256+NAA)/CyaB1.

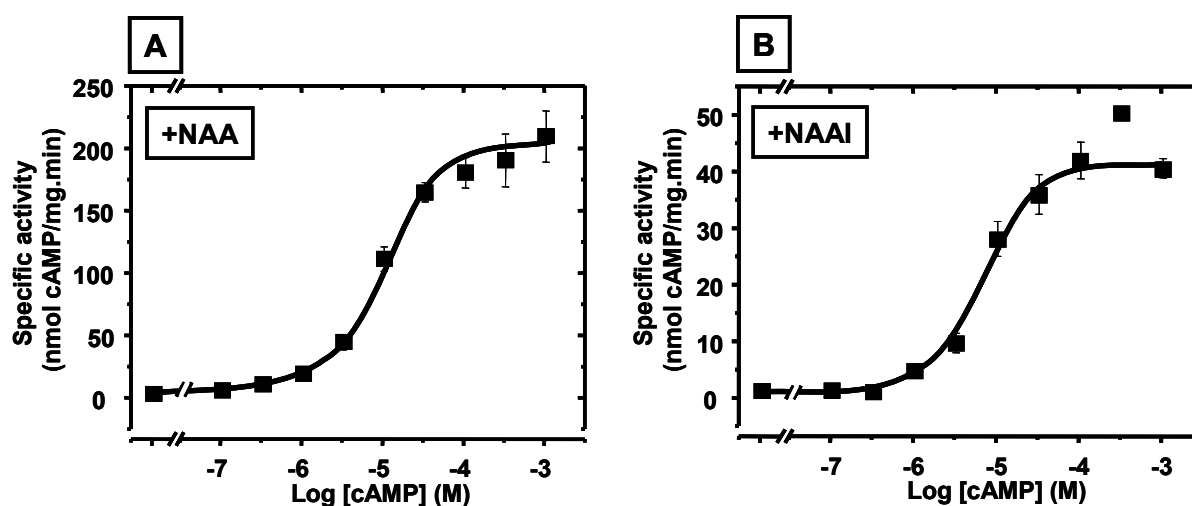


Fig. 4.31: Dose response curve of CyaB2 elongated GAF constructs. Assay condition: 4 min, 37°C, 75 μ M Mg+2-ATP, 0.1M Tris/HCl pH 7.5 (n = 4). **(A)** CyaB2 (256+NAA)/CyaB1, 20 nM protein. **(B)** CyaB2 (256+NAAI)/CyaB1, 9 nM protein.

4.2.1.2.3 Exchange of the connecting helix

Next, the whole connecting helix was exchanged with that of CyaB1 (Fig.4.32). The region (P233-K263) was replaced by the same number of amino acids (A199-Q229) from CyaB1.

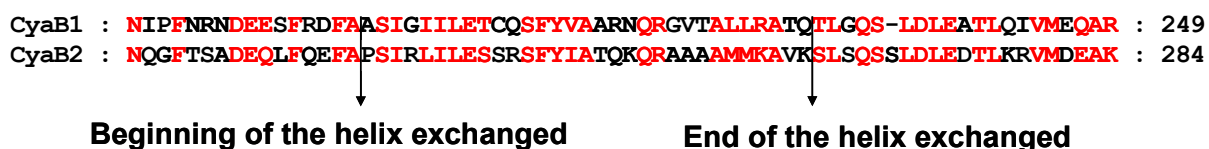


Fig.4.32: ClustalW alignment of CyaB1 and CyaB2 connecting helix region showing the amino acids exchanged between CyaB2 and CyaB1 tandem GAFs.

The chimera was cloned (section 3.4.2.10), expressed at different concentrations of IPTG at 18°C (fig.4.33) and purified as the CyaB2 wild type chimera. Expression using 30 μ M IPTG have the least degradation. Lowering the temperature to 16°C increased degradation.

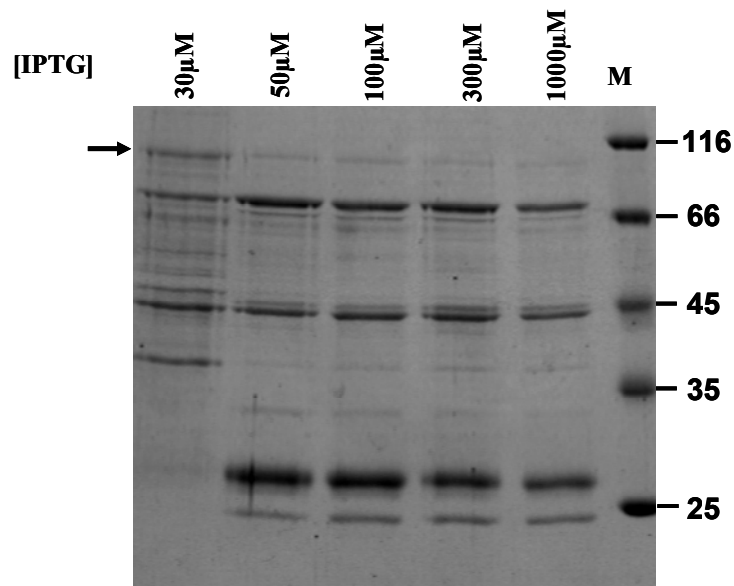


Fig.4.33: SDS-PAGE (12.5%) of optimization of expression conditions of CyaB2 (CyaB1 connecting helix)/CyaB1 chimera at different concentration of IPTG and 18°C.

According to the dose-response curve (Fig.4.34), the stimulation factor of CyaB2GAF (CyaB1 connecting helix)/CyaB1 was 181.4 ± 26.1 , the cAMP-EC₅₀ was 0.62 ± 0.146 and Hill coefficient was 0.912 ± 0.018 ($R^2 = 0.9581$, $n = 4$)

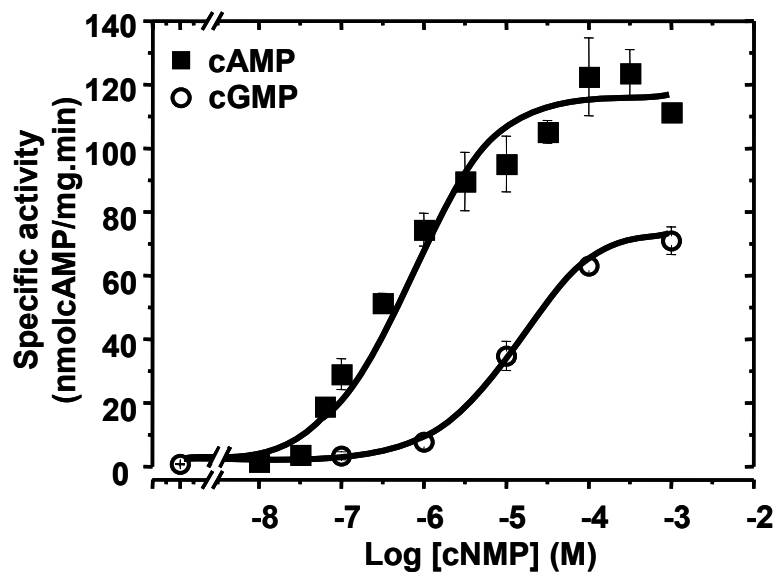


Fig.4.34: Dose response curve of CyaB2GAF (CyaB1 connecting helix)/CyaB1 Assay conditions: 37°C, 75 μ M ATP, 0.1M Tris/HCl pH 7.5, 4 min, 92 nM protein ($n = 4$)

Results

Table 4.2: Summary of the different parameters for constructs of deleted or inserted aa's compared to those of CyaB1 (WT) chimera

Construct (aa inserted or deleted)	Basal activity (nmol/mg.min)	EC ₅₀ (μM)	Fold- stimulation (by cAMP)	Hill coefficient (R ² is between parenthesis)	figure
CyaB2NGAF/CyaB1 (wild type)	1.85 ± 0.216	0.53 ± 0.013	747± 82	2.84 ± 0.3 (0.9223)	4.25.B
CyaB2 (Δ253)/CyaB1 (-R)	3.39 ± 0.440	16.3 ± 3.40	31.1 ± 2.43	0.788 ± 0.040 (0.9766)	4.29.A
CyaB2 (Δ253-254)/ CyaB1 (-RA)	1.04 ± 0.152	14.9 ± 1.7	3.35 ± 0.32	0.458± 0.054 (0.9793)	4.29.B
CyaB2 (Δ 253-255)/ CyaB1 (-RAA)	3.77 ± 0.185	17.9 ± 2.00	21.4 ± 1.3	0.547 ± 0.034 (0.9801)	4.29.C
CyaB2 (Δ 253-256)/ CyaB1 (-RAAA)	3.23 ± 0.434	335 ± 1.00	4.9 ± 0.44	0.26 ± 0.013 (0.9833)	4.29.D
CyaB2 (256+NAA)/CyaB1 (+ NAA)	4.34 ± 1.143	10.6 ± 0.28	54.1 ± 6.6	0.82 ± 0.07 (0.9833)	4.31.A
CyaB2 (256+NAAI)/CyaB1 (+NAAI)	1.22 ± 0.28	8.11 ± 1.10	42.43 ± 5.01	0.72 ± 0.05 (0.9828)	4.31.B
CyaB2GAF(CyaB1 connecting helix)/ CyaB1	0.74 ± 0.133	0.62 ± 0.146	181.4 ± 26.1	0.91 ± 0.02 (0.9581)	4.34

4.2.1.3 Crystallization of CyaB2 (Δ R253-A255) and CyaB2 (256+NAA)

In order to understand the conformational changes caused by shortening or elongation of the GAF connecting helix, attempts to crystallize one construct of each group were carried out.

4.2.1.3.1 CyaB2GAF (Δ R253-A255)

The coding region for amino acids V58-Q445 of CyaB2 was amplified by PCR using non-mutated primers and CyaB2 (ΔR253-A255)/CyaB1 as template and subcloned into the expression vector pQE60. The resultant plasmid pQE-CyaB2 (ΔR253-A255) was transferred into *E. coli* strain *BL21 (DE3)[pREP4]* for overexpression (0.3 mM IPTG, 22°C for 5-7 hr). The recombinant CyaB2 (Δ R253-A255) protein was purified by binding to 200 μl of Ni²⁺-NTA agarose slurry for 3 hr. The purification yielded 1.8 mg with a purity >95% from 600 ml cell culture. The C-terminal His-tagged protein has a calculated molecular weight of 43.92 kDa. The expression, size and purity of the protein were evaluated by SDS-PAGE and western blot (fig. 4.35)

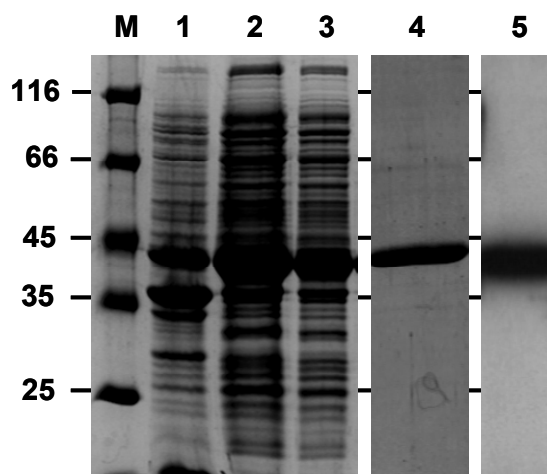


Fig.4.35: SDS-PAGE (12.5%) of CyaB2 (Δ R253-A255)cr (**M**) PeqGold protein marker (**1**) Pellet (**2**) Supernatant (**3**) Supernatant after Ni²⁺-NTA (**4**) Purified protein (2 μ g) (**5**) Western blot (0.2 μ g)

The size exclusion chromatography of the protein produced a one peak-profile with a calculated MW of 84.6 kDa proves a dimer (42.3 kDa for the monomer) and this is consistent with the calculated MW mentioned above (Fig.4.36).

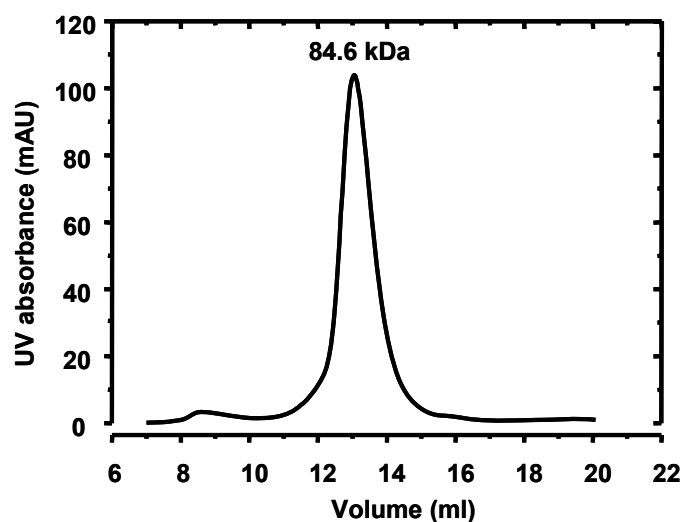


Fig. 4.36: Gel filtration of CyaB2 (Δ R253-A255)cr using Supradex 200 (50 mM Tris/HCl pH 7.5, 200mM NaCl, 10% glycerol and 2 mM MgCl₂), No fractions were collected.

The protein was dialyzed overnight at 4°C against the crystallization buffer, concentrated by ultrafiltration to 21.5 mg/ml, mixed with 2 mM cAMP and screened by crystal screen I, II and lite (from Hampton) using the hanging drop vapour diffusion method and the plates were kept at 12°C and examined.

Large separated plates (300 × 200 μ m) or rod clusters (300 × 50 μ m) appeared one week later in Crystal screen II # 23 (1.6 M ammonium sulphate, 0.1M MES pH 6.5 and 10% v/v 1,4-dioxane). Although the crystals were large, their thickness didn't exceed 15 μ m, and that was

Results

not enough for having an image with good resolution. Further optimization of the size and form of the crystals was performed (see table 4.3).

Table 4.3: optimization of the crystals of obtained CyaB2 ($\Delta R253-A255$)cr

Fixed condition	Variable	Result
0.1M MES pH 6.5 1.6M (NH ₄) ₂ SO ₄ , 21.5 mg/ml protein, 12°C	1,4-dioxane (5,10,15,20,30%)	10%1,4-dioxane was the only concentration which gave crystals (300 × 30)
10% 1,4-dioxane, 0.1M MES pH 6.5, 21.5 mg/ml protein, 12°C	(NH ₄) ₂ SO ₄ (M) (0.8,1.6,2.0,2.4, 3.2)	Only 1.6M (NH ₄) ₂ SO ₄ gave crystals
10% 1,4-dioxane, 0.1M MES pH 6.5, 21.5 mg/ml protein, 12°C	1.6M of different salts	None of the salts gave crystals so (NH ₄) ₂ SO ₄ was a second precipitant.
10% 1,4-dioxane, 1.6M (NH ₄) ₂ SO ₄ , 21.5 mg/ml protein, 12°C	Buffer and pH Acetate and MES pH< 6.5 MES pH 6.5 Tris/HCl pH 7.5-9.0	No crystals (only precipitate) Large crystals (300 × 30) Different sizes of crystals with the largest with pH 7.5.

Different sizes of plate-shaped crystals have been obtained but with a maximum thickness of 30 μm . Some of the crystals were measured by Dr. Schal from the department of Biochemistry, Tübingen University, but the resolution was 8 Å upon diffraction. No further optimization has been done. The shape and size of the crystals obtained by the first trial and by optimization are shown in Fig.4.37.

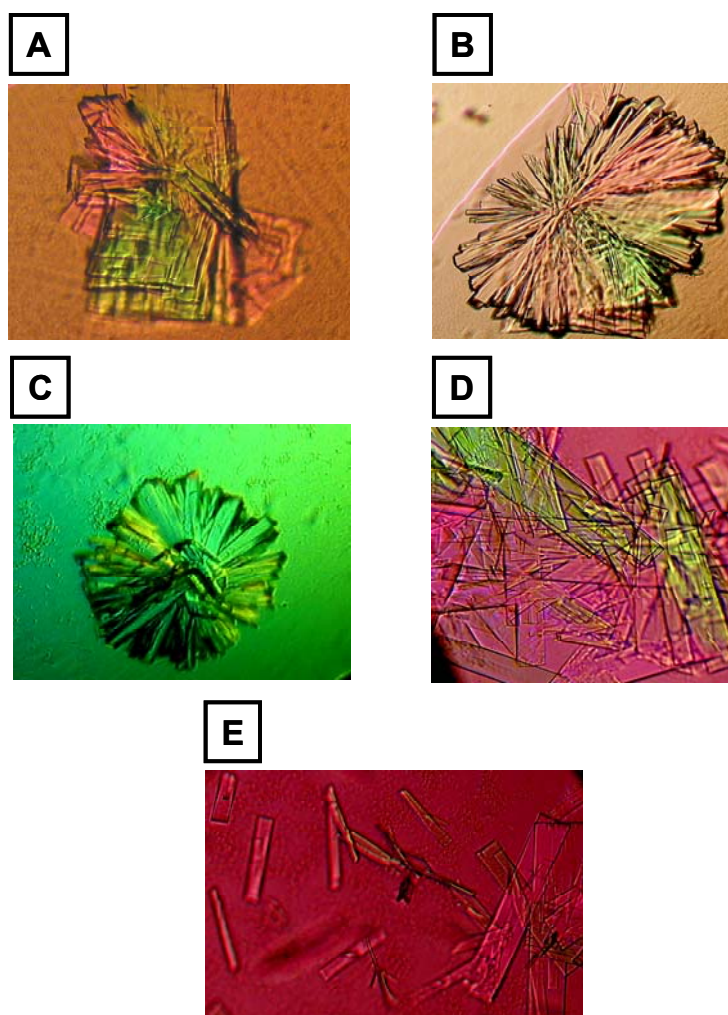


Fig. 4.37: Crystals of CyaB2 (Δ R253-A255)cr (A and B) Initial crystallization trials by crystal screen II # 23 (C) The reproducibility of the crystallization by my own solutions (D) Crystals optimized by 10% dioxane 0.1M Tris/HCl pH 7.5, 1.6M $(\text{NH}_4)_2\text{SO}_4$ (E) Crystals obtained by 10% dioxane, 0.1M Tris/HCl pH 8.5, 1.6M $(\text{NH}_4)_2\text{SO}_4$.

4.2.1.3.2 CyaB2GAF (256 + NAA)cr

The cloning, overexpression and purification of CyaB2 (256+NAA)cr used the same protocols as for CyaB2 (Δ R253-A255)cr. The resulting protein has a calculated MW of 44.47 kDa and excellent purity (fig.4.38, A). Crystallization was set as mentioned before, but no crystals were obtained after time interval reaches to one year. The gel filtration of 200 μ l (2 mg/ml) of the purified protein shows a dimer of 81.2 kDa (40.6 kDa for the monomer) (see Fig.4.38, B)

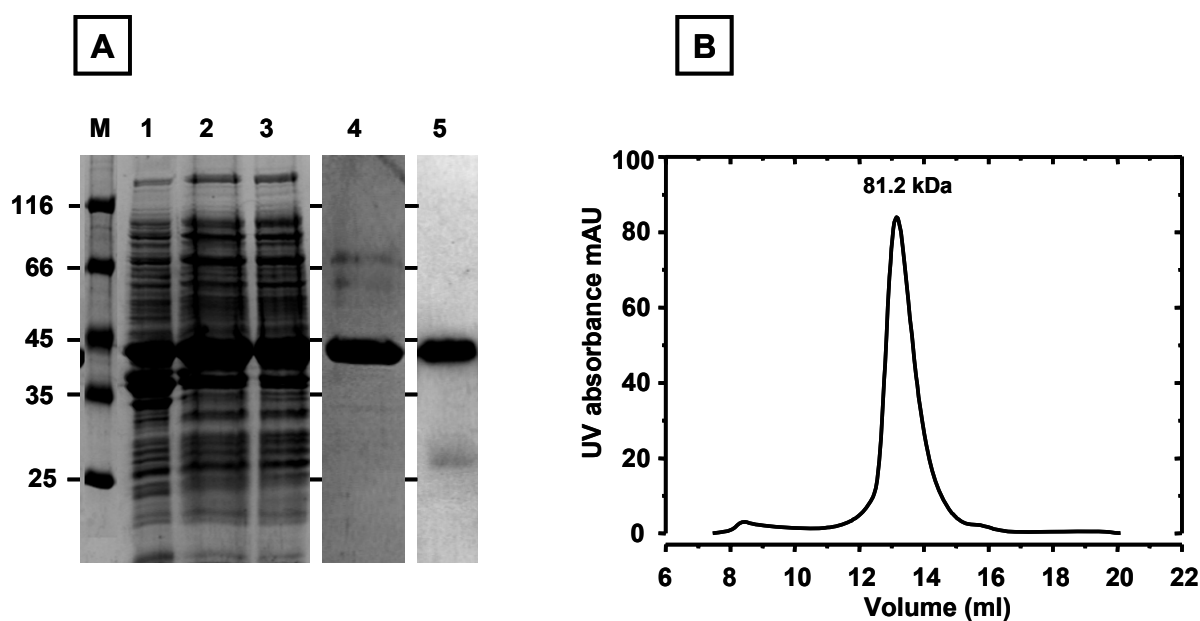


Fig. 4.38: (A) SDS-PAGE of CyaB2 GAF (256+NAA)cr (M) PeqGold protein marker (1) Pellet (2) Supernatant (3) Supernatant after Ni-NTA (4) Purified protein (2 μ g) (5) Western blot (0.2 μ g) (B) Gel filtration of 40 μ g of CyaB2 (256+NAA) showing single peak for a dimer. No fractions were collected.

4.2.1.4 Mutation of GAF α – helices

4.2.1.4.1 α 1 – helix

according to results obtained from shortening and elongation of the CyaB2 GAF connecting helix and the dramatic decrease in the fold stimulation and affinity to cAMP, I have observed another 2 similar hydrophobic aa's (methionine, leucine or isoleucine) in the α 1–helix in the alignment prepared by Martinez et al [24]. All α 1–helices of CyaB and PDE GAF α domains were aligned (fig.4.39) and the alignment showed the poor homology in the presumed α 1–helix.

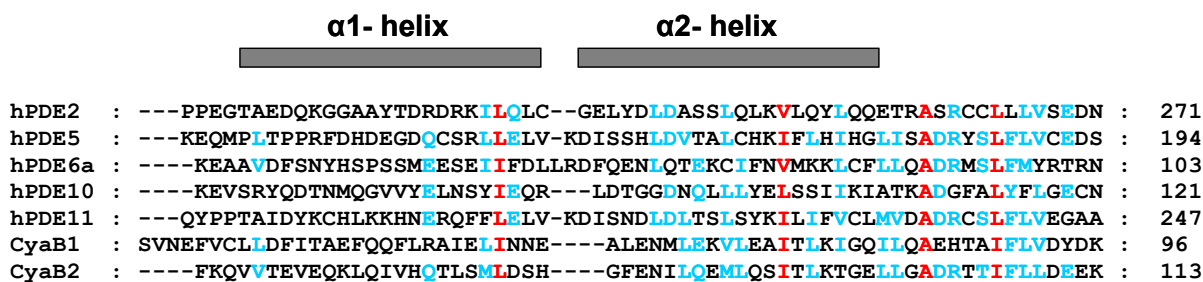


Fig.4.39: Alignment of cyanobacterial AC's and human PDE's α 1-helices preceding the GAFa domain determined according to the crystal structure of mouse PDE2 and CyaB2

In CyaB2, these residues are methionine and leucine (ML). M74 and L75 were either mutated to Glycines or to M74S and L75T which are hydrophilic in nature. The protein dependence curves (fig.4.40) were not linear over the tested range.

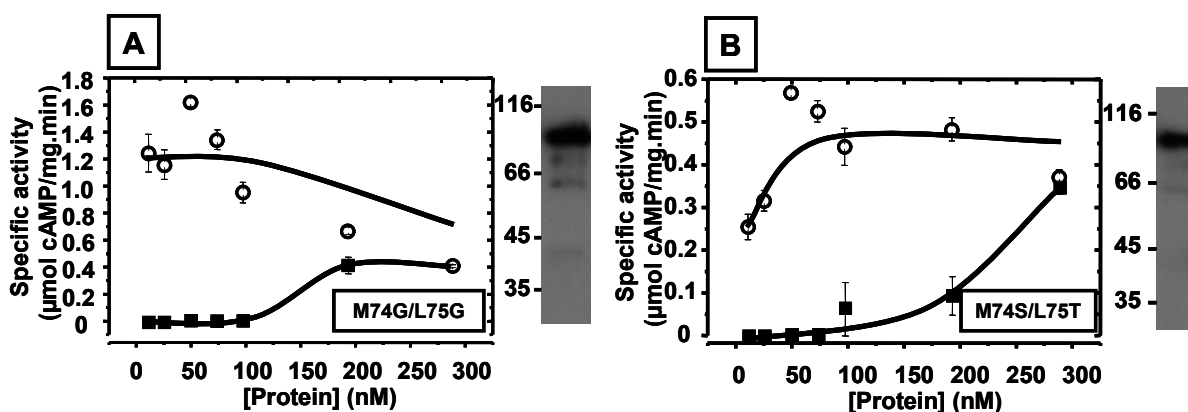


Fig. 4.40: Protein dependence (A) CyaB2 (M74G/L75G)/CyaB1 (B) CyaB2 (M74S/L75T)/CyaB1. Assay conditions: 4 min, 37°C, 0.1M Tris/HCl pH 7.5, 75 μ M ATP, 10 mM MgCl₂ (n = 4)

The cAMP-dose response of CyaB2 (M74G/L75G)/CyaB1 (fig.4.41) shows a 261 fold stimulation (± 14.4), and cAMP-EC₅₀ of $7.95 \pm 0.17 \mu$ M. CyaB2 (M74S/L75T)/CyaB1 mutant has 133 fold stimulation (± 13.9) and cAMP-EC₅₀ of $4.16 \pm 0.3 \mu$ M. The Hill coefficients of both mutants were showing no or little cooperativity (1.19 ± 0.02 ($R^2=0.9877$), 1.29 ± 0.07 ($R^2=0.9758$), respectively).

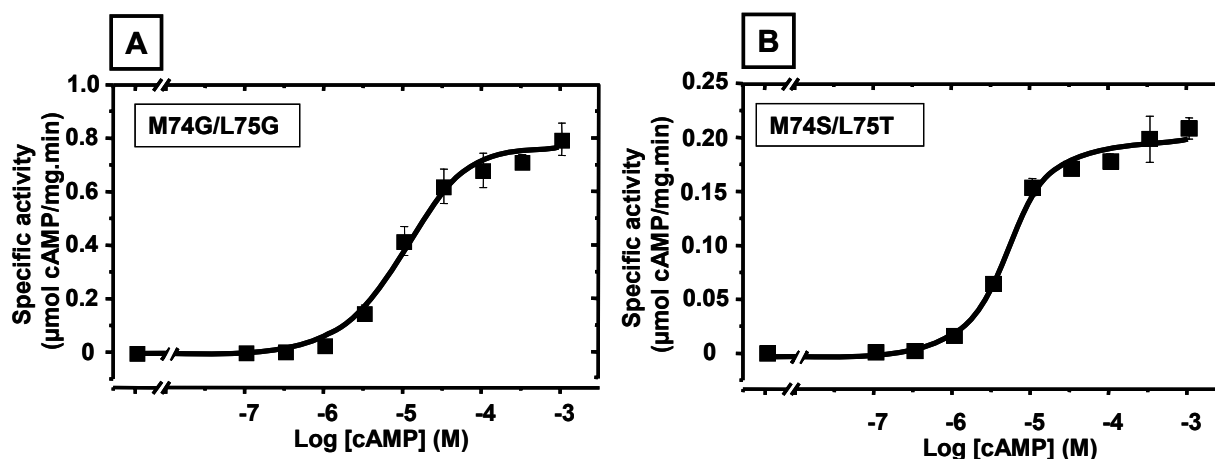


Fig. 4.41: Dose response of (A) CyaB2 (M74G/L75G)/CyaB1 (B) CyaB2 (M74S/L75T)/CyaB1. Assay conditions: 4 min, 37°C, 0.1M Tris/HCl pH 7.5, 75 μM ATP, 10 mM MgCl_2 , 25 nM protein (n = 4)

4.2.1.4.2 α 2- helix

Similar to the ML residues in α 1-helix, another ML residues were observed in the α 2- helix of CyaB2. Single mutation of each one of them to serine followed by double mutation for both of them to alanine/serine produced three different constructs.

The protein dependence curves of the three mutants (Fig.4.42) showed an increase in the specific activity by increasing the protein concentration which levels off at a concentration of 100 nM.

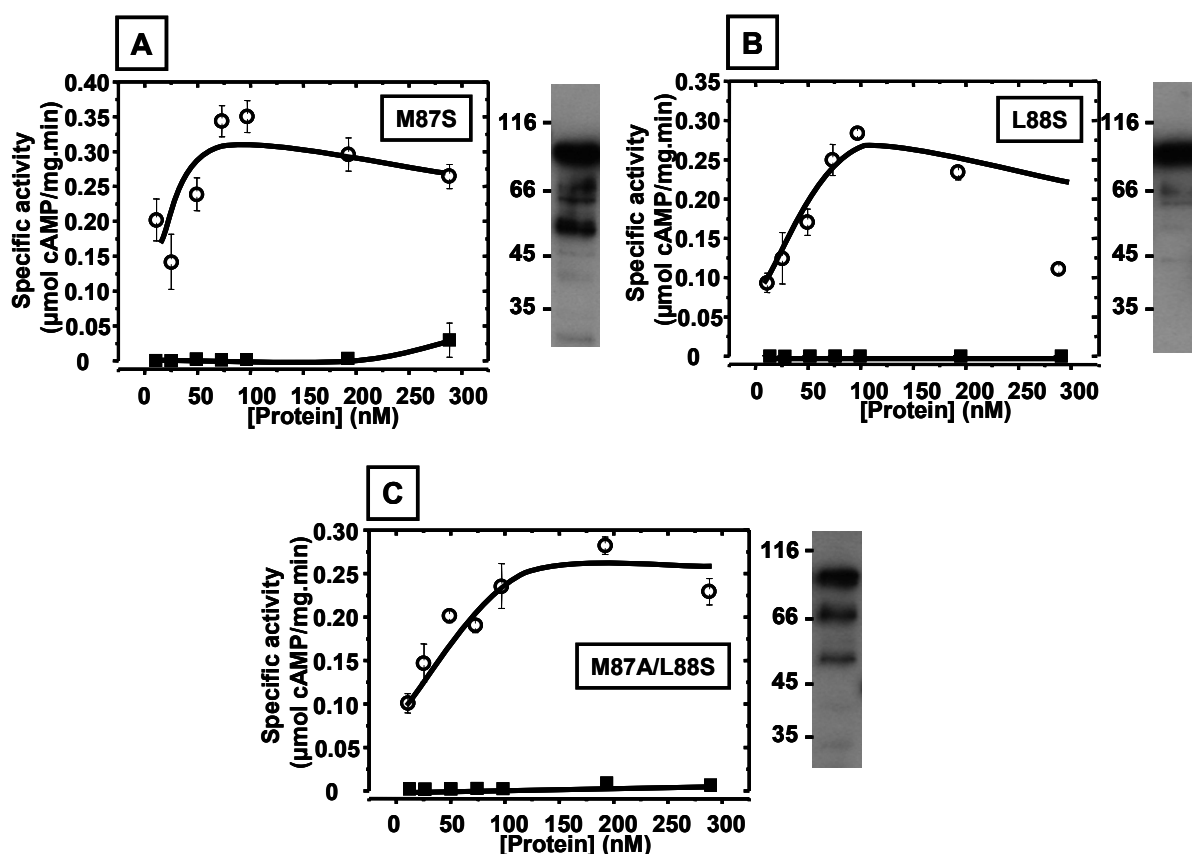


Fig. 4.42: Protein dependence of $\alpha 2$ -helix mutants. Assay condition: 4 min, 37°C, 75 μM ATP, 10 mM MgCl_2 , 0.1M Tris/HCl pH 7.5 (A) CyaB2 (M87S)/CyaB1 (B) CyaB2 (L88S)/CyaB1 (C) CyaB2 (M87A/L88S)/CyaB1

CyaB2 (M87S)/CyaB1 had a 128 fold-stimulation of (± 7.6), an EC_{50} of 1.15 ± 0.03 and a Hill coefficient of 3.07 ± 0.2 according to the curve in fig.4.43.A, so the EC_{50} and the Hill coefficient were comparable to the WT but the mutant had a lower fold stimulation. The second mutant, CyaB2 (L88S)/CyaB1, had 343 fold-stimulation (± 14.0) and higher EC_{50} of 12.0 ± 1.69 μM cAMP. The Hill coefficient was showing cooperativity with a value of 1.43 ± 0.07 ($R^2 = 0.9737$, $n = 4$) (curve B). The double mutant, CyaB2 (M87A/L88S)/CyaB1 was sharing the characteristics of both mutants, the low fold stimulation of 145 ± 4.5 fold and the low EC_{50} of 1.16 ± 0.27 μM cAMP, which is similar to the first mutant and a Hill coefficient of 1.57 ± 0.21 ($R^2 = 0.945$) of the second mutant.

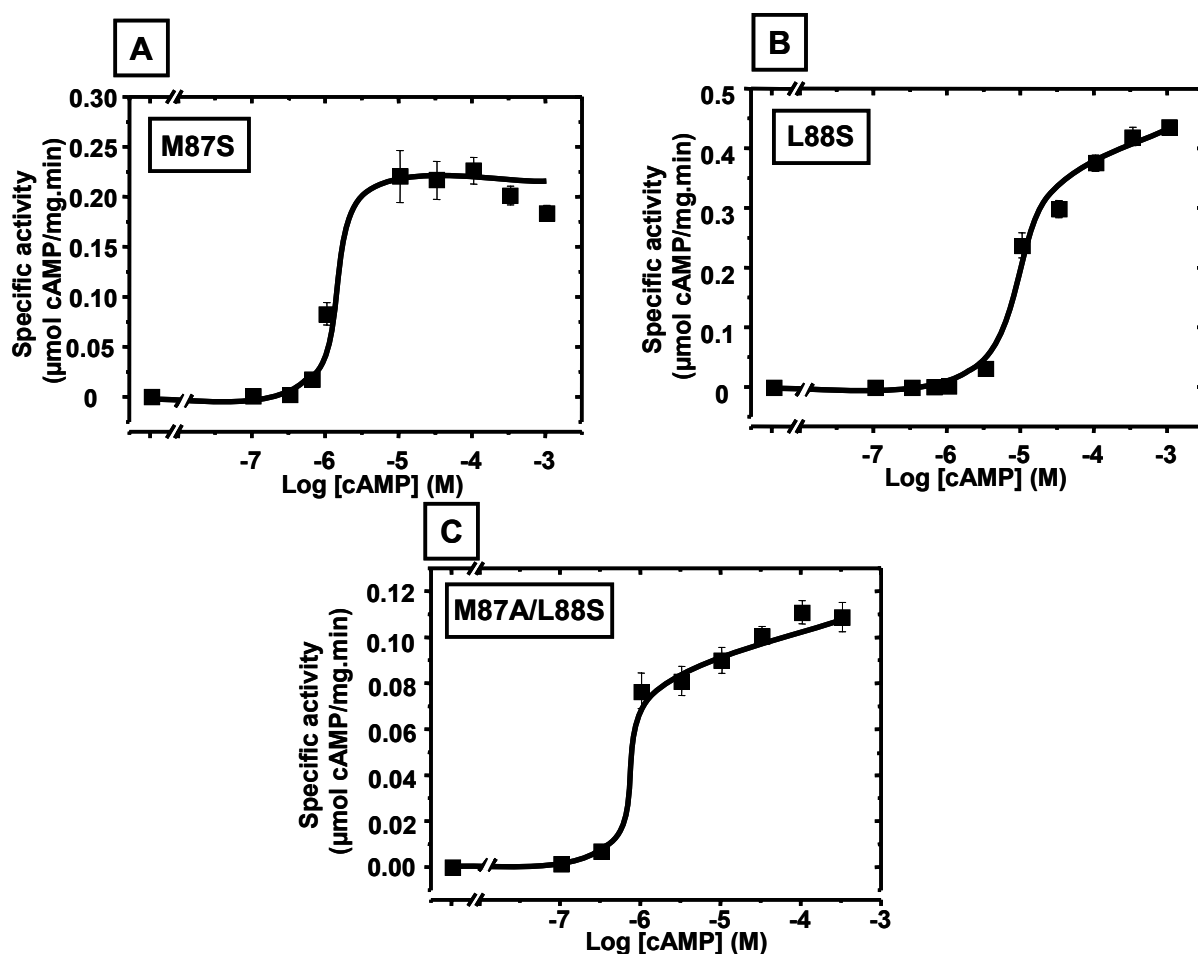


Fig. 4.43: Dose response curves of α 2-helix mutants. Assay conditions: 4 min, 37°C, 75 μ M ATP, 10 mM $MgCl_2$, 0.1M Tris/HCl pH 7.5, 40-50 nM protein (n = 4) (A) CyaB2 (M87S)/CyaB1 (B) CyaB2 (L88S)/CyaB1 (C) CyaB2 (M87A/L88S)/CyaB1

Table 4.4: summary of enzyme parameters of CyaB2 α -helix mutants.

construct	Basal activity (nmol/mg.min)	EC_{50} (μ M)	Fold-stimulation (by cAMP)	Hill coefficient	figure
CyaB2NGAF/CyaB1	1.85 ± 0.216	0.53 ± 0.013	746.8 ± 82.4	2.84 ± 0.3 (0.9223)	4.25.B
CyaB2(ML74GG)/CyaB1	2.86 ± 0.195	7.95 ± 0.17	260.9 ± 14.4	1.19 ± 0.02 (0.9877)	4.41.A
CyaB2(ML74ST)/CyaB1	1.64 ± 0.187	4.16 ± 0.3	133.5 ± 13.9	1.29 ± 0.07 (0.9758)	4.41.B
CyaB2(M87S)/CyaB1	1.64 ± 0.131	1.15 ± 0.03	127.8 ± 7.6	3.07 ± 0.2 (0.9825)	4.43.A
CyaB2(L88S)/CyaB1	1.23 ± 0.058	12.0 ± 1.69	342.5 ± 14.0	1.43 ± 0.07 (0.9737)	4.43.B
CyaB2(ML87AS)/CyaB1	0.77 ± 0.049	1.16 ± 0.27	144.8 ± 4.5	1.57 ± 0.21 (0.9448)	4.43.C

4.2.1.5 Mutation of connecting helix of CyaB2 GAF

According to the alignment in fig.4.27, the two conserved hydrophobic amino acids were leucines in almost all the PDE GAF connecting helices. Five mutants in which one or both methionines were mutated were prepared. The first mutant contained the accidental mutation of M258T and this was recloned as in section (3.4.2.9) to get rid other mutations, the next four mutants had both methionines mutated, once to glycines, to alanines, to leucines and fourth to serine/threonine. These were cloned, expressed and run on the SDS-PAGE to check purity (Fig.4.44). All constructs were well-expressed with good yield. The protein dependence assays of four of them are shown in figure 4.45. All activated proteins had low activity at low protein concentration which increased with protein concentration. Although leucine does not differ in size from methionine, CyaB2 (M258L/M259L)/CyaB1 protein was dead with zero activity and activation, possibly due to misfolding.

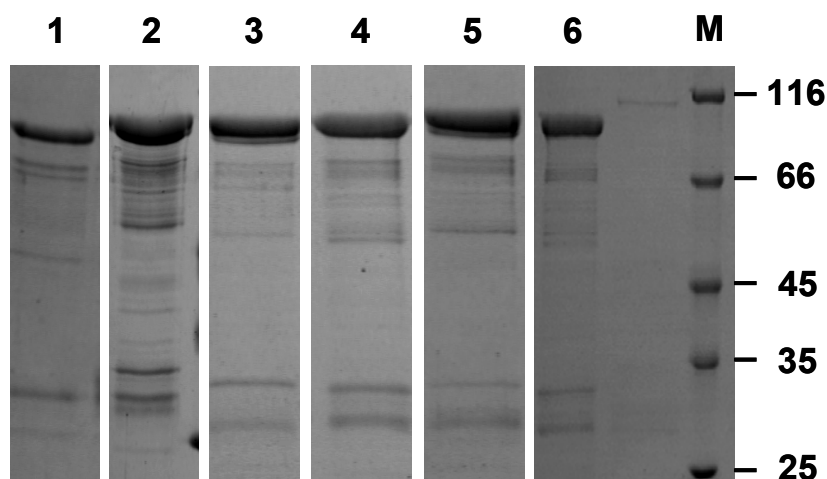


Fig.4.44: The expression of the five mutants in addition to the WT (4 μ g each) **(1)** CyaB2NGAF/CyaB1 **(2)** CyaB2 (M258T)/CyaB1 **(3)** CyaB2 (M258A/M259A)/CyaB1 **(4)** CyaB2 (M258S/M259T)/CyaB1 **(5)** CyaB2 (M258L/M259L)/CyaB1 **(6)** CyaB2 (M258G/M259G)/CyaB1.

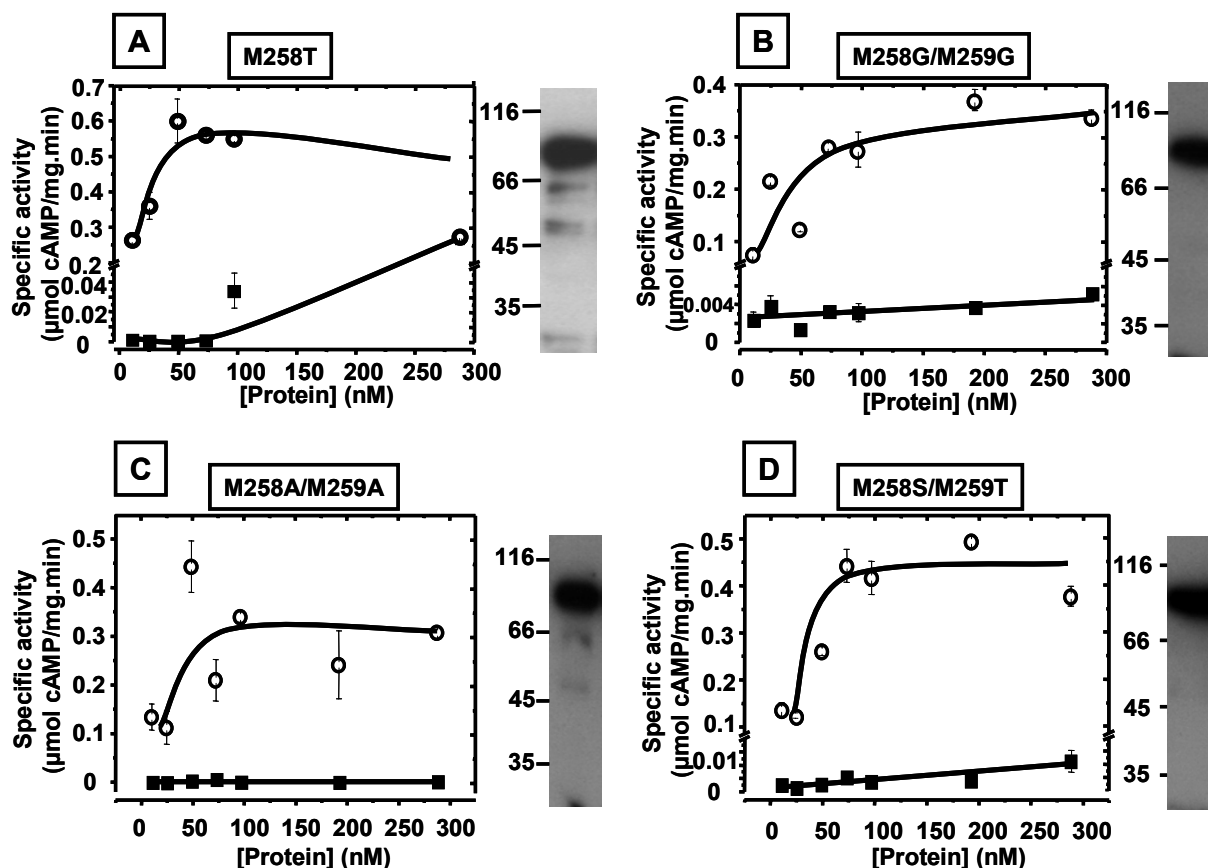


Fig. 4.45: Protein dependence of CyaB2GAF connecting helix mutants. Assay conditions: 4 min, 37°C, 75 μM ATP, 10 mM MgCl₂, 0.1M Tris/HCl pH 7.5 (n = 4) **(A)** CyaB2 (M258T)/CyaB1 **(B)** CyaB2 (M258G/M259G)/CyaB1 **(C)** CyaB2 (M258A/M259A)/CyaB1 **(D)** CyaB2 (M258S/M259T)/CyaB1.

In the cAMP-dose response curves, the fold-stimulation of CyaB2 (M258T)/CyaB1 was 223.5 ± 14.2 , the EC_{50} was 2.42 ± 0.09 μM cAMP and a Hill coefficient of 1.56 ± 0.023 . CyaB2 (M258G/M259G)/CyaB1 had a fold-stimulation of 60.0 ± 10.24 , an EC_{50} of 19.2 ± 1.24 μM cAMP and Hill coefficient of 0.926 ± 0.04 . For the third construct, CyaB2 (M258A/M259A)/CyaB1, the fold-stimulation was 199.2 ± 8.5 , an EC_{50} of 27.7 ± 2.4 μM and a Hill coefficient of 1.55 ± 0.2 . The last mutant, CyaB2 (M258S/M259T)/CyaB1, had a fold-stimulation of 102.5 ± 5.7 , an EC_{50} of 7.85 ± 0.58 and a Hill coefficient of 1.54 ± 0.06 (Fig.4.46.A-D).

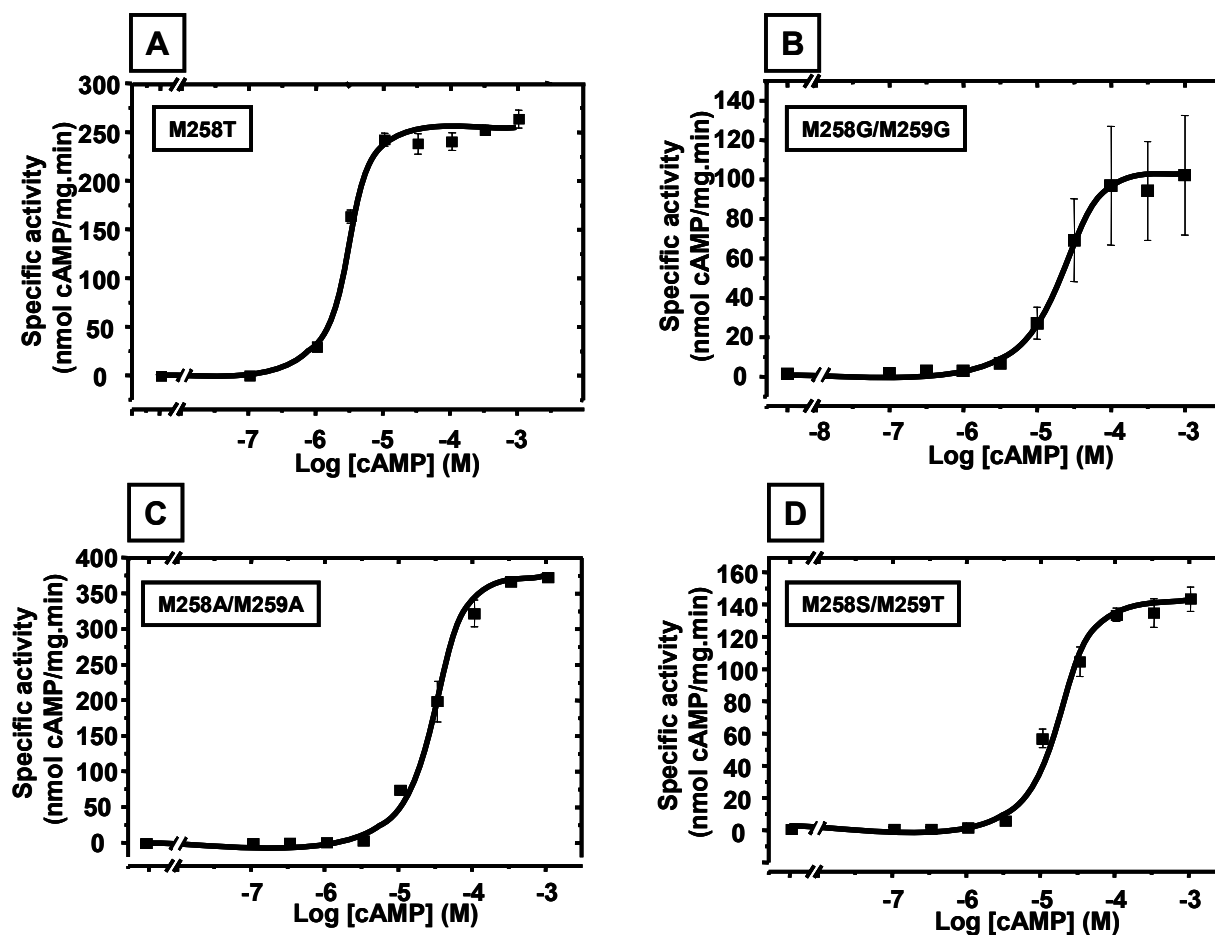


Fig.4.46: Dose response curve of the CyaB2 connecting helix mutants. Assay conditions: 4 min, 37°C, 75 μ M ATP, 10 mM MgCl₂, 0.1M Tris/HCl pH 7.5, 40-50 nM protein (n = 4)

From the two mutants of the α 1-helix, CyaB1 (M74S/L75T)/CyaB1 had lower fold stimulation and from that of the connecting helix, CyaB2 (M258S/M259T)/CyaB1 and CyaB2 (M258G/M259G)/CyaB1 had the least fold-stimulation. The mutants to hydrophilic amino acids of both helices were combined in a chimeric quadruple mutation, expressed and assayed for protein dependence and dose response. The protein dependence curve was showing an interesting result as the activity was increasing in a parabolic manner and the specific activity in a linear manner. The effect could be due to disturbance in the dimerization of the GAF domain which led to a decrease in the specific activity of the enzyme at low concentration of the protein and as the concentration increases, the dimerization increases and the response to the cAMP increases as well (fig.4.47).

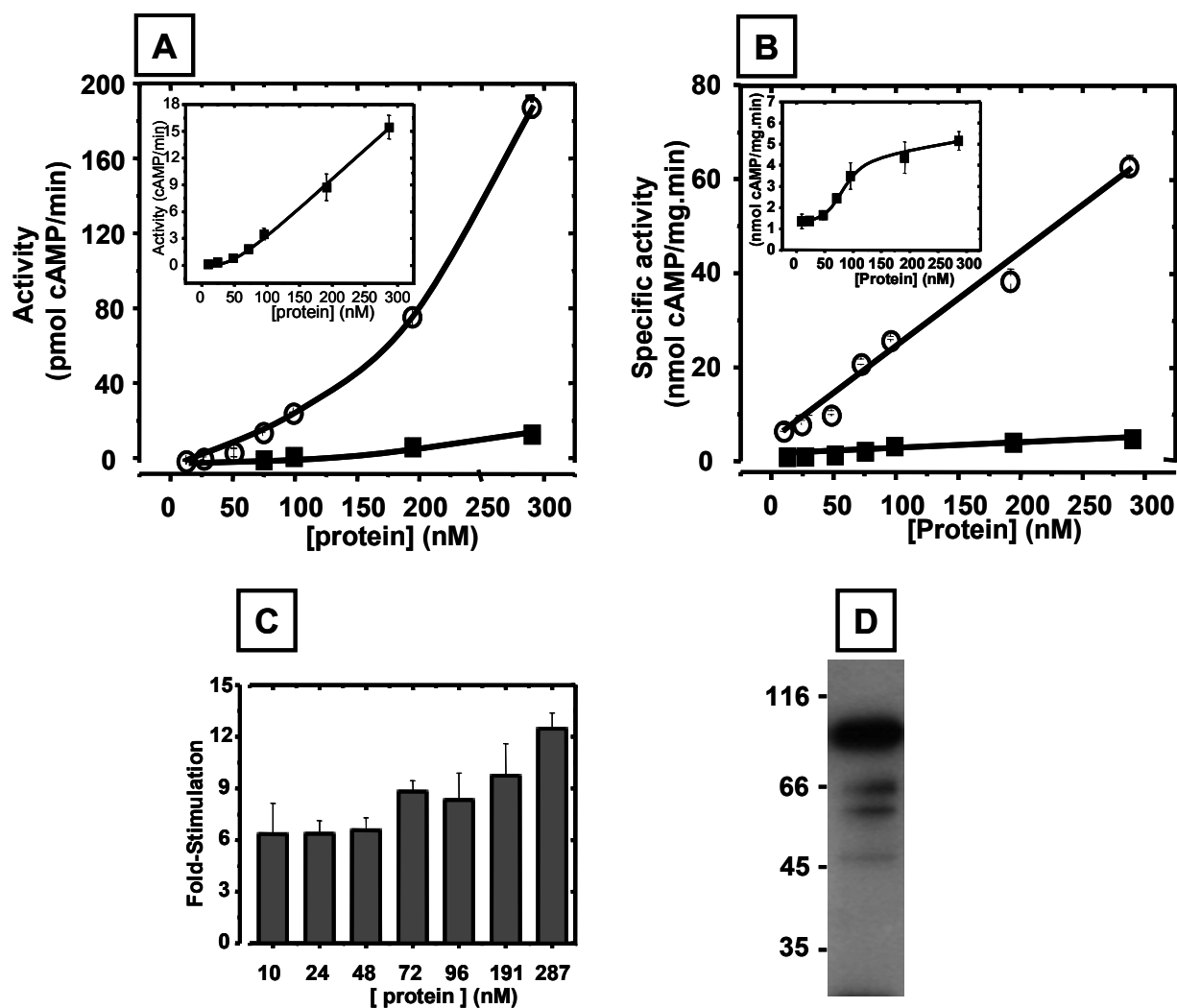


Fig. 4.47: Protein dependence of Cya2 (M74S/L75T/M258S/M259T)/CyaB1. Assay conditions: 4 min, 37°C, 75 μ M ATP, 10 mM MgCl₂, 0.1M Tris/HCl pH 7.5 (n = 4) **(A)** Activity against protein concentration **(B)** Specific activity against protein concentration. **(C)** Plot shows the effect of protein concentration on the fold-stimulation **(D)** Western blot of 0.3 μ g protein.

The dose response curve of Cya2 (M74S/L75T/M258S/M259T)/CyaB1 (Fig.4.48) showed a fold stimulation of 6.4 ± 0.56 , an EC₅₀ of 9.1 ± 0.04 μ M cAMP and a Hill coefficient of 0.47 ± 0.06 , i.e loss of cooperativity.

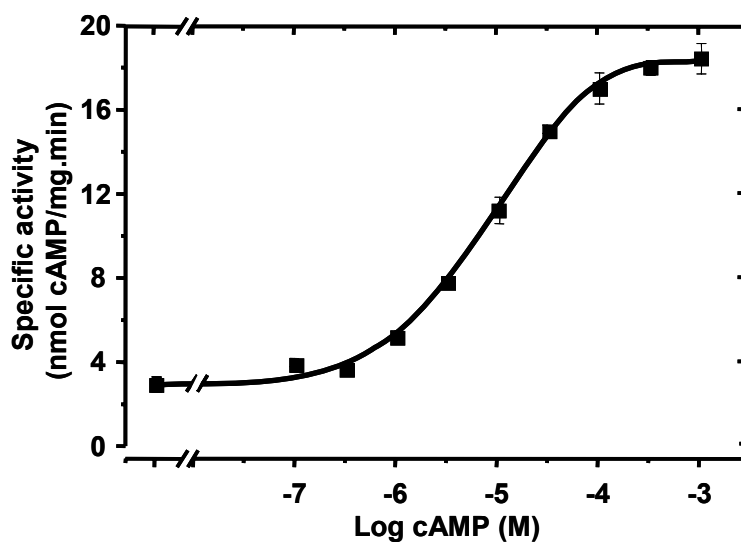


Fig. 4.48: Dose response curve of CyaB2 (M74S/L75T/M258S/M259T)/CyaB1. Assay conditions: 4 min, 37°C, 75 μ M ATP, 10 mM MgCl₂, 0.1M Tris/HCl pH 7.5, 30 nM protein (n = 4).

Table 4.5: different parameters of CyaB2 GAF connecting helix mutants compared to the wild type

Mutation	Basal activity (nmol/mg.min)	EC ₅₀ (μ M)	Activation factor (x) (by cAMP)	Hill coefficient	figure
WT	1.85 \pm 0.216	0.53 \pm 0.013	746.8 \pm 82.4	2.84 \pm 0.3 (0.9223)	4.26.B
M258T	1.01 \pm 0.189	2.42 \pm 0.09	223.5 \pm 14.2	1.56 \pm 0.023 (0.9883)	4.48.A
M258G/M259G	1.59 \pm 0.25	19.2 \pm 1.24	60.0 \pm 10.24	0.926 \pm 0.04 (0.9774)	4.48.B
M258A/M259A	1.89 \pm 0.123	27.7 \pm 2.4	199.2 \pm 8.5	1.554 \pm 0.2 (0.9764)	4.48.C
M258L/M259L	Inactive enzyme				
M258S/M259T	1.70 \pm 0.455	7.85 \pm 0.58	102.5 \pm 5.7	1.54 \pm 0.06 (0.9782)	4.48.D
M74S/M75T/M258S/M259T	3.01 \pm 0.358	9.08 \pm 0.036	6.4 \pm 0.56	0.47 \pm 0.06 (0.9907)	4.50

4.2.1.6 Dimerization study and gel filtration.

From the above constructs, two GAF domains were selected to be cloned in pQE60 and studied for the dimerization to see if this decrease in the fold stimulation and affinity toward cAMP is due to dimerization proposed to occur through these two amino acids or it was a folding problem. CyaB2 (M258S/M259T) and CyaB2 (M258L/M259L) were selected and checked for dimerization, using both glutaraldehyde and gel filtration. The two constructs were cloned using the same primers as used in the preparation of the crystallized CyaB2GAF (V58-Q445), transformed into *BL21 (DE3)[pREP4] E.coli* cells, overexpressed at 22°C, 300 µM IPTG for 6 hrs. Both proteins were expressed in good yield (600 µg/200 ml culture) and evaluated by SDS-PAGE for size and purity (fig.4.49). Good purity was observed for CyaB2 (M258S/M259T) and the size was matching the calculated MW (44.7 kDa). For CyaB2 (M258L/M259L), the purity was excellent but the size was much higher so the sequencing of the DNA was repeated to exclude frame shifting by mutations and it was found to be correct which suggested the increase in protein volume due to misfolding and this explains the earlier results obtained for the chimera of this mutant which produced inactive enzyme.

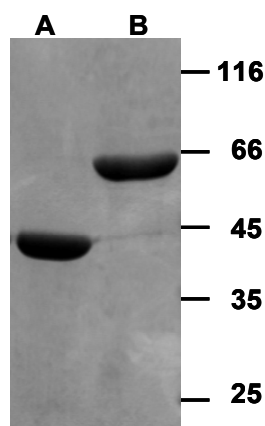


Fig.4.49: SDS-PAGE (12.5%) showing the correct size of CyaB2 GAF (M258S/M259T) (**A**) and the wrong size for CyaB2 GAF (M258L/M259L) (**B**)

The gel filtration was performed for both constructs and they were showing a dimer in both mutants with a broad peak of larger size than calculated for CyaB2GAF (M258L/M259L) (see fig.4.50)

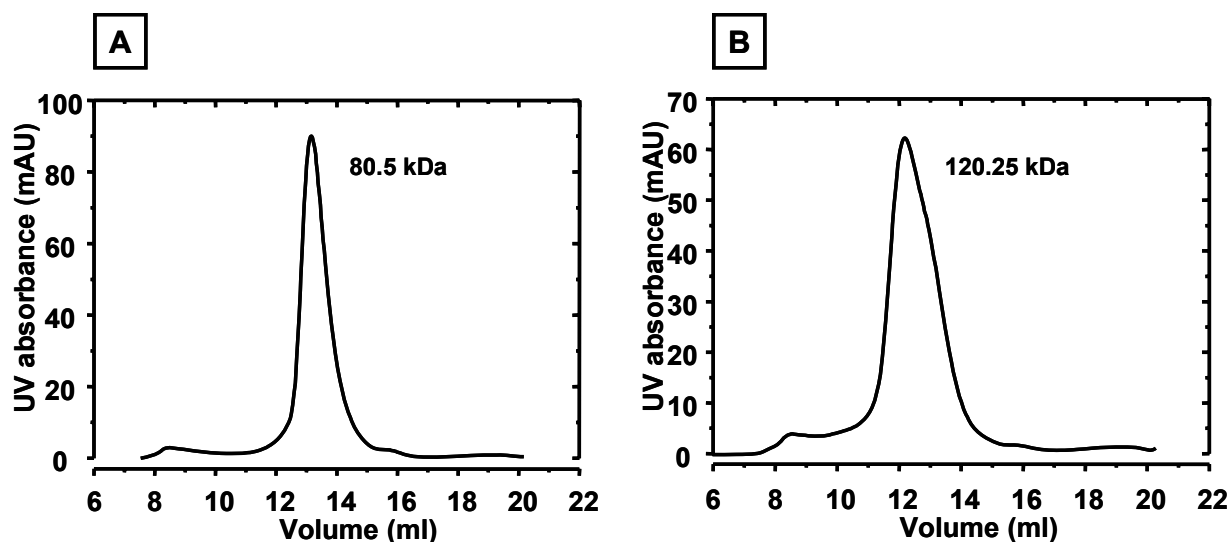


Fig.4.50: Gel filtration of CyaB2GAF connecting helix mutants **(A)** CyaB2GAF (M258S/M259T) and **(B)** CyaB2GAF (M258L/M259L). No fractions were collected.

4.2.1.7 Crystallization of CyaB2 PAS (444-568), Catalytic (569-860) and PAS/Catalytic (444-860) domains.

The different domains of CyaB2 enzyme were cloned. CyaB2 PAS (E444-R568), PAS/Catalytic (E444-K860), Catalytic (L569-K860) were cloned in pQE30, transformed into *E.coli BL21 (DE3) [pREP4]* cells and expressed (27°C, 300 µM IPTG, 6 hr). The washed-cell pellets were suspended in lysis buffer, lysed by passing twice through French press and purified by shaking with 200 µl Ni-NTA agarose for 3 hr.

In fig.4.51, CyaB2 PAS/catalytic was degraded and no band of 48.43 kDa appears on the gel which make the crystallization experiments not possible. For CyaB2 catalytic, one band appears at the correct size (34.89 kDa) but with a lot of impurities, in addition to the low concentration of protein so optimization of expression was required but it was not done due large number of domains prepared at the same time from both CyaB1 and CyaB2 enzymes for crystallization purposes. The CyaB2 PAS domain was expressed in a very high purity (see fig.4.51) but the estimated MW of the protein (19 kDa) was higher than the calculated one (15.09 kDa). Nevertheless, the protein was expressed again on large scale, purified, dialysed against crystallization buffer (10% glycerol) and concentrated (NANOSEF[®]) to 21.5 mg/ml. Crystal screens I, II, and lite were used. Yet, no crystals were obtained.

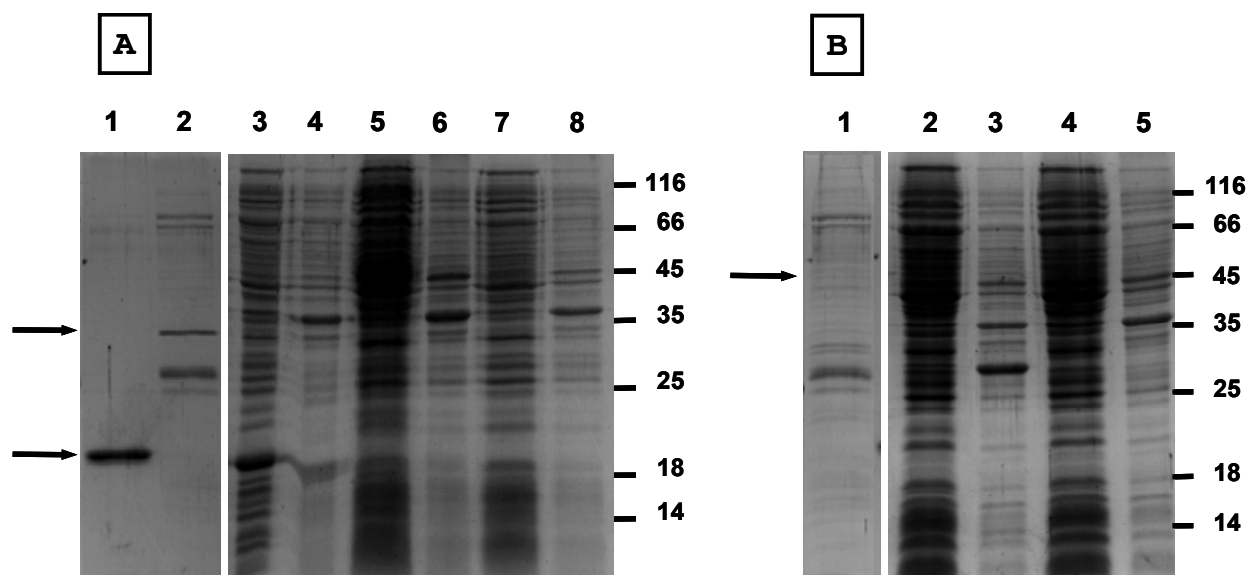


Fig.4.51: (A) SDS-PAGE (15%) of CyaB2 PAS and CyaB2 catalytic compared to pQE30 (1) Purified CyaB2 PAS (2 μ g) (2) purified CyaB2 catalytic (2 μ g) (3 and 4) Supernatant and pellets of CyaB2 PAS respectively (5 and 6) Supernatant and pellets of CyaB2 catalytic respectively (7 and 8) Supernatant and pellets of pQE30, respectively.

(B) SDS-PAGE (15%) of CyaB2 PAS/Catalytic compared to pQE30 (1) Purified protein (2 μ g) (2 and 3) Supernatant and pellets of CyaB2 PAS/Catalytic (4 and 5) Supernatant and pellets of pQE30 as control.

4.2.2 hPDE2 GAF domain

4.2.2.1 Mutation of GAF α α 1- helix

In the crystal structure of the mouse PDE2A GAF tandem, the dimer observed was consistent with earlier data of PDE2A holoenzyme that suggested that the N-terminal region is responsible for dimerization [104]. GAF α rather than GAF β was involved in the dimerization as observed from the crystal structure shown in fig.4.52.

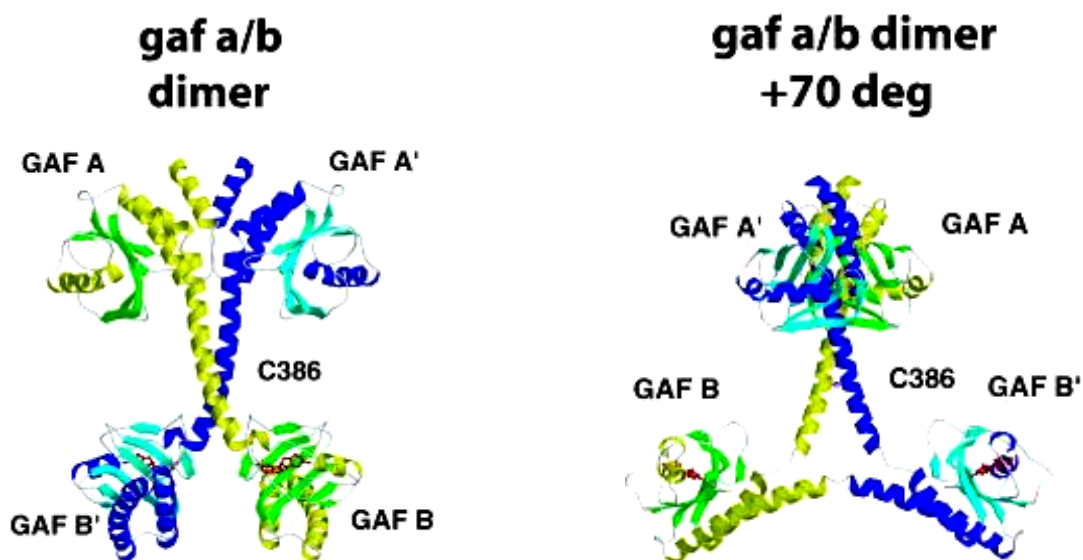


Fig.4.52: The crystal structure of mouse PDE2 GAF domain showing the dimerization involving the GAFa motif

In PDE2A, several hydrophobic residues in GAFa are involved in the dimer interface between the two monomers, including L223 of helix $\alpha 1$ which inserts into a hydrophobic pocket formed by I222', L223', C226', all from helix $\alpha 1'$, and Y365' from the kink between $\alpha 5'$ and the connecting helix. D219' on $\alpha 1'$ seals the pocket from the solvent [24]. These amino acids mentioned in the dimerization of mPDE2 GAFa (I222, L223, C226, Y365 and D219) correspond to residues I230, L231, C234, Y372, and D227 in human PDE2 GAFa.

The two corresponding amino acids in the $\alpha 1$ -helix were mutated to explore the effect of dimerization on the affinity to cGMP and on stimulation. Either I230S or L231S were prepared. The constructs were cloned in pQE30 and were expressed in *E.coli* BL21(DE3)[pREP4] for overnight at 16°C and induced by 30 μ M IPTG and 10 mM MgCl₂. The washed, frozen pellets were resuspended in lysis buffer, lysed by French Press and the proteins were purified by binding to Ni⁺²-NTA agarose for 3 hr with a yield of 240 μ g/200 ml culture. The purified proteins had a calculated MW of 116.2 kDa.

The protein dependence was assayed (Fig.4.53.A and B). hPDE2 (I230S)/CyaB1 was linear while for hPDE2 (L231S)/CyaB1, higher activity was observed at lower protein concentrations. The proteins were run on SDS-PAGE (12.5%) followed by Western blot.

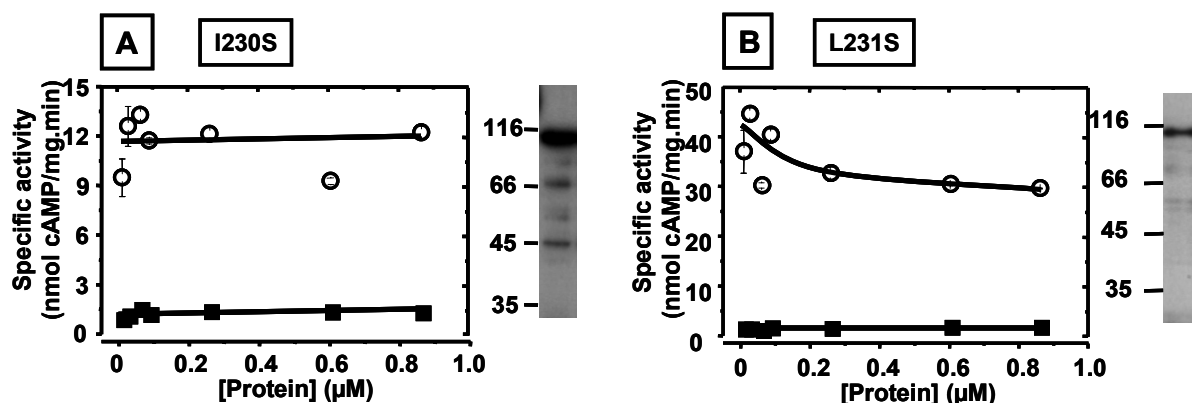


Fig. 4.53: Protein dependence of α 1-helix hPDE2 mutants. (■) Unactivated protein (○) +300 μ M cGMP. Assay conditions: 4 min, 37°C, 75 μ M ATP, 10 mM MgCl₂, 0.1M Tris/HCl pH 7.5 (A) hPDE2NGAF (I230S)/CyaB1, to the right western blot (0.5 μ g) (B) hPDE2NGAF (L231S)/CyaB1. Western blots (0.1 μ g) at right.

In figure 4.54, hPDE2NGAF (I230S)/CyaB1 and hPDE2NGAF (L231S)/CyaB1 were showing a stimulation factor of 16.9 ± 0.8 and 23.9 ± 0.9 respectively, which is higher than that of wild type (5.2 ± 0.4) (Section 4.1.1), the EC₅₀ for cGMP was 6.5 ± 0.53 and 5.9 ± 0.4 , respectively, i.e. not different from the wild type. Although Hill coefficient was higher for both of them (1.18 ± 0.118 $R^2 = 0.9670$ for I230S and 0.844 ± 0.072 , $R^2 = 0.9844$ for L231S), only I230S was showing some cooperativity.

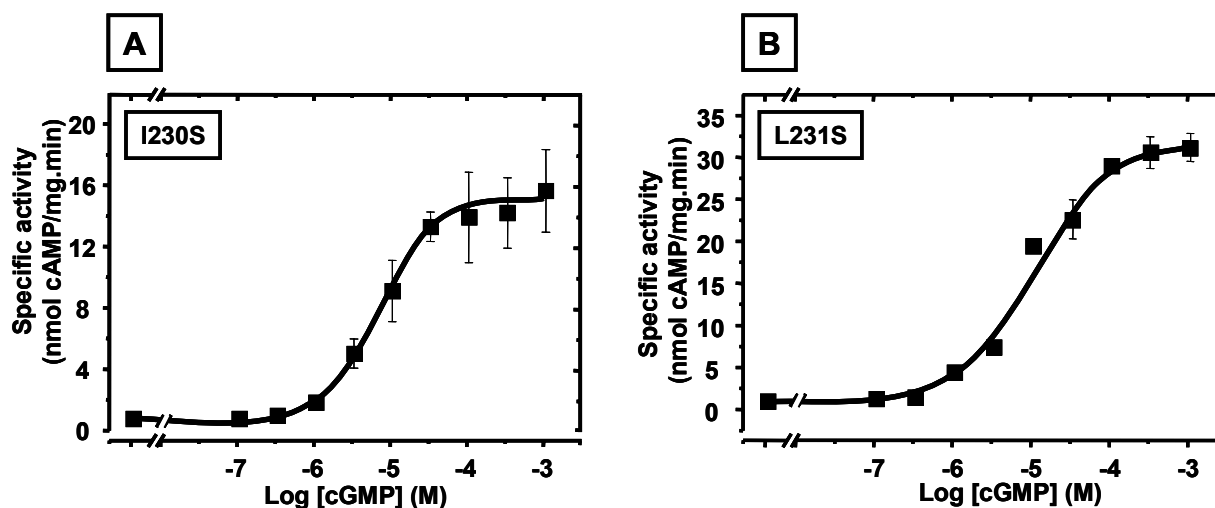


Fig. 4.54: Dose response curve of α 1-helix hPDE2 mutants. Assay conditions: 37°C, 75 μ M ATP, 10 mM MgCl₂, Tris/HCl pH 7.5, 10 min, 86 nM protein (n = 4) (A) hPDE2 NGAF (I230S)/CyaB1. (B) hPDE2 NGAF (L231S)/CyaB1.

4.2.2.2 Mutation of the connecting helix of hPDE2NGAF/CyaB1

According to the alignment of the hPDE2GAF and CyaB2 GAF connecting helix (Fig. 4.55), the helix connecting the two GAF domains has a poor homology (15 % identity and 27 % similarity).

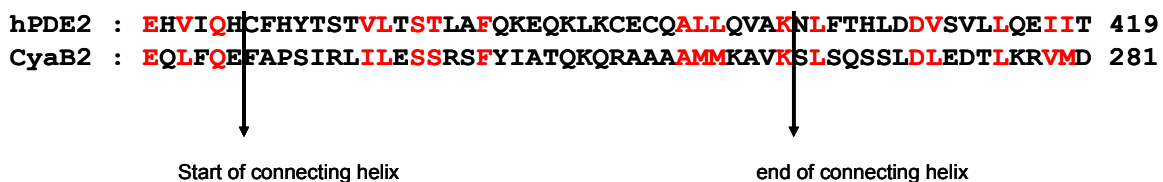


Figure 4.55: ClustalW alignment of CyaB2 and hPDE2 GAF connecting helices as determined from their crystal structures. Arrows determine the beginning and end. [24].

To study the effect of cysteine and the two leucine residues on signal transduction, three mutants were generated. The first mutant was a triple mutation (C393S/L396A/L397A). The construct was cloned in pQE30 with an N-terminal His-tag, expressed in *BL-21(DE3)* [*pREP4*]. Protein expression was induced by 50 μ M IPTG, 10 mM MgCl₂ at (16°C, 210 rpm, overnight), and the protein was purified using 200 μ l Ni-NTA agarose (0°C, 3 hrs). The purified protein was dialysed overnight at 4°C against dialysis buffer and assayed immediately.

The protein dependence was linear (0.0088-0.88 μ M) with lower fold stimulation than the wild type (fig.4.56)

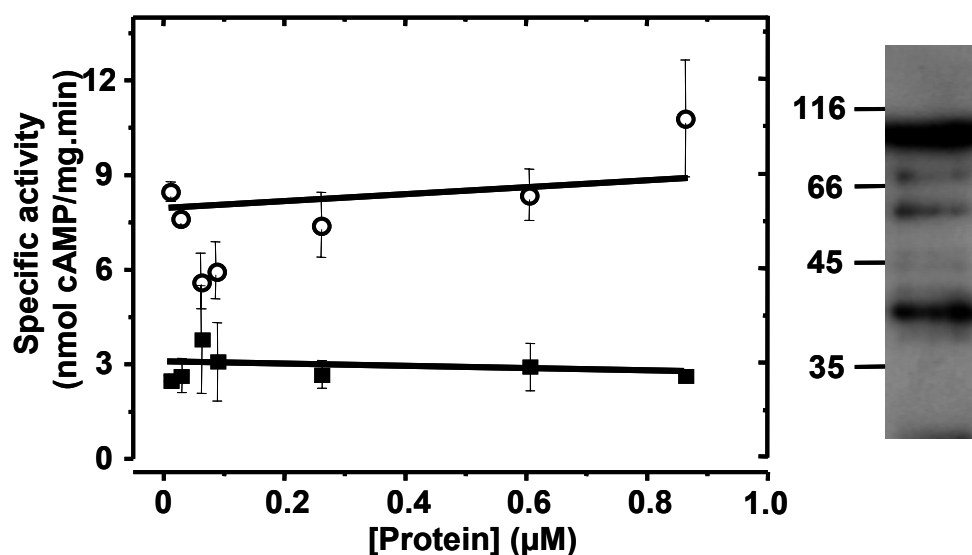


Fig. 4.56: Protein dependence of hPDE2 (C393S/L396A/L397A)/CyaB1. (■) unactivated protein (○) +300 μ M cGMP. Assay conditions: 10 min, 37°C, 75 μ M ATP, 10 mM MgCl₂, 0.1M Tris/HCl pH 7.5 (n = 4). Western blot (0.5 μ g) at right.

Results

The cGMP-EC₅₀ was calculated to be $0.354 \pm 0.077 \mu\text{M}$ ($n = 6$) which is 28-fold lower than that of the WT chimera ($9.92 \pm 1.04 \mu\text{M}$). The stimulation factor was also lower (3.37 ± 0.2 , $n = 6$) and the Hill coefficient of 0.57 ± 0.08 ($R^2 = 0.9901$, $n = 6$) indicated no cooperativity (see Fig.4.57).

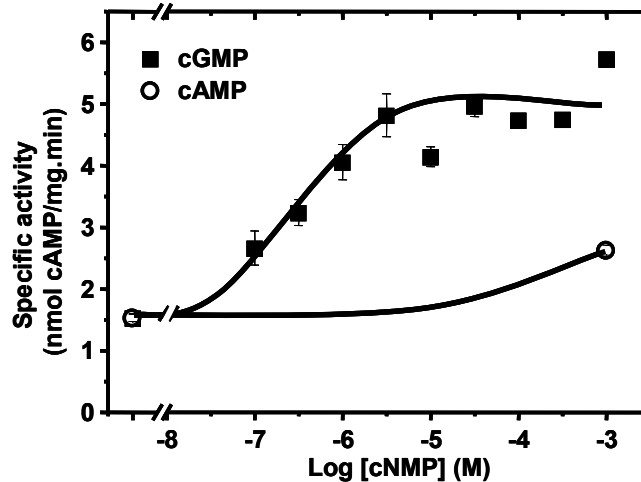


Fig.4.57: Dose response curve of hPDE2NGAF (C393S/L396A/L397A)/CyaB1 chimera. Assay conditions: 4 min, 37°C, 75 μM Mg⁺²-ATP, 0.1M Tris/HCl pH 7.5, 90 nM protein ($n = 6$)

Because it was difficult to know whether cysteine or the two leucines were responsible for this data, mutation was separated by cloning of two constructs, i.e. C393S and L396A/L397A. The mutants were expressed and purified as the triple mutated construct.

The protein dependence (fig.4.58.A and B) was linear for hPDE2NGAF (C393S)/CyaB1 but for hPDE2NGAF (L396A/L397A)/ CyaB1, the specific activity was increasing up to 90 nM and then it leveled off.

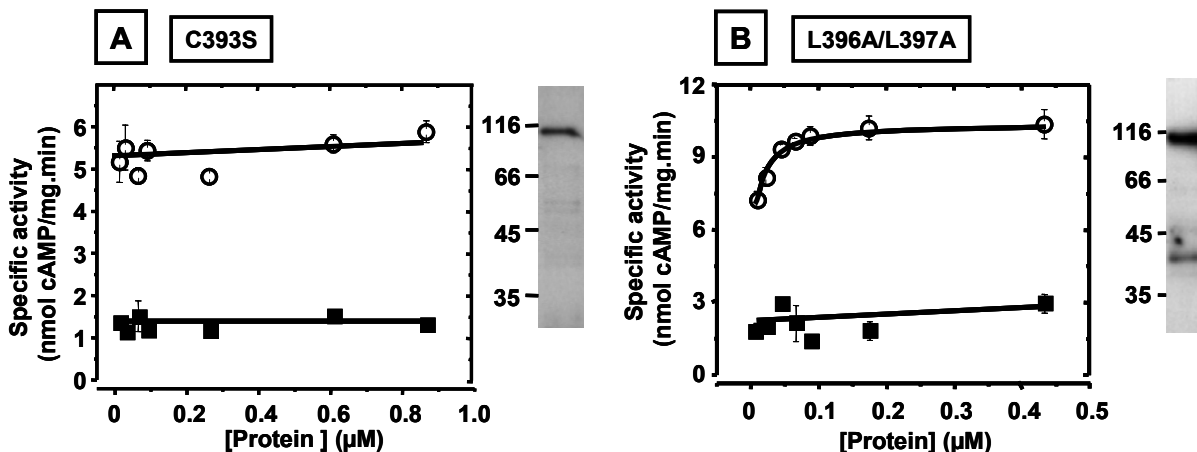


Fig.4.58: Protein dependence of (A) hPDE2NGAF (C393S)/CyaB1 and (B) hPDE2NGAF (L396A/L397A)/CyaB1. (■) Unactivated protein (○) +100 μM cGMP. Assay conditions: 75 μM ATP, 10 mM MgCl₂, 37°C, 0.1M Tris/HCl pH 7.5, 10 min ($n = 4$).

cGMP stimulated 4.8 fold (± 0.17) (Fig.4.59) and the EC₅₀ and Hill coefficient of were 4.80, $5.1 \pm 0.06 \mu\text{M}$ and 0.54 ± 0.03 ($R^2 = 0.987$, $n = 4$), respectively, i.e. not significantly different

Results

from those of hPDE2NGAF/ CyaB1. The construct, hPDE2NGAF (L396A/L397A)/CyaB1, had a fold-stimulation of 3.8 ± 0.07 , an EC_{50} of 0.44 ± 0.0335 and a Hill coefficient of 0.9 ± 0.17 ($R^2 = 0.9518$) consistent with the triple mutated construct so the decrease in EC_{50} was due to the leucines residues and not the disulfide bridging of the cysteine.

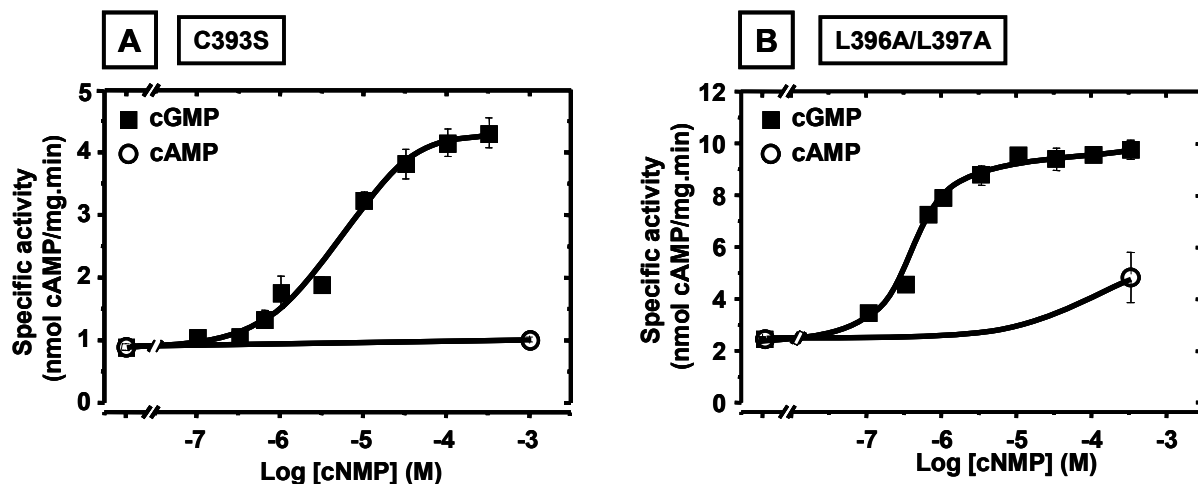


Fig. 4.59: Dose response curves of (A) hPDE2 (C393S)/CyaB1 (B) hPDE2 (L396A/L397A)/CyaB1. Assay conditions: $75\mu\text{M Mg}^{+2}$ -ATP, 37°C , $0.1\text{M Tris/HCl pH } 7.5$, 10 min ($n = 4$)

4.2.2.3 Quadruple mutation of both helices

Accordingly, a truncated $\Delta 1$ -227 construct with quadruple mutation in both GAF α 1 helix and the connecting helix was prepared. The Δ N hPDE2GAF (I230A/L231A/L396A/L397A)/CyaB1 was cloned in pQE30, expressed in *BL21 (DE3)* [*pREP4*] as for other mutants, the purified protein has a MW of 91.8 kDa. The protein dependence curve was linear (Fig.4.60).

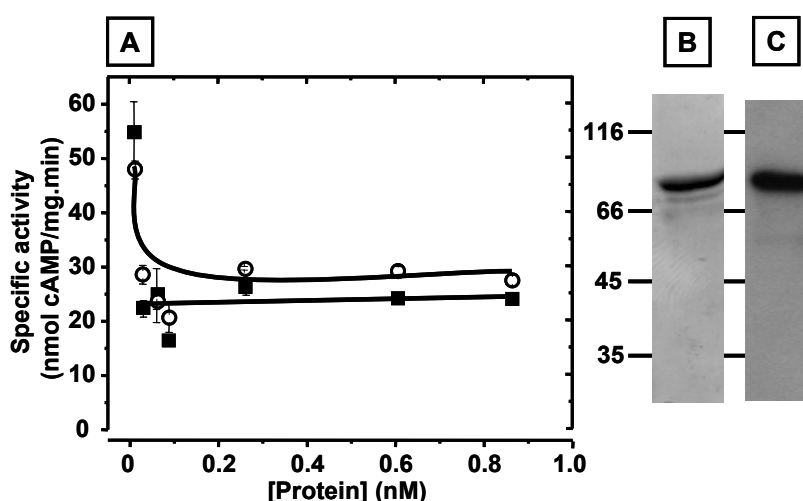


Fig. 4.60: (A) protein dependence of Δ N-hPDE2GAF (I230A/L231A/L396A/L397A)/CyaB1. (■) Unactivated protein (○) + $100\mu\text{M}$ cGMP. Assay conditions: 37°C , 10 min , $75\mu\text{M Mg}^{+2}$ -ATP, $0.1\text{M Tris/HCl pH } 7.5$ ($n = 4$). (B) SDS-PAGE (12.5%) with $4\mu\text{g}$ protein (C) Western blot ($0.2\mu\text{g}$).

Results

The construct was not activated by cGMP. In addition, basal activity was higher than all PDE2 constructs and mutants (Fig.4.61).

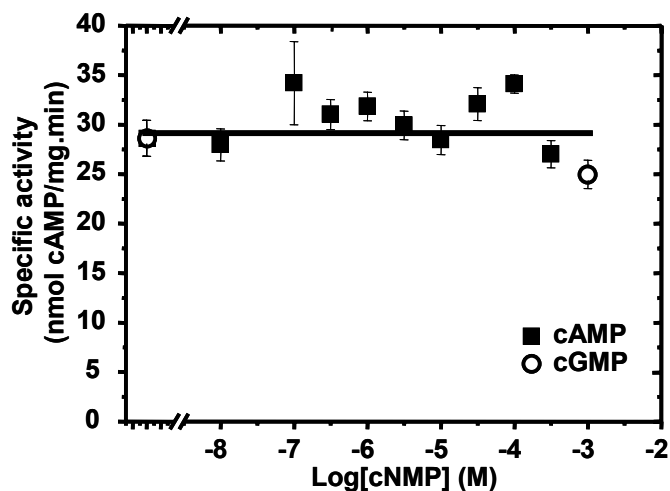


Fig. 4.61: Dose response curve of Δ N- hPDE2 (I230A/L 231A/L396A/L397A)/CyaB1. Assay conditions: 37°C, 10 min, 75 μ M Mg^{+2} -ATP, 0.1M Tris/HCl pH 7.5, 109 nM protein (n = 4)

The time dependence was examined \pm 100 μ M cGMP. It was linear and cGMP did not stimulate (Fig.4.62.A and B). The parameters of hPDE2 chimeras and mutants are summarized in table 4.6

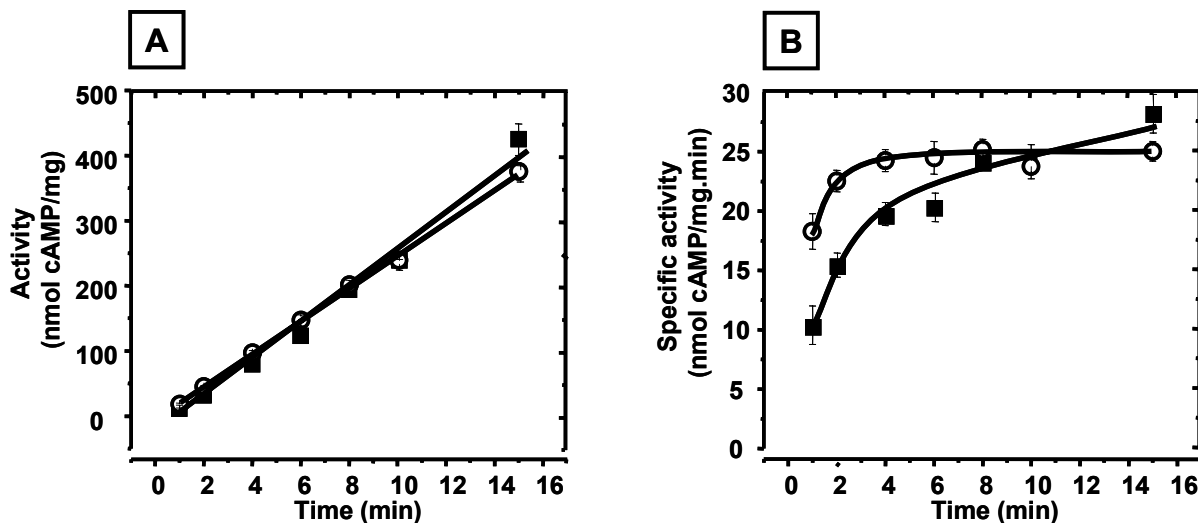


Fig.4.62: Time dependence of Δ N- hPDE2 (I230A/L231A/L396A/L397A)/CyaB1. (■) unactivated protein (○) +100 μ M cGMP. Assay conditions: 37°C, 0.1M Tris/HCl pH 7.5, 75 μ M Mg^{+2} -ATP, 1-15 min, 109 nM protein (n = 4) (A) activity against time (B) specific activity against time.

Table 4.6: Summary for the parameters of hPDE2 chimeras and mutants.

construct	Basal activity (nmol/mg.min)	EC ₅₀ (μM) (n=4)	Activation factor (x) (by cAMP)	Hill coefficient
hPDE2NGAF/CyaB1	1.32 ± 0.08	9.92 ± 1.04	5.2 ± 0.37	0.477 ± 0.042 (R ² = 0.9754)
Δ N -hPDE2 GAF/CyaB1	12.2 ± 0.8	7.7 ± 0.072	4.2 ± 0.092	0.469 ± 0.020 (R ² = 0.9760)
hPDE2 (I230S)/CyaB1	0.9 ± 0.14	6.49 ± 0.53	16.9 ± 0.9 (n = 4)	1.18 ± 0.118 (R ² = 0.9670)
hPDE2 (L231S)/CyaB1	1.3 ± 0.04	5.94 ± 0.37	23.9 ± 0.9 (n = 4)	0.844 ± 0.072 (R ² = 0.9844)
hPDE2 (C393S)/CyaB1	0.89 ± 0.05	5.1 ± 0.063	4.8 ± 0.17 (n = 4)	0.539 ± 0.032 (R ² = 0.9871)
hPDE2 (LL396AA)/CyaB1	2.5 ± 0.03	0.44 ± 0.034	3.79 ± 0.068 (n = 4)	0.897 ± 0.172 (R ² = 0.9518)
hPDE2 (C393S/LL396AA)/CyaB1	0.74 ± 0.06	0.35 ± 0.08	3.366 ± 0.18 (n = 4)	0.571 ± 0.075 (R ² = 0.9901)
Δ N-hPDE2 (I230A/L231A/L396A/L397A) / CyaB1	28.3 ± 0.93	ND*	1.11 ± 0.055 (n = 4)	ND*

* ND means not determined.

4.2.2.4 Crystallization of hPDE2GAF ± N-terminus

4.2.2.4.1 hPDE2NGAFcr

hPDE2NGAF (M1-562) was cloned in pQE30 and transformed into *BL21 (DE3) [pREP4]* for expression. 200-ml batches of LB-medium were inoculated by 5 ml of an overnight culture and induced (0.3 mM IPTG, 22°C for 6 hr). The protein was purified by 200 μl Ni²⁺-NTA agarose for three hours. The 62.9-kDa, His₆-tagged protein was analysed by SDS-PAGE and Western blot (fig.4.63). 200 ml culture produced 0.16 mg protein. The protein was concentrated by ultrafiltration (NANOSEP filters) yet much was lost on the filter and only a concentration of 3-7.5 mg/ml was obtained.

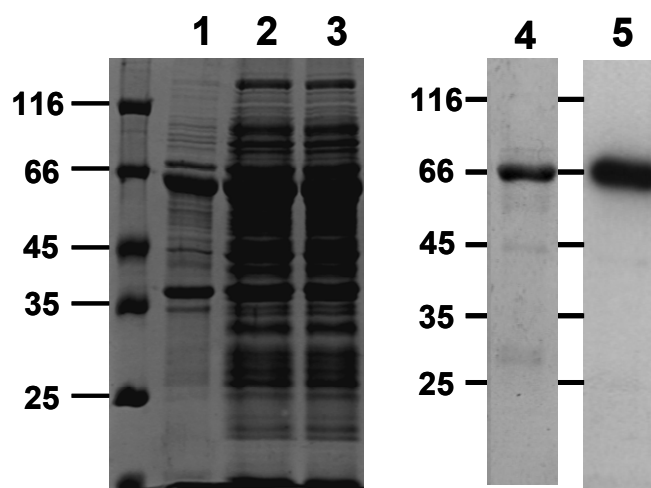


Fig 4.63: SDS-PAGE (12.5%) of hPDE2NGAFcr (1) Pellets (5 μ l) (2) Supernatant (10 μ l) (3) Supernatant after Ni-NTA (10 μ l) (4) Purified protein (2 μ g) (5) Western blot (100 ng)

No crystals were obtained.

4.2.2.4.2 Δ N-hPDE2 GAF

The Δ N-hPDE2 GAF was cloned in pQE30 with an N-terminal His-tag, expressed and purified as mentioned for hPDE2NGAF protein (Fig.4.64). The protein of a calculated MW of 38.5 kDa, was pure (yield 0.4 mg/200 ml culture), a concentration of 12 mg/ml was obtained by ultrafiltration (Vivaspin, Sartorius) as described (section 3.3.11.2). Crystallization trials were performed \pm 2 mM cGMP using the sitting drop method. Crystal screens I, II, lite, PEG/Ion 2 were used for the initial screening of the crystals. No crystals were obtained for a time as long as one year.

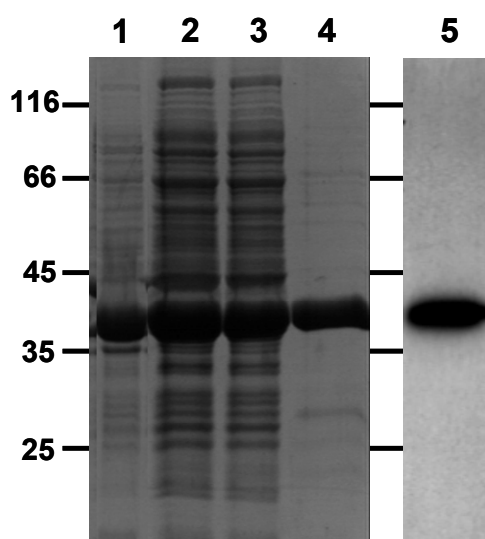


Fig. 4.64: SDS-PAGE (12.5%) of Δ N₁₋₂₂₇-hPDE2 GAF. (1) Pellet (2) Supernatant (3) Supernatant after Ni²⁺-NTA (4) Purified protein (4 μ g) (5) Western blot (0.1 μ g)

4.2.2.5 Glutaraldehyde dimerization and gel filtration of hPDE2GAF and mutants.

GAF domain or their mutants were purified as usual, washed by 2 ml of wash buffer D, E, and F and eluted using elution buffer 2 and dialyzed against crosslinking buffer (50 mM phosphate pH 7.4, 10 mM NaCl, 22% glycerol). In 16 μ l, GAF or mutant proteins (0.1, 0.3 or 1 μ g) were incubated with freshly diluted glutaraldehyde (0.06 and 0.12%) at RT for 60 min. The reactions were stopped by the addition of SDS loading dye, boiled at 95°C for 5 min, and subjected to 10-15% SDS-PAGE followed by Western blotting.

The gel chromatography of the hPDE2NGAF (the crystallized construct) is indicating a dimer as a major peak with a calculated MW of 175.8 kDa, a small peak of a monomer and another for an oligomer were also observed, similar results were obtained by dimerization experiments with glutaraldehyde which has demonstrated a dimer (fig.4.65.A and B).

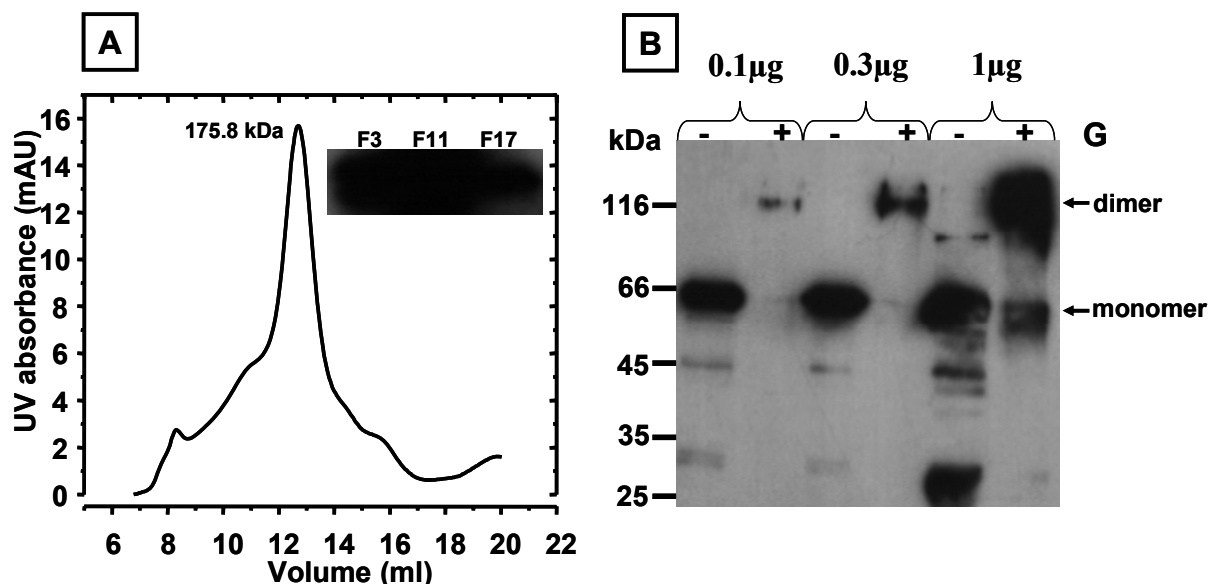


Fig. 4.65: Dimerization study of hPDE2NGAFcr performed by **(A)** Gel filtration showing a size of 175.8 kDa which was a dimer. Fraction collection started 7 ml and fractions mentioned above corresponds to F3: 8.5 ml retention volume, F11: 12.5 ml and F17: 15.5 ml. **(B)** Glutaraldehyde crosslinking shows dimer formation.

The removal of the N-terminus showed one peak for a dimer with a shoulder corresponding to monomer, the first peak and the major peak gave a band for a monomer on the western blot (Fig.4.68.A). The glutaraldehyde study of Δ N-hPDE2 GAFcr shows a band for the unreacted and proves the presence of dimer for the protein crosslinked (Fig.4.66.B).

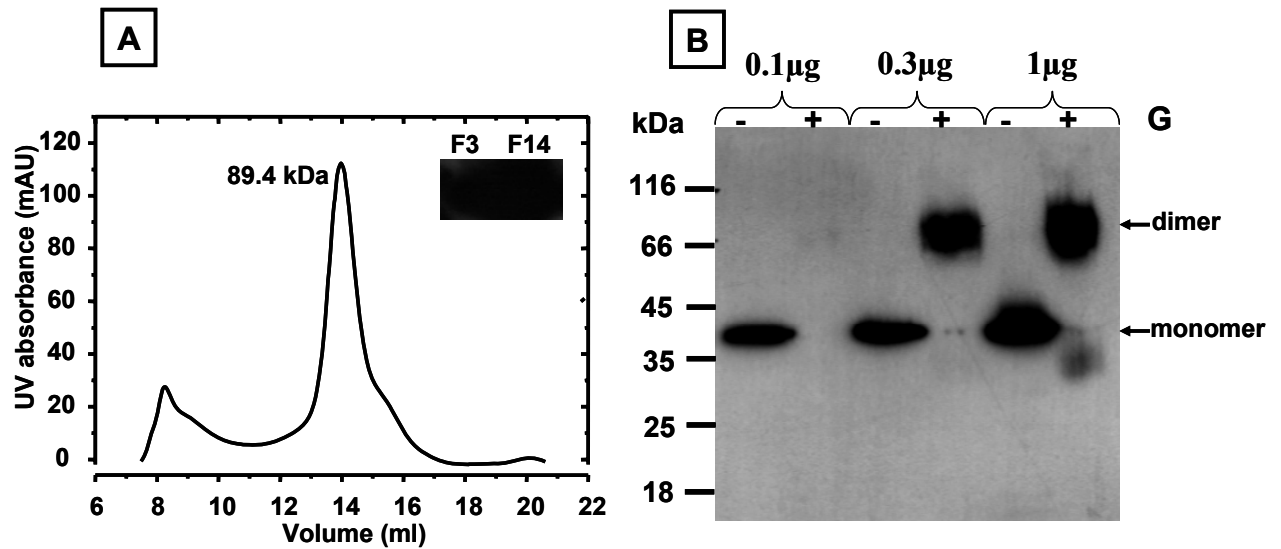


Fig.4.66: Dimerization study of Δ N-hPDE2 GAFcr. **(A)** Gel filtration showing a size of 89.4 kDa which was estimated to be a dimer Fractions collection starts at 7 ml and fractions mentioned above corresponds to F3: 8.5 ml retention volume, F14: 14 ml **(B)** Glutaraldehyde dimerization study performed at different protein concentrations 0.1, 0.3 and 1 μ g/16 μ l reaction \pm 10 mM glutaraldehyde.

Then the GAF domain of the mutant hPDE2NGAF (L396A/L397A)cr was cloned in pQE30 and run on the gel chromatography. A peak appears at the beginning due to oligomerization when tested by Western blotting, monomers were observed (data not shown). The second peak at retention volume of 11 ml was due to membrane fraction of the hPDE2 NGAF. The third peak indicates a dimer and the fourth a monomer. The crosslinking experiment shows two faint bands at the sizes of monomer and dimer (Fig.4.67.A and B).

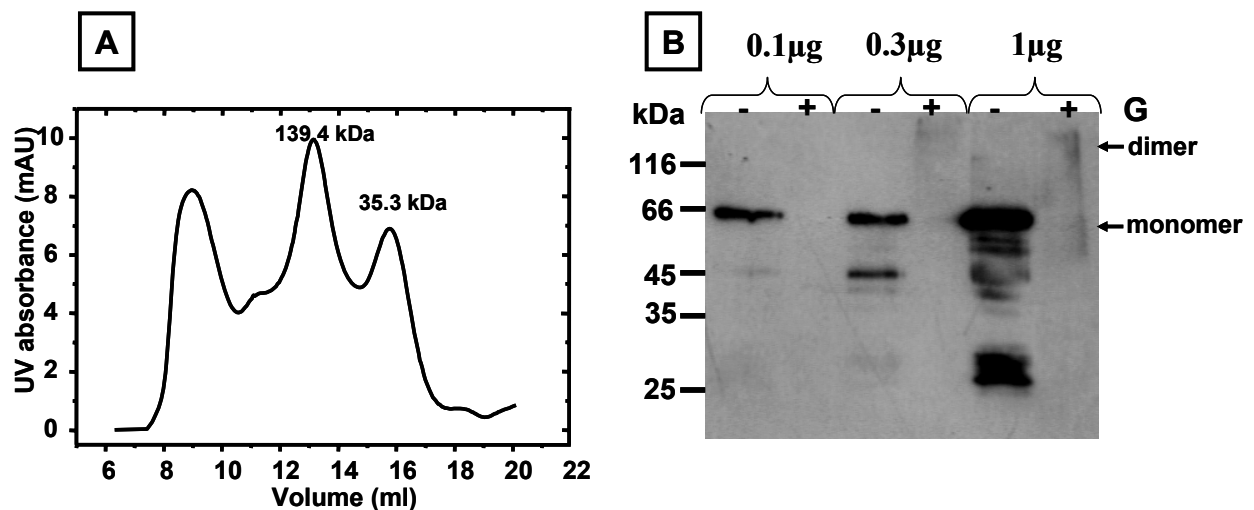


Fig.4.67: Dimerization study of hPDE2NGAF (L396A/L397A)cr **(A)** Gel filtration shows a large peak of oligomer at the beginning of plot and one peak for a monomer **(B)** Glutaraldehyde crosslinking experiment showing a two faint bands of monomer and dimer at 1 μ g amount of protein.

Results

The removal of the N-terminus and mutating the leucines in the connecting helix showed a different profile (fig.4.68.A). Only three peaks appeared an oligomer, a dimer and a monomer. With the mutation, the monomer peak is distinct compared to that of the Δ N-hPDE2GAF in figure 4.66.A. The glutaraldehyde crosslinking study shows the three peaks as bands at 1 μ g protein so double mutation in the connecting helix and N-terminus truncation, did not abolish dimerization.

The quadruple mutation in both α 1-helix and connecting helix with the truncation of the N-terminus produced a major peak of a monomer and small dimer peak (Fig.4.69.A). The glutaraldehyde crosslinking shows a monomer, dimer and oligomer at 1 μ g protein, which indicating that the dimerization was disturbed but not abolished (Fig.4.69.B).

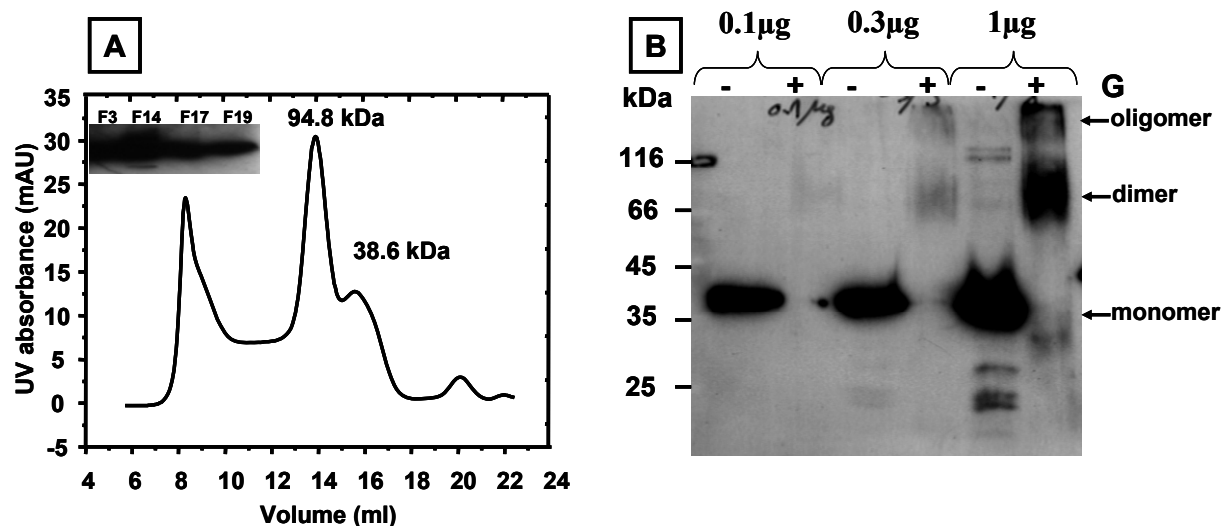


Fig.4.68: Dimerization of Δ N-hPDE2 (L396A/L397A) **(A)** Gel filtration showed a large peak of oligomer at the beginning and a higher peak for a dimer and smaller one for a monomer, fractions were collected starting at 7 ml, and the numbers corresponds to the following volumes, F3: 8.5, F14: 14 ml, F17: 15.5 ml and F19: 16.5 ml. **(B)** Glutaraldehyde crosslinking experiment showing three bands of monomer, dimer and oligomer which is more evident at higher protein concentrations (1 μ g)

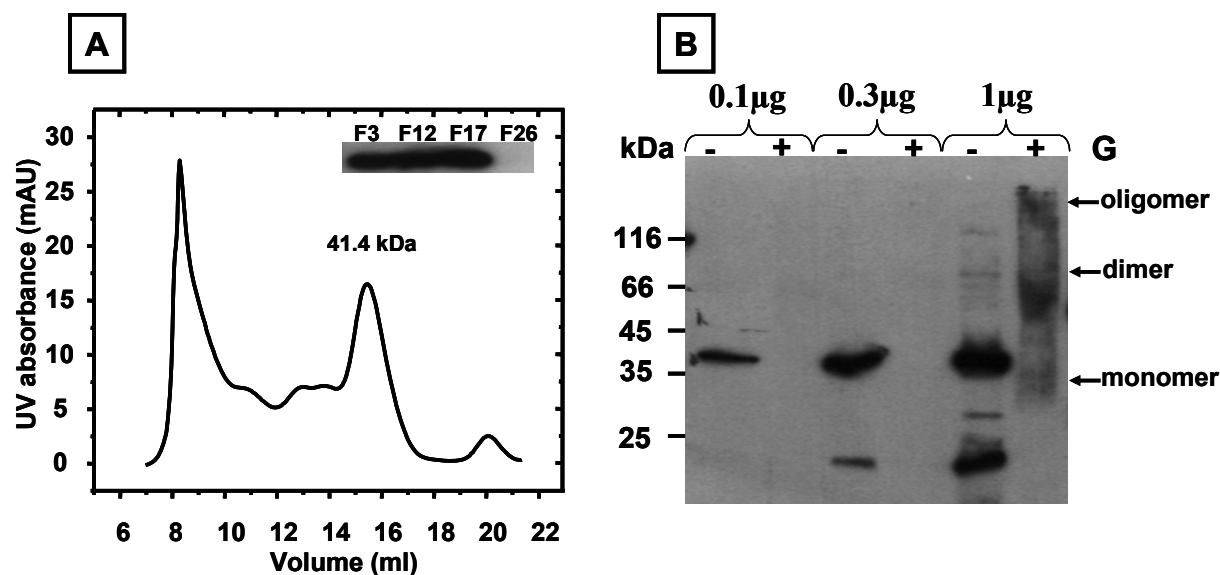


Fig.4.69: Dimerization study of Δ N-hPDE2 (I230A/L231A/L396A/L397A) **(A)** Gel filtration showed a large peak of oligomer at the beginning and a peak for a monomer. Fraction at 7 ml, F3 corresponds to 8.5 ml, F12: 13 ml, F17: 15.5 ml and F26: 20 ml **(B)** Glutaraldehyde crosslinking experiment showing a streak of monomer, dimer and oligomer at 1 μ g protein.

4.2.3 hPDE5 GAF tandem

Similar to the CyaB2 and hPDE2 GAF mutations, the corresponding residues present in the α 1 helix and connecting helix of hPDE5 were mutated. 3 different mutated chimeras were generated and compared to hPDE5NGAF/CyaB1 chimera obtained from S.Bruder. Figure 4.70 shows the domain organization of this protein.

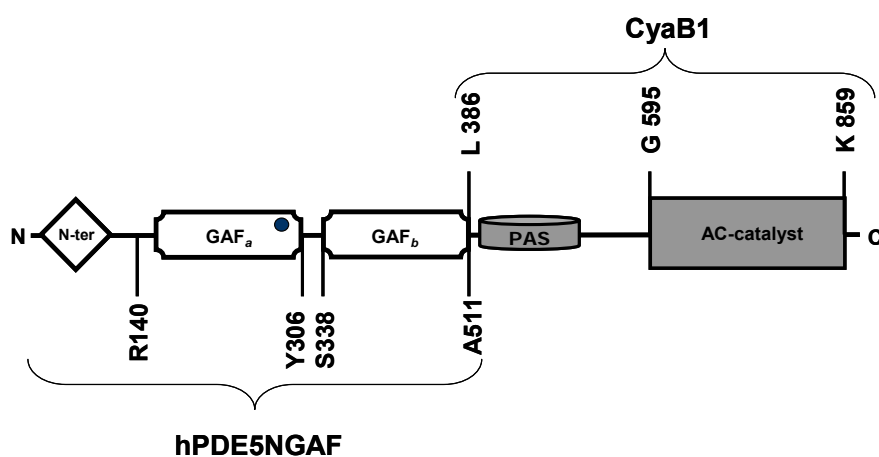


Fig. 4.70: Domain organization of hPDE5NGAF/CyaB1 chimera with aa boundaries of the GAF domain determined according to an alignment with CyaB2 and hPDE2 GAF domains. The blue circle in GAFa domain indicates the allosteric binding site of cGMP.

Results

Three hPDE5 mutants were prepared: one with mutations of the two corresponding leucines in the $\alpha 1$ helix to alanines, the second has a double mutation of the two respective leucines in the connecting helix to AA and the third is a quadruple.

The three proteins, including the wild type PDE5 chimera, were cloned in pET-pQE30 MCS, expressed in *E.coli BL21 (DE3) [pREP4]* at 16°C overnight using 50 μM IPTG and 10 mM MgCl_2 for induction. Proteins were purified by binding to 110 μl Ni^{+2} -NTA agarose for 90 min. The four proteins had an N-terminal hexaHis-tag with a calculated MW of 113 kDa and pI of 5.62. The mutants were compared to the wild type through the protein dependence and dose response assays.

The purified protein dependence of hPDE5NGAF/CyaB1 was linear (Fig.4.71.A). The cGMP dose response curve showed a basal activity of 21.25 ± 1.55 nmol/mg.min, EC_{50} of 22.3 ± 1.8 μM , a fold-stimulation of 14.5 ± 0.56 and a Hill coefficient of 0.769 ± 0.04 ($R^2 = 0.9762$) i.e. not cooperative.

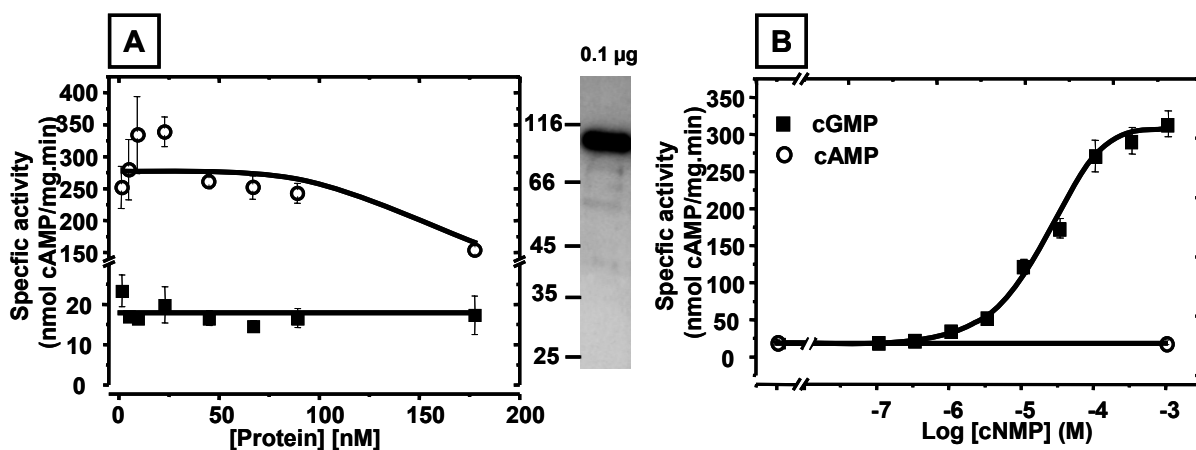


Fig.4.71: Evaluation of hPDE5NGAF/CyaB1 chimera. Assay conditions: 10 min, 75 μM Mg^{+2} -ATP, 37°C, 0.1M Tris/HCl pH 7.5 (n = 4) (A) Protein dependence ((■) Unactivated protein (○) +100 μM cGMP), western blot of 0.1 μg protein is to the right (B) Dose response curve with the same assay conditions and 9 nM protein.

4.2.3.1 hPDE5/CyaB1 mutants

For the hPDE5 mutants, protein dependence was established. Usually, the protein is in the monomeric form and dimerizes at increasing protein concentrations. For the first mutant of hPDE5, hPDE5 (L152A/L153A)/CyaB1, the curves were linear. In the mutant of the connecting helix and the quadruple mutant, hPDE5 (L333A/L334A)/CyaB1 and hPDE5 (L152A/L153A/L333A/L334A)/CyaB1, the curves decreased by increasing protein concentration (Fig.4.72.A-C).

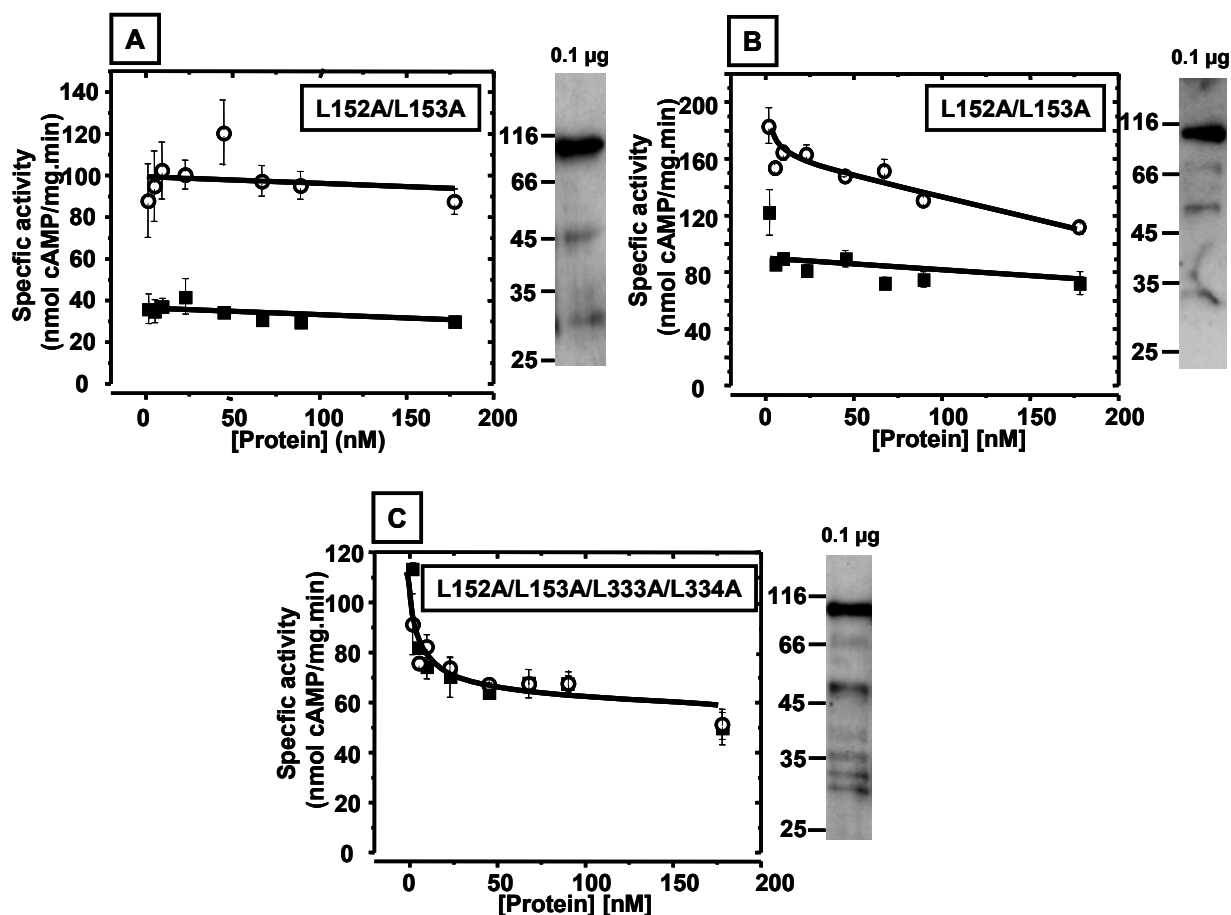


Fig. 4.72: Protein dependence of hPDE5 mutants (■) Unactivated protein (○) +100µM cGMP (A) hPDE5NGAF (L152A/L153A)/CyaB1 (B) hPDE5NGAF (L333A/L334A)/CyaB1 (C) hPDE5NGAF (L152A/L153A/L333A/L334A)/CyaB1, Western blot is shown to the right of each curve (0.3 µg). Assay conditions: 10 min, 75 µM Mg^{+2} -ATP, 37°C, 0.1M Tris/HCl pH 7.5 (n = 4)

The dose response curves showed a decreased fold-stimulation and cGMP- EC_{50} for the two constructs with double mutations. In hPDE5 (L152A/L153A)/CyaB1, the fold-stimulation was 3.4 ± 0.1 , the EC_{50} was 1.7 ± 0.2 µM cGMP and the Hill coefficient was 0.51 ± 0.04 ($R^2 = 0.977$, n = 4). hPDE5 (L333A/L334A)/CyaB1 has also lower fold stimulation and EC_{50} of 1.64 ± 0.072 and 0.327 ± 0.07 , respectively. The Hill coefficient of 0.585 ± 0.14 ($R^2 = 0.9402$, n = 4) showed no cooperativity. A quadruple mutations of both helices caused loss of regulation. Regarding basal activity of the mutants, the double mutations in the connecting helix had the highest basal activity (94.8 ± 7.5 nmol/mg.min), the mutations in the $\alpha 1$ -helix had the lowest basal activity (41.8 ± 2.3 nmol/mg.min) while the quadruple mutant had a basal activity between the two (72.19 ± 3.42 nmol/mg.min) (see Fig.4.73 and table 4.7).

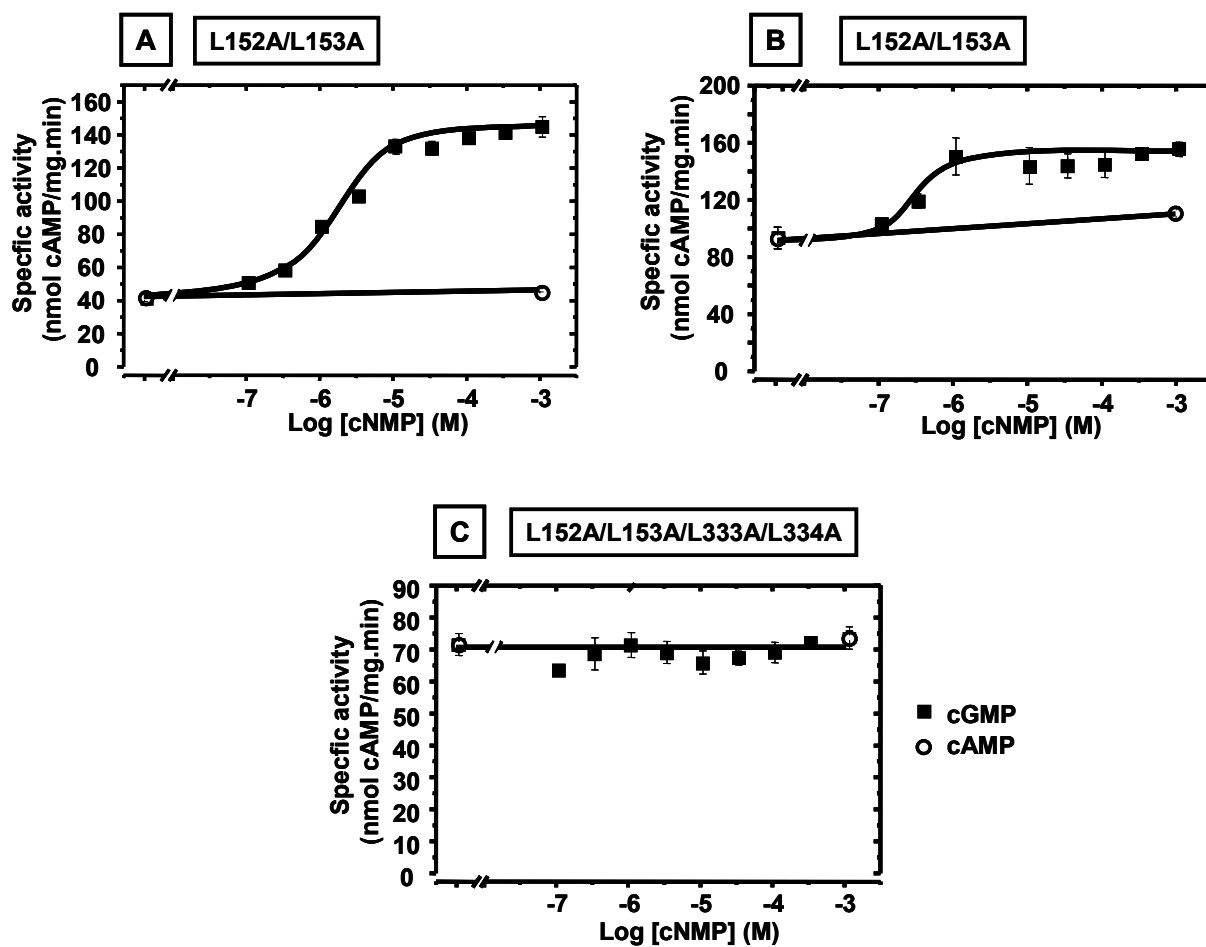


Fig.4.73: Dose response curves of (A) hPDE5NGAF(L152A/L153A).CyaB1 (B) hPDE5NGAF(L333A/L334A)/CyaB1 (C) hPDE5NGAF(L152A/L153A/L333A/L334A)/CyaB1. Assay conditions: 10 min, 75 μ M Mg^{+2} -ATP, 37°C, 0.1M Tris/HCl pH 7.5, 9-18 nM protein (n = 4).

Table 4.7: Kinetic parameters characterizing hPDE5NGAF/CyaB1 chimera and its mutants

construct	Basal activity (nmol/mg.min)	EC ₅₀ (μ M)	Fold-stimulation (by cAMP) (x)	Hill coefficient (Correlation factor)
hPDE5NGAF/CyaB1	21.3 \pm 1.6	22.3 \pm 1.8	14.50 \pm 0.56	0.769 \pm 0.04 (R ² = 0.9762)
hPDE5 (L152A/L153A)/CyaB1	41.8 \pm 2.3	1.7 \pm 0.19	3.4 \pm 0.1	0.512 \pm 0.04 (R ² = 0.9770)
hPDE5(L333A/L334A)/CyaB1	94.8 \pm 7.5	0.33 \pm 0.07	1.6 \pm 0.072	0.585 \pm 0.14 (R ² = 0.9402)
hPDE5(L152A/L153A/L333A/L334A)/CyaB1	72.2 \pm 3.4	ND*	1.01 \pm 0.02	ND*

* ND means Not Determined

4.2.3.2 Dimerization by Glutaraldehyde and gel filtration of hPDE5 and mutants:

To reasonably interpret the results from above, the GAF domain of the hPDE5 and mutants \pm N-terminus were cloned. The dimerization was investigated for different GAF domains of hPDE5 in the presence and absence of the N-terminus. In the gel filtration curve (4.74.A), a large peak in the size of dimer is skewed to the left due to the presence of oligomers. A small peak for a monomer (41.3 kDa) was also observed. Figure 4.74.B shows the formation of a dimer upon crosslinking with glutaraldehyde at the three protein concentrations.

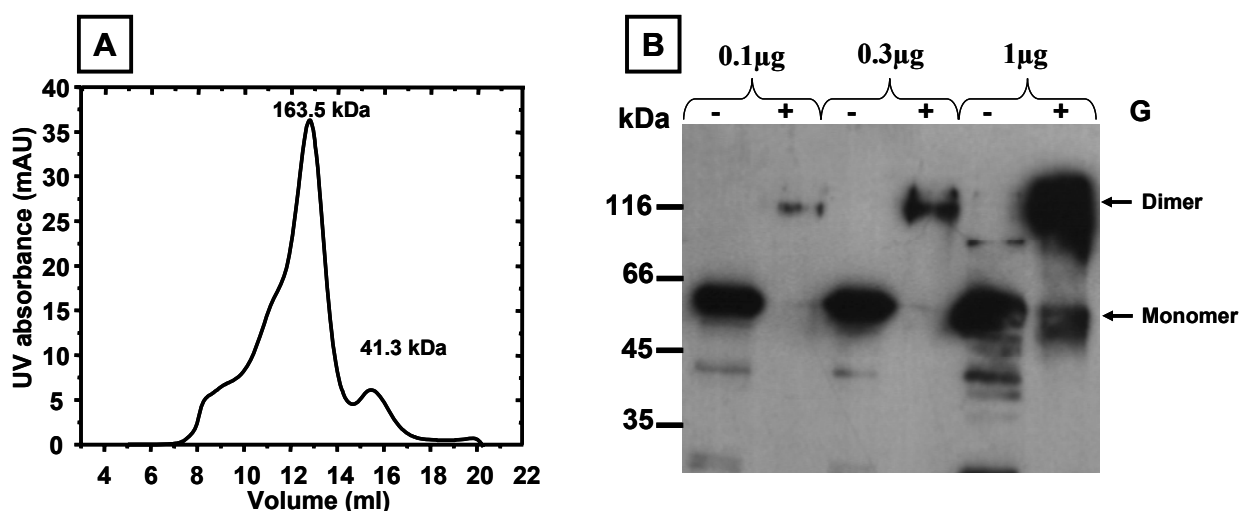


Fig.4.74: Dimerization of hPDE5NGAF performed by (A) Gel filtration showing a size of 163.5 kDa which was estimated to be a dimer. Fractions collection starts at 7 ml and fractions mentioned above corresponds to the following volumes, F3: 8.5 ml retention volume, F11: 12.5 ml and F17: 15.5 ml (B) Glutaraldehyde dimerization shows dimer formation.

The gel filtration of hPDE5 (L152A/L153A) showed similar curves to the hPDE5NGAF in which the dimerization was not disrupted by double mutations in the α 1-helix (Fig.4.75). The glutaraldehyde crosslinking experiment showed formation of dimers at all protein concentrations (Data not shown).

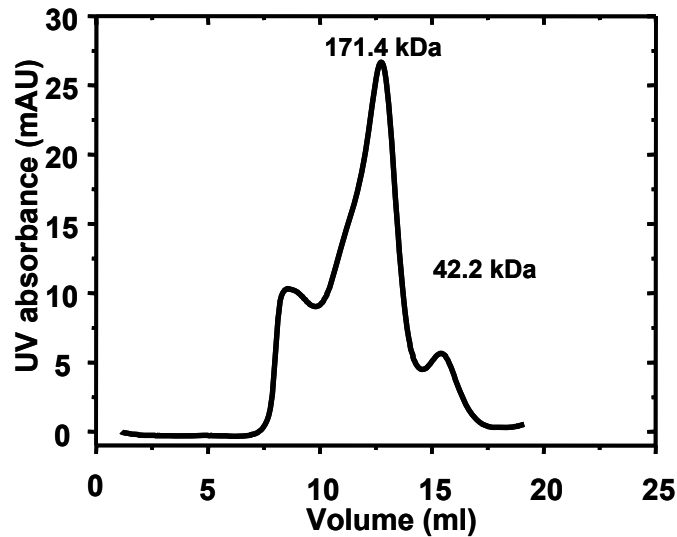


Fig.4.75: Dimerization of hPDE5NGAF (L152A/L153A) performed by gel filtration showing a size of 171.4 kDa which was estimated to be a dimer and another of a monomer

hPDE5 (L333A/L334A) which contains the mutation in the connecting helix also exhibited a similar profile with the four peaks with the dimer as the major peak. This means that double mutations of the connecting helix alone do not affect the dimerization of the hPDE5 GAF domain (Fig.4.76.A). The glutaraldehyde crosslinking experiment didn't show any difference (Fig.4.76.B).

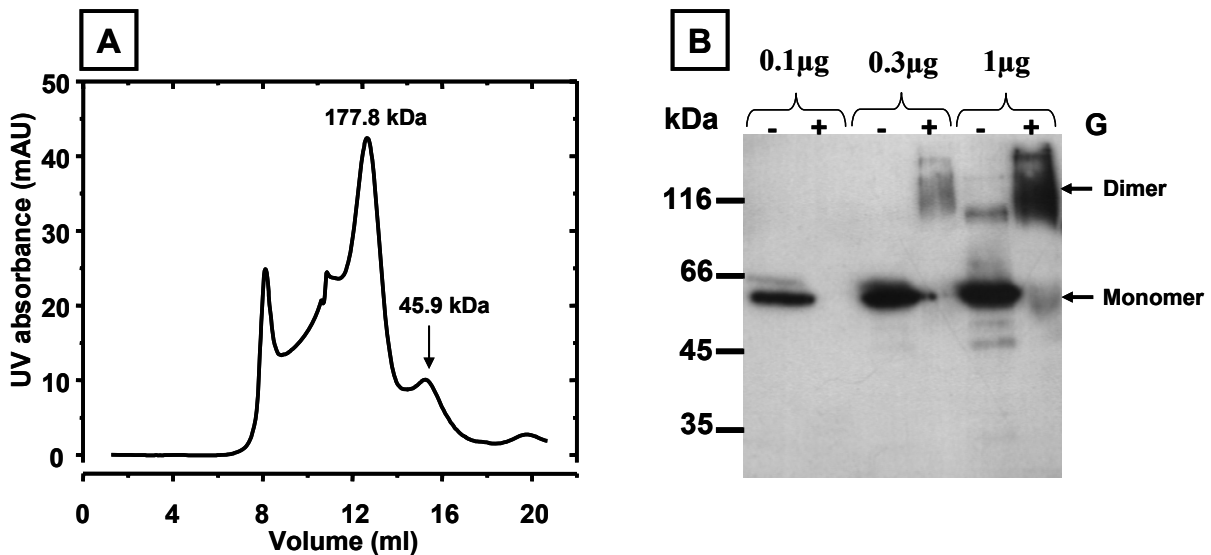


Fig.4.76: Dimerization of hPDE5NGAF (L333A/L334A) performed by (A) Gel filtration showing a size of 177.8 kDa which was estimated to be a dimer and another of a monomer (B) Glutaraldehyde dimerization shows dimer formation.

The quadruple mutant had a different profile (Fig.4.77.A). The three peaks became distinct for an oligomer, dimer and monomer. The Western blot of the fractions of the last three peaks showed a band for the first two but no band for the third.

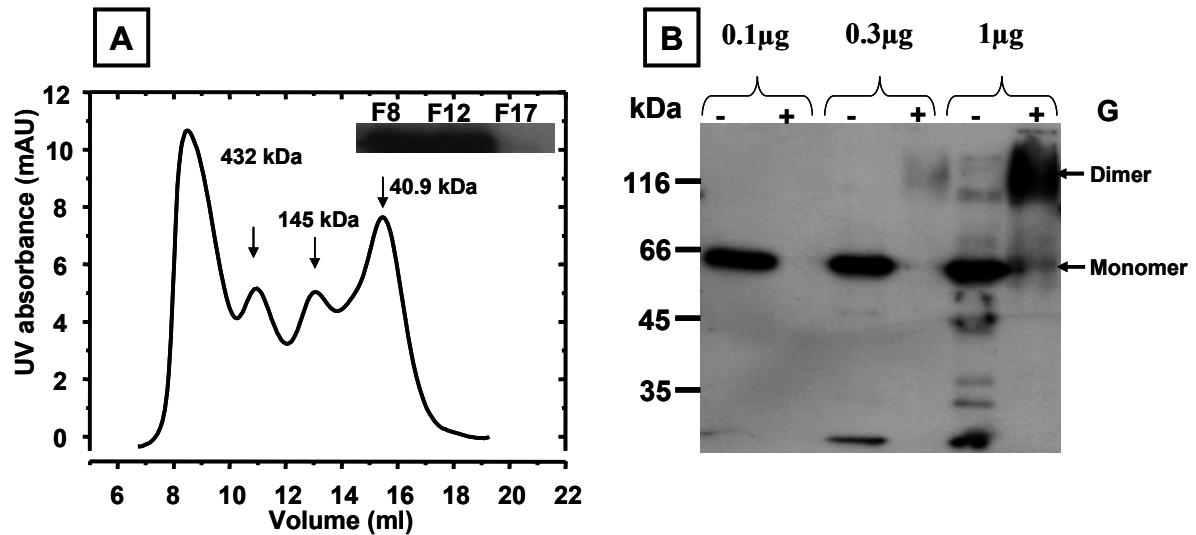


Fig.4.77: Dimerization study of hPDE5NGAF (L152A/L153A/L333A/L334A) **(A)** Gel filtration showing three different peaks: oligomer, dimer and monomer. Fraction collected started at 7 ml F8: 11 ml, F12: 13 ml and F17: 15.5 ml **(B)** Glutaraldehyde crosslinking showing a band for a dimer at high protein concentration with a smaller band for a monomer.

The truncation of the N-terminus of hPDE5 had a MW of 44.4 kDa (with His-tag). In ΔN_{1-135} -hPDE5GAF, the truncation of the N-terminus increased the ratio of monomer to dimer as seen in the gel chromatogram (fig.4.78.A), but the dimer was still the major peak. A third peak to the left of the dimer was a distinct peak for an oligomer which is not distinct in the presence of the N-terminus and this could be due to the larger size of the proteins with N-terminus so the two peaks are not well-separated. Application of the fractions to SDS-PAGE showed bands of monomer size for all peaks. In the glutaraldehyde crosslinking, only dimer is seen at low concentration, while at higher protein concentration (1 μ g) both monomer and dimer were observed (Fig.4.78.B).

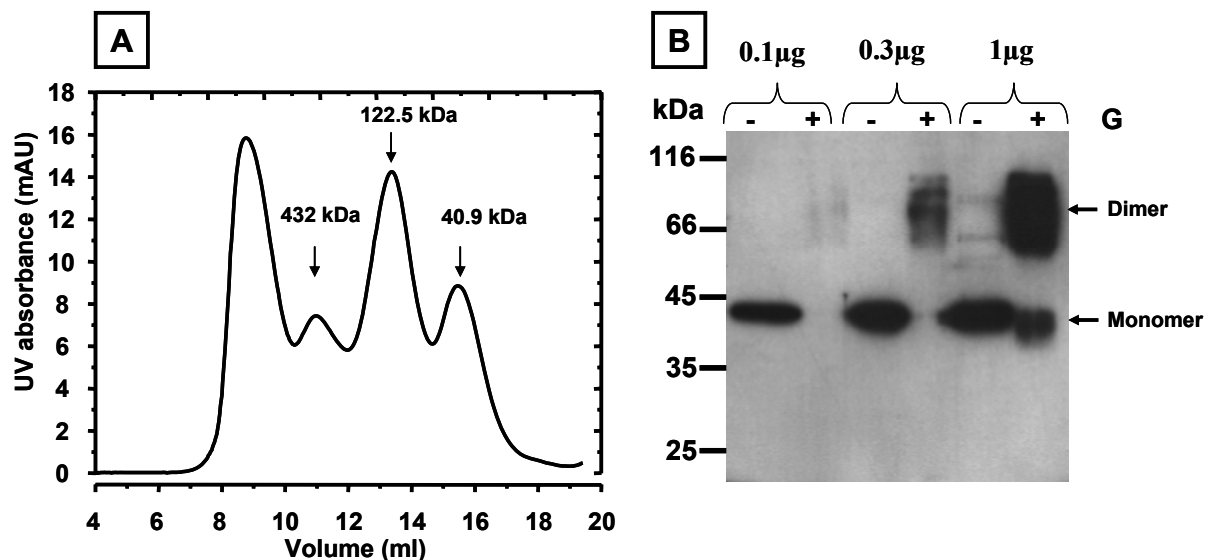


Fig.4.78: Dimerization of ΔN_{1-135} -hPDE5GAF performed by **(A)** Gel filtration showing a size of 122.5 kDa which was estimated to be a dimer **(B)** Glutaraldehyde dimerization shows dimer formation as a major band.

Results

The truncation of the N-terminus in the presence of the connecting helix mutation increased the ratio of monomer to dimer which means that it disturbed dimerization but didn't abolish it (Fig.4.79.A). The glutaraldehyde crosslinking showed bands of the unreacted protein but faint ones for the crosslinked (Fig.4.79.B).

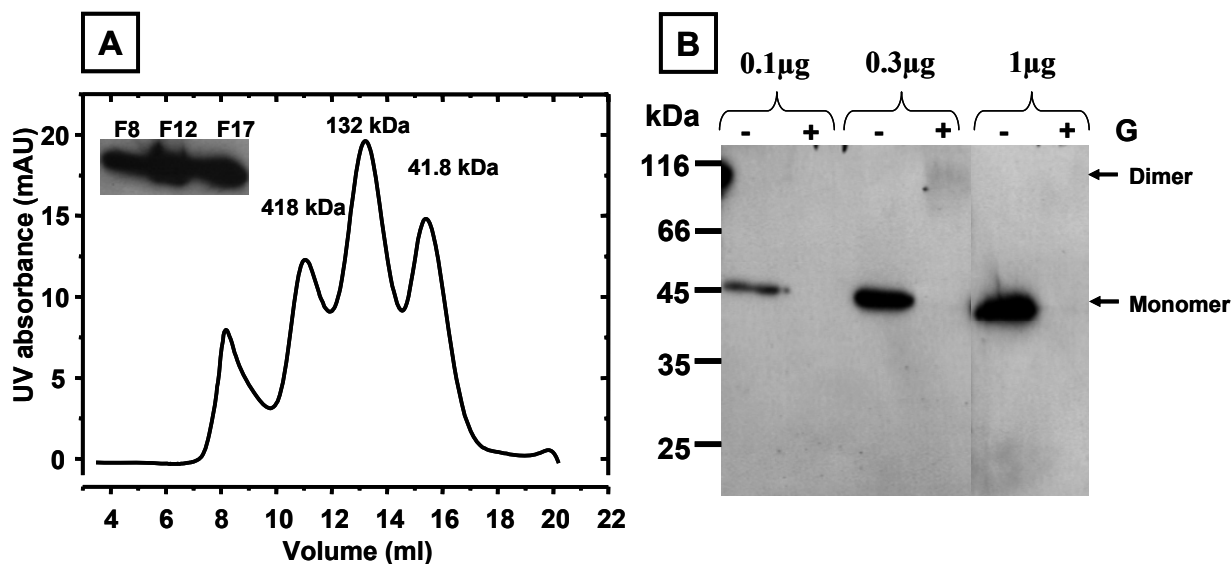


Fig.4.79: Dimerization of ΔN_{1-135} -hPDE5GAF (L333A/L334A) performed by **(A)** Gel filtration showing a size of 418 kDa for oligomer, 132 kDa for a dimer and 41.8 for a monomer and three peaks proved to be ΔN_{1-135} -hPDE5GAF (L333A/L334A) protein by exposing the fractions to western blot F8: 11 ml, F12: 13 ml, F17: 15.5 ml **(B)** Glutaraldehyde dimerization shows clear bands for the unreacted protein and faint bands for a monomer and a dimer for the crosslinked ones.

The truncation of the N-terminus accompanied by quadruple mutation has obviously disturbed dimerization. For ΔN_{1-135} -hPDE5GAF (L152A/L153A/L333A/L334), the gel filtration (Fig.4.80.A) showed three peaks again but with the monomer as a major peak. Applying the fractions of each peak to SDS-PAGE followed by Western blot showed a band of a monomer size (Fig.4.80.A). Glutaraldehyde crosslinking showed a band for a monomer and a streak of dimer-oligomer only at high protein concentration (Fig.4.80.B).

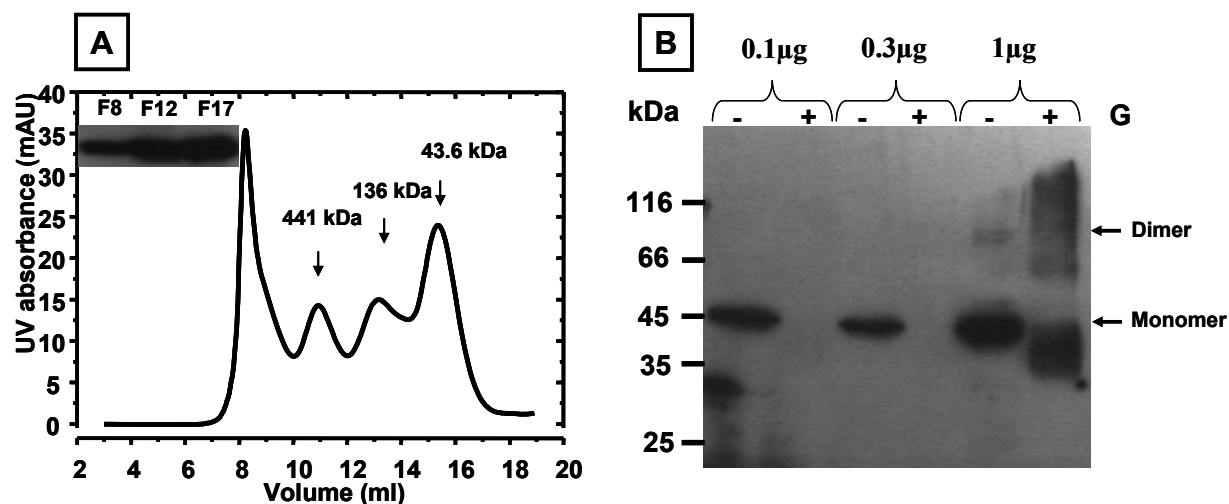


Fig.4.80: Dimerization of ΔN_{1-135} -hPDE5GAF (L152A/L153A/L333A/L334) performed by **(A)** Gel filtration showing a size of 441 kDa for oligomer, 136 kDa for a dimer and 43.6 for a monomer and three peaks proved to be protein by exposing the fractions to western blot, F8: 11 ml, F12: 13 ml, F17: 15.5 ml **(B)** Glutaraldehyde dimerization shows no bands at low amount of protein and mainly a monomer with a streak for the dimer and oligomer.

4.3 Signal transduction through the PAS domain of CyaB1

Comparing the domain organizations of cyanobacterial adenylyl cyclases, CyaB1 and CyaB2, with PDEs 2, 5, 6, 10 and 11, figure 4.81 shows that the cyclases possess a PAS domain of 100-180 aa in front of the catalytic domain. Removal of the PAS domain of CyaB1 and linkage the GAF domain directly in front of the catalytic domain was found to abolish signaling (J.Linder, personal communication).

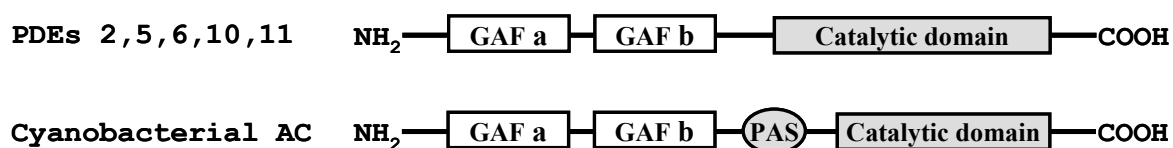


Fig.4.81: Domain organization of Cyanobacteria adenylyl cyclases (CyaB1 and CyaB2) and GAF domain containing mammalian PDEs. Image modified according to ref [16].

According to a BLAST search, the amino acids from 389 to 468 were annotated as a PAS domain while the amino acids 469 to 562 may represent a linker of unknown function. The catalytic domain is from 563 to 795. Three approaches were used to examine signal transduction through the PAS domain of CyaB1. First, the PAS domain was replaced by the linker from hPDE5 which joins the GAF tandem to the catalytic region. Two different lengths were used. Second, the CyaB1 PAS domain was replaced by the PAS domain of CyaB2 enzyme which is longer than the PAS of CyaB1 and lacks the linker region. Third, a flexible linker was inserted between PAS and catalytic domains. The CyaB1 (WT) holoenzyme served as positive control. The kinetic values were in agreement with the published data [80].

It was attempted to crystallize the different domains of CyaB1.

4.3.1 Exchange of CyaB1 PAS domain by the PDE5 linker.

To study the mechanism by which GAF domain tandem signals to the catalytic domain, the PAS domain was replaced by the hPDE5 linker. Two different lengths of the hPDE5 were used (fig. 4.82.A); (A) hPDE5 linker consists of 25 aa's (E513-T537) and (B) consists of 36 aa's, starting exactly the same as (A) and ends at V548. Four different N-terminally truncated catalytic domains were used (fig.4.82.B).

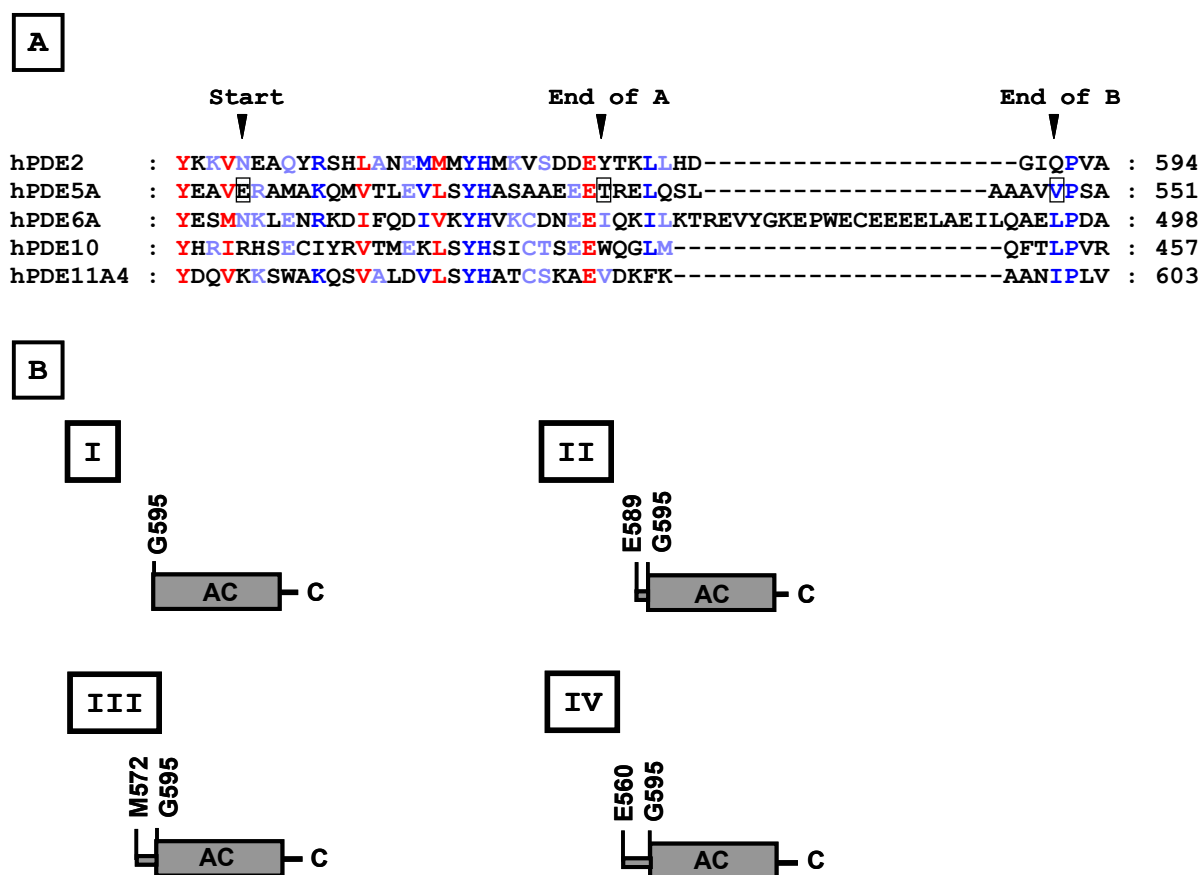


Fig.4.82: (A) Alignment of the PDE5 linker region with that of hPDEs 2, 6, 10 and 11. Rectangles and arrows show the beginning and the end of the PDE5 linker regions used in the study. **(B)** Domain organization of the N-terminally truncated catalytic domains used showing the beginning of each construct.

4.3.1.1 Control (truncated catalytic domains):

To explain the difference in the basal activities obtained by different constructs, the four truncated catalytic domains (fig.4.81.B) were transformed into *BL21 (DE3) [pREP4] E.coli* cells, expressed and assayed. The expression was induced by 300 μ M of IPTG, 10 mM MgCl_2 (27°C, 300 min). Cells were harvested, washed, centrifuged and frozen at -80°C. The pellets were suspended in cell lysis buffer, lysed by passing twice through French press and purified by shaking with 350 μ l of Ni^{+2} -NTA for 90 min. The eluted proteins were dialysed against dialysis buffer overnight at 4°C and used immediately or stored at -20°C. The yield and MW of the four constructs are in table 4.11 in section 4.3.4.3. The SDS-PAGE (Fig.4.83) showed the high purity of the four catalytic domains.

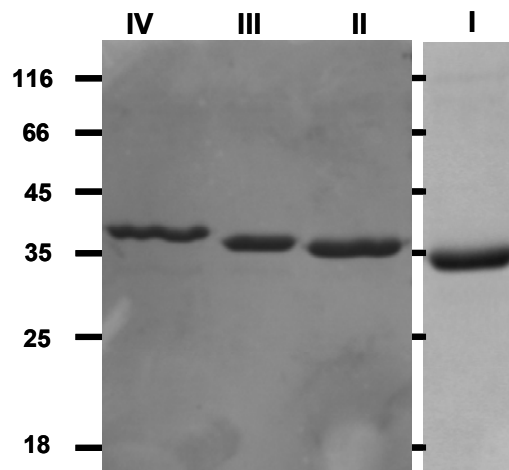


Fig.4.83: SDS-PAGE (15%) of N-terminally truncated catalytic domains (2 μ g)

Constructs I and II to achieve a steady activity at lower protein concentrations with while the constructs III and IV were do no achieve maximal activity at 3 μ M protein. Furthermore, the highest activities were several fold higher for the shorter constructs than the longer ones which could be due to dimerization of the catalytic domain. Dimerization can be observed by a band of construct IV (Fig.4.84)

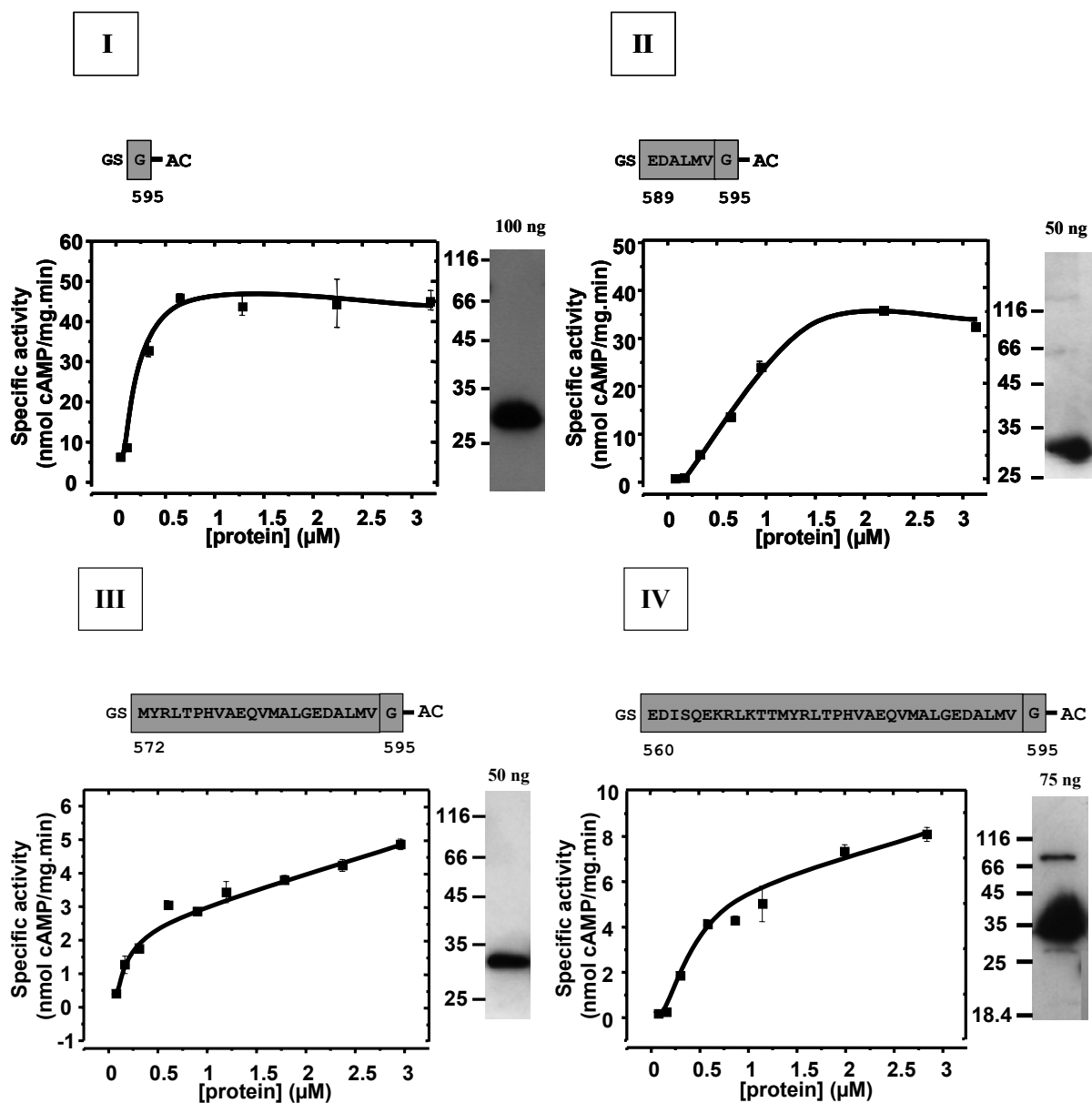
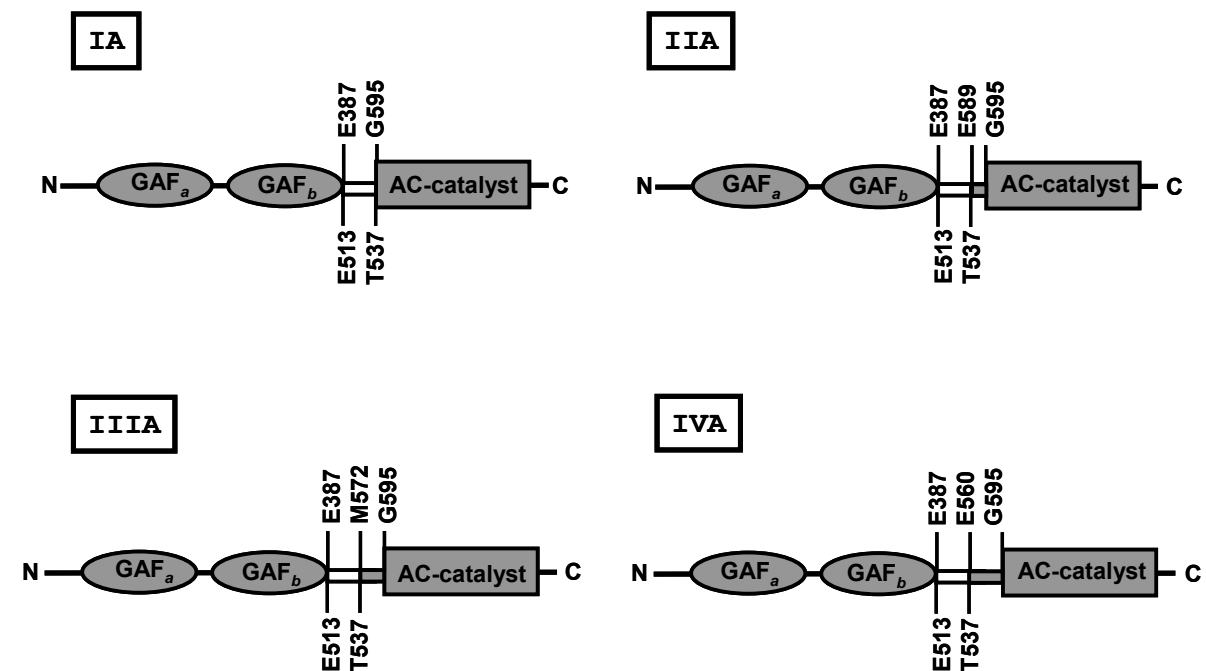


Figure 4.84: Protein dependence of N-terminally-truncated CyaB1 AC's. Assay conditions: 37°C, min, 75 μM Mg^{+2} -ATP, 0.1M Tris/HCl pH 7.5, 10 min (n = 4). Western blots are shown to the right.

The protein dependence was established for the constructs. The basal activity of the truncated catalytic domains mirror the basal activities obtained by their corresponding constructs in categories A and B (see below)

All constructs have similar domain organization but differ in sequence of the linker (Fig.4.85). GAF domain was from A.Schultz and the four catalytic domain constructs were from J.Linder.

Category A



Category B

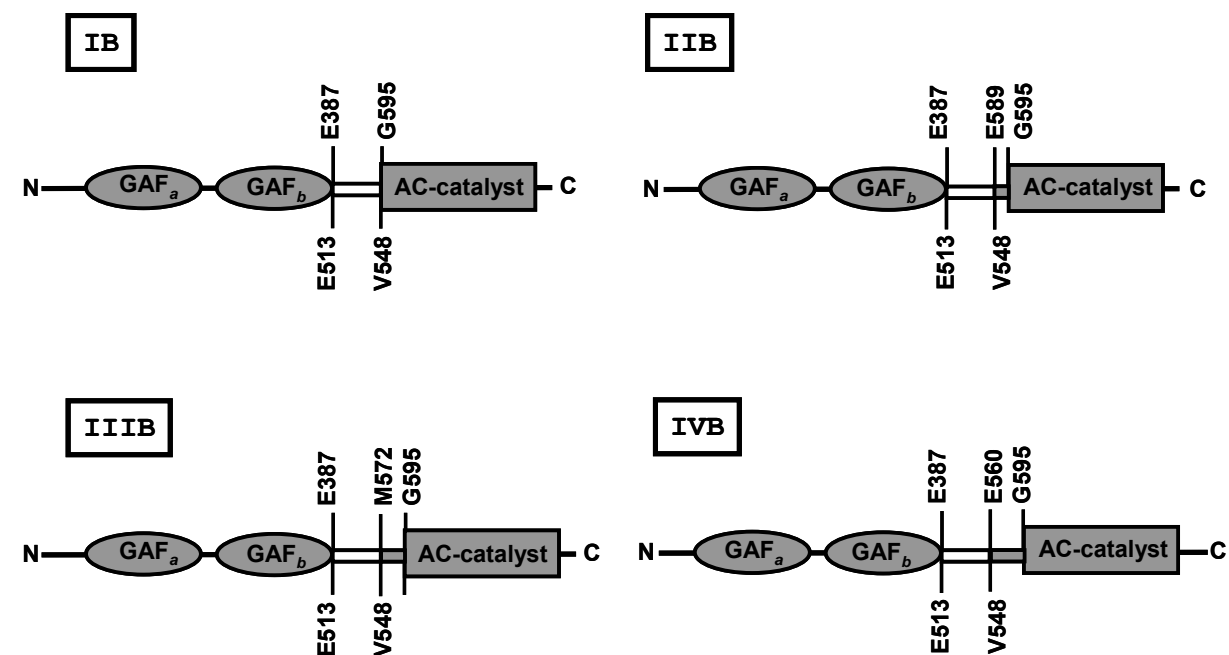


Fig.4.85: Domain organizations of constructs of category A and B of CyaB1 (PDE5linker).

A total of 8 constructs (2 linkers \times 4 N-truncated AC's) were generated (3.4.5.1), transformed into *BL21(DE3)[pREP4]* *E.coli* cells, expressed (30 μ M IPTG, 18°C, 10 mM MgCl₂,

Results

overnight) and purified (200 μ l Ni⁺²-NTA agarose, 3 hr). The proteins were well-expressed with good yield and purity (fig.4.86).

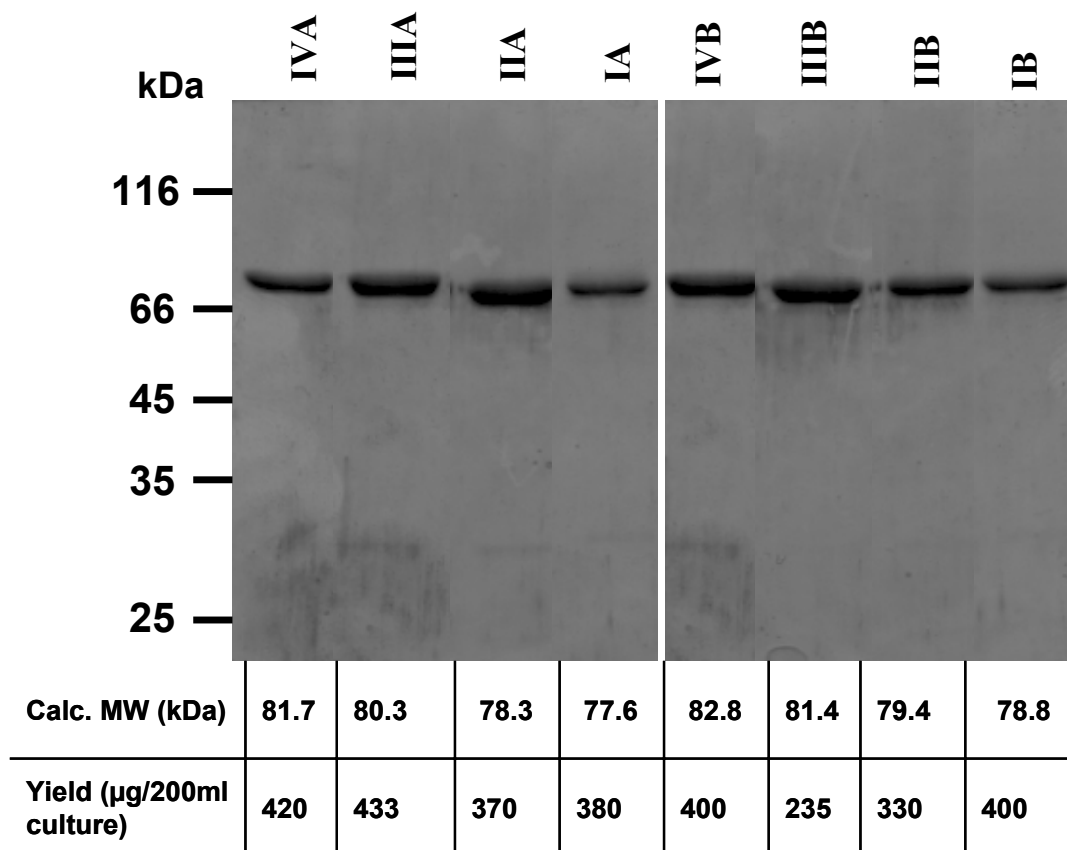


Fig.4.86: SDS-PAGE (12.5%) of 4 μ g of the eight constructs (both category A and B)

N-terminally truncated catalytic domains were used as controls. Category A contains CyaB1 GAF₁₋₃₈₇, hPDE5₅₁₃₋₅₃₇ and the four catalytic domains. Category B has the CyaB1 GAF₁₋₃₈₇, hPDE5₅₁₃₋₅₄₈ and the four catalytic domains.

4.3.1.2 Category A

The protein dependence was established \pm cAMP for the four constructs (Fig.4.87). None of them was activated by cAMP. The specific activity was high for the two shorter construct (15 and 18 nmol/mg.min for IA and IIA respectively) and low for the longer constructs (5 and 4 nmol/mg.min for IIIA and IVA respectively). Western blots for all constructs showed no degradation products.

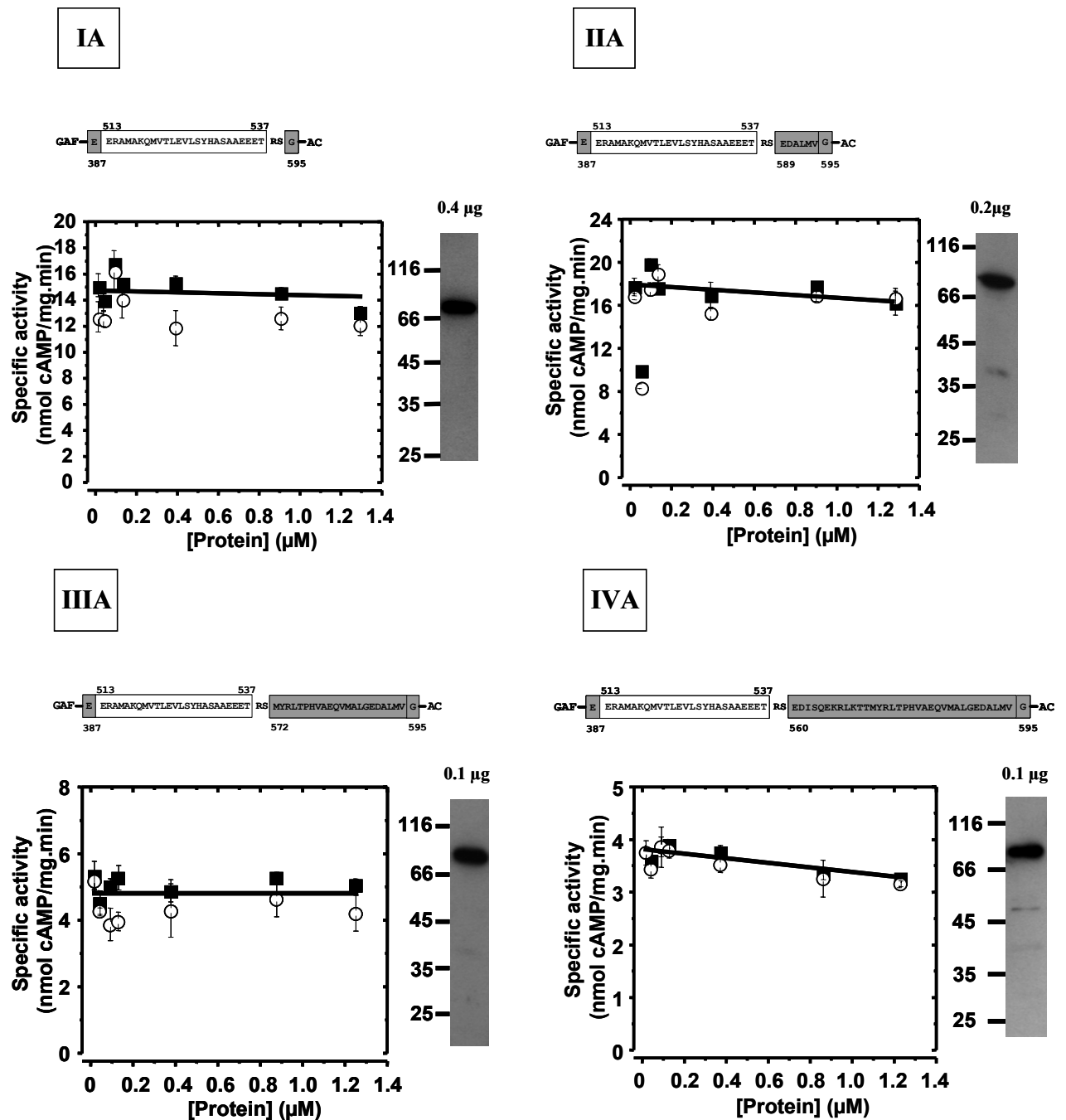


Fig.4.87: Protein dependence of constructs of **Category A**. (■) Basal activity, (○) + 1mM cAMP Assay conditions: 75 µM Mg⁺²-ATP, 37°C, 4 min and 0.1M Tris/HCl pH 7.5

4.3.1.3 Category B

The protein dependence was mostly linear for these constructs (Fig.4.88). The shorter three constructs were not affected by cAMP and they have similar basal activities. The fourth construct IVB was the only construct activated by cAMP. Basal activity of the unactivated construct was lower.

Results

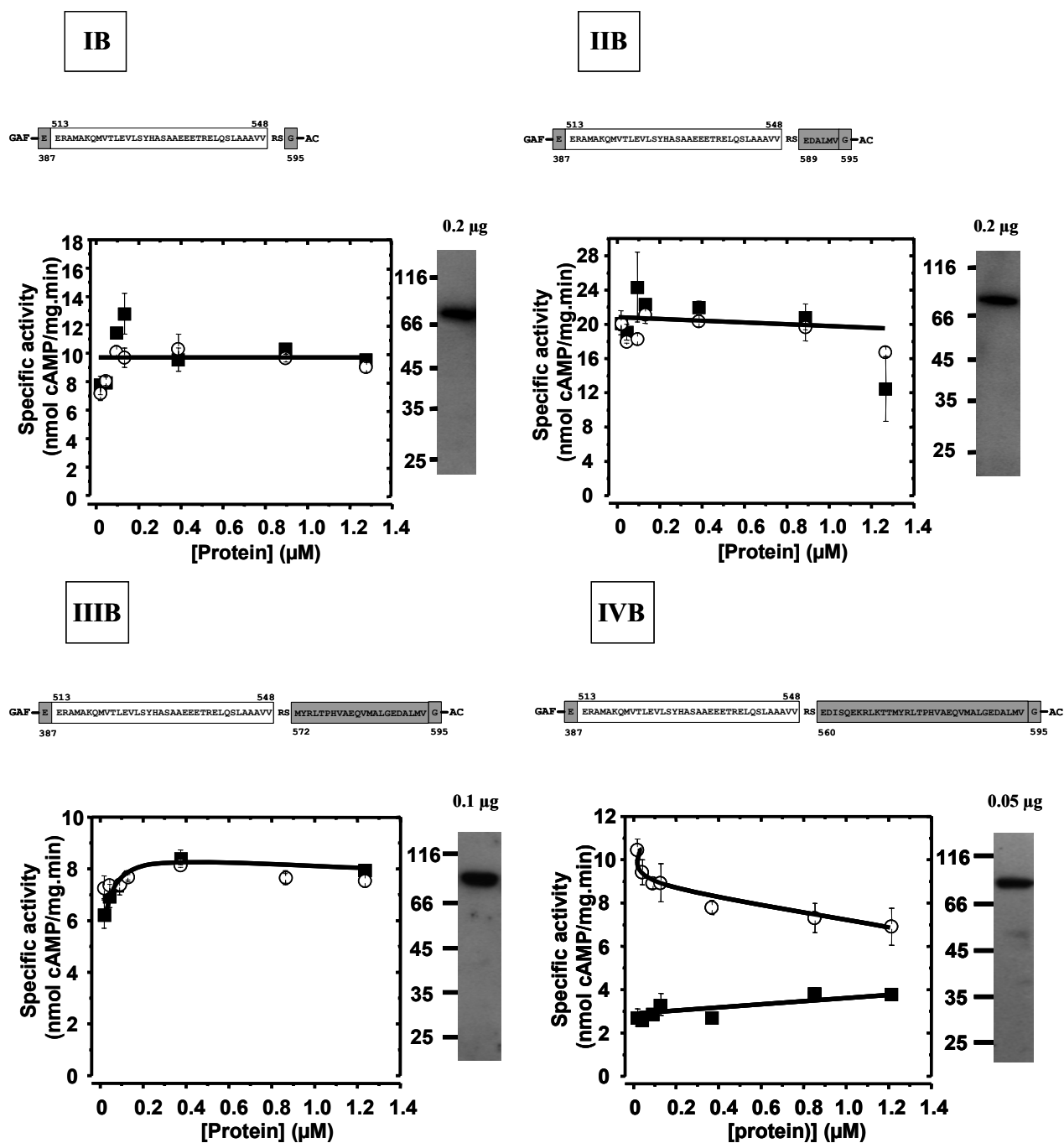


Fig.4.88: Protein dependence of **category B**. (■) Basal activity, (○) + 1 mM cAMP. Assay conditions: 4 min, 37°C, 75 μM Mg^{+2} -ATP, 0.1M Tris/HCl pH 7.5

A cAMP-dose response curve for construct IVB was established. The EC_{50} of $1.58 \pm 0.15 \mu\text{M}$ was similar to the wild type ($0.40 \pm 0.023 \mu\text{M}$). The Hill coefficient of 0.5818 ± 0.064 ($R^2 = 0.9865$, $n = 4$) showed no cooperativity. However, the fold stimulation was only 3.34 ± 0.070 ($n = 4$); i.e. about one tenth that of CyaB1 (fig.4.89).

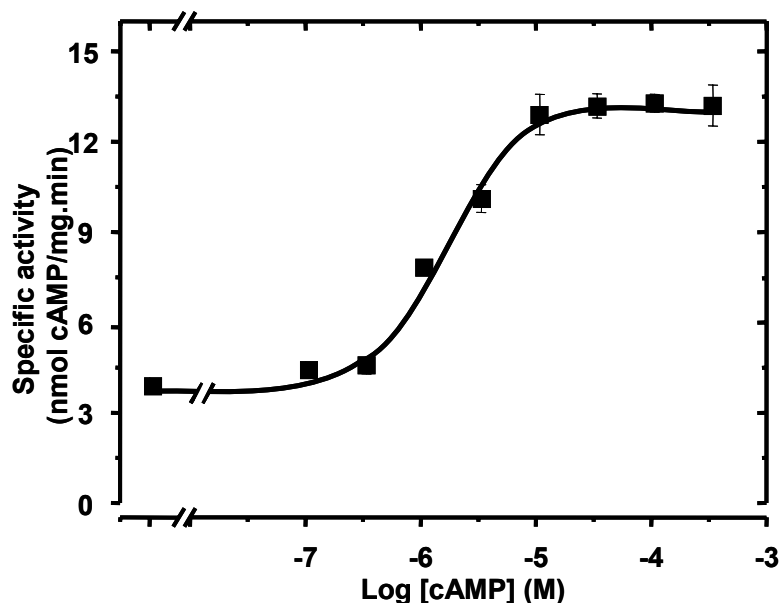


Figure 4.89: The cAMP-dose response of construct (IVB). Assay conditions: 4 min, 37°C, 75 μ M Mg^{+2} -ATP and 0.1M Tris/HCl pH 7.5, 81 nM protein (n = 4).

According to T.Kanacher [79], a metal was required for CyaB1 catalytic domain. D606 and D650 were responsible for metal binding in CyaB1. I have observed presence of similar residues in the PAS domain (see figure 4.90)

```

          ▼                               ▼
CyaB1.Cat : GE-RKEVTVLFSDIRGYTTLTENLGAAEVVSLLNQYFETMVEAVFNVEGTLDKFIGDA : 651
CyaB1.PAS : KQYQKDIQLQSLSDA----VISTDM-AGRIVTINDAALELIGC-----PLGDA : 429

```

Fig.4.90: Alignment by ClustalW showing the 21% identity and 48% similarities between the beginning of the PAS domain and the beginning of the AC catalytic domain. The triangles determine the aspartate residues responsible for the metal binding in the AC catalytic domains.

4.3.2 Exchange of CyaB1 PAS domain by CyaB2 PAS domain.

The PAS domain of CyaB1 was aligned with that of CyaB2 and segment from K388-K569 from CyaB1 holoenzyme was exchanged by PAS of CyaB2 (E444-K570) (Fig.4.91.A).

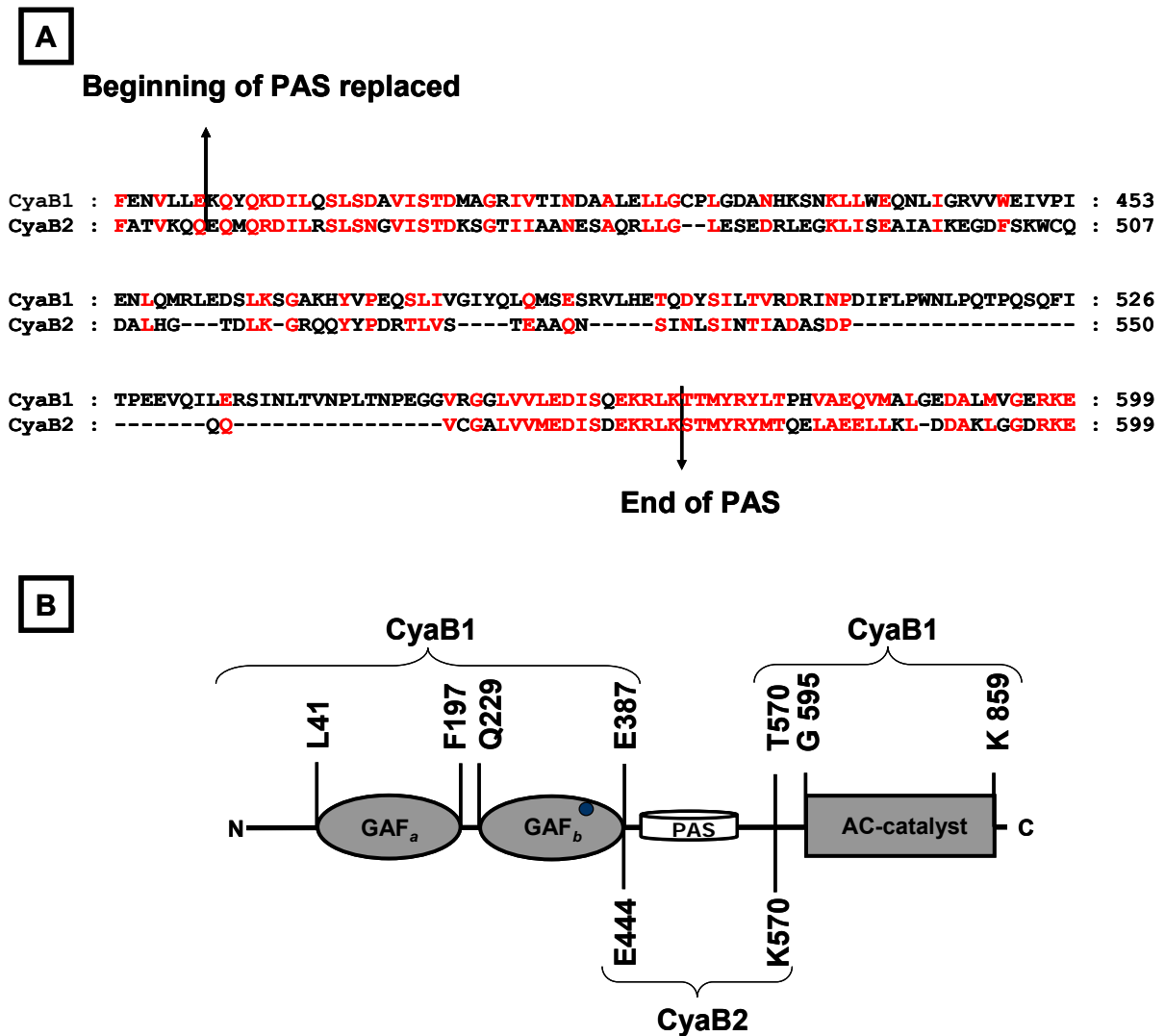


Fig.4.91: Construction of CyaB1(PAS2) construct (A) Alignment shows similarities and identities and the amino acid boundaries of the PAS domain, (B) Domain organization of CyaB1 (PAS2) construct. Blue circle indicates the cAMP binding to the GAF_b domain.

The construct (4.92.b) was cloned in pQE30 and expressed as usual Two hours after induction, 1 ml was pipetted, treated as mentioned in section 3.3.2 and the supernatant and pellets were compared with that of empty pQE30. The protein was well-expressed as soluble protein (Fig.4.92), and purified by Ni⁺²-NTA agarose. Relatively clean bands were obtained on the SDS-PAGE and Western blot. The protein has a calculated MW of 91.49 kDa and an isoelectric point of 5.52.

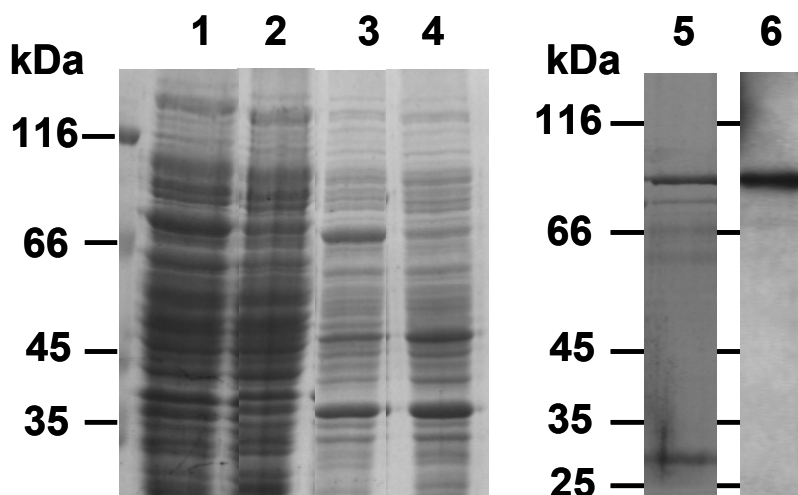


Fig.4.92: SDS-PAGE (10%) and Western blot of CyaB1 (PAS2) (1 and 3) supernatant and pellet of CyaB1 (PAS2), respectively, (2 and 4) Supernatant and pellet of pQE30, respectively, (5) 1.8 μg of purified CyaB1(PAS2) and (6) Western blot (0.5 μg).

The protein dependence was linear \pm 1 mM cAMP (Fig.4.93). The construct was stimulated by cAMP, but less than CyaB1.

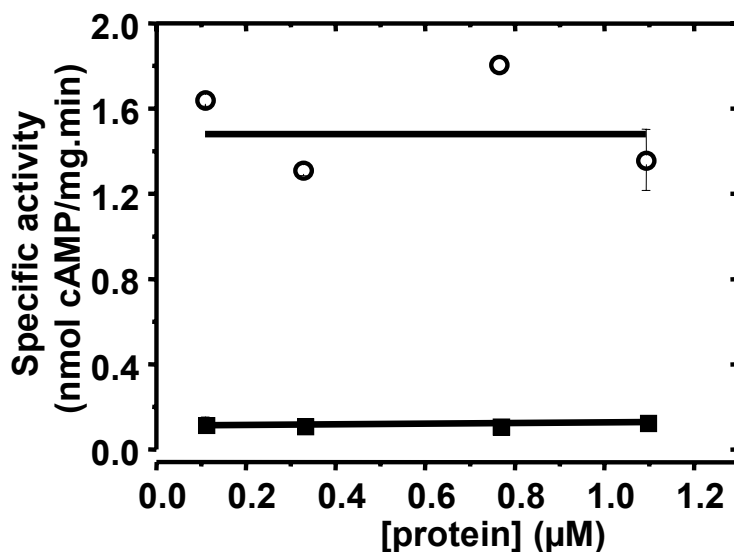


Fig.4.93: Protein dependence of CyaB1 (PAS2). (■) Basal activity, (○) + 1 mM cAMP. Assay conditions: 4 min, 75 μM Mg^{+2} -ATP, 37°C, 0.1M Tris/HCl pH 7.5, (n = 4).

Dose response curve (Fig.4.94) yielded an activation factor of 8.8 ± 0.5 for cAMP, an EC_{50} of 3.2 ± 0.23 μM and a Hill coefficient of 0.588 ± 0.023 ($R^2 = 0.9765$, n = 4) which shows no cooperativity.

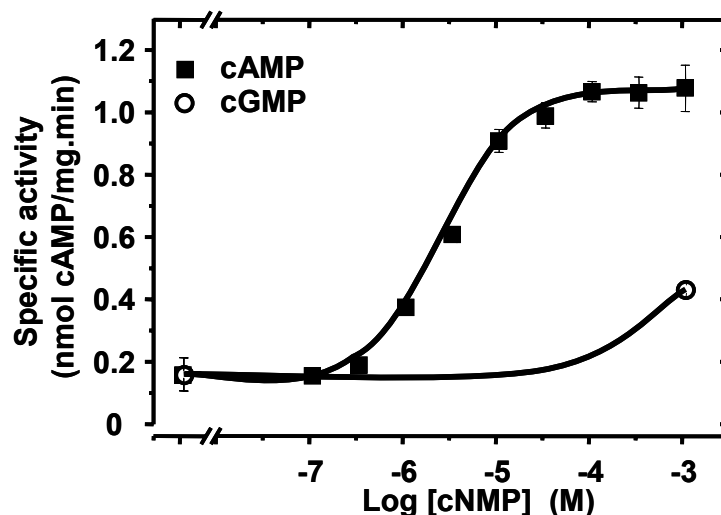


Fig.4.94: Dose response curve of CyaB1 (PAS2).

Assay conditions: 4 min, 37°C, 75 μ M Mg^{+2} -ATP, 0.1 M Tris/HCl pH 7.5, 325 nM (n = 4).

4.3.3 Insertion of tetradekapeptide linker between PAS and catalytic domains of CyaB1.

A flexible tetradekapeptide linker used by Y.Guo produced an active heterodimer from Rv1625 [105]. Here, the same peptide linker was inserted between the PAS and catalytic domains of CyaB1. Accordingly, the GAF, PAS of CyaB1 were separated from the catalytic domain via the insertion of a DNA sequence that codes for the peptide linker “TRAAGGPPAAGGLE” (abbreviated as L) using conventional molecular biology techniques. The peptide linker was inserted between T571 and M572.

The construct was cloned in pQE30, transformed into *BL21 (DE3) [pREP4] E.coli* cells, expressed and purified (section 4.3.1). The purified dialysed N-His tagged- protein had a calculated MW of 99.2 kDa and an isoelectric point of 5.65 (Fig.4.95).

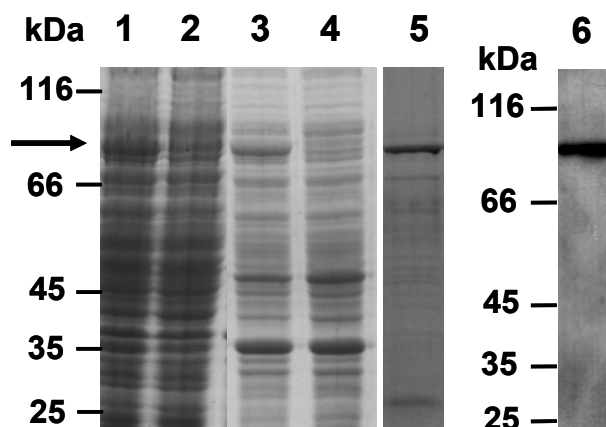


Fig.4.95: SDS-PAGE (10%) and Western blot of CyaB1 (571+L) (1 and 3) Supernatant and pellet of CyaB1 (571+L), respectively, (2 and 4) Supernatant and pellet for pQE30, respectively, (5) 1.9 μ g of purified CyaB1 (571 + L) (6) Western blot of 0.5 μ g (12.5%SDS-PAGE).

Results

The protein has low basal activity (0.457 ± 0.057 , $n = 14$) and was not stimulated by 1 mM cAMP (fig.4.96).

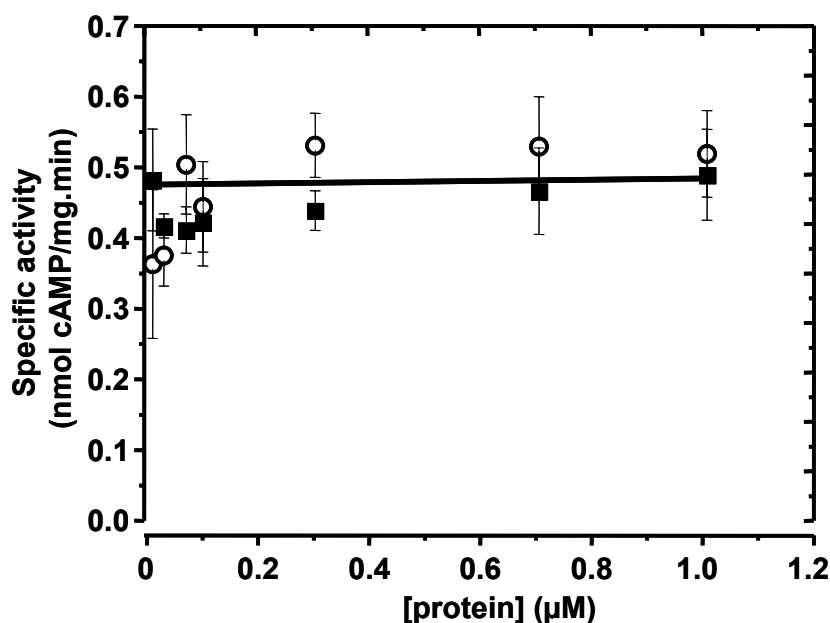


Fig.4.96: Protein dependence of CyaB1 (571 + L) \pm 1 mM cAMP. (■) Basal activity, (○) + 1mM cAMP. Assay conditions: 10 min, $75 \mu\text{M Mg}^{+2}$ -ATP, 0.1 M Tris/HCl pH 7.5, 37°C .

To exclude any effect of the insertion of the linker on the folding of the catalytic domain, substrate kinetics were established \pm 1 mM cAMP (Fig.4.97). The K_m value was $18.56 \pm 1.42 \mu\text{M}$ ATP, a V_{max} of $0.65 \pm 0.008 \text{ nmol/mg.min}$ and a Hill coefficient of 1.05 ± 0.02 ($R^2 = 0.9887$, $n = 2$) for both activated and unactivated forms. The V_{max} for the CyaB1 (571 + L) was much lower (less than 1%) than for CyaB1 whereas K_m and Hill coefficient were comparable.

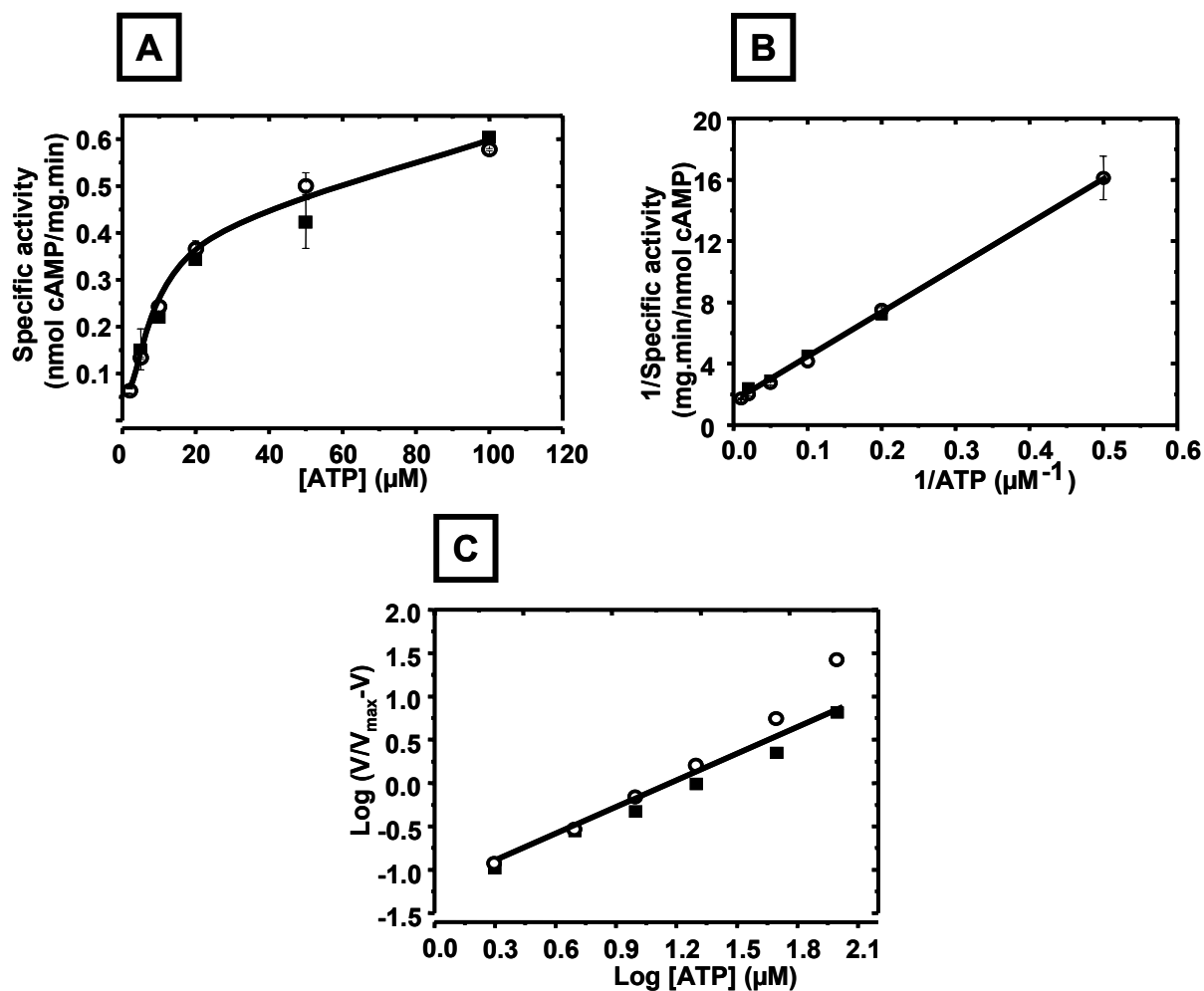


Fig.4.97: Substrate kinetics of CyaB1 (571 + L). (■) basal activity, (○) + 1mM cAMP. Assay conditions: 37°C, 4 min, 75 μM Mg-ATP and 0.1M Tris/HCl pH 7.5, 300 nM protein (n = 2) (A) Michaelis-Menten curve, (B) Lineweaver- Burke, and (C) Hill Plot

4.3.4 Crystallization trials of the CyaB1 domains

4.3.4.1 Crystallization of CyaB1 GAF domain

The crystal structure of CyaB2 GAF tandem had shown an antiparallel dimer in contrast to the parallel structure of mPDE2 GAF-tandem. In spite of that, the two tandems were functional upon exchanging the GAF domain of CyaB1 [80, 101]. The crystallization of CyaB1 GAF domain could shed light on the dimerization of this unique enzyme. CyaB1GAF boundaries were determined by J.Linder according to the crystallized mouse PDE2 GAF and CyaB2 GAF, cloned in pQE60 by A.Schultz and DNA-plasmid was transformed into *E.coli BL21 (DE3) [pREP4]* cells for expression (see fig.4.98).

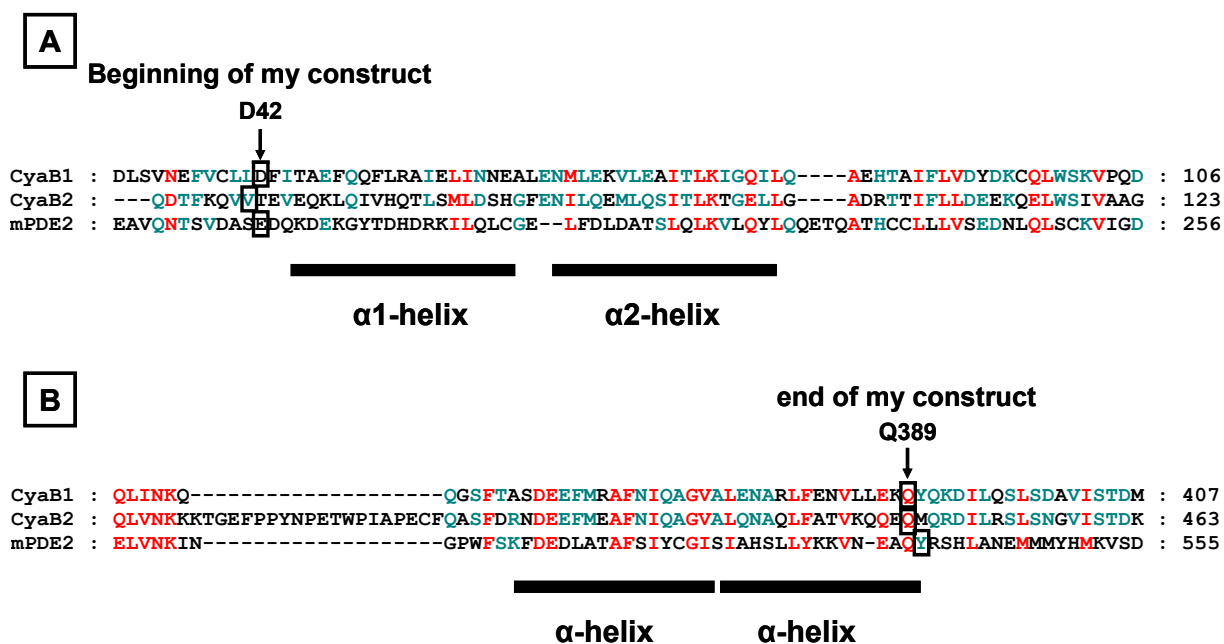


Fig.4.98: Construction of the CyaB1 GAF by alignment the GAF domain of CyaB1 with that of CyaB2 and mPDE2

(A) Alignment shows the beginning of the three constructs with the first amino acid indicated by a rectangle (note that the only conserved residues in the α 1-helix are the two hydrophobic residues followed by a carboxylic amino acid)

(B) The end of the alignment of the three GAF domains and the last amino acids are determined by a rectangle, code of the alignment: red: highly conserved, blue: more the 60% similarity, Black: unconserved. The secondary structure appears below the alignment is according to the crystal structures of both GAF-tandems.

Several 200-ml batches were inoculated by 5 ml of an overnight culture. The cultures (30°C until $OD_{600} \sim 0.5-0.6$) were induced with 0.3 μ M IPTG (22°C for 6 hrs). Cells were harvested and the washed pellets were frozen at -80°C. The pellets were resuspended and passed twice through a French Press (1000 Psi). The lysate was centrifuged at 18000 \times g, 4°C for 40 min. The protein was purified by 200 μ l Ni-NTA agarose for three hours and dialyzed against crystallization buffer (with 10% Glycerol). The 40.0-kDa, C-terminally hexahistidine-tagged protein was analyzed by SDS-PAGE (see fig.4.99). Each 200 ml culture produced 0.3 mg protein.

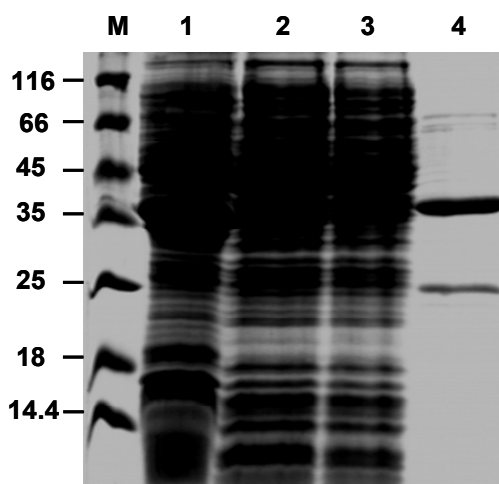


Fig.4.99: SDS-PAGE (15% polyacrylamide) of CyaB1GAF crystallized. **(M)** PeqGold marker **(1)** Pellet **(2)** Supernatant after centrifugation **(3)** Supernatant after Ni⁺²-NTA binding **(4)** Purified protein (4 μ g).

The protein was concentrated by ultrafiltration (NANOSEP 10K centrifugal devices) to 11-12 mg/ml and 2 mM cAMP was added. The mixture was centrifuged and screened by crystal screen I, II and lite (from Hampton) and Wizard I and II (from genetic deCode Biostructures) using the hanging drop diffusion method (section 3.3.11.1) at 16°C. The plates were inspected every day for the first week and then weekly.

Clusters of needles have appeared with crystal screen II # 39 (3.4M 1,6-hexanediol, 0.1M Tris/HCl pH 8.5 and 0.2M MgCl₂) after 4 days and increased in number with time but not in size (see fig.4.100). Crystallization was reproducible.

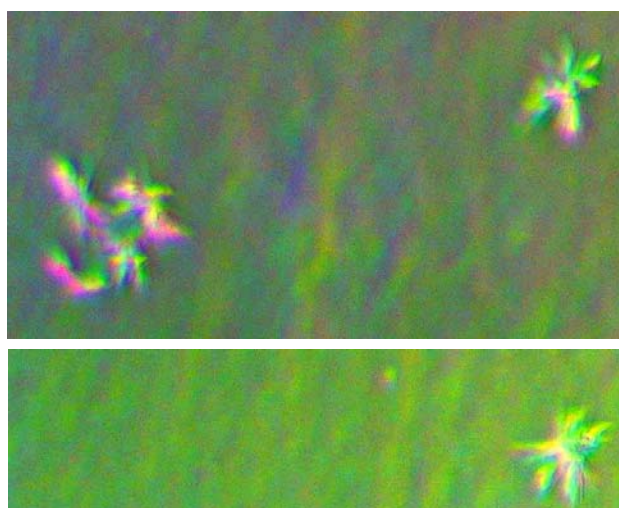


Fig.4.100: Clusters of needle-shape crystals of CyaB1GAF obtained by the hanging drop method using crystal screen II #39 (3.4M 1,6-hexanediol, 0.1M Tris/HCl pH 8.5 and 0.2M MgCl₂) as precipitant.

Results

To make sure that these needles are protein, the crystallization was performed without protein \pm 2 mM cAMP. No needles appeared.

Further optimization of the crystal size and shape have been tried by varying the concentration of 1,6-hexandiol, pH and the type and concentration of salt. The conditions produced crystals as listed in table 4.8.

Table 4.8: crystals-containing conditions obtained by optimization of the size and shape of CyaB1 GAF crystals

1,6-Hexanediol	Tris/HCl	pH	MgCl ₂	[Protein] +2mM cAMP	Crystallization conditions	Storage Temp.
2.6/3.0/3.4/3.8/ 4.2	0.1M	8.5	0.2 M	11 mg/ml	Needle bundles of 10-35 μ m the largest appears at 3.8M	12°C
3.4 M	0.1M	8.5	0.1, 0.2, 0.4, 0.67M	11 mg/ml	Needles of 5-40 μ m. the crystals decrease in number and increase in size with more MgCl ₂ , largest at 0.67M	
3.4 M	0.1M	7.5	0.2	11 mg/ml	Many needle shape crystals as bundles (15 μ m)	
	0.1M	8.0	0.2	11 mg/ml	Few needles 20-25 μ m	
	0.1M	9.0	0.2	11 mg/ml	Few crystal bundles 20-30 μ m	

The optimization of these crystals did not succeed.

4.3.4.2 Crystallization of CyaB1 PAS domain

According to the SMART search (Schultz, 1998), the PAS domain of CyaB1 boundaries starts at CyaB1 PAS (K388-T571) was cloned in pQE30 and expressed in *BL21 (DE3) [pREP4]* *E.coli* cells. Cells were induced at an OD₆₀₀ of 0.5-0.6 by 300 μ M IPTG at 27°C. After 6 h, cells were harvested, freeze shocked in liquid nitrogen. Pellets were lysed by passing twice through French Press and protein was purified by 200 μ l of Ni⁺²-NTA agarose for three hours. The eluted protein was dialysed overnight at 4°C against crystallization buffer (20 % Glycerol, 10 mM Tris/HCl pH 7.5, 10 mM MgCl₂ and 0.05% thioglycerol). The yield was 600 μ g/200 ml. The purity of CyaB1 PAS protein was monitored by SDS-PAGE and Western blot (fig.4.101). The protein has a calculated MW of 22.05 kDa.

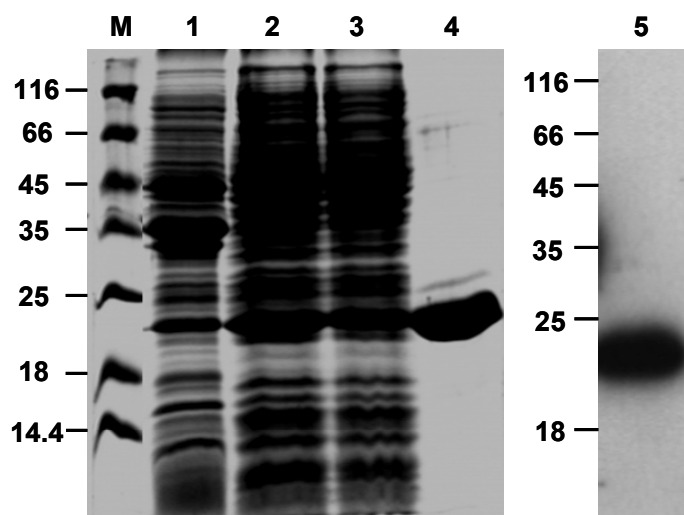


Fig. 4.101: SDS-PAGE (15%) and western blot of CyaB1 PAS crystallized. **(M)** PeqGold marker **(1)** Pellets **(2)** Supernatant **(3)** Supernatant after Ni-NTA **(4)** 12 µg of purified protein showing high purity **(5)** Western blot (15% SDS-PAGE and 0.1 µg protein), the protein has N-terminal His-tag and was detected by anti RGS-His4 as primary antibodies.

Samples were concentrated by ultrafiltration over a 10 kDa cut-off filter (Nanosep) to 11.5 mg/ml and used for crystallization or stored at 4°C. The protein was screened by Crystal screen I, II and lite (from Hampton) by the hanging drop method. 1 µl of protein sample was mixed with 1 µl of each screening buffer (drop mixture 1:1). In the reagent reservoir 0.4 ml of the precipitant solution were mixed with 100 µl glycerol 87% to obtain a concentration of glycerol 7% higher than the glycerol present in the drop mixture because the crystallization buffer contains 20% glycerol. The 24-well plates were incubated at 12°C and examined under a polarization microscope every day for the first week and then once a week.

A huge number of very small cubic crystals (10 × 10 µm) have appeared after 5 days of storage at 12°C by the unbuffered crystal screen II # 7 which consists of 10% PEG1000 and 10% of PEG 8000. Repetition at lower protein concentration (8mg/ml) produced fewer and bigger cube-like crystals (35×35 µm) (see fig 4.102.A). Further optimization varied the concentration of precipitant components, protein concentration, pH's, and incubation of the plate at lower temperatures to produce nuclei followed by higher temperature to grow the crystal.

First, different concentrations of PEG1500 and PEG8000 were tried but none of the conditions produced crystals. In addition, 10% of PEG1000 and 10% of PEG8000 with 0.2M of different salts: MgCl₂, sodium formate, sodium acetate, ammonium sulphate, sodium citrate, lithium chloride, lithium nitrate, potassium nitrate, potassium acetate, potassium iodide, sodium thiocyanate, sodium chloride, ammonium acetate in addition to 2% isopropanol with protein concentration of 6 mg/ml and incubation temperature of 12°C but

Results

none of these conditions produced crystals. Varying the concentration of PEG1000 and PEG8000 proved that 10% of each reagent is the optimum to give crystals. 0.1M Tris/HCl with different pH's were tried concomitantly with incubation conditions of the plate at lower temperature (12°C) for 2 days followed by higher temperature (18°C) (see table 4.9 and fig. 4.102.B and C).

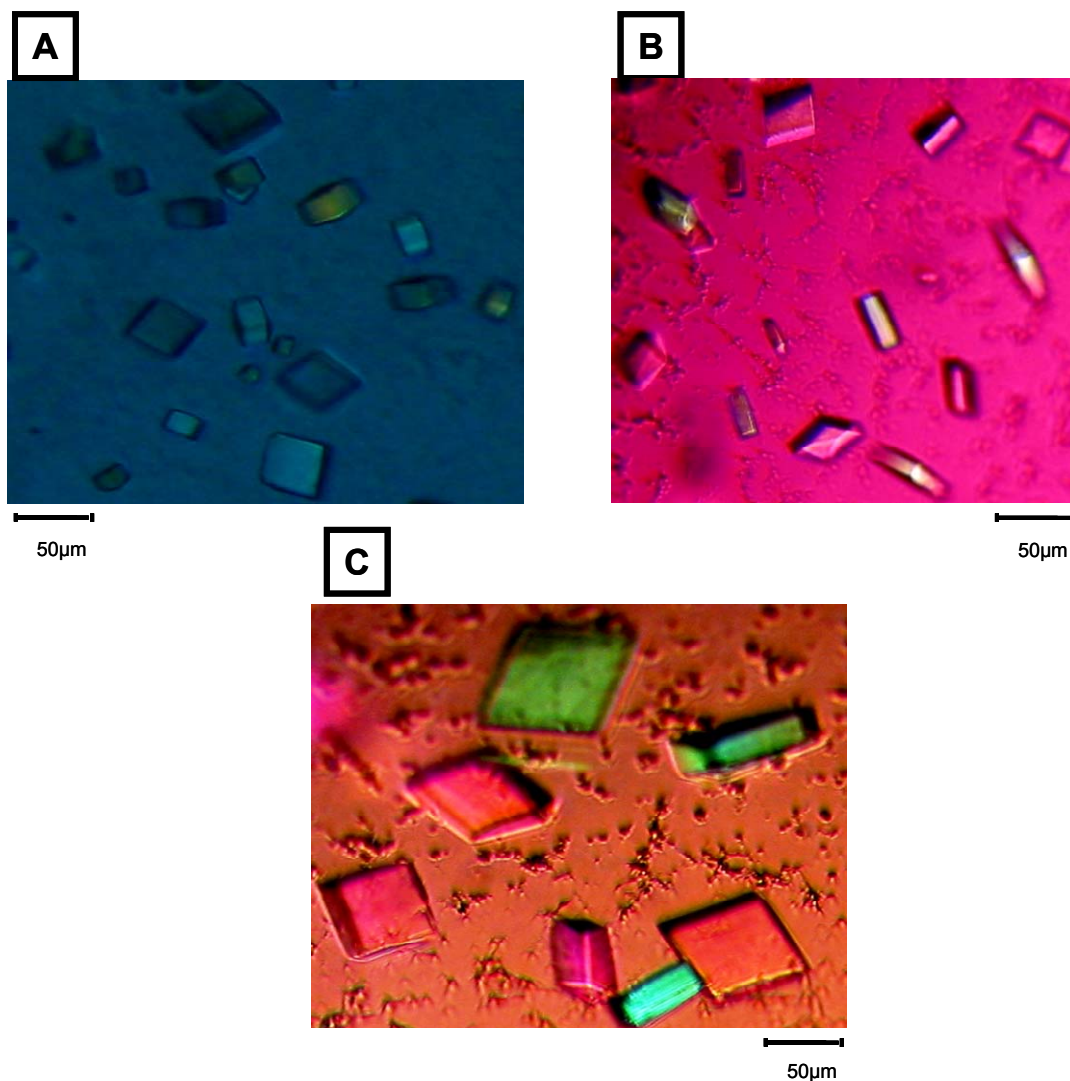


Fig. 4.102: Crystals obtained from CyaB1 PAS. **(A)** Crystals with crystal screen II # 7 which consists of 10% PEG 1000 and 10% PEG 8000 incubated at 12°C with protein concentration of 8 mg/ml **(B)** the crystals obtained with 10 % PEG1000, 10% PEG8000 and 0.1M Tris/HCl pH 8.5 **(C)** crystals obtained with 10% PEG1000, 10% PEG8000 and 0.1M Tris/HCl pH 9.0 **(B and C)** contain protein concentration of 6 mg/ml and incubation conditions of 12°C for 2 days followed by 18°C for another 5 days.

Results

Table 4.9: The results of crystallization optimization of CyaB1 PAS protein

PEG 1000 (%)	PEG 8000 (%)	Additives	[Protein]	Crystallization conditions	Storage Temp.
7.5, 10, 12.5, 15, 17.5, 20	10	-	6.5 mg/ml	Large number of small cubic crystals appeared four days after storage only with concentrations between 7.5-12.5%	12°C
10	7.5, 10, 12.5, 15, 17.5, 20	-	6.5 mg/ml	Large number of very small cubes appeared with the same storage conditions as above with 7.5-17.5%	
10	10	Tris/HCl pH 7.5	6 mg/ml	No crystals	12°C for 2 days then 18°C for 5 days
10	10	Tris/HCl pH 8.0	6 mg/ml	No crystals	
10	10	Tris/HCl pH 8.5	6 mg/ml	Tetragonal crystals (60 × 50 μm) figure 4.102.B	
10	10	Tris/HCl pH 9.0	6 mg/ml	Tetragonal crystals (90 × 80 μm) figure 4.102.C	

Analysis and Data collection

The crystals were sent to the Biochemistry Center (BZH) in Heidelberg University to elucidate the crystal structure. Several X-ray diffraction data sets were recorded from individual crystals at the ESRF in Grenoble, and images with a resolution of 2.1-2.3 Å were obtained with three different crystals (data are shown in table 4.10).

Table 4.10: Statistics for datasets P2-5, P1-5 and P1-2 collected from the x-ray of three different crystals (from analysis report obtained from I.Tews)

	P2-5	P1-5	P1-2
Space group	1 (P1)	1 (P1)	4 (P2 ₁)
Unit cell dimensions (a b c [Å] α β γ [°])	35.846 45.777 118.809 90.189 89.951 89.588	35.960 45.781 118.874 89.933 89.980 89.465	45.858 117.825 35.783 90.000 90.571 90.000
Beamline	Id-23	Id-23	Id-14-2
Wavelength	0.976	0.976	0.931
Frames recorded	400	151	400
Molecules / AU	4	4	2
Matthews coefficient	2.2	2.21	2.18
Solvent content	44.0	44.3	43.6
Resolution [Å]	2.3	2.1	2.18
Rsym [%]	5.1	4.4	8.1
I / σ	13.1	14.5	13.4

Completeness [%]	96.2	31.2	99.9
Average redundancy	1.7	1.3	4.1
Unique reflections	32275	13795	19795
Average B factor	49.1	46.4	36.0
Highest resolution bin [Å]	2.3-2.35	2.1-2.15	2.18-2.21
Rsym (highest bin) [%]	16.4	23.4	25.4

Phase determination, model building and refinement

In Heidelberg University, Molecular replacement was performed with several search models derived from the heme binding PAS domain of the bacterial histidine kinase FixL, as these bear the highest sequence similarity to the *cyaB1* PAS domain, according to the structure-based alignment and a sequence alignment computed with ClustalX 1.8366, and also with models derived from flavin binding or photoactive yellow protein PAS domains. Five models were calculated for each alignment and scores based on the energy of the conformation were calculated with PROSA2003. The models in Figure 4.103 represent the more likely models according to this scoring with model B as the best. The impact of the sequence alignment used for the modelling is clearly visible, as the first model has a large insert between helices E and F, which appears unstructured. In the second model a large and also unstructured insert can be found between helices C and D, and in the third model a large insert can be found between helices C and D, along with several smaller inserts in the loop regions between the beta sheets.

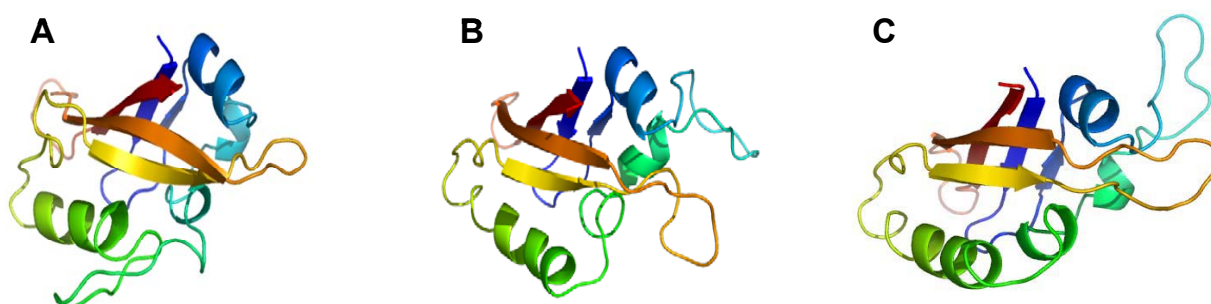


Fig.4.103: Homology models of the *cyaB1* PAS domain derived from alignments based on (A) Pfam 00989.11 (B) Smart00091.101, and (C) based on the alignment obtained with the Modeller v8.2 align2d command. The secondary structure was in the order: A_β-B_β-C_α-D_α-E_α-F_α-G_β-H_β-I_β.

4.3.4.3 Crystallization of Catalytic and PAS/catalytic domains of CyaB1

The CyaB1 PAS/catalytic domain was cloned in pQE30 (section 3.4.5.5) and the DNA's of four N-terminally truncated catalytic domains were obtained from J.Linder. The five

Results

constructs were transformed into *BL21 (DE3)[pREP4]*, overexpressed and purified as mentioned above for the CyaB1 PAS domain. The size and purity was evaluated by SDS-PAGE and Western blot (fig.4.82 and 4.83), the AC activity was also assayed (Table 4.11).

Table 4.11: Characteristics of the four truncated catalytic domains and the PAS/catalytic of CyaB1 enzyme

	I	II	III	IV	PAS/Catalytic
Description	G595-K859	E589-K859	M572-K859	E560-K859	388-K859
Calculated size (kDa)	31.5	32.1	34.1	35.5	54.9
Steady state activity (nmol/mg.min)	46.2 ± 0.78	48.7 ± 1.1	4.9 ± 0.16	8.3 ± 0.3	5.26 ± 0.26
Yield (µg)	710	360	700	620	590
Concentration used in the crystallization (mg/ml)	-	8.36	-	7.72	8.46

The CyaB1 PAS/catalytic and two of the truncated catalytic domains (II and IV) were chosen for crystallization.

The constructs II and IV of the catalytic domain had a purity > 95%. They were expressed in larger scale, concentrated by ultrafiltration (Nanosep filter) at 11,000 ×g and 4°C and crystallized using crystal screen I, crystal screen II and crystal screen lite (from Hampton). The plates were left at 16°C and screened as mentioned in section 3.3.11.1

No crystals were obtained for a time as long as 2 years. Gel filtration for both constructs shows presence of a monomer as a major form and in case of construct IV a small shoulder for a dimer appears in the curve (fig.4.104)

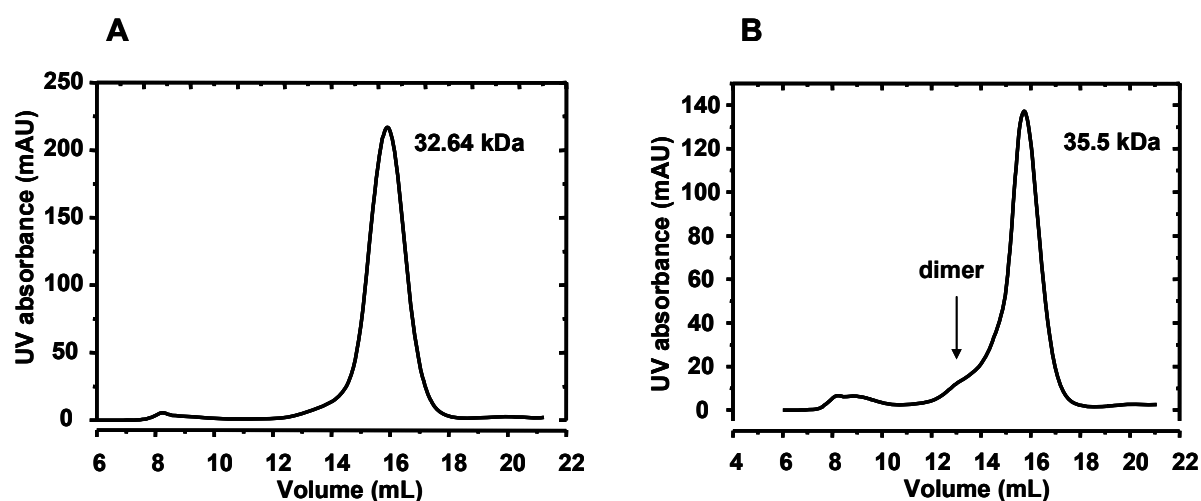


Fig.4.104: Gel filtration of the crystallized constructs: Construct II (A) and IV (B) of the CyaB1 catalytic domain 200 µl of 2 mg/ml were loaded to the column and the sample was run without fractionation.

Results

For CyaB1 PAS/catalytic, the purity of the protein was not sufficient for crystallization so I tried to improve it by:

1. Taking larger volume of bacterial culture (600 ml instead of 400 ml) and these were combined after harvesting, during the washing of pellets.
2. Incubation of the lysed cells with DNAase solution (2 mg/ml) for 30 min during purification prior to the centrifugation of pellets.
3. Use of less quantity of Ni-NTA (150 or 200 μ l)

According to the above steps, the purity has improved but the use of 150 μ l Ni-NTA reduced the yield of protein without improving its purity so the 200 μ l Ni-NTA was used in the purification of the protein on larger scale (see fig.4.105)

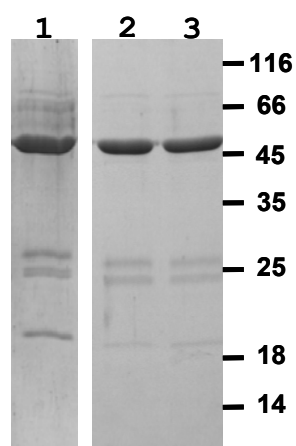


Fig.4.105: Optimization of overexpression of CyaB1 PAS/Catalytic **(1)** Before optimization 200 μ l Ni-NTA and 400 ml culture media **(2)** 600 ml culture media, DNase after lysis of the cells and 150 μ l Ni-NTA **(3)** 600 ml culture media, DNase after lysis of the cells and 200 μ l Ni-NTA.

The protein was overexpressed in larger quantities, concentrated and crystallized as mentioned for the catalytic domain constructs and again no crystals were obtained with this construct.

The gel filtration and glutaraldehyde dimerization experiments of CyaB1 PAS/catalytic showed formation of a dimer of 107 kDa and the smaller peak for 24.5 kDa which appears also in the run is suggested to be an impurity or degradation product of the protein (fig.4.106). The formation of the dimer in the PAS/catalytic and a monomer in case of catalytic domain proves that the PAS domain is responsible for the dimerization of the enzyme.

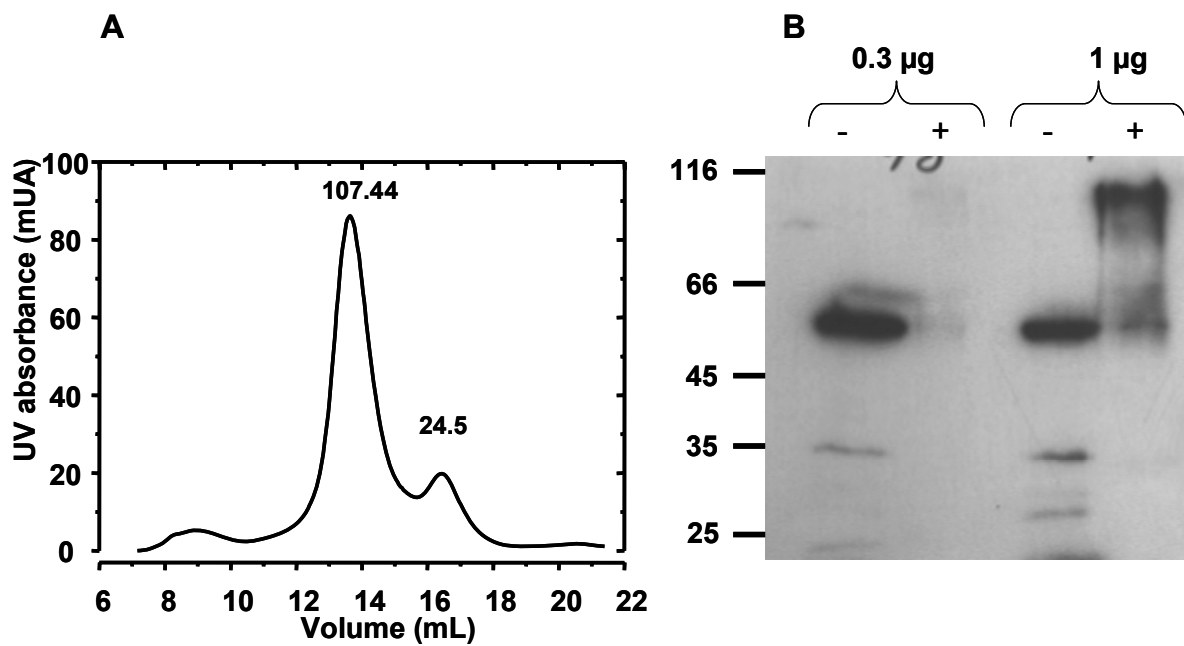


Fig.4.106: Dimerization of CyaB1PAS/catalytic (**A**) the gel filtration showing single peak of a dimer with another smaller peak in the size of impurity (see SDS-PAGE in fig.4.105) and (**B**) Dimerization by Glutaraldehyde showing presence of a dimer.

5 Discussion

Although great progress has been made in characterizing the different groups of phosphodiesterases, we are still unable to grasp the idea of how regulation and intramolecular signaling occurs within these enzymes. In the last few years, the crystal structure of the mPDE2 GAF tandem revealed a parallel dimer with cGMP bound to the GAFb domain of each monomer, on the other hand the CyaB2 GAF tandem which was elucidated three years later showed an antiparallel dimer with cAMP binding to each of the four subdomains. The success of producing the chimeras of rPDE2/CyaB1 and CyaB2/CyaB1 which were regulated by different cyclic nucleotides addressed the question: what is the mechanism by which the signal is transduced through the PAS domain to the catalytic domain?

5.1 Biochemical characterization of hPDE2NGAF/CyaB1 chimera

5.1.1 hPDE2NGAF/CyaB1 chimera had a 5-fold stimulation upon binding of cGMP

In CyaB1, cAMP binding to the GAF domain is responsible for regulation of the catalytic domain. Previously, CyaB1 PAS/catalytic (L386-K859) was used as a reporter to study GAF domains of CyaB2 and mammalian PDEs 2, 5, 10 and 11 [19, 80, 101, 106].

In PDE2, there is only one gene coding for this family, which is the PDE2A. PDE2 has two binding sites one is a high affinity, non-catalytic binding site, specific for cGMP and the other is low affinity catalytic binding site which can hydrolyze both cAMP and cGMP. Because PDE2 was found in cells that express little or no PKG, PDE2 is considered to be one of the main receptors for cGMP in cGMP-mediated signal-transduction mechanisms, and represents a classic site of cross-talk between cAMP and cGMP signaling pathways [5].

Although the crystal structure of the GAF domain (Y215-Y555 rat PDE2 numbering) of mPDE2 and the catalytic domain of hPDE2 (578-919) were elucidated [24, 53], little information is available about the structure of the holoenzyme.

The regulatory domain of hPDE2 was characterized through the generation of hPDE2NGAF/CyaB1 AC chimera. The chimera was regulated by cGMP with 5-fold stimulation. A recombinant bPDE2A assayed in a mammalian cell extract showed approximately 3.5-fold stimulation by cGMP [107]. Purified bPDE2 proteins showed 5–6-fold stimulation in one report [108] and >50-fold stimulation in another [109]. The rPDE2A1

had 1.4-2.3-fold-stimulation while rPDE2A2 had 2.5-3 fold-stimulation depending on the method of purification from liver cells [110]. Almost 3-fold stimulation for the unpurified recombinant hPDE2 was produced by the addition of 10 mM cGMP [111]. The differences in these values may reflect differences in methodology and enzyme status. Alterations in assay temperature, assay pH, cGMP concentration and proteolysis of the enzyme affect the activation state of the enzyme. In addition, the presence of fatty acids or short chain alcohols has been reported to inhibit the activation of cAMP hydrolysis by cGMP [111].

The cGMP-EC₅₀ of $9.9 \pm 1 \mu\text{M}$ of hPDE2NGAF/CyaB1 chimera was comparable to the other hPDE/CyaB1 chimeras. In hPDE5/CyaB1 chimera, the cGMP-EC₅₀ was $9.6 \pm 1.8 \mu\text{M}$ [106], $72.5 \pm 10.1 \mu\text{M}$ for hPDE11A4/CyaB1 while the cAMP-EC₅₀ of PDE10A1/CyaB1 was $18.1 \pm 1 \mu\text{M}$ [19]. The value of the EC₅₀ of human PDE2 has been calculated in one report to be $0.3 \mu\text{M}$ which is much less than the value obtained here. The Hill coefficients that represent the cooperativity of cNMP binding to the GAF domain were ≤ 1 for all PDE/CyaB1 chimeras and CyaB1 holoenzyme but cooperative for CyaB2/CyaB1 chimera which may be explained by the allosteric binding of the cyclic nucleotide to one GAF motif of each monomer of PDEs and CyaB1 GAF but to both motifs of the CyaB2 GAF domain. The Hill coefficient for the unactivated hydrolysis of cAMP was ranging from 1.5-2.0 in different variants of mammalian PDE2 but it was 1 for the activated hydrolysis of cAMP and for cGMP [104, 110].

The time dependence of hPDE2/CyaB1 chimera showed a steady state achieved at as short interval as two minutes and this was used as a control to compare other PDE2 mutants. The optimum temperatures for the activated and the unactivated differ by 5°C which suggests differences in the conformation of the catalytic domain between the activated and the unactivated states. The ATP kinetics showed different K_m values for the unactivated and the activated form of the enzyme as activation reduced the K_m value of ATP. This agrees with a report evaluating the kinetic of cAMP hydrolysis in PDE2 holoenzyme in the presence and absence of cGMP where they found that cGMP reduced the K_m value of cAMP rather than V_{max} [110].

The optimum pH for hPDE2NGAF/CyaB1 chimera was 8.5. Plotting the fold stimulation obtained by the pH-dependence study against pH showed presence of two peaks one at pH 6.5 (8.5 fold) and the other at pH 8.5 (6.1 fold). This indicates the presence of two optimum pH's one for the non-catalytic binding of cGMP (pH 6.5) and the other for the AC catalytic activity (pH 8.5).

5.2 Role of the N-terminal domain on the activity and regulation of PDE2/CyaB1 chimera

5.2.1 Effect of the hPDE2 N-terminus

From the three splice variants, the PDE2A1, PDE2A2 and PDE2A3 (PDE2A2 has only been found in rats) [107, 111-113], PDE2A1 is cytosolic whereas -A2 and -A3 are membrane bound. It has been suggested that different localization of PDE2A2 and -A3 is due to a unique N-terminal sequence, which is absent in PDE2A1 (Fig.5.1). These differences in hydrophobicity may be the base for the partitioning of the PDE2A activity between membrane-associated and soluble fractions of the cell [114]. Despite the PDE2A splice variants being different; there is no known difference in their kinetic behaviour [115].

PDE2A1			MRRQPAASR	DLFAQEPVPP	GSGDGA	25
PDE2A2	MVL	VLHHILIAVV	QFLRRGQQVF	LKPDE-P-PP	QPCADS	37
PDE2A3	MGQACGHSIL	CRSQQYPAAR	PAEPRGQQVF	LKPDEPPPPP	QPCADS	46

Fig.5.1: Comparison of the amino-terminal sequence of PDE2A1, PDE2A2, and PDE2A3. Sequences are from bovine (PDE2A1), rat (PDE2A2), and human (PDE2A3). Hydrophobic regions are highlighted in grey. Alignment re-drawn from ref [115].

Human PDE2A3, discovered in the brain, has a unique hydrophobic proline-rich N-terminus. The truncation of the whole N-terminus of hPDE2 (Δ 1-227 aa) had little or no effect on the cGMP-EC₅₀, fold stimulation and Hill coefficient, in addition to that the substrate kinetics showed similar K_m value but higher V_{max} for the both activated and unactivated chimeras. An increase in the basal activity of about 9 times was observed in the N-terminally truncated construct. This increase in the activity of the enzyme can be due to its direct effect on the catalytic domain or by reducing the soluble fraction of the enzyme. This could be checked by solubilization of hPDE2NGAF/CyaB1 chimera by 1% lubrol and the evaluation of its effect on the activity of the enzyme.

It is note worthy that the N-termini of PDE5 and PDE11 were important for regulation and their truncation increased basal activity and the affinity toward cGMP accompanied by reduction of the fold-stimulation [106, 116].

5.2.2 Effect of hPDE5 N-terminus on the regulation and activity of hPDE2/CyaB1 AC chimera

Similar to PDE2, a significant dissimilarity in the protein sequence of the N-terminus of rat, bovine and human PDE5 was observed. Alterations in the N-terminal sequence among the three species may lead to differences in the subcellular localization. An N-terminal Gln-rich sequence was found in human homolog [117].

The effect of different lengths of the N-terminus of PDE5 was studied earlier and truncation of more than 101 aa's of the N-terminus increased the affinity of the GAF domain toward cGMP, increased the basal activity and decreased the fold-stimulation in hPDE5/CyaB1 chimera [106]. Swapping the N-terminus of hPDE5 in front of PDE2/CyaB1 AC chimera had also an inhibitory effect on the AC activity compared to the N-terminally truncated construct. Although the hPDE5 N-terminus is hydrophilic in nature and had a significant regulatory effect on the hPDE5/CyaB1 chimera [106], this effect was not obvious in conjunction with PDE2 and only a small decrease in the EC_{50} with a small increase in the fold-stimulation was observed. This means that regardless the hydrophilicity of the N-terminus, it has an inhibitory effect on the enzyme without affecting the affinity toward cGMP or the folding of the GAF domain. This suggests a difference in the folding of hPDE5 GAF and hPDE2 GAF where no interaction between the N terminus of PDE5 and GAF domain of hPDE2 was observed at the time it regulates the activity of its GAF domain.

5.2.3 The CyaB1 N-terminus reduced the fold stimulation by cGMP of rat PDE2 GAF

The different expressions of CyaB1N-rPDE2/CyaB1 protein had different values of fold stimulation which range from 2-5 fold while the different expressions of Δ N-rPDE2/CyaB1 had a fold-stimulation of 15-33 fold. In the results obtained by T.Kanacher, the fold-stimulation was 10-fold by CyaB1N-rPDE2/CyaB1 with basal activity of 2.5 nmol/mg.min[80].

In all assays, the fold stimulation of the N-terminally truncated chimera was higher than the construct with the CyaB1 N-terminus. The CyaB1 N-terminus may inhibit signal transduction from the GAF domain to the catalytic domain without having an effect on the affinity of the GAF domain toward cGMP. The same effect of CyaB1 N-terminus was observed in CyaB1.N-ter.hPDE11/CyaB1 [116].

5.3 Role of the connecting helix in the signal transduction

5.3.1 Shortening and elongation of the connecting helix of CyaB2GAF disturb dimerization and signaling

What is the nature of the signal transmitted by a helix? An obvious answer is dimerization of protein monomers. Another possibility is that the helix might be a structural relay. Both of these appear to play a role in signaling between CyaB2 GAF motifs. According to the crystal structure of CyaB2 GAF, the α 1-helix and the connecting helix are responsible for dimerization [23]. Shortening or elongation of the connecting helix by 1-3 aa reduced the stimulation and the cAMP-affinity, demonstrating that dimerization is essential for full potency. Deletion of more than three amino acids led to a dramatic reduction of both fold stimulation and cAMP-affinity, while the insertion of aa's affected the stability, indicating the importance of the helix length in signalling and protein stabilization. The enormous reduction in the stimulation can be due to several reasons: no dimerization, a change in the rotational orientation of the helix will affect the amino acids embedded in the helix and those exposed, in addition to the proper orientation of the two GAF motifs. It has been proposed that such shifts could occur gradually, without disruption of the helix, by a change in supercoiling about the dimer axis; these gradual shifts would require an intermediate region of relatively weak interhelical packing [118]. Such an interface shift might be expected to cause significant reorientation of CyaB2 GAF motifs at the other end of the helix, capable of suppressing activity. Another reason for the effect of such mutations is the signal transduction within the GAF domain of CyaB2 itself. In the crystal structure of CyaB2 GAF, cAMP was found to bind to both GAFa and GAFb which may explain the cooperativity in CyaB2/CyaB1 chimera. The α 1, α 2, and the connecting helix in the crystal structure look like the HAMP domain in their arrangement. The increase in the EC_{50} of cAMP by both deletion and insertion mutants can be due to the disruption of the signaling between the GAFa and GAFb.

Although the four helices of the two chains are present in the same environment, the interaction was inter- rather than intrasubunit which performed the dimerization between the two monomers and what stabilized the CyaB2 GAF tandem. In more details, the intrasubunit interaction between the α 1-helix and the connecting helix in CyaB1 GAF was observed to be poor with only one site of hydrophobic interaction (L75 with F245). Intersubunit interaction was achieved through the α 1-helices, the two connecting helices and α 1-helix-connecting helix interactions (Fig.5.2).

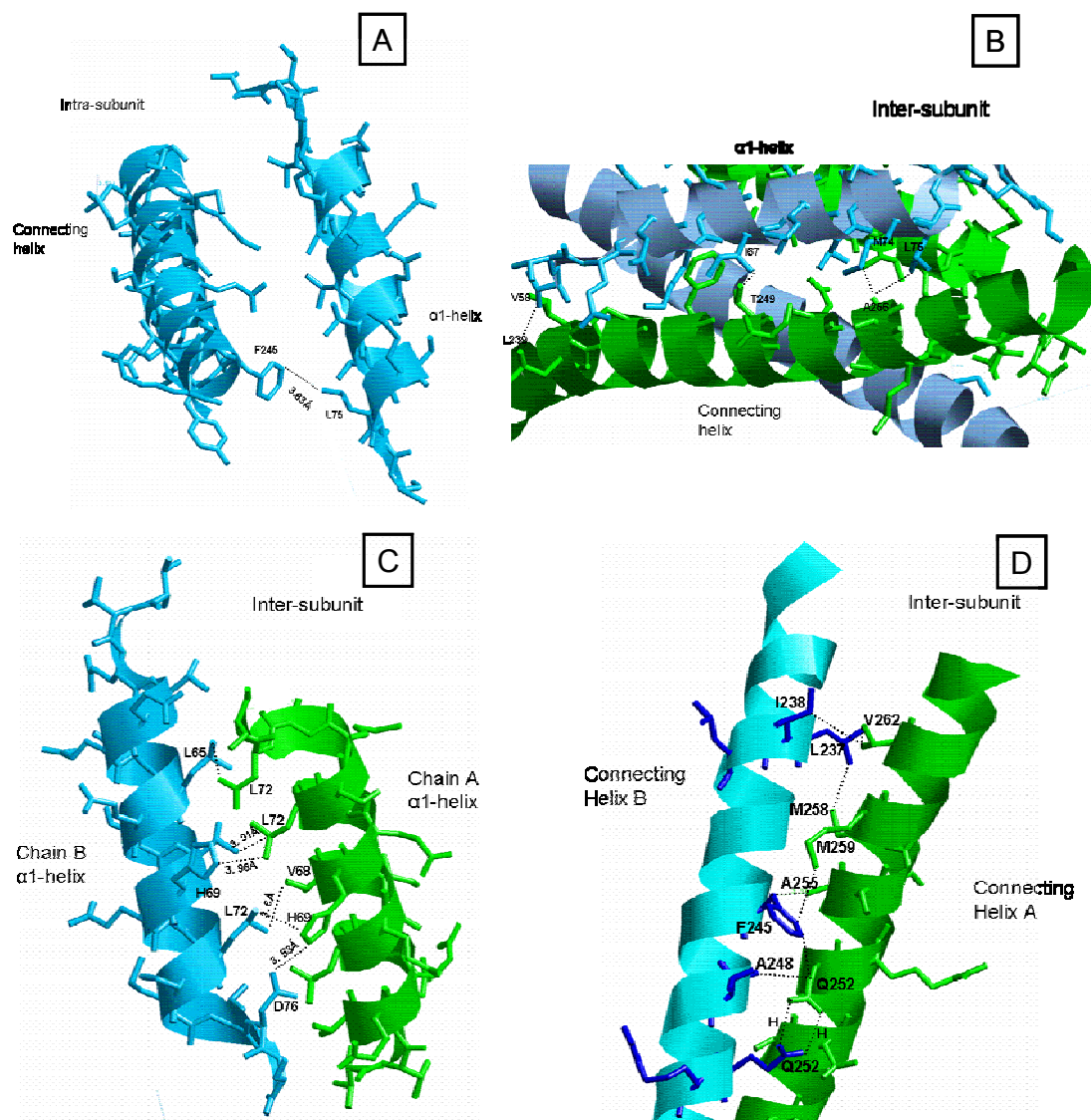


Fig.5.2: Different diagrams from CyaB2 GAF crystal structure showing the intra and inter subunit interactions between the α 1-helices and the connecting helices.

The interesting observation in these models was that although all helices were dimerizing with each other by hydrophobic bonds, two hydrogen bonds ($<3 \text{ \AA}$) at the crossing of the two connecting helices formed by Gln252 were supporting the whole structure and I will guess that mutation of this amino acid residue may dramatically affect signaling between the two GAF tandems and hence to the catalytic domain (Fig.5.3)

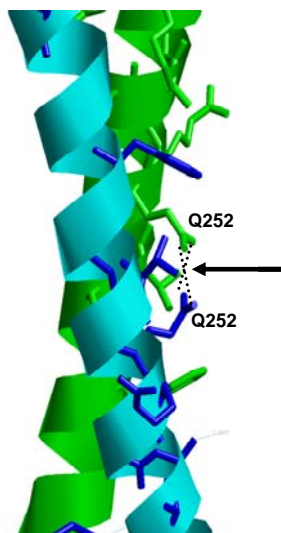


Fig.5.3: The hydrogen bonding between N-O of Gln252 observed at the crossing of the connecting helices of the two GAF subunits.

5.3.2 The effect of CyaB1 connecting helix on the signaling of CyaB2 GAF

The exchange of the CyaB2 GAF connecting helix by that of CyaB1 had decreased the fold stimulation to about one fourth without having a great effect on the cAMP-EC₅₀. Although 31 aa were exchanged, none of them was found to have a stabilization affect on the GAF motifs, in addition, there was no rotation in the GAF tandem around the dimerization axis which didn't affect the interaction between the two GAF tandems and hence, the affinity toward cAMP was not changed. The exchange of this helix has shown to cause loss of cooperativity and this means that the decrease in the fold stimulation could be due to the loss in the cross-talking between the two GAF motifs a and b which is governed by the linker between the two GAFs.

5.3.3 The role of the two hydrophobic residues (ML) in $\alpha 1$ and $\alpha 2$ helices of CyaB2 GAF

My observation of the presence of the two hydrophobic amino acids in the $\alpha 1$ -helix of the GAF domain was beneficial in the determination of the beginning of this domain in other PDEs, e.g. the re-cloning of the GAF domain of hPDE10 which included this $\alpha 1$ -helix has produced large crystals.

The different mutations performed in the different aa's had included mutation to the small non-chiral aa, glycine, the small side chain aa, alanine, the small hydrophilic aa, serine, the branched hydrophilic aa, threonine, and the larger branched hydrophobic aa, leucine (Fig.5.4)

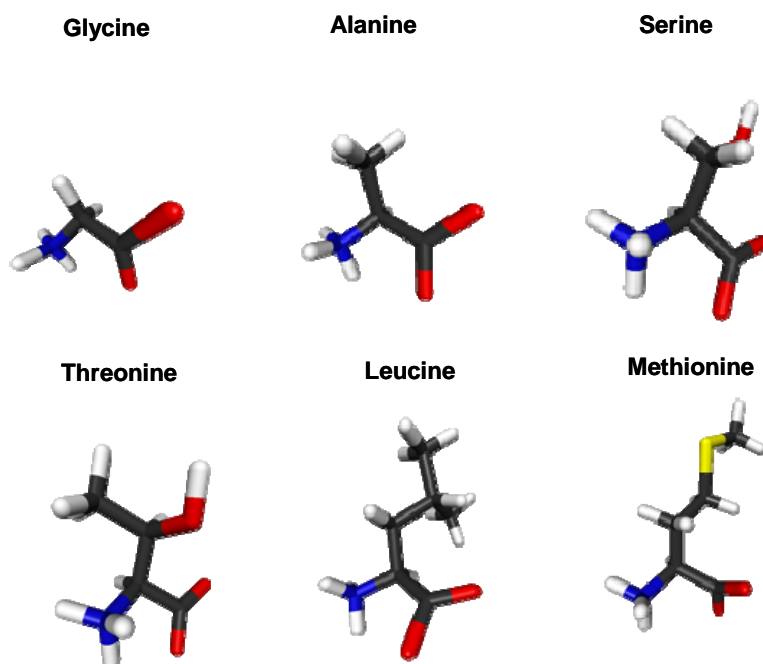


Fig.5.4: Stick model of the amino acids used in the different mutants. Black: carbon, red: oxygen, blue: nitrogen, yellow: sulfur and white: hydrogen.

M74 and L75 have different hydrophobic interactions with different residues. L75 forms van der Waal forces with F245 and F80 within the same subunit and M259 of the other subunit. The mutation of these two amino acids to the small flexible glycines didn't have a great effect on the fold stimulation but obviously decreased the affinity and the Hill coefficient of the mutant. The mutation to hydrophilic amino acids (S, T) reduced the fold stimulation more than the GG mutant did with less effect on the cAMP-EC₅₀ of the enzyme. Both mutants were found to reduce the cooperativity of cAMP binding.

Other mutations in the α 2-helix were done on the M87 and L88 residues. These two residues were found to have interactions with I238, L239 within the same subunit and S266 of the other subunit. The mutation of the first residue to the hydrophilic serine reduced the fold-stimulation dramatically but the EC₅₀ was not affected with a Hill coefficient not changed. This can be explained by the involvement of this aa residue in dimerization and signaling but not in the stabilization of the GAFa domain. For the second mutant (L88S), the protein dependence curve was non-linear with a dose response curve that doesn't reach a plateau. L88 has interaction with L239, I119 and V120, the last two residues are part of a β -sheet within the GAFa and this explains the dose response curve wherever L88 is mutated (Fig.5.5).

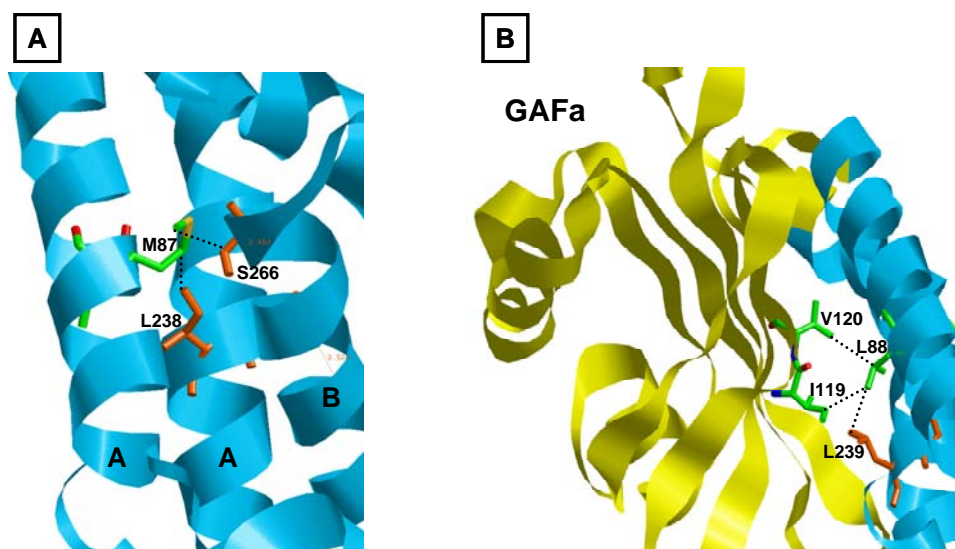


Fig.5.5: The crystal structure of CyaB2 GAF domain shows the hydrophobic interactions by which M87 (**A**) and L88 (**B**) stabilize the GAF structure.

The double mutation of both residues had produced a mutant with lower fold stimulation of both single mutants and shares the no effect on the EC_{50} of M87 mutant and the reduction in the Hill coefficient and the same profile of dose response curve of L88 mutant.

5.3.4 The role of two methionines in the connecting helix on dimerization and signaling

An unplanned mutation of the M258T in the presence of other mutations in the GAF domain had showed an obvious decrease in the fold stimulation of the enzyme which shed light on the importance of the linker region in general and specifically these two amino acids in the signal transduction. I generated a single mutant (M258T). The fold stimulation and the affinity toward cAMP were reduced only to one third. The interaction of these aa residues were checked in CyaB2 GAF crystal structure. M258 had intrasubunit interactions with I425 and intersubunit interaction with L237 while M259 interacts with L75 and L84 of the other subunit. I have observed that these 2 aa with their different interactions are holding the two GAFa domain together until the distance between D375 of GAFb of one monomer with E187 of GAFa from the other monomer is 3.7\AA . The four mutants prepared later included double mutants of methionines. The mutations of MM to GG or AA were found to decrease the cAMP-affinity more than other mutants without having a great effect on the fold stimulation. The least fold stimulation was observed for GG and ST mutants. This decrease in both, fold stimulation and cAMP-affinity in the GG mutant is due to the fact that glycine is the smallest

aa with no chiral carbon. The ST residues are hydrophilic in nature and smaller in size which may not only disturb the dimerization but also affect the surrounding aa by its hydrophilicity. The most interesting result was obtained with the quadruple mutant (α 1-helix (ML) and connecting helix (MM) to ST; CyaB2 (M74S/M75T/M258S/M259T)/CyaB1). Calculating the fold stimulation with different protein concentrations showed an increase which meant that dimerization within the GAF enhances binding of cAMP to the GAF domain or signaling to the catalytic domain. The cAMP-EC₅₀ was higher than that of the double mutants. Although these double mutants were still showing some cooperativity, the Hill coefficient of the quadruple mutant showed no cooperativity.

Another interesting result was the mutation of the two methionines to leucines. All PDE GAFs and CyaB1 GAF contain two leucines in their connecting helix while methionines were unique for the CyaB2 GAF connecting helix. Methionine and leucine are considered equivalent as they have almost similar size and hydrophobicity but the truth was something else. The mutation of the methionines to leucines misfolded the protein and produced an absolutely inactive enzyme. The isolated GAF domain of leucine mutant also proved the misfolding on the SDS-PAGE and gel chromatography. Although the connecting helix of CyaB1 displaced contained two leucines, it was still having its own intersubunit interface of CyaB1. This result can be explained by the rigidity of the side chain of leucine represented by the branched carbons which may have a steric effect on the dimerization interface between the connecting helices of the two monomers compared to the more flexible sulfur containing methionine (see Fig.5.4). A question mark is put on the reliability of the thousands of alignments we are making every day and rely on it in the comparison of proteins in which M is considered similar to L and I, Q is similar to E, D is similar to N at the time all these aa residues compared are different in size or physical properties.

5.3.5 Mutation of two hydrophobic aa residues in the α 1-helix and another in the connecting helix disturbed the dimerization of hPDE2 and hPDE5 GAF domain.

PDEs are dimeric. However, the dimerization is not required for catalytic activity, because the monomeric short catalytic domain of PDE5 is active. The structural and functional roles of PDE dimerization are poorly understood [119]. The first molecular informations about PDE dimerization have been provided by the structure of the mPDE2A tandem GAF [24]. This crystal structure demonstrates that GAFa domain is responsible for dimerization of PDE2A, in addition to some aa's in the connecting helix between the two GAF's. In the hPDE2 α 1-helix

mutants, the mutation of either I230 or L231 residue, involved in the dimerization of the GAF_a, increased the fold stimulation by cGMP by 17 and 24-fold, respectively, without an effect on basal activity or EC₅₀ of cGMP. The Hill coefficient for L231S mutant was not affected but it increased to above 1 for I230S mutant. As the PDE2 GAF_a doesn't bind cGMP, the 3-5 times increase in the fold stimulation by cGMP would suggest that a real effect on the GAF_b folding and signal transduction to the catalytic domain had occurred as the affinity toward cGMP was not affected.

In the connecting helix mutants a slight decrease in the fold stimulation, an 28-fold increase in the affinity toward cGMP and no effect on the Hill coefficient were observed with hPDE2 (L396A/L397A)/CyaB1 mutant, another mutant (C393S), which was found in the crystal structure to be involved in the dimerization by forming a disulfide bond, didn't have any effect on the kinetic parameters of cGMP-binding to the GAF domain which agrees with the results obtained by Martinez et al [24]. The truncation of the N-terminus accompanied by quadruple mutation of the two hydrophobic amino acids in both α 1-helix and the connecting helix had led to having persistent high basal activity and loss of regulation by cGMP. The interesting result of this mutant was although cGMP doesn't stimulate, it has a stabilizing effect on the GAF domain. In order to correlate the parameters obtained from the AC assay with the dimerization, a crosslinking experiment was performed for the WT and the mutated chimeras. As the PAS domain proved to enhance the dimerization of the catalytic domain of CyaB1, the isolated tandem GAF domains \pm N-terminus and mutants were cloned. The gel filtration and glutaraldehyde crosslinking experiments showed that hPDE2 GAF \pm N-terminus are dimers which mean that the N-terminus has no effect on the dimerization of the enzyme.

The dimerization appears to be very important for the stabilization of the GAF folding and for providing certain conformation that can bind cGMP.

In PDE5/CyaB1 mutants the double mutation of the two leucine residues in the either α 1-helix or the connecting helix increased the affinity of the GAF domain toward cGMP significantly and reduced the fold stimulation. The quadruple mutant had lost the regulation by cGMP completely. In these mutants, the basal activity of the enzyme was significantly affected, at the time hPDE5 (L152A/L153A)/CyaB1 had the double basal activity of WT, hPDE5 (L333A/L334A)/CyaB1 had 7-fold increase in the basal activity and mutant combine all four mutations had produced a construct of 3.5-fold basal activity. To discover if these results are due to disturbance of the GAF domain dimerization, the different GAF mutants \pm N-terminus were cloned and evaluated for dimerization by glutaraldehyde crosslinking and gel filtration. Δ 135-hPDE5 has shown to enhance monomerization by increasing the ratio of monomer to

dimer. The double mutation in either α 1-helix or connecting helix had little or no effect on the dimerization of the GAF domain while the combination of both mutations in a quadruple mutant in the presence of the N-terminus had disturbed the dimerization significantly by producing a profile in which the monomer is the major peak. Combination of the Δ N-terminus with the quadruple mutant had produced similar profile in which the monomer is the major peak. This suggests the presence of three dimerization interfaces: one in the region from 101-135 aa of the N-terminus, a second in the α 1-helix and the third in the connecting helix. It was obvious that disruption of the dimer interface shifts the conformation of the enzyme toward the activated state which requires usually the binding of cGMP to the GAF domain. Such a result supports the presence of different conformations for PDE5 and proves that the unactivated conformation had higher energy and is the unpreferred conformation in comparison to the activated form.

In the unactivated state, the dimerization decreases the flexibility of the GAF domain of both PDEs and form more rigid structure. In the presence of the cGMP, the binding to the GAFa in PDE5 and GAFb in PDE2 changes the conformation of the GAF it bound leading to rotation of the connecting helix between the two GAFs, weakening the dimerization at the other GAF motif and gave more flexibility of the whole regulatory domain. As the different domains: N-terminal domain, GAFa, GAFb, PAS, and catalytic domain were all attached with each other by α -helices, the change in the conformation of one domain will transfer the signal as a 'domino' to the other domains and then to the catalytic domain in which the action of the signal transmitted is observed. The length of the helix and the angle, around which this helix rotates, determine the amount of signal transferred from one domain to another. In addition any substances that may bind directly to any domain will lead to conformational changes in that domain and change in the amount of signal transmitted.

5.4 Signal transduction through CyaB1 PAS domain

5.4.1 Is it determined by the binding of a divalent cation to the PAS domain?

CyaB1 has been characterized by Ohmori et al [83]. Later, CyaB1 enzyme was evaluated as a holoenzyme and a truncated catalytic domain [79].

The kinetic properties of the shortest catalytic domain, construct I, CyaB1595-859, were assayed at 45°C and pH 8.5 in the presence of Mn^{+2} or Mg^{+2} as a divalent metal ion. In the presence of Mn^{+2} , the enzyme had higher affinity toward ATP (K_m values of 11 vs. 334 μ M)

and lower V_{\max} (309 vs. 655 nmol/mg.min) when compared to kinetics in presence of Mg^{+2} [80].

Unlike the truncated catalytic domain, CyaB1 holoenzyme prefers Mg^{+2} over Mn^{+2} as a metal cofactor. Using Mn^{+2} , as divalent cation, a biphasic curve was obtained by cAMP-dose response assays but a monophasic in the presence of Mg^{+2} . This was explained to be due to the presence of two different cAMP-binding sites (high and low-affinity) in the presence of Mn^{+2} but only one high affinity binding site in the presence of Mg^{+2} [80].

The presence of two aspartate residue in the PAS domain similar to those responsible for the metal binding in the catalytic domain, opened the question whether this high and low metal binding sites are really required for the binding of cAMP to the GAF domain or it was the binding of this metal to the PAS domain which decides the amount of signal transferred from the GAF domain to the catalytic domain. To answer this question, the substrate kinetics in the presence of Mg^{+2} and Mn^{+2} should be carried out for the following constructs: construct IV (beginning of the dimerization without PAS or GAF), CyaB1 PAS/catalytic (dimer with PAS domain and no GAF), Construct IVB (GAF domain with no PAS which is able to transmit the signal) and CyaB1 WT (GAF, PAS and catalytic are all there).

5.4.2 CyaB1 catalytic domain utilizes only one ATP catalytic core depends on the truncation

The truncated CyaB1 catalytic domains are monomers as observed by gel filtration curves. The protein dependence of the two shorter catalytic domains (constructs I and II) had higher activity and achieved the steady activity at lower protein concentrations while the two longer ones (constructs III and IV) had lower activity and didn't achieve steady state up to 3 μ M protein. In addition, the Western blots of the four constructs showed bands in the size of monomer for all constructs and another band for a dimer only with the longest one (construct IV). The secondary structure of the four constructs as predicted by the Protean program (Fig.5.6) indicated that the two short catalytic domains are missing part of the long α -helix, a β -sheet and a short α -helix, the third construct lacks the α -helix and the fourth has all.

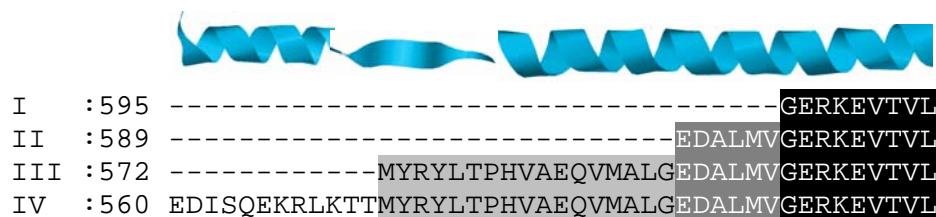


Fig.5.6: An alignment of the truncated catalytic domains shows the beginning of each construct and above their secondary structure according to Protean program.

I suggest that the catalytic domain of CyaB1 is a monomer in solution. During the assay, ATP is inducing homodimerization. In the shorter constructs (I and II), both ATP binding sites were utilized to yield the high activity, while the presence of the β -sheet in the third construct and a β -sheet and α -helix in construct IV hindered the proper dimerization of the enzyme leading to only partial dimerization and utilization of one ATP catalytic site. This explains the lower steady activity and failure in achieving steady state. The CyaB1 PAS/catalytic gave a result similar to the longer catalytic domain, which suggests the same catalytic domain conformation with the one ATP-catalytic core. A scissor like mechanism was suggested for this enzyme in which figure 5.7.A represents the more active short truncations of the enzyme while B represents the longer less active constructs.

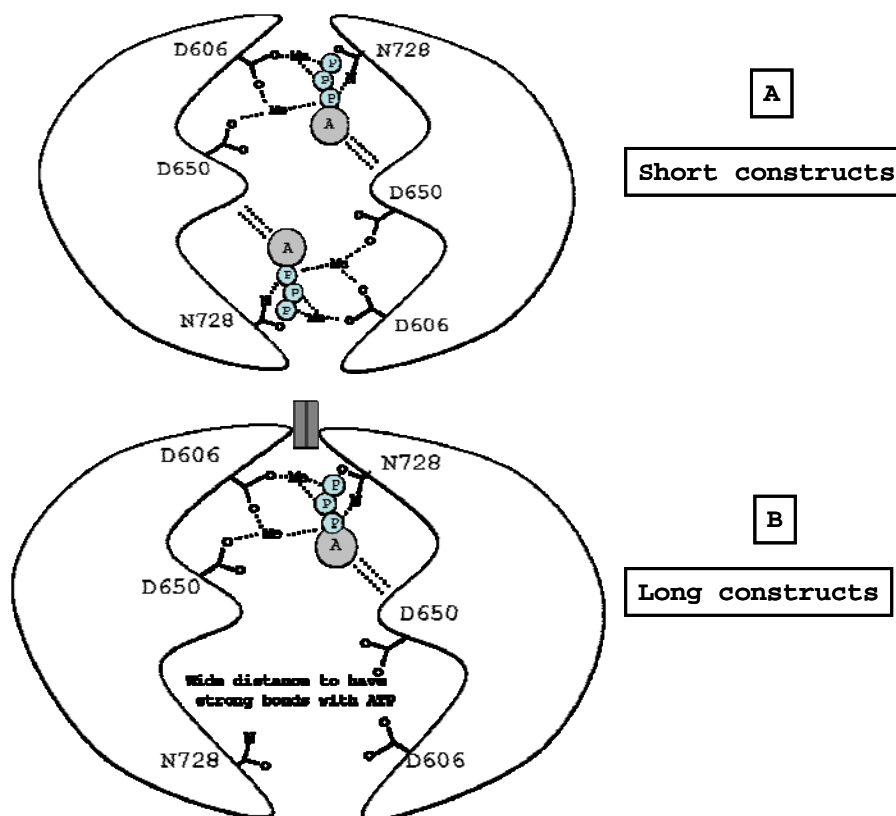


Fig.5.7: A schematic diagram suggests and explains the decrease in basal activity of CyaB1 catalytic domain by elongation of the linker preceding the catalytic domain. **(A)** Diagram represents the catalytic domain in the activated state or short constructs, Modified from [79]. **(B)** The proposed one catalytic pocket theory in the presence of longer catalytic linker.

To see whether the CyaB1 catalytic linker represent any of the domains, its sequence was checked by Blast search to find it aligned well with hPDE2 with 22% identity and 44% similarity (CyaB1 516-560 and hPDE2 126-165) which suggest for this linker to have an inhibitory effect on the activity of the enzyme as observed in hPDE2 N-terminus.

5.4.3 The linker of hPDE5 can transduce the signal between GAF and catalytic domains of CyaB1 with less efficiency

From the eight constructs cloned with different lengths of hPDE5 linker and CyaB1 catalytic domain, only the construct with the longest hPDE5 linker and the longest CyaB1 catalytic linker (construct IVB) was regulated by cAMP. The other seven constructs had different activities depending on the truncated catalytic domain attached but they were not regulated at all. Construct IVB had similar cAMP-EC₅₀ but only one tenth of the fold-stimulation of CyaB1. Different theories were suggested for signaling from the GAF domain to the catalytic domain in PDE5. Rybalkin et al. suggested presence of 3 different conformations, unactivated, activated by cGMP and one with higher activity which is not regulated by cGMP after long storage of the enzyme and it was suggested a physical interaction between the GAF and the catalytic domain [120]. Dr. Omori suggested the presence of three conformations, two for the activated and one for the unactivated [9] (see Fig.5.8).

According to this, in construct IVB, hPDE5 linker placed CyaB1 GAF and catalytic domain in certain angle to allow physical interaction between the two domains as suggested by the above theories which require the CyaB1 catalytic domain to be a monomer to allow this physical interaction. I would propose (first) that the PDE5 two helices are holding the GAF and catalytic domain in certain angle and once cGMP binds the GAF domain, conformational changes in the GAF cause rotation of the first helix which causes a rotation in the second helix leading to conformational changes in the catalytic domain to utilize both ATP catalytic sites and be activated. The second possibility is that the two α -helices of hPDE5 are parallel to each other and not perpendicular which means that the enzyme as a dimer forms a 4-helix bundle that may function as a signaling domain. In order to strengthen this possibility, the linker of construct IVB was aligned with 2 different PAS domains, CyaB1 PAS which had 19% identity and 33% similarity and PYP which had 29% identity and 44% similarity. This doesn't mean that hPDE5 linker represents a PAS domain but it looks like and may function as a signal transducing domain.

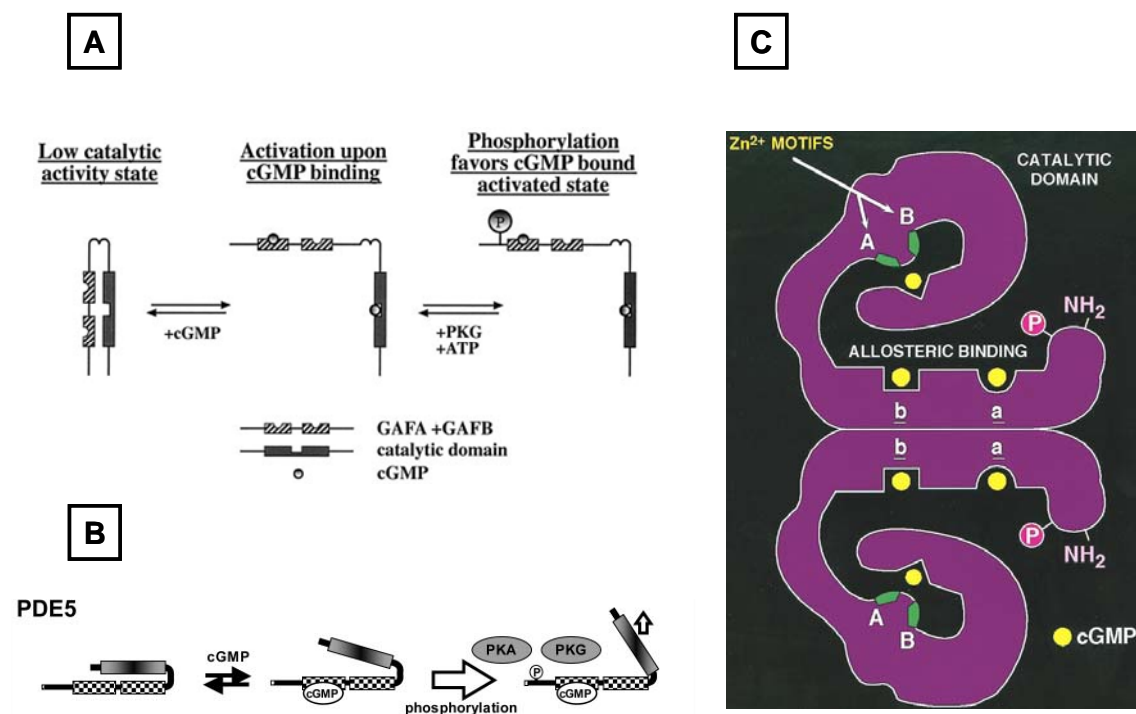


Fig.5.8: Mechanism of signaling from the GAF domain to the catalytic domain in hPDE5 upon binding of cGMP and phosphorylation of the regulatory domain. PDE5 is directly activated upon cGMP binding to its GAF A domain. Without cGMP bound, PDE5 is in a nonactivated state. PDE5 is converted into an activated state after binding of cGMP to the GAF A domain. Only activated PDE5 is phosphorylated by PKG. **(A)** As suggested by Rybalkin et al. [10, 120] **(B)** As suggested by Omori et al [9]. **(C)** Working model of PDE5. The regulatory domain in the amino terminal portion of PDE5 contains the phosphorylation site (Ser-92), the two allosteric cGMP-binding sites *a* and *b*, and at least a portion of the dimerization domain. The catalytic domain in the carboxyl-terminal portion of the protein contains the two Zn²⁺-binding motifs A and B and a cGMP-binding substrate site. Amino acids that are potentially involved in the catalytic mechanism are indicated in *green* and those involved in binding cGMP in an allosteric or catalytic site are indicated in *yellow* suggested by Corbin et al [121].

The secondary structure of IVB linker was predicted by Protean and found to form two α -helices each of 17 aa in length, which may suggest a HAMP-like domain which is also a transmitter domain present in many organisms, and consists of four α -helices that dimerize and interact with each other to transduce the signal in mechanical and interactive modes [122]. The alignment of hPDE5 linker with different HAMP domains showed little similarities with most of them but some similarity with the HAMP domain of methyl accepting chemotaxis protein from *Rhodospirillum centenum* with 29% identity and 40% similarity was observed.

Accordingly, I would suggest that the CyaB1 catalytic linker arrests the catalytic domain in a conformation to be activated while the hPDE5 linker has worked as signal transducing domain in this construct. The decrease in the signal transduction to one tenth could be due to the difference in the length and transduction properties of IVB linker compared to the PAS domain.

5.4.4 Exchange of the PAS domain by that of CyaB2 is still able to transduce the signal but with less efficiency

The exchange of the CyaB1 PAS with that of CyaB2 didn't have a significant effect on the affinity of the CyaB1 GAF toward cAMP which means that the folding of the GAF domain was not affected. The fold-stimulation and the basal activity were affected, the decrease in the fold stimulation may be due to the disruption of the signal transduction through the PAS domain of CyaB2 as the two PAS domains can't have the same efficiency in signal transduction or they may bind different ligands that help in the transduction of the signal. The effect of CyaB2 PAS domain on the folding or dimerization of the catalytic domain of CyaB1 should also be evaluated by carrying out the substrate kinetics of the chimera. I would expect that the CyaB2 PAS domain affects in one way or another the folding of the enzyme or that the region replaced doesn't only include the PAS domain of CyaB1 but another 130 aa between the PAS and the catalytic domain which are missed in the sequence of CyaB2 and I expect it to have a role in the folding and the function of the catalytic domain due to the fact that construct I of CyaB1 catalytic has a different activity from construct IV which has 35 aa from this linker.

5.4.5 The insertion of a flexible linker between the catalytic linker and the catalytic domain of CyaB1 completely destroyed signaling to the catalytic domain

The insertion of the flexible linker didn't only reduce the catalytic activity but also stopped signal transduction from the GAF domain to the catalytic domain. In order to see whether this linker affected the folding of the CyaB1 catalytic domain, the ATP-Kinetics were carried out to find no significant effect on the K_m value or the Hill coefficient but a decrease in the V_{max} compared to CyaB1 holoenzyme which means that the catalytic domain is correctly folded. The loss of regulation can be due to the interruption of a very important secondary structured element in the catalytic linker as this flexible linker was inserted between T571 and M572. The construct which was regulated in the constructs prepared with hPDE5 linker, construct IVB, had a linker which starts at E560. Accordingly, although the flexible linker inserted can free the movement of the GAF domain over the catalytic domain and allow the physical interaction and hence should be regulated, the failure of this construct to transmit the signal can't disprove the theory of the physical interaction between the GAF domain and the catalytic domain due to the reason mentioned above.

5.4.6 Crystallization of CyaB1 PAS domain

The discussion for this part of work was written according to the report provided by F.Voigts-Hoffmann from Heidelberg University.

The importance of the PAS domain family is shown by its presence in most forms of life (plants, animals, and bacteria). There are as many as 140 and 87 different PAS and GAF domains identified in *Anabaena* alone, and many hundreds have been identified in genomes sequenced to date [123].

Protein sequence analysis [27, 33] and molecular modelling [32] suggested a common fold for putative PAS domains from a wide variety of prokaryote and eukaryote sensor proteins. PAS domains from PYP [42], FixL [43] and the human HERG potassium channel [124] have a distinctive $\alpha\beta$ fold with a five stranded antiparallel β -barrel core. It is expected that the more than 300 known PAS domains will have a similar three-dimensional structure. At this time, relatively little is known about the mechanisms of signal transduction by PAS domains other than PYP, HERG and FixL. The common structure of PAS domains suggests that there might be different strategies for signalling and different cofactors associated with the fold may introduce significant variation in the signaling pathways [125]. According to that solving another crystal structure, like CyaB1 PAS, will be important for exploring a new unique signalling pathway.

The crystals CyaB1 PAS produced an image of 2.1 Å. It has been suggested that 40-50% sequence identity and a reasonable complete model are required for successful molecular replacement but recent studies have demonstrated that successful model can be built on the basis of 25-30% sequence identity using data from 1.8-2.1 Å resolution [126]. Although some weak sequence homologies have been reported between CyaB1 PAS and other proteins, the construction of reliable model suitable for molecular replacement experiments as the resolution of 2.1 Å was considered low. The efforts to solve the structure by molecular replacement method using different PAS domain structures as search model have so far proven unsuccessful. The SeMet method was used but no crystals were obtained with the first trial, the purification and the crystallization conditions needed to be modified to get crystals. Accordingly, the expected model of the three dimensional structure indicates a similar core structure as the 'PAS fold', nevertheless, a significant deviations were observed which may be required for the interaction with the regulatory GAF domain of the enzyme.

5.4.7 Discovering of metal ligand for the CayB1 PAS

Although the crystal structure of CyaB1 PAS was not solved, the expectation of the PAS domain to have a metal binding site was mentioned before. Finding the type of metal bound to the PAS will be a strong point in this work but needed some experiments. The exact method was mentioned in section 5.4.1. Any difference on the K_m and V_{max} values of these constructs and the effect of this difference on signaling, if any, can be evaluated.

5.4.8 Importance of this work

PDEs were considered for decades a good drug targets for the treatment of many diseases. Drugs known to date are targeted to the catalytic domain of these enzymes. The high similarities in the catalytic domain cause side effects by inhibition of other PDEs. There are more than 50 splice variants of PDEs. GAF domains are present in 5 of the 11 families (2, 5, 6, 10 and 11) while a PAS domain is present in one family (PDE8). This makes the GAF domains attractive as drug target. In all the drugs designed so far, a ligand-based rational design was performed. Here, the structure-function relationship of the GAF domains (PDE2, PDE5 and CyaB2) and PAS domain of CyaB1 provided here were attempts to shift the drug design from ligand based rational design to protein based rational design and to use different biochemical techniques, x-ray and gel chromatography to provide a new insight into signalling by these sensory domains.

5.4.9 Open questions and outlook

As the hydrophobic N-terminus of hPDE2 was found to have an inhibitory effect on PDE2 activity, and the fatty acid and short chains polyalcohols activate the enzyme at low concentrations followed by inhibition at higher concentration, I would guess that this happens by micellization of the hydrophobic N-terminus by these amphoteric compounds at low concentration and binding to hydrophobic regions in the enzyme at higher concentration that may affect enzyme activity. The effect of these compounds on activity and activation of the hPDE2NGAF/CyaB1 can be evaluated in the presence and absence of the N-terminus. Regarding the different mutants of hPDE2/CyaB1 chimeras, I think that the preparation of a chimera of hPDE2/CyaB1 and the isolated GAF in the presence of the N-terminus and the quadruple mutation in both the $\alpha 1$ -helix and the connecting helix hydrophobic residues will complete the story of the dimerization effect on the activity of the enzyme.

The agreement in the fold stimulation by cGMP between the PDE2 holoenzyme, which hydrolyses cAMP, and CyaB1 AC, which cyclizes ATP to cAMP, would suggest the

possibility of physical interaction between the GAF domain and the catalytic domain. In order to prove or disprove this possibility, the assay of PAS/catalytic activity in the presence of different isolated GAF domains \pm cNMP would be one way.

In CyaB2GAF, the presence of two hydrogen bonds between Q252 residues of the two chains represents an important interaction for the dimerization interface of the two monomers. Mutation of this aa residue may severely affect dimerization as this strong interaction is localized at the middle of the helix.

Furthermore, the project of the PAS domain was not completed, and further experiments are required to shed light on the signaling of this unique PAS domain.

The trials to crystallize the CyaB1 GAF (D42-389) domain have produced only small needles and all attempts to optimize did not succeed. Applying the sequence of the crystallized construct to the protean program showed the presence of an α -helix which starts 9 amino acids before (S33). The recloning of this construct with this beginning could be worthy if it is interesting to elucidate the crystal structure of another GAF to have a clearer idea about this group of SMBDs.

The efforts spent to solve the crystal structure of the CyaB1 PAS domain were not enough and a diploma student for 4 weeks doesn't have the time and the experience to elucidate a crystal structure. Further work is required to reveal not a crystal structure of a PAS domain but a new mechanism in signal transduction.

And lastly, trials by Dr. J.Linder to express CyaB2 holoenzyme and my trials to express the PAS/catalytic of this enzyme didn't succeed. I cloned and expressed the CyaB2 catalytic domain for crystallization purposes in this project but its purity was not enough for crystallization. The expression can be further optimized and the catalytic domain can be characterized with different divalent metals similar to CyaB1.

6 Conclusion

The human cGMP-stimulated PDE2 has a long proline-rich N-terminus while the hPDE5 had a glutamine-rich hydrophilic N-terminus ahead of the respective tandem GAF. The swapping of any of them in front of hPDE2/CyaB1 chimera had inhibitory effect. In rPDE2/CyaB1 chimera, CyaB1 N-terminus had a regulatory effect on the enzyme by either reducing the binding of cGMP to the GAF domain or reducing the signal transduction from the GAF domain to the catalytic domain.

The CyaB2 GAF linker was important with regard to the length and its amino acid sequence. Shortening the length of the connecting helix reduced signalling represented by fold stimulation and increased the cAMP-EC₅₀. The difference in the fold stimulation between the different mutants can be due to a shift in the dimerization or the differences in the exposed and embedded amino acids in the helix which affect dimerization. In the constructs with three inserted aa, the effect on fold stimulation and cAMP-EC₅₀ was less dramatic but the mutant with 4 aa inserted was unstable which indicates the importance of this linker not only for the proper signalling but also for the stability of this domain. The cooperativity was lost in all deletion and insertion mutants. The loss of the cooperativity may be due to the interruption of signalling between GAFa and GAFb motifs. Mutations of the Met/Leu couple in the α 1-helix or the two methionines in the connecting helix partially disrupted dimerization leading to dramatic reduction in the fold stimulation, decrease in the affinity toward cAMP and reduction in the Hill coefficient for most constructs. A quadruple mutation in the four amino acids reduced the fold stimulation more than 100 times, in addition to the need of high concentrations of protein to achieve steady state. Unlike CyaB2 GAF α -helices, the mutation in any of the helices preceding the GAF motifs in hPDE5 increased the basal activity and the cGMP-affinity. The quadruple mutation in leucines of both helices led to complete loss of regulation and increase in the basal activity. Mutations of the α 1-helix to serines in PDE2 GAFs increased the fold stimulation without affecting cGMP affinity while the mutations in the connecting helix caused little reduction in the fold-stimulation with an 28-fold increase in the cGMP affinity. The quadruple mutation in both helices and the truncation of the N-terminus showed loss of regulation and a 25-fold increase in the basal activity. The disruption of dimerization of the GAF in three enzymes had different effects on regulation of each of them. This indicates that each GAF domain has a unique structure and drugs may be targeted toward it without cross-inhibition between different GAF domains.

Conclusion

The PAS domain of CyaB1 was shown to be important for the proper and efficient signalling from the GAF domain to the catalytic domain. The exchange of the PAS domain by the hPDE5 linker showed that it is required between the GAF and catalytic for signalling. This applies also to the exchange by PAS domain of CyaB2 which was able to transduce the signal. Regarding the mechanism of signalling between the different domains, the situation was highly complicated. I expect that the N-terminus of hPDE2 was only for anchoring the enzyme to the membrane but PDE5 N-terminus had physical interaction with the GAF domain that regulates the binding of cGMP. The GAF domain tandems are responsible for dimerization and the allosteric activation by cNMP, the binding of the cyclic nucleotide to one of the GAF motifs is changing the conformation of that GAF leading to rotation of the connecting helix which will loosen the dimerization interface in the other GAF motif and cause further conformational changes in the other GAF that will be transferred to the catalytic domain by rotational mechanism that will cause the change in the conformation of the catalytic domain and affect the K_m or the V_{max} for that enzyme accordingly.

7. Appendix

A. kinetic parameters of PDE2A

Isoform substrate	K_m (μ M)	V_{max} (unit/mg protein)	stimulation (x)*	Hill coefficient	Ref.
<u>rPDE2A1 (Cytosolic)</u>					[110]
cAMP	40 ± 2	4.8 ± 0.25		1.6 ± 0.05	
cAMP + 2 μ M cGMP	20 ± 2	4.2 ± 0.13	2-fold	1.0 ± 0.1	
cGMP	25 ± 2	1.6 ± 0.12		1.0 ± 0.05	
<u>rPDE2A2 (Particulate)</u>					[110]
cAMP	34 ± 2	4.0 ± 0.2		1.5 ± 0.05	
cAMP + 2 μ M cGMP	20 ± 2	3.8 ± 0.1	4-fold	1.0 ± 0.05	
cGMP	31 ± 3	2.1 ± 0.15		1.0 ± 0.05	

Isoform	cGMP	cAMP	stimulation (x)*	inhibitors	Ref.
hPDE2A3	28.5 nmol/mg.min	20.5 nmol/mg.min	3-fold	EHNA	[111]
hPDE2A catalytic domain (579-921)					[53]
in vitro translated	43 ± 7	34 ± 6	-		
bacterially expressed	34 ± 4	32 ± 8	-		

* Allosteric stimulation of cAMP hydrolysis by cGMP

	Affinity toward cyclic nucleotide		Ref.
	IC ₅₀ (nM)		
mPDE2A	cAMP	cGMP	[127]
GAFa	ND	ND	
GAFb	146 ± 10	7 ± 1	
GAF a + b	247 ± 14	25 ± 2	
GAF a + b +C	400 ± 20	20 ± 2	
Holoenzyme	598 ± 47	22 ± 1	

B. DNA and protein sequences of the enzymes used in this study**B-1 CyaB2 (all1904)**

gi: 1754639

Acc no.: D89624

GeneID: 1105496 Protein ID: BAA13999.1

														<u>bp</u>	<u>aa</u>
atg	tca	ttg	caa	cag	cgt	aat	ttt	ggg	gag	act	ggc	gat	ttg	42	
M	S	L	Q	Q	R	N	F	G	E	T	G	D	L		14
atc	tta	ggt	acg	caa	aac	caa	gag	caa	aac	ttg	cca	gaa	act	84	
I	L	G	T	Q	N	Q	E	Q	N	L	P	E	T		28
tcg	gct	cct	gtc	ggc	aca	cta	gcc	cgc	aga	aaa	ggt	act	att	126	
S	A	P	V	G	T	L	A	R	R	K	G	T	I		42
tcg	aca	ttt	ctt	gct	ccc	tta	act	cag	gat	act	ttt	aaa	caa	168	
S	T	F	L	A	P	L	T	Q	D	T	F	K	Q		56
gtt	gtt	aca	gaa	gtc	gag	caa	aaa	ctc	caa	att	gtg	cat	caa	210	
V	V	T	E	V	E	Q	K	L	Q	I	V	H	Q		70
acc	ctg	tca	atg	ttg	gat	tct	cac	ggg	ttt	gaa	aat	atc	ctg	252	
T	L	S	M	L	D	S	H	G	F	E	N	I	L		84
caa	gag	atg	ttg	cag	tca	att	acc	tta	aaa	act	ggg	gaa	ttg	294	
Q	E	M	L	Q	S	I	T	L	K	T	G	E	L		98
ttg	ggg	gca	gat	cgg	acg	act	ata	ttt	ttg	cta	gat	gaa	gaa	336	
L	G	A	D	R	T	T	I	F	L	L	D	E	E		112
aaa	caa	gaa	ttg	tgg	tcg	att	gtc	gcc	gcc	gga	gga	ggc	gat	378	
K	Q	E	L	W	S	I	V	A	A	G	E	G	D		126
cgc	tcc	cta	gaa	att	cgc	atc	ccc	gcc	gac	aag	ggg	att	gcc	420	
R	S	L	E	I	R	I	P	A	D	K	G	I	A		140
ggt	gaa	gtc	gct	act	ttt	aaa	caa	gta	gtt	aat	ata	ccc	ttt	462	
G	E	V	A	T	F	K	Q	V	V	N	I	P	F		154

Appendix

														<u>bp</u>	<u>aa</u>
gac	ttt	tat	cac	gat	cct	cgg	tcg	ata	ttt	gcc	caa	aaa	caa	504	
D	F	Y	H	D	P	R	S	I	F	A	Q	K	Q		168
gag	aaa	atc	act	ggc	tac	cgc	aca	tat	aca	atg	ctg	gct	tta	546	
E	K	I	T	G	Y	R	T	Y	T	M	L	A	L		182
ccg	cta	ttg	agt	gag	caa	ggg	cga	tta	gtc	gcg	gtg	gta	cag	588	
P	L	L	S	E	Q	G	R	L	V	A	V	V	Q		196
tta	ctc	aac	aaa	tta	aaa	cct	tac	agt	cct	cct	gat	gca	ctg	630	
L	L	N	K	L	K	P	Y	S	P	P	D	A	L		210
cta	gca	gaa	cgg	att	gat	aat	caa	ggt	ttt	acc	agt	gca	gat	672	
L	A	E	R	I	D	N	Q	G	F	T	S	A	D		224
gag	caa	ttg	ttt	caa	gaa	ttt	gcg	ccc	tca	att	cgc	ttg	att	714	
E	Q	L	F	Q	E	F	A	P	S	I	R	L	I		238
ttg	gag	tcg	tca	cgc	tcc	ttt	tat	ata	gcg	acg	caa	aaa	caa	756	
L	E	S	S	T	S	F	Y	I	A	T	Q	K	Q		252
agg	gcg	gcg	gcg	gcg	atg	atg	aag	gcg	gta	aag	tct	ctg	agc	798	
R	A	A	A	A	M	M	K	A	V	K	S	L	S		266
caa	agt	agt	ctg	gat	tta	gaa	gat	acc	ctc	aaa	cgg	gta	atg	840	
Q	S	S	L	D	L	E	D	T	L	K	R	V	M		280
gat	gaa	gcc	aag	gaa	ctg	atg	aac	gcc	gat	cgc	agt	acc	tta	882	
D	E	A	K	E	L	M	N	A	D	R	S	T	L		294
tgg	ctg	ata	gac	cgc	gat	cgc	cat	gaa	tta	tgg	acg	aaa	att	924	
W	L	I	D	R	D	R	H	E	L	W	T	K	I		308
act	caa	gat	aat	ggt	tct	act	aag	gag	ttg	cgc	ggt	ccc	ata	966	
T	Q	D	N	G	S	T	K	E	L	R	V	P	I		322
ggt	aaa	ggt	ttt	gcc	ggg	atc	gtc	gcc	gca	tcc	ggt	caa	aaa	1008	
G	K	G	F	A	G	I	V	A	A	S	G	Q	K		336
ctc	aac	atc	cct	ttt	gat	tta	tac	gac	cat	cca	gac	tcg	gca	1050	
L	N	I	P	F	D	L	Y	D	H	P	D	S	A		350

Appendix

														<u>bp</u>	<u>aa</u>
act	gcc	aaa	caa	atc	gac	cag	caa	aat	ggc	tac	cgc	acc	tgt	1092	
T	A	K	Q	I	D	Q	Q	N	G	Y	R	T	C		364
agt	tta	tta	tgt	atg	cct	gta	ttt	aac	ggc	caa	gaa	caa	tta	1134	
S	L	L	C	M	P	V	F	N	G	D	Q	E	L		378
att	ggt	gtg	acc	caa	ctg	gta	aat	aaa	aag	aaa	acc	gga	gag	1176	
I	G	V	T	Q	L	V	N	K	K	K	T	G	E		392
ttc	ccc	ccc	tat	aat	cca	gaa	act	tgg	ccg	ata	gcg	ccc	gaa	1218	
F	P	P	Y	N	P	E	T	W	P	I	A	P	E		406
tgc	ttc	caa	gcg	agt	ttt	gac	cgc	aac	gac	gaa	gaa	ttc	atg	1260	
C	F	Q	A	S	F	D	R	N	D	E	E	F	M		420
gaa	gct	ttt	aat	att	caa	gcc	ggg	gtg	gct	tta	caa	aat	gct	1302	
E	A	F	N	I	Q	A	G	V	A	L	Q	N	A		434
cag	ttg	ttt	gcc	aca	gtc	aag	caa	caa	gag	caa	atg	caa	cgg	1344	
Q	L	F	A	T	V	K	Q	Q	E	Q	M	Q	R		448
gat	att	ctg	cgg	agt	ttg	tcc	aac	ggt	gtg	att	tcc	aca	gat	1386	
D	I	L	R	S	L	S	N	G	V	I	S	T	D		462
aag	tct	ggg	aca	att	att	gca	gcg	aat	gaa	agc	gcc	cag	cgt	1428	
K	S	G	T	I	I	A	A	N	E	S	A	Q	R		476
ttg	ttg	ggg	ctg	gaa	tca	gaa	gat	cgt	ttg	gaa	ggt	aaa	ctc	1470	
L	L	G	L	E	S	E	D	R	L	E	G	K	L		490
atc	agt	gag	gcg	atc	gcc	att	aaa	gaa	ggc	gat	ttt	agc	aaa	1512	
I	S	E	A	I	A	I	K	E	G	D	F	S	K		504
tgg	tgt	caa	gat	gcc	tta	cat	ggg	aca	gac	ctc	aaa	ggc	cgc	1554	
W	C	Q	D	A	L	H	G	T	D	L	K	G	R		518
cag	caa	tat	tac	cca	gac	cgc	aca	cta	gta	agc	act	gaa	gca	1596	
Q	Q	Y	Y	P	D	R	T	L	V	S	T	E	A		532
gca	caa	aat	agc	att	aac	cta	tcg	att	aat	acc	att	gcc	gat	1638	
A	Q	N	S	I	N	L	S	I	N	T	I	A	D		546

Appendix

														<u>bp</u>	<u>aa</u>
gct	agc	gat	ccc	cag	caa	gtc	tgc	ggc	gcg	ttg	gtg	gtg	atg	1680	
A	S	D	P	Q	Q	V	C	G	A	L	V	V	M		560
gaa	gat	att	agc	gat	gag	aag	cgc	ctc	aag	agt	acg	atg	tat	1722	
E	D	I	S	D	E	K	R	L	K	S	T	M	Y		574
cgc	tac	atg	act	cag	gaa	tta	gcc	gag	gaa	ttg	ctg	aaa	tta	1764	
R	Y	M	T	Q	E	L	A	E	E	L	L	K	L		588
gac	gat	gct	aaa	ctg	gga	ggc	gat	cgc	aaa	gaa	gtt	tcc	atc	1806	
D	D	A	K	L	G	G	D	R	K	E	V	S	I		602
ctc	ttt	tcg	gat	att	cgc	ggt	tac	acc	act	ttg	acg	gaa	aat	1848	
L	F	S	D	I	R	G	Y	T	T	L	T	E	N		616
ctg	gaa	gcc	gaa	gaa	gtc	gta	agt	atg	ctc	aat	gaa	tat	ttt	1890	
L	E	A	E	E	V	V	S	M	L	N	E	Y	F		630
gag	tcg	atg	gta	gag	gct	gta	ttc	aaa	cac	aaa	ggc	act	ctg	1932	
E	S	M	V	E	A	V	F	K	H	K	G	T	L		644
gat	aaa	tac	atc	ggt	gat	gcg	att	atg	gcc	gtg	ttt	ggt	tca	1974	
D	K	Y	I	G	D	A	I	M	A	V	F	G	S		658
cct	ttg	ccc	tta	gaa	gaa	cac	gct	tgg	atg	gct	gta	aaa	aca	2016	
P	L	P	L	E	E	H	A	W	M	A	V	K	T		672
tct	ata	gaa	atg	cgt	cat	cgc	tta	caa	gaa	ttt	aat	caa	aaa	2058	
S	I	E	M	R	H	R	L	Q	E	F	N	Q	K		686
cgt	tat	gca	gct	aat	aaa	ccc	cga	atc	aat	atc	ggt	att	ggc	2100	
R	Y	A	A	N	K	P	R	I	N	I	G	I	G		700
atc	aat	tcc	gac	acc	gta	att	agt	ggc	aac	att	ggc	tct	agt	2142	
I	N	S	D	T	V	I	S	G	N	I	G	S	S		714
aaa	cgt	atg	gaa	ttt	aca	gct	att	ggt	gat	ggt	gtg	aat	ctg	2184	
K	R	M	E	F	T	A	I	G	D	G	V	N	L		728
ggt	tcc	cgc	tta	gaa	agt	gtg	agt	aag	cag	tat	ggt	tgc	gac	2226	
G	S	R	L	E	S	V	S	K	Q	Y	G	C	D		742

Appendix

													<u>bp</u>	<u>aa</u>	
att	att	ctc	agt	gat	aat	act	ttt	aaa	cca	tgc	cag	gaa	aat	2268	
I	I	L	S	D	N	T	F	K	P	C	Q	E	N		756
att	tgg	gct	aga	gaa	cta	gat	ttt	atc	cgt	gtt	aaa	ggc	aga	2310	
I	W	A	R	E	L	D	F	I	R	V	K	G	R		770
aat	gag	cca	gta	tct	ata	tac	gag	tta	att	ggt	tta	cgt	tct	2352	
N	E	P	V	S	I	Y	E	L	I	G	L	R	S		784
gac	ccc	att	gct	agt	gaa	aaa	ttg	cag	gta	att	gag	cat	tat	2394	
D	P	I	A	S	E	K	L	Q	V	I	E	H	Y		798
cac	aag	gga	cgg	gaa	tat	tac	ctg	caa	cgt	caa	ttt	tcc	tta	2436	
H	K	G	R	E	Y	Y	L	Q	R	Q	F	S	L		812
gca	aga	gca	gaa	ttt	gcc	aat	gtt	tta	gca	gtt	gat	aaa	cat	2478	
A	R	A	E	F	A	N	V	L	A	V	D	K	H		826
gac	aaa	gcc	gcg	atg	ttg	cat	ctg	cta	cgc	tgt	cag	cat	tgg	2520	
D	K	A	A	M	L	H	L	L	R	C	Q	H	W		840
tta	caa	tca	cct	cca	aca	gat	tca	gaa	tgg	gat	gaa	ggg	gtg	2562	
L	Q	S	P	P	T	D	S	E	W	D	E	G	V		854
tgg	acg	ttt	cag	gag	aag	tga								2583	
W	T	F	Q	E	K	.									860

B-2 Human PDE2A3: N-terminus with GAF-A and -B

gi: 4505657

chromosome: 11 Location: 11q13.4

Acc. No.: NP_002590.1

GeneID (PDE2A): 5138

													<u>bp</u>	<u>aa</u>	
atg	ggg	cag	gca	tgc	ggc	cac	tcc	atc	ctc	tgc	agg	agc	cag	42	
M	G	Q	A	C	G	H	S	I	L	C	R	S	Q		14
cag	tac	ccg	gca	gcg	cga	ccg	gct	gag	ccg	cgg	ggc	cag	cag	84	
Q	Y	P	A	A	R	P	A	E	P	R	G	Q	Q		28

Appendix

													<u>bp</u>	<u>aa</u>	
gtc	ttc	ctc	aag	ccg	gac	gag	ccg	ccg	ccg	ccg	ccg	cag	cca	126	
V	F	L	K	P	D	E	P	P	P	P	P	Q	P		42
tgc	gcc	gac	agc	ctg	cag	gac	gcc	ttg	ctg	agt	ctg	ggc	tct	168	
C	A	D	S	L	Q	D	A	L	L	S	L	G	S		56
gtc	atc	gac	att	tca	ggc	ctg	caa	cgt	gct	gtc	aag	gag	gcc	210	
V	I	D	I	S	G	L	Q	R	A	V	K	E	A		70
ctg	tca	gct	gtg	ctc	ccc	cga	gtg	gaa	act	gtc	tac	acc	tac	252	
L	S	A	V	L	P	R	V	E	T	V	Y	T	Y		84
cta	ctg	gat	ggg	gag	tcc	cag	ctg	gtg	tgt	gag	gac	ccc	cca	294	
L	L	D	G	E	S	Q	L	V	C	E	D	P	P		98
cat	gag	ctg	ccc	cag	gag	ggg	aaa	gtc	cgg	gag	gct	atc	atc	336	
H	E	L	P	Q	E	G	K	V	R	E	A	I	I		112
tcc	cag	aag	cgg	ctg	ggc	tgc	aat	ggg	ctg	ggc	ttc	tca	gac	378	
S	Q	K	R	L	G	C	N	G	L	G	F	S	D		126
ctg	cca	ggg	aag	ccc	ttg	gcc	agg	ctg	gtg	gct	cca	ctg	gct	420	
L	P	G	K	P	L	A	R	L	V	A	P	L	A		140
cct	gat	acc	caa	gtg	ctg	gtc	atg	ccg	cta	gcg	gac	aag	gag	462	
P	D	T	Q	V	L	V	M	P	L	A	D	K	E		154
gct	ggg	gcc	gtg	gca	gct	gtc	atc	ttg	gtg	cac	tgt	ggc	cag	504	
A	G	A	V	A	A	V	I	L	V	H	C	G	Q		168
ctg	agt	gat	aat	gag	gaa	tgg	agc	ctg	cag	gcg	gtg	gag	aag	546	
L	S	D	N	E	E	W	S	L	Q	A	V	E	K		182
cat	acc	ctg	gtc	gcc	ctg	cgg	agg	gtg	cag	gtc	ctg	cag	cag	588	
H	T	L	V	A	L	R	R	V	Q	V	L	Q	Q		196
cgc	ggg	ccc	agg	gag	gct	ccc	cga	gcc	gtc	cag	aac	ccc	ccg	630	
R	G	P	R	E	A	P	R	A	V	Q	N	P	P		210
gag	ggg	acg	gcg	gaa	gac	cag	aag	ggc	ggg	gcg	gcg	tac	acc	672	
E	G	T	A	E	D	Q	K	G	G	A	A	Y	T		224

Appendix

													<u>bp</u>	<u>aa</u>	
gac	cgc	gac	cgc	aag	atc	ctc	caa	ctg	tgc	ggg	gaa	ctc	tac	714	
D	R	D	R	K	I	L	Q	L	C	G	E	L	Y		238
gac	ctg	gat	gcc	tct	tcc	ctg	cag	ctc	aaa	gtg	ctc	caa	tac	756	
D	L	D	A	S	S	L	Q	L	K	V	L	Q	Y		252
ctg	cag	cag	gag	acc	cgg	gca	tcc	cgc	tgc	tgc	ctc	ctg	ctg	798	
L	Q	Q	E	T	R	A	S	R	C	C	L	L	L		266
gtg	tgc	gag	gac	aat	ctc	cag	ctt	tct	tgc	aag	gtc	atc	gga	840	
V	S	E	D	N	L	Q	L	S	C	K	V	I	G		280
gac	aaa	gtg	ctc	ggg	gaa	gag	gtc	agc	ttt	ccc	ttg	aca	gga	882	
D	K	V	L	G	E	E	V	S	F	P	L	T	G		294
tgc	ctg	ggc	cag	gtg	gtg	gaa	gac	aag	aag	tcc	atc	cag	ctg	924	
C	L	G	Q	V	V	E	D	K	K	S	I	Q	L		308
aag	gac	ctc	acc	tcc	gag	gat	gta	caa	cag	ctg	cag	agc	atg	966	
K	D	L	T	S	E	D	V	Q	Q	L	Q	S	M		322
ttg	ggc	tgt	gag	ctg	cag	gcc	atg	ctc	tgt	gtc	cct	gtc	atc	1008	
L	G	C	E	L	Q	A	M	L	C	V	P	V	I		336
agc	cgg	gcc	act	gac	cag	gtg	gtg	gcc	ttg	gcc	tgc	gcc	ttc	1050	
S	R	A	T	D	Q	V	V	A	L	A	C	A	F		350
aac	aag	cta	gaa	gga	gac	ttg	ttc	acc	gac	gag	gac	gag	cat	1092	
N	K	L	E	G	D	L	F	T	D	E	D	E	H		364
gtg	atc	cag	cac	tgc	ttc	cac	tac	acc	agc	acc	gtg	ctc	acc	1134	
V	I	Q	H	C	F	H	Y	T	S	T	V	L	T		378
agc	acc	ctg	gcc	ttc	cag	aag	gaa	cag	aaa	ctc	aag	tgt	gag	1176	
S	T	L	A	F	Q	K	E	Q	K	L	K	C	E		392
tgc	cag	gct	ctt	ctc	caa	gtg	gca	aag	aac	ctc	ttc	acc	cac	1218	
C	Q	A	L	L	Q	V	A	K	N	L	F	T	H		406
ctg	gat	gac	gtc	tct	gtc	ctg	ctc	cag	gag	atc	atc	acg	gag	1260	
L	D	D	V	S	V	L	L	Q	E	I	I	T	E		420

Appendix

														<u>bp</u>	<u>aa</u>
gcc	aga	aac	ctc	agc	aac	gca	gag	atc	tgc	tct	gtg	ttc	ctg	1302	
A	R	N	L	S	N	A	E	I	C	S	V	F	L		434
ctg	gat	cag	aat	gag	ctg	gtg	gcc	aag	gtg	ttc	gac	ggg	ggc	1344	
L	D	Q	N	E	L	V	A	K	V	F	D	G	G		448
gtg	gtg	gat	gat	gag	agc	tat	gag	atc	cgc	atc	ccg	gcc	gat	1386	
V	V	D	D	E	S	Y	E	I	R	I	P	A	D		462
cag	ggc	atc	gcg	gga	cac	gtg	gcg	acc	acg	ggc	cag	atc	ctg	1428	
Q	G	I	A	G	H	V	A	T	T	G	Q	I	L		476
aac	atc	cct	gac	gca	tat	gcc	cat	ccg	ctt	ttc	tac	cgc	ggc	1470	
N	I	P	D	A	Y	A	H	P	L	F	Y	R	G		490
gtg	gac	gac	agc	acc	ggc	ttc	cgc	acg	cgc	aac	atc	ctc	tgc	1512	
V	D	D	S	T	G	F	R	T	R	N	I	L	C		504
ttc	ccc	atc	aag	aac	gag	aac	cag	gag	gtc	atc	ggt	gtg	gcc	1554	
F	P	I	K	N	E	N	Q	E	V	I	G	V	A		518
gag	ctg	gtg	aac	aag	atc	aat	ggg	cca	tgg	ttc	agc	aag	ttc	1596	
E	L	V	N	K	I	N	G	P	W	F	S	K	F		532
gac	gag	gac	ctg	gcg	acg	gcc	ttc	tcc	atc	tac	tgc	ggc	atc	1638	
D	E	D	L	A	T	A	F	S	I	Y	C	G	I		546
agc	atc	gcc	cat	tct	ctc	cta	tac	aaa	aaa	gtg	aat	gag	gct	1680	
S	I	A	H	S	L	L	Y	K	K	V	N	E	A		560
cag	tat														
Q	Y														562

B-3 Rat PDE2A: GAF-A and -B

gi: 13592021

chromosome: 1 ; Location: 1q32

Acc.no.: NM_031079.1

GeneID: 81743 ProteinID: NP_112341

GAF domain from E207-546

Appendix

														<u>bp</u>	<u>aa</u>
gaa	aag	gga	tac	acc	gcc	cat	gac	cga	aag	atc	ctg	caa	ctg	660	
E	K	G	Y	T	A	H	D	R	K	I	L	Q	L		220
tgt	gga	gaa	ctc	tat	gac	ttg	gat	gcc	act	tct	ctg	cag	ctc	702	
C	G	E	L	Y	D	L	D	A	T	S	L	Q	L		234
aaa	gtc	ctt	cga	tat	ctt	cag	cag	gag	aca	cag	gcc	act	cac	744	
K	V	L	R	Y	L	Q	Q	E	T	Q	A	T	H		248
tgc	tgc	ctc	ctg	ctg	gtg	tca	gag	gac	aac	ctg	cag	ctt	tcc	786	
C	C	L	L	L	V	S	E	D	N	L	Q	L	S		262
tgc	aag	gtc	att	gga	gag	aaa	gtg	ctg	gga	gaa	gag	gtc	agc	828	
C	K	V	I	G	E	K	V	L	G	E	E	V	S		276
ttt	cca	ttg	acc	atg	gga	cgc	ctg	ggc	cag	gtg	gtg	gag	gac	870	
F	P	L	T	M	G	R	L	G	Q	V	V	E	D		290
aaa	cag	tgt	atc	cag	ttg	aag	gac	cta	acc	tct	gac	gat	gtg	912	
K	Q	C	I	Q	L	K	D	L	T	S	D	D	V		304
caa	cag	cta	caa	aac	atg	ttc	ggg	tgt	gag	ctt	cgg	gct	atg	954	
Q	Q	L	Q	N	M	L	G	C	E	L	R	A	M		318
cta	tgt	gtc	cct	gtc	atc	agt	cga	gcc	act	gac	cag	gtg	gtg	996	
L	C	V	P	V	I	S	R	A	T	D	Q	V	V		332
gcc	ctg	gct	tgc	gcc	ttc	aac	aag	ctt	gga	gga	gac	ttc	ttc	1038	
A	L	A	C	A	F	N	K	L	G	G	D	F	F		346
aca	gat	gag	gat	gaa	cgt	gcg	atc	caa	cac	tgc	ttc	cac	tac	1080	
T	D	E	D	E	R	A	I	Q	H	C	F	H	Y		360
aca	ggc	acg	gtg	ctc	acc	agt	acc	ttg	gcc	ttc	cag	aag	gag	1122	
T	G	T	V	L	T	S	T	L	A	F	Q	K	E		374
cag	aag	ctc	aag	tgg	tga	tgc	cag	gct	ctt	ctc	caa	gtg	gca	1164	
Q	K	L	K	C	E	C	Q	A	L	L	Q	V	A		388
aag	aac	ctc	ttc	acc	cac	ctg	gat	gac	gtc	tct	gtc	ctg	cta	1206	
K	N	L	F	T	H	L	D	D	V	S	V	L	L		402

Appendix

														<u>bp</u>	<u>aa</u>
cag	gag	atc	atc	aca	gag	gcc	aga	aac	ctc	agc	aac	gca	gag	1248	
Q	E	I	I	T	E	A	R	N	L	S	N	A	E		416
atc	tgc	tcc	gtg	ttc	ctg	ctg	gat	cag	aat	gag	ctg	gtt	gcc	1290	
I	C	S	V	F	L	L	D	Q	N	E	L	V	A		430
aag	gtg	ttc	gat	ggc	ggt	gta	gtg	gac	gat	gag	agt	tat	gag	1332	
K	V	F	D	G	G	V	V	D	D	E	S	Y	E		444
atc	cgc	atc	cct	gcg	gac	caa	ggc	atc	gcg	ggc	cac	gtg	gcg	1374	
I	R	I	P	A	D	Q	G	I	A	G	H	V	A		458
acc	acg	ggc	cag	atc	ctg	aac	atc	cca	gat	gca	tac	gcc	cat	1416	
T	T	G	Q	I	L	N	I	P	D	A	Y	A	H		472
ccg	ctt	ttc	tat	cgc	ggc	gta	gac	gac	agc	act	ggc	ttc	cgc	1458	
P	L	F	Y	R	G	V	D	D	S	T	G	F	R		486
acg	cgc	aac	att	ctc	tgc	ttc	cct	atc	aag	aac	gag	aac	caa	1500	
T	R	N	I	L	C	F	P	I	K	N	E	N	Q		500
gag	gtc	atc	ggt	gtg	gct	gag	cta	gtg	aac	aag	atc	aat	ggg	1542	
E	V	I	G	V	A	E	L	V	N	K	I	N	G		514
cca	tgg	ttc	agc	aaa	ttt	gat	gag	gac	ctg	gcc	aca	gcc	ttc	1584	
P	W	F	S	K	F	D	E	D	L	A	T	A	F		528
tcc	atc	tac	tgt	ggc	att	agc	atc	gct	cac	tct	ctc	cta	Tac	1626	
S	I	Y	C	G	I	S	I	A	H	S	L	L	Y		542
aaa	aag	gtg	aat											1638	
K	K	V	N												546

B-4 Human PDE5A1: N-Terminus with GAF-A and -B

gi: 61744435

Chromosome no.: 4 Location: 4q25-q27

Acc. no.: NM_001083.3

GeneID (PDE5A): 8654

Appendix

														<u>bp</u>	<u>aa</u>
atg	gag	cgg	gcc	ggc	ccc	agc	ttc	ggg	cag	cag	cga	cag	cag	42	
M	E	R	A	G	P	S	F	G	Q	Q	R	Q	Q		14
cag	cag	ccc	cag	cag	cag	aag	cag	cag	cag	agg	gat	cag	gac	84	
Q	Q	P	Q	Q	Q	K	Q	Q	Q	R	D	Q	D		28
tcg	gtc	gaa	gca	tgg	ctg	gac	gat	cac	tgg	gac	ttt	acc	ttc	126	
S	V	E	A	W	L	D	D	H	W	D	F	T	F		42
tca	tac	ttt	gtt	aga	aaa	gcc	acc	aga	gaa	atg	gtc	aat	gca	168	
S	Y	F	V	R	K	A	T	R	E	M	V	N	A		56
tgg	ttt	gct	gag	aga	gtt	cac	acc	atc	cct	gtg	tgc	aag	gaa	210	
W	F	A	E	R	V	H	T	I	P	V	C	K	E		70
ggt	atc	aga	ggc	cac	acc	gaa	tct	tgc	tct	tgt	ccc	ttg	cag	252	
GE	E	R	G	H	T	E	S	C	S	C	P	L	Q		84
cag	agt	cct	cgt	gca	gat	aac	agt	gtc	cct	gga	aca	cca	acc	294	
Q	S	P	R	A	D	N	S	V	P	G	T	P	T		98
agg	aaa	atc	tct	gcc	tct	gaa	ttt	gac	cgg	cct	ctt	aga	ccc	336	
R	K	I	S	A	S	E	F	D	R	P	L	R	P		112
att	gtt	gtc	aag	gat	tct	gag	gga	act	gtg	agc	ttc	ctc	tct	378	
I	V	V	K	D	S	E	G	T	V	S	F	L	S		126
gac	tca	gaa	aag	aag	gaa	cag	atg	cct	cta	acc	cct	cca	agg	420	
D	S	E	K	K	E	Q	M	P	L	T	P	P	R		140
ttt	gat	cat	gat	gaa	ggg	gac	cag	tgc	tca	aga	tct	ttg	gaa	462	
F	D	H	D	R	G	D	Q	C	S	R	L	L	E		154
tta	gtg	aag	gat	att	tct	agt	cat	ttg	gat	gtc	aca	gcc	tta	504	
L	V	K	D	I	S	S	H	L	D	V	T	A	L		168
tgt	cac	aaa	att	ttc	ttg	cat	atc	cat	gga	ctg	ata	tct	gct	546	
C	H	K	I	F	L	H	I	H	G	L	I	S	A		182
gac	cgc	tat	tcc	ctg	ttc	ctt	gtc	tgt	gaa	gac	agc	tcc	aat	588	
D	R	Y	S	L	F	L	V	C	E	D	S	S	N		196

Appendix

														<u>bp</u>	<u>aa</u>
gac	aag	ttt	ctt	atc	agc	cgc	ctc	ttt	gat	gtt	gct	gaa	ggt	630	
D	K	F	L	I	S	R	L	F	D	V	A	E	G		210
tca	aca	ctg	gaa	gaa	gtt	tca	aat	aac	tgt	atc	cgc	tta	gaa	672	
S	T	L	E	E	V	S	N	N	C	I	R	L	E		224
tgg	aac	aaa	ggc	att	gtg	gga	cat	gtg	gca	gcg	ctt	ggt	gag	714	
W	N	K	G	I	V	G	H	V	A	A	L	G	E		238
ccc	ttg	aac	atc	aaa	gat	gca	tat	gag	gat	cct	cgg	ttc	aat	756	
P	L	N	I	K	D	A	Y	E	D	P	R	F	N		252
gca	gaa	gtt	gac	caa	att	aca	ggc	tac	aag	aca	caa	agc	att	798	
A	E	V	D	Q	I	T	G	Y	K	T	Q	S	I		266
ctt	tgt	atg	cca	att	aag	aat	cat	agg	gaa	gag	gtt	gtt	ggt	840	
L	C	M	P	I	K	N	H	R	E	E	V	V	G		280
gta	gcc	cag	gcc	atc	aac	aag	aaa	tca	gga	aac	ggt	ggg	aca	882	
V	A	Q	A	I	N	K	K	S	G	N	G	G	T		294
ttt	act	gaa	aaa	gat	gaa	aag	gac	ttt	gct	gct	tat	ttg	gca	924	
F	T	E	K	D	E	K	D	F	A	A	Y	L	A		308
ttt	tgt	ggt	att	gtt	ctt	cat	aat	gct	cag	ctc	tat	gag	act	966	
F	C	G	I	V	L	H	N	A	Q	L	Y	E	T		322
tca	ctg	ctg	gag	aac	aag	aga	aat	cag	gtg	ctg	ctt	gac	ctt	1008	
S	L	L	E	N	K	R	N	Q	V	L	L	D	L		336
gct	agt	tta	att	ttt	gaa	gaa	caa	caa	tca	tta	gaa	gta	att	1050	
A	S	L	I	F	E	E	Q	Q	S	L	E	V	I		350
ttg	aag	aaa	ata	gct	gcc	act	att	atc	tct	ttc	atg	caa	gtg	1092	
L	K	K	I	A	A	T	I	I	S	F	M	Q	V		364
cag	aaa	tgc	acc	att	ttc	ata	gtg	gat	gaa	gat	tgc	tcc	gat	1134	
Q	K	C	T	I	F	I	V	D	E	D	C	S	D		378
tct	ttt	tct	agt	gtg	ttt	cac	atg	gag	tgt	gag	gaa	tta	gaa	1176	
S	F	S	S	V	F	H	M	E	C	E	E	L	E		392

Appendix

														<u>bp</u>	<u>aa</u>
aaa	tca	tct	gat	aca	tta	aca	agg	gaa	cat	gat	gca	aac	aaa	1218	
K	S	S	D	T	L	T	R	E	H	D	A	N	K		406
atc	aat	tac	atg	tat	gct	cag	tat	gtc	aaa	aat	act	atg	gaa	1260	
I	N	Y	M	Y	A	Q	Y	V	K	N	T	M	E		420
cca	ctt	aat	atc	cca	gat	gtc	agt	aag	gat	aaa	aga	ttt	ccc	1302	
P	L	N	I	P	D	V	S	K	D	K	R	F	P		434
tgg	aca	act	gaa	aat	aca	gga	aat	gta	aac	cag	cag	tgc	att	1344	
W	T	T	E	N	T	G	N	V	N	Q	Q	C	I		448
aga	agt	ttg	ctt	tgt	aca	cct	ata	aaa	aat	gga	aag	aag	aat	1386	
R	S	L	L	C	T	P	I	K	N	G	K	K	N		462
aaa	gtt	ata	ggg	gtt	tgc	caa	ctt	gtt	aat	aag	atg	gag	gag	1428	
K	V	I	G	V	C	Q	L	V	N	K	M	E	E		476
aat	act	ggc	aag	gtt	aag	cct	ttc	aac	cga	aat	gac	gaa	cag	1470	
N	T	G	K	V	K	P	F	N	R	N	D	E	Q		490
ttt	ctg	gaa	gct	ttt	gtc	atc	ttt	tgt	ggc	ttg	ggg	atc	cag	1512	
F	L	E	A	F	V	I	F	C	Q	L	G	I	Q		504
aac	acg	cag	atg	tat	gaa	gca	gtg	gag	aga	gtt	ctg	tcg	tat	1554	
N	T	Q	M	Y	E	A	V	E	R	A	M	A	K		518
cat	gct	tca	gca	gca	gag	gaa	gaa	aca	aga	gag	cta	cag	tcg	1596	
Q	M	V	T	L	E	V	L	S	Y	H	A	S	A		532
tta	gcg	gct	gct	gtg	gtg	cca	tct	gcc	cag	acc	ctt	aaa	att	1638	
A	E	E	E	T	R	E	L	Q	S	L	A	A	A		546
act	gac													1644	
V	V														548

B-5 CyaB1 (alr2266)

gi: 15553050

Acc. no.: D89623.2

GeneID (CyaB1): 1105863 proteinID: BAA13998

Appendix

													<u>bp</u>	<u>aa</u>	
atg	act	ctt	ccc	aat	cct	ggt	agc	gtt	ttg	gct	tcg	tta	aca	42	
M	T	L	P	N	P	G	S	V	L	A	S	L	T		14
gaa	ctg	act	caa	gtt	aat	cgt	acc	cac	gct	tta	ttg	cgt	cgg	84	
E	L	T	Q	V	N	R	T	H	A	L	L	R	R		28
gtc	aaa	gac	ctt	tct	gtt	aac	gaa	ttt	gtt	tgc	ttg	cta	gac	126	
V	K	D	L	S	V	N	E	F	V	C	L	L	D		42
ttt	atc	act	gcc	gaa	tcc	gaa	caa	ttt	ctc	aga	gca	att	gaa	168	
F	I	T	A	E	F	E	Q	F	L	R	A	I	E		56
ctc	att	aat	aat	gaa	gcc	cta	gaa	aat	atg	ttg	gag	aaa	gtg	210	
L	I	N	N	E	A	L	E	N	M	L	E	K	V		70
ttg	gaa	gca	att	aca	ctg	aaa	atc	ggt	caa	att	ctc	caa	gca	252	
L	E	A	I	T	L	K	I	G	Q	I	L	Q	A		84
gaa	cat	aca	gcc	att	ttc	tta	gtt	gac	tat	gat	aaa	tgt	caa	294	
E	H	T	A	I	F	L	V	D	Y	D	K	C	Q		98
tta	tgg	tca	aaa	gta	ccc	caa	gat	aat	ggg	cag	aaa	ttt	tta	336	
L	W	S	K	V	P	Q	D	N	G	Q	G	F	L		112
gaa	att	cgt	act	ccc	att	act	gta	gga	att	cct	ggt	cat	Gtt	378	
E	I	R	T	P	I	T	V	G	I	P	G	H	V		126
gct	agt	aca	ggt	caa	tat	tta	aat	atc	tca	gaa	act	gct	act	420	
A	S	T	G	Q	Y	L	N	I	S	E	T	A	T		140
cat	cct	ttg	ttt	agc	cca	gga	tta	gag	aga	caa	atg	ggc	tat	462	
H	P	L	F	S	P	E	L	E	R	Q	M	G	Y		154
aag	att	aat	aat	att	tta	tgt	atg	cct	gtc	gtt	agt	agc	aaa	504	
K	I	N	N	I	L	C	M	P	V	V	S	S	K		168
gat	cca	att	gtc	gca	gta	gta	caa	tta	gct	aat	aag	aca	gga	546	
D	Q	I	V	A	V	V	Q	L	A	N	K	T	G		182
aat	ata	ccc	ttc	aat	cga	aat	gat	gaa	gag	tct	ttt	cgt	gat	588	
N	I	P	F	N	R	N	D	E	E	S	F	R	D		196

Appendix

														<u>bp</u>	<u>aa</u>
ttt	gct	gct	tct	att	ggg	att	att	tta	gaa	acc	tgt	caa	tct	630	
F	A	A	S	I	G	I	I	L	E	T	C	Q	S		210
ttt	tat	gtt	gca	gct	cgc	aat	caa	cgg	gga	gtc	aca	gca	ctt	672	
F	Y	V	A	A	R	N	Q	R	G	V	T	A	L		224
tta	cgc	gct	act	caa	aca	cta	ggg	caa	agt	cta	gat	tta	gag	714	
L	R	A	T	Q	T	L	G	Q	S	L	D	L	E		238
gct	act	ttg	caa	ata	gtg	atg	gaa	caa	gcc	cga	att	ttg	atg	756	
A	T	L	Q	I	V	M	E	Q	A	R	I	L	M		252
cag	gca	gac	cgc	agc	aca	tta	ttt	ctg	tat	cgc	aaa	gaa	atg	798	
Q	A	D	R	S	T	L	F	L	Y	R	K	E	M		266
ggc	gaa	ctc	tgg	act	aaa	gta	gca	gca	gca	gca	gat	acc	aca	840	
G	E	L	W	T	K	V	A	A	A	A	D	T	T		280
cag	tta	ata	gaa	att	cgg	att	ccg	gcg	aat	cgc	ggt	att	gtc	882	
Q	L	I	E	I	R	I	P	A	N	R	G	I	V		294
ggc	tat	gtg	gca	tct	aca	ggc	gat	gcg	ctg	aat	atc	tct	gat	924	
G	Y	V	A	S	T	G	D	A	L	N	I	S	D		308
gct	tat	aaa	gac	ccc	cgg	ttt	gat	cca	aca	aca	gac	aga	aaa	966	
A	Y	K	D	P	R	F	D	P	T	T	D	R	K		322
aca	ggc	tat	ttg	acc	aga	aat	att	ttg	tgt	ttg	cca	gtc	ttt	1008	
T	G	Y	L	T	R	N	I	L	C	L	P	V	F		336
aat	tca	gcc	aat	gaa	ttg	atc	gga	gta	aca	cag	tta	att	aat	1050	
N	S	A	N	E	L	I	G	V	T	Q	L	I	N		350
aag	caa	caa	gga	agt	ttt	acg	gct	tct	gat	gaa	gag	ttt	atg	1092	
K	Q	Q	G	S	F	T	A	S	D	E	E	F	M		364
cgg	gct	ttt	aat	att	caa	gcc	gga	gtt	gct	tta	gaa	aat	gct	1134	
R	A	F	N	I	Q	A	G	V	A	L	E	N	A		378
cgt	tta	ttt	gaa	aat	gta	tta	ctc	gag	aaa	caa	tat	caa	aaa	1176	
R	L	F	E	N	V	L	L	E	K	Q	Y	Q	K		392

Appendix

													<u>bp</u>	<u>aa</u>	
gac	att	tta	caa	agc	ttg	tca	gat	gct	gta	att	tct	aca	gat	1218	
D	I	L	Q	S	L	S	D	A	V	I	S	T	D		406
atg	gcc	ggg	aga	att	gtc	aca	att	aat	gat	gca	gcc	ttg	gaa	1260	
M	A	G	R	I	V	T	I	N	D	A	A	L	E		420
tta	ctc	ggt	tgt	cct	tta	ggt	gat	gct	aat	cat	aaa	agt	aat	1302	
L	L	G	C	P	L	G	D	A	N	H	K	S	N		434
aag	ctg	ctg	tgg	gaa	caa	aat	tta	att	ggt	cgc	gta	gtt	tgg	1344	
K	L	L	W	E	Q	N	L	I	G	R	V	V	W		448
gaa	att	gta	cca	att	gaa	aat	ttg	cag	atg	cgc	tta	gaa	gat	1386	
E	I	V	P	I	E	N	L	Q	M	R	L	E	D		462
agt	tta	aaa	agt	ggt	gct	aaa	cat	tat	gtg	cca	gaa	caa	agt	1428	
S	L	K	S	G	A	K	H	Y	V	P	E	Q	S		476
ttg	ata	gtg	gga	att	tat	caa	tta	caa	atg	tct	gaa	agt	cgg	1470	
L	I	V	G	I	Y	Q	L	Q	M	S	E	S	R		490
gtt	ttg	cat	gaa	act	caa	gac	tac	tct	att	ttg	aca	gta	cgc	1512	
V	L	H	E	T	Q	D	Y	S	I	L	T	V	R		504
gat	cgc	atc	aac	cca	gat	att	ttt	ctc	ccc	tgg	aat	tta	ccc	1554	
D	R	I	N	P	D	I	F	L	P	W	N	L	P		518
caa	acc	ccc	cag	tcg	caa	ttt	atc	acc	ccg	gaa	gaa	gta	caa	1596	
Q	T	P	Q	S	Q	F	I	T	P	E	E	V	Q		532
atc	tta	gaa	cgc	agt	att	aat	ctt	acc	gtt	aat	cct	ttg	acg	1638	
I	L	E	R	S	I	N	L	T	V	N	P	L	T		546
aac	cca	gaa	ggc	ggt	gtc	cgt	ggt	ggt	ttg	gta	gtt	ttg	gaa	1680	
N	P	E	G	G	V	R	G	G	L	V	V	L	E		560
gat	att	agt	caa	gag	aag	cgc	ctc	aaa	act	act	atg	tat	cgc	1722	
D	I	S	Q	E	K	R	L	K	T	T	M	Y	R		574
tac	ctt	aca	ccc	cat	gta	gct	gaa	cag	gta	atg	gct	tta	ggg	1764	
Y	L	T	P	H	V	A	E	Q	V	M	A	L	G		588

Appendix

													<u>bp</u>	<u>aa</u>	
gaa	gat	gcc	tta	atg	gtt	ggt	gaa	cgc	aag	gag	gtg	act	gtt	1806	
E	D	A	L	M	V	G	E	R	K	E	V	T	V		602
tta	ttt	tca	gat	atc	cga	ggc	tac	acc	aca	ctt	acg	gaa	aat	1848	
L	F	S	D	I	R	G	Y	T	T	L	T	E	N		616
cta	ggt	gcg	gct	gaa	gtg	gta	tca	ctc	ctg	aac	caa	tat	ttt	1890	
L	G	A	A	E	V	V	S	L	L	N	Q	Y	F		630
gaa	aca	atg	gtt	gaa	gca	gtt	ttc	aac	tat	gaa	ggc	aca	ctg	1932	
E	T	M	V	E	A	V	F	N	Y	E	G	T	L		644
gat	aaa	ttt	atc	ggt	gat	gct	tta	atg	gct	gtt	ttt	ggt	gcg	1974	
D	K	F	I	G	D	A	L	M	A	V	F	G	A		658
cca	cta	cca	ctc	aca	gaa	aat	cat	gct	tgg	caa	gca	gta	cag	2016	
P	L	P	L	T	E	N	H	A	W	Q	A	V	Q		672
tca	gca	tta	gat	atg	cgc	caa	cgc	ctg	aag	gaa	ttt	aac	caa	2058	
S	A	L	D	M	R	Q	R	L	K	E	F	N	Q		686
cga	cgc	atc	att	cag	gca	caa	cca	caa	atc	aaa	atc	ggt	att	2100	
R	R	I	I	Q	A	Q	P	Q	I	K	I	G	I		700
ggt	att	agt	tct	gga	gaa	gta	gtt	tct	ggt	aac	atc	ggt	tct	2142	
G	I	S	S	G	E	V	V	S	G	N	I	G	G		714
cac	aag	cgt	atg	gat	tac	aca	gtc	att	ggt	gat	ggt	gtg	aat	2184	
H	K	R	M	D	Y	T	V	I	G	D	G	V	N		728
tta	agt	tcc	cgc	ttg	gaa	act	gtc	acc	aaa	gaa	tat	ggc	tgt	2226	
L	S	S	R	L	E	T	V	T	K	E	Y	G	C		742
gat	att	atc	ctc	agt	gag	ttt	act	tac	caa	tta	tgc	agc	gat	2268	
D	I	I	L	S	E	F	T	Y	Q	L	C	S	D		756
cgc	att	tgg	gta	cgt	cag	tta	gat	aaa	atc	cga	gtc	aaa	ggg	2310	
R	I	W	V	R	Q	L	D	K	I	R	V	K	G		770
aaa	cac	caa	gct	gtc	aat	atc	tat	gag	ttg	att	agc	gat	cgc	2352	
K	H	Q	A	V	N	I	Y	E	L	I	S	D	R		784

Appendix

														<u>bp</u>	<u>aa</u>
agt	act	ccc	tta	gat	gac	aac	acc	caa	gag	ttc	ctc	ttt	cac	2394	
S	T	P	L	D	D	N	T	Q	E	F	L	F	H		798
tat	cat	aat	ggt	cgg	act	gcc	tac	tta	gtc	cgc	gat	ttt	acc	2436	
Y	H	N	G	R	T	A	Y	L	V	R	D	F	T		812
cag	gcg	atc	gct	tgt	ttt	aac	tca	gct	aaa	cat	att	cga	ccc	2478	
Q	A	I	A	C	F	N	S	A	K	H	I	R	P		826
aca	gac	caa	gct	gct	aat	att	cac	cta	gaa	cgc	gcc	tac	aat	2520	
T	D	Q	A	V	N	I	H	L	E	R	A	Y	N		840
tat	caa	caa	act	cca	cca	cct	cct	cca	tgg	gac	ggc	gta	tgg	2562	
Y	Q	Q	T	P	P	P	P	Q	W	D	G	V	W		854
aca	att	ttc	aca	aag	tag									2580	
T	I	F	T	K	.										859

1 References

- 1 Anantharaman, V., Koonin, E. V. and Aravind, L. (2001) Regulatory potential, phyletic distribution and evolution of ancient, intracellular small-molecule-binding domains. *J Mol Biol* **307**, 1271-1292
- 2 Sutherland, E. W. and Rall, T. W. (1958) Fractionation and characterization of a cyclic adenine ribonucleotide formed by tissue particles. *J Biol Chem* **232**, 1077-1091
- 3 Ashman, D. F., Lipton, R., Melicow, M. M. and Price, T. D. (1963) Isolation of adenosine 3', 5'-monophosphate and guanosine 3', 5'-monophosphate from rat urine. *Biochem Biophys Res Commun* **11**, 330-334
- 4 Lipkin, D., Cook, W. H. and Markham, R. (1959) Adenosine-3': 5'-phosphoric Acid: A Proof of Structure. *J Am Chem Soc* **81**, 6198-6203
- 5 Beavo, J. A. (1995) Cyclic nucleotide phosphodiesterases: functional implications of multiple isoforms. *Physiol Rev* **75**, 725-748
- 6 Francis, S. H., Turko, I. V. and Corbin, J. D. (2001) Cyclic nucleotide phosphodiesterases: relating structure and function. *Prog Nucleic Acid Res Mol Biol* **65**, 1-52
- 7 Soderling, S. H. and Beavo, J. A. (2000) Regulation of cAMP and cGMP signaling: new phosphodiesterases and new functions. *Curr Opin Cell Biol* **12**, 174-179
- 8 Beavo, J. A. and Brunton, L. L. (2002) Cyclic nucleotide research -- still expanding after half a century. *Nat Rev Mol Cell Biol* **3**, 710-718
- 9 Omori, K. and Kotera, J. (2007) Overview of PDEs and their regulation. *Circ Res* **100**, 309-327
- 10 Rybalkin, S. D., Yan, C., Bornfeldt, K. E. and Beavo, J. A. (2003) Cyclic GMP phosphodiesterases and regulation of smooth muscle function. *Circ Res* **93**, 280-291
- 11 Ma, X., Sayed, N., Baskaran, P., Beuve, A. and van den Akker, F. (2008) PAS-mediated dimerization of soluble guanylyl cyclase revealed by signal transduction histidine kinase domain crystal structure. *J Biol Chem* **283**, 1167-1178
- 12 Ponting, C. P., Aravind, L., Schultz, J., Bork, P. and Koonin, E. V. (1999) Eukaryotic signalling domain homologues in archaea and bacteria. Ancient ancestry and horizontal gene transfer. *J Mol Biol* **289**, 729-745
- 13 Martinez, S. E., Beavo, J. A. and Hol, W. G. (2002) GAF Domains: Two-Billion-Year-Old Molecular Switches that Bind Cyclic Nucleotides. *Mol Interv* **2**, 317-323
- 14 Aravind, L. and Ponting, C. P. (1997) The GAF domain: an evolutionary link between diverse phototransducing proteins. *Trends Biochem Sci* **22**, 458-459
- 15 Zoraghi, R., Bessay, E. P., Corbin, J. D. and Francis, S. H. (2005) Structural and functional features in human PDE5A1 regulatory domain that provide for allosteric cGMP binding, dimerization, and regulation. *J Biol Chem* **280**, 12051-12063
- 16 Zoraghi, R., Corbin, J. D. and Francis, S. H. (2004) Properties and functions of GAF domains in cyclic nucleotide phosphodiesterases and other proteins. *Mol Pharmacol* **65**, 267-278

References

- 17 Ho, Y. S., Burden, L. M. and Hurley, J. H. (2000) Structure of the GAF domain, a ubiquitous signaling motif and a new class of cyclic GMP receptor. *Embo J* **19**, 5288-5299
- 18 Francis, S. H., Lincoln, T. M. and Corbin, J. D. (1980) Characterization of a novel cGMP binding protein from rat lung. *J Biol Chem* **255**, 620-626
- 19 Gross-Langenhoff, M., Hofbauer, K., Weber, J., Schultz, A. and Schultz, J. E. (2006) cAMP is a ligand for the tandem GAF domain of human phosphodiesterase 10 and cGMP for the tandem GAF domain of phosphodiesterase 11. *J Biol Chem* **281**, 2841-2846
- 20 Muradov, H., Boyd, K. K. and Artemyev, N. O. (2004) Structural determinants of the PDE6 GAF A domain for binding the inhibitory gamma-subunit and noncatalytic cGMP. *Vision Res* **44**, 2437-2444
- 21 Farber, D. B. and Danciger, M. (1997) Identification of genes causing photoreceptor degenerations leading to blindness. *Curr Opin Neurobiol* **7**, 666-673
- 22 McLaughlin, M. E., Sandberg, M. A., Berson, E. L. and Dryja, T. P. (1993) Recessive mutations in the gene encoding the beta-subunit of rod phosphodiesterase in patients with retinitis pigmentosa. *Nat Genet* **4**, 130-134
- 23 Martinez, S. E., Bruder, S., Schultz, A., Zheng, N., Schultz, J. E., Beavo, J. A. and Linder, J. U. (2005) Crystal structure of the tandem GAF domains from a cyanobacterial adenylyl cyclase: modes of ligand binding and dimerization. *Proc Natl Acad Sci U S A* **102**, 3082-3087
- 24 Martinez, S. E., Wu, A. Y., Glavas, N. A., Tang, X. B., Turley, S., Hol, W. G. and Beavo, J. A. (2002) The two GAF domains in phosphodiesterase 2A have distinct roles in dimerization and in cGMP binding. *Proc Natl Acad Sci U S A* **99**, 13260-13265
- 25 Lin, Z., Johnson, L. C., Weissbach, H., Brot, N., Lively, M. O. and Lowther, W. T. (2007) Free methionine-(R)-sulfoxide reductase from *Escherichia coli* reveals a new GAF domain function. *Proc Natl Acad Sci U S A* **104**, 9597-9602
- 26 Taylor, B. L. and Zhulin, I. B. (1999) PAS domains: internal sensors of oxygen, redox potential, and light. *Microbiol Mol Biol Rev* **63**, 479-506
- 27 Zhulin, I. B., Taylor, B. L. and Dixon, R. (1997) PAS domain S-boxes in Archaea, Bacteria and sensors for oxygen and redox. *Trends Biochem Sci* **22**, 331-333
- 28 Rutter, J., Michnoff, C. H., Harper, S. M., Gardner, K. H. and McKnight, S. L. (2001) PAS kinase: an evolutionarily conserved PAS domain-regulated serine/threonine kinase. *Proc Natl Acad Sci U S A* **98**, 8991-8996
- 29 Nambu, J. R., Lewis, J. O., Wharton, K. A., Jr. and Crews, S. T. (1991) The *Drosophila* single-minded gene encodes a helix-loop-helix protein that acts as a master regulator of CNS midline development. *Cell* **67**, 1157-1167
- 30 Narikawa, R., Okamoto, S., Ikeuchi, M. and Ohmori, M. (2004) Molecular evolution of PAS domain-containing proteins of filamentous cyanobacteria through domain shuffling and domain duplication. *DNA Res* **11**, 69-81
- 31 Hefti, M. H., Francoijs, K. J., de Vries, S. C., Dixon, R. and Vervoort, J. (2004) The PAS fold. A redefinition of the PAS domain based upon structural prediction. *Eur J Biochem* **271**, 1198-1208

References

- 32 Pellequer, J. L., Wager-Smith, K. A., Kay, S. A. and Getzoff, E. D. (1998) Photoactive yellow protein: a structural prototype for the three-dimensional fold of the PAS domain superfamily. *Proc Natl Acad Sci U S A* **95**, 5884-5890
- 33 Ponting, C. P. and Aravind, L. (1997) PAS: a multifunctional domain family comes to light. *Curr Biol* **7**, R674-677
- 34 Alex, L. A. and Simon, M. I. (1994) Protein histidine kinases and signal transduction in prokaryotes and eukaryotes. *Trends Genet* **10**, 133-138
- 35 Sprenger, W. W., Hoff, W. D., Armitage, J. P. and Hellingwerf, K. J. (1993) The eubacterium *Ectothiorhodospira halophila* is negatively phototactic, with a wavelength dependence that fits the absorption spectrum of the photoactive yellow protein. *J Bacteriol* **175**, 3096-3104
- 36 Soderling, S. H., Bayuga, S. J. and Beavo, J. A. (1998) Identification and characterization of a novel family of cyclic nucleotide phosphodiesterases. *J Biol Chem* **273**, 15553-15558
- 37 Schibler, U. (1998) Circadian rhythms. New cogwheels in the clockworks. *Nature* **393**, 620-621
- 38 Kay, S. A. (1997) PAS, present, and future: clues to the origins of circadian clocks. *Science* **276**, 753-754
- 39 Warmke, J. W. and Ganetzky, B. (1994) A family of potassium channel genes related to *eag* in *Drosophila* and mammals. *Proc Natl Acad Sci U S A* **91**, 3438-3442
- 40 Jiang, B. H., Semenza, G. L., Bauer, C. and Marti, H. H. (1996) Hypoxia-inducible factor 1 levels vary exponentially over a physiologically relevant range of O₂ tension. *Am J Physiol* **271**, C1172-1180
- 41 Kurokawa, H., Lee, D. S., Watanabe, M., Sagami, I., Mikami, B., Raman, C. S. and Shimizu, T. (2004) A redox-controlled molecular switch revealed by the crystal structure of a bacterial heme PAS sensor. *J Biol Chem* **279**, 20186-20193
- 42 Borgstahl, G. E., Williams, D. R. and Getzoff, E. D. (1995) 1.4 Å structure of photoactive yellow protein, a cytosolic photoreceptor: unusual fold, active site, and chromophore. *Biochemistry* **34**, 6278-6287
- 43 Gong, W., Hao, B., Mansy, S. S., Gonzalez, G., Gilles-Gonzalez, M. A. and Chan, M. K. (1998) Structure of a biological oxygen sensor: a new mechanism for heme-driven signal transduction. *Proc Natl Acad Sci U S A* **95**, 15177-15182
- 44 Soderback, E., Reyes-Ramirez, F., Eydmann, T., Austin, S., Hill, S. and Dixon, R. (1998) The redox- and fixed nitrogen-responsive regulatory protein NIFL from *Azotobacter vinelandii* comprises discrete flavin and nucleotide-binding domains. *Mol Microbiol* **28**, 179-192
- 45 Christie, J. M., Salomon, M., Nozue, K., Wada, M. and Briggs, W. R. (1999) LOV (light, oxygen, or voltage) domains of the blue-light photoreceptor phototropin (*nph1*): binding sites for the chromophore flavin mononucleotide. *Proc Natl Acad Sci U S A* **96**, 8779-8783
- 46 Vreede, J., van der Horst, M. A., Hellingwerf, K. J., Crielgaard, W. and van Aalten, D. M. (2003) PAS domains. Common structure and common flexibility. *J Biol Chem* **278**, 18434-18439

References

- 47 Paulussen, A., Raes, A., Matthijs, G., Snyders, D. J., Cohen, N. and Aerssens, J. (2002) A novel mutation (T65P) in the PAS domain of the human potassium channel HERG results in the long QT syndrome by trafficking deficiency. *J Biol Chem* **277**, 48610-48616
- 48 Richter, W. (2002) 3',5' Cyclic nucleotide phosphodiesterases class III: members, structure, and catalytic mechanism. *Proteins* **46**, 278-286
- 49 Aravind, L. and Koonin, E. V. (1998) The HD domain defines a new superfamily of metal-dependent phosphohydrolases. *Trends Biochem Sci* **23**, 469-472
- 50 Lander, E. S. and et.al (2001) Initial sequencing and analysis of the human genome. *Nature* **409**, 860-921
- 51 Venter, J. C. and et.al (2001) The sequence of the human genome. *Science* **291**, 1304-1351
- 52 Beavo, J. A., Conti, M. and Heaslip, R. J. (1994) Multiple cyclic nucleotide phosphodiesterases. *Mol Pharmacol* **46**, 399-405
- 53 Iffland, A., Kohls, D., Low, S., Luan, J., Zhang, Y., Kothe, M., Cao, Q., Kamath, A. V., Ding, Y. H. and Ellenberger, T. (2005) Structural determinants for inhibitor specificity and selectivity in PDE2A using the wheat germ in vitro translation system. *Biochemistry* **44**, 8312-8325
- 54 Chew, K. K., Stuckey, B. G. and Thompson, P. L. (2000) Erectile dysfunction, sildenafil and cardiovascular risk. *Med J Aust* **172**, 279-283
- 55 Hemnes, A. R. and Champion, H. C. (2006) Sildenafil, a PDE5 inhibitor, in the treatment of pulmonary hypertension. *Expert Rev Cardiovasc Ther* **4**, 293-300
- 56 Sandner, P., Hutter, J., Tinel, H., Ziegelbauer, K. and Bischoff, E. (2007) PDE5 inhibitors beyond erectile dysfunction. *Int J Impot Res* **19**, 533-543
- 57 Card, G. L., Blasdel, L., England, B. P., Zhang, C., Suzuki, Y., Gillette, S., Fong, D., Ibrahim, P. N., Artis, D. R., Bollag, G., Milburn, M. V., Kim, S. H., Schlessinger, J. and Zhang, K. Y. (2005) A family of phosphodiesterase inhibitors discovered by cocrystallography and scaffold-based drug design. *Nat Biotechnol* **23**, 201-207
- 58 Bender, A. T. and Beavo, J. A. (2006) Cyclic nucleotide phosphodiesterases: molecular regulation to clinical use. *Pharmacol Rev* **58**, 488-520
- 59 Conti, M. (2000) Phosphodiesterases and cyclic nucleotide signaling in endocrine cells. *Mol Endocrinol* **14**, 1317-1327
- 60 Richter, W. and Conti, M. (2002) Dimerization of the type 4 cAMP-specific phosphodiesterases is mediated by the upstream conserved regions (UCRs). *J Biol Chem* **277**, 40212-40221
- 61 Bentley, J. K. (2005) Immunoprecipitation of PDE2 phosphorylated and inactivated by an associated protein kinase. *Methods Mol Biol* **307**, 211-223
- 62 Conti, M. and Beavo, J. (2007) Biochemistry and physiology of cyclic nucleotide phosphodiesterases: essential components in cyclic nucleotide signaling. *Annu Rev Biochem* **76**, 481-511
- 63 Sette, C. and Conti, M. (1996) Phosphorylation and activation of a cAMP-specific phosphodiesterase by the cAMP-dependent protein kinase. Involvement of serine 54 in the enzyme activation. *J Biol Chem* **271**, 16526-16534

References

- 64 Sharma, R. K. and Wang, J. H. (1985) Differential regulation of bovine brain calmodulin-dependent cyclic nucleotide phosphodiesterase isoenzymes by cyclic AMP-dependent protein kinase and calmodulin-dependent phosphatase. *Proc Natl Acad Sci U S A* **82**, 2603-2607
- 65 Degerman, E., Belfrage, P. and Manganiello, V. C. (1997) Structure, localization, and regulation of cGMP-inhibited phosphodiesterase (PDE3). *J Biol Chem* **272**, 6823-6826
- 66 Menniti, F. S., Faraci, W. S. and Schmidt, C. J. (2006) Phosphodiesterases in the CNS: targets for drug development. *Nat Rev Drug Discov* **5**, 660-670
- 67 Pandit, J. M., CT, US) (2005) Crystal structure of 3', 5'-cyclic nucleotide phosphodiesterase (PDE1B) and uses thereof. United States Pfizer Inc **20050075795**
- 68 Scapin, G., Patel, S. B., Chung, C., Varnerin, J. P., Edmondson, S. D., Mastracchio, A., Parmee, E. R., Singh, S. B., Becker, J. W., Van der Ploeg, L. H. and Tota, M. R. (2004) Crystal structure of human phosphodiesterase 3B: atomic basis for substrate and inhibitor specificity. *Biochemistry* **43**, 6091-6100
- 69 Xu, R. X., Hassell, A. M., Vanderwall, D., Lambert, M. H., Holmes, W. D., Luther, M. A., Rocque, W. J., Milburn, M. V., Zhao, Y., Ke, H. and Nolte, R. T. (2000) Atomic structure of PDE4: insights into phosphodiesterase mechanism and specificity. *Science* **288**, 1822-1825
- 70 Huai, Q., Colicelli, J. and Ke, H. (2003) The crystal structure of AMP-bound PDE4 suggests a mechanism for phosphodiesterase catalysis. *Biochemistry* **42**, 13220-13226
- 71 Huai, Q., Wang, H., Sun, Y., Kim, H. Y., Liu, Y. and Ke, H. (2003) Three-dimensional structures of PDE4D in complex with roliprams and implication on inhibitor selectivity. *Structure* **11**, 865-873
- 72 sung, B., Hwang, KY, Jeon, YH, Lee, JI, Heo, YS, Kim, JH, Moon, J, Yoon, JM, Hyun, YL, Kim, E, Eum, SJ, Park, SY, Lee, JO, Lee, TG, Ro, S, Cho, JM (2003) structure of the catalytic domain of human phosphodiesterase 5 with bound drug molecules. *Nature* **425**, 98-102
- 73 Wang, H., Liu, Y., Chen, Y., Robinson, H. and Ke, H. (2005) Multiple elements jointly determine inhibitor selectivity of cyclic nucleotide phosphodiesterases 4 and 7. *J Biol Chem* **280**, 30949-30955
- 74 Huai, Q., Wang, H., Zhang, W., Colman, R. W., Robinson, H. and Ke, H. (2004) Crystal structure of phosphodiesterase 9 shows orientation variation of inhibitor 3-isobutyl-1-methylxanthine binding. *Proc Natl Acad Sci U S A* **101**, 9624-9629
- 75 Wang, H., Liu, Y., Hou, J., Zheng, M., Robinson, H. and Ke, H. (2007) Structural insight into substrate specificity of phosphodiesterase 10. *Proc Natl Acad Sci U S A* **104**, 5782-5787
- 76 Zhang, K. Y., Card, G. L., Suzuki, Y., Artis, D. R., Fong, D., Gillette, S., Hsieh, D., Neiman, J., West, B. L., Zhang, C., Milburn, M. V., Kim, S. H., Schlessinger, J. and Bollag, G. (2004) A glutamine switch mechanism for nucleotide selectivity by phosphodiesterases. *Mol Cell* **15**, 279-286
- 77 Wang, H., Robinson, H. and Ke, H. (2007) The molecular basis for different recognition of substrates by phosphodiesterase families 4 and 10. *J Mol Biol* **371**, 302-307

References

- 78 Linder, J. U. and Schultz, J. E. (2003) The class III adenylyl cyclases: multi-purpose signalling modules. *Cell Signal* **15**, 1081-1089
- 79 Kanacher, T. (2003) Die Adenylatcyclase CyaB1 aus *Anabaena* sp. PCC 7120 ist ein cAMP-sensitives Protein., Dissertation der Universität Tübingen
- 80 Kanacher, T., Schultz, A., Linder, J. U. and Schultz, J. E. (2002) A GAF-domain-regulated adenylyl cyclase from *Anabaena* is a self-activating cAMP switch. *Embo J* **21**, 3672-3680
- 81 Ohmori, M. and Okamoto, S. (2004) Photoresponsive cAMP signal transduction in cyanobacteria. *Photochem Photobiol Sci* **3**, 503-511
- 82 Kaneko, T., Nakamura, Y., Wolk, C. P., Kuritz, T., Sasamoto, S., Watanabe, A., Iriguchi, M., Ishikawa, A., Kawashima, K., Kimura, T., Kishida, Y., Kohara, M., Matsumoto, M., Matsuno, A., Muraki, A., Nakazaki, N., Shimpo, S., Sugimoto, M., Takazawa, M., Yamada, M., Yasuda, M. and Tabata, S. (2001) Complete genomic sequence of the filamentous nitrogen-fixing cyanobacterium *Anabaena* sp. strain PCC 7120. *DNA Res* **8**, 205-213; 227-253
- 83 Tada, T., Sekimoto, H, Ohmori, M (2001) Biochemical characterization of an adenylate cyclase, CyaB1, in the Cyanobacterium *Anabaena* sp. strain PCC 7120. *journal of plant research* **114**, 387-394
- 84 Linder, J. U. (2006) Class III adenylyl cyclases: molecular mechanisms of catalysis and regulation. *Cell Mol Life Sci* **63**, 1736-1751
- 85 Cann, M. (2007) A subset of GAF domains are evolutionarily conserved sodium sensors. *Mol Microbiol* **64**, 461-472
- 86 Altschul, S. F., Madden, T. L., Schaffer, A. A., Zhang, J., Zhang, Z., Miller, W. and Lipman, D. J. (1997) Gapped BLAST and PSI-BLAST: a new generation of protein database search programs. *Nucleic Acids Res* **25**, 3389-3402
- 87 Bairoch, A., Bucher, P. and Hofmann, K. (1997) The PROSITE database, its status in 1997. *Nucleic Acids Res* **25**, 217-221
- 88 Schultz, J., Milpetz, F., Bork, P. and Ponting, C. P. (1998) SMART, a simple modular architecture research tool: identification of signaling domains. *Proc Natl Acad Sci U S A* **95**, 5857-5864
- 89 Tautz, D. and Renz, M. (1983) An optimized freeze-squeeze method for the recovery of DNA fragments from agarose gels. *Anal Biochem* **132**, 14-19
- 90 Cohen, S. N., Chang, A. C., Boyer, H. W. and Helling, R. B. (1973) Construction of biologically functional bacterial plasmids in vitro. *Proc Natl Acad Sci U S A* **70**, 3240-3244
- 91 Sanger, F., Nicklen, S. and Coulson, A. R. (1977) DNA sequencing with chain-terminating inhibitors. *Proc Natl Acad Sci U S A* **74**, 5463-5467
- 92 Karger, A. E. (1996) Separation of DNA sequencing fragments using an automated capillary electrophoresis instrument. *Electrophoresis* **17**, 144-151
- 93 Cohen, A. S., Najarian, D. R., Paulus, A., Guttman, A., Smith, J. A. and Karger, B. L. (1988) Rapid separation and purification of oligonucleotides by high-performance capillary gel electrophoresis. *Proc Natl Acad Sci U S A* **85**, 9660-9663

References

- 94 Bradford, M. M. (1976) A rapid and sensitive method for the quantitation of microgram quantities of protein utilizing the principle of protein-dye binding. *Anal Biochem* **72**, 248-254
- 95 Laemmli, U. K. (1970) Cleavage of structural proteins during the assembly of the head of bacteriophage T4. *Nature* **227**, 680-685
- 96 Towbin, H., Staehelin, T. and Gordon, J. (1979) Electrophoretic transfer of proteins from polyacrylamide gels to nitrocellulose sheets: procedure and some applications. *Proc Natl Acad Sci U S A* **76**, 4350-4354
- 97 Salomon, Y., Londos, C. and Rodbell, M. (1974) A highly sensitive adenylyl cyclase assay. *Anal Biochem* **58**, 541-548
- 98 Adachi, H., Takano, K., Morikawa, M., Kanaya, S., Yoshimura, M., Mori, Y. and Sasaki, T. (2003) Application of a two-liquid system to sitting-drop vapour-diffusion protein crystallization. *Acta Crystallogr D Biol Crystallogr* **59**, 194-196
- 99 Molin, S. O., Nygren, H. and Dolonius, L. (1978) A new method for the study of glutaraldehyde-induced crosslinking properties in proteins with special reference to the reaction with amino groups. *J Histochem Cytochem* **26**, 412-414
- 100 Ramesh, V. and Nagaraja, V. (1996) Sequence-specific DNA binding of the phage Mu C protein: footprinting analysis reveals altered DNA conformation upon protein binding. *J Mol Biol* **260**, 22-33
- 101 Bruder, S., Linder, J. U., Martinez, S. E., Zheng, N., Beavo, J. A. and Schultz, J. E. (2005) The cyanobacterial tandem GAF domains from the *cyaB2* adenylyl cyclase signal via both cAMP-binding sites. *Proc Natl Acad Sci U S A* **102**, 3088-3092
- 102 Armbruster, B. N., Banik, S. S., Guo, C., Smith, A. C. and Counter, C. M. (2001) N-terminal domains of the human telomerase catalytic subunit required for enzyme activity in vivo. *Mol Cell Biol* **21**, 7775-7786
- 103 Sellers, W. R., Novitch, B. G., Miyake, S., Heith, A., Otterson, G. A., Kaye, F. J., Lassar, A. B. and Kaelin, W. G., Jr. (1998) Stable binding to E2F is not required for the retinoblastoma protein to activate transcription, promote differentiation, and suppress tumor cell growth. *Genes Dev* **12**, 95-106
- 104 Stroop, S. D. and Beavo, J. A. (1991) Structure and function studies of the cGMP-stimulated phosphodiesterase. *J Biol Chem* **266**, 23802-23809
- 105 Guo, Y. L., Seebacher, T., Kurz, U., Linder, J. U. and Schultz, J. E. (2001) Adenylyl cyclase Rv1625c of *Mycobacterium tuberculosis*: a progenitor of mammalian adenylyl cyclases. *Embo J* **20**, 3667-3675
- 106 Bruder, S., Schultz, A. and Schultz, J. E. (2006) Characterization of the tandem GAF domain of human phosphodiesterase 5 using a cyanobacterial adenylyl cyclase as a reporter enzyme. *J Biol Chem* **281**, 19969-19976
- 107 Sonnenburg, W. K., Mullaney, P. J. and Beavo, J. A. (1991) Molecular cloning of a cyclic GMP-stimulated cyclic nucleotide phosphodiesterase cDNA. Identification and distribution of isozyme variants. *J Biol Chem* **266**, 17655-17661
- 108 Martins, T. J., Mumby, M. C. and Beavo, J. A. (1982) Purification and characterization of a cyclic GMP-stimulated cyclic nucleotide phosphodiesterase from bovine tissues. *J Biol Chem* **257**, 1973-1979

References

- 109 Mumby, M. C., Martins, T. J., Chang, M. L. and Beavo, J. A. (1982) Identification of cGMP-stimulated cyclic nucleotide phosphodiesterase in lung tissue with monoclonal antibodies. *J Biol Chem* **257**, 13283-13290
- 110 Pyne, N. J., Cooper, M. E. and Houslay, M. D. (1986) Identification and characterization of both the cytosolic and particulate forms of cyclic GMP-stimulated cyclic AMP phosphodiesterase from rat liver. *Biochem J* **234**, 325-334
- 111 Rosman, G. J., Martins, T. J., Sonnenburg, W. K., Beavo, J. A., Ferguson, K. and Loughney, K. (1997) Isolation and characterization of human cDNAs encoding a cGMP-stimulated 3',5'-cyclic nucleotide phosphodiesterase. *Gene* **191**, 89-95
- 112 Tanaka, T., Hockman, S., Moos, M., Jr., Taira, M., Meacci, E., Murashima, S. and Manganiello, V. C. (1991) Comparison of putative cGMP-binding regions in bovine brain and cardiac cGMP-stimulated phosphodiesterases. *Second Messengers Phosphoproteins* **13**, 87-98
- 113 Yang, Q., Paskind, M., Bolger, G., Thompson, W. J., Repaske, D. R., Cutler, L. S. and Epstein, P. M. (1994) A novel cyclic GMP stimulated phosphodiesterase from rat brain. *Biochem Biophys Res Commun* **205**, 1850-1858
- 114 Whalin, M. E., Strada, S. J. and Thompson, W. J. (1988) Purification and partial characterization of membrane-associated type II (cGMP-activatable) cyclic nucleotide phosphodiesterase from rabbit brain. *Biochim Biophys Acta* **972**, 79-94
- 115 Zaccolo, M. and Movsesian, M. A. (2007) cAMP and cGMP signaling cross-talk: role of phosphodiesterases and implications for cardiac pathophysiology. *Circ Res* **100**, 1569-1578
- 116 Groß-Langenhoff, M. (2007) Biochemische Charakterisierung der Funktion der GAF Domänen der Phosphodiesterase 11A4. dissertation der universität Tübingen
- 117 Yanaka, N., Kotera, J., Ohtsuka, A., Akatsuka, H., Imai, Y., Michibata, H., Fujishige, K., Kawai, E., Takebayashi, S., Okumura, K. and Omori, K. (1998) Expression, structure and chromosomal localization of the human cGMP-binding cGMP-specific phosphodiesterase PDE5A gene. *Eur J Biochem* **255**, 391-399
- 118 Brown, J. H., Cohen, C. and Parry, D. A. (1996) Heptad breaks in alpha-helical coiled coils: stutters and stammers. *Proteins* **26**, 134-145
- 119 Muradov, K. G., Boyd, K. K., Martinez, S. E., Beavo, J. A. and Artemyev, N. O. (2003) The GAFa domains of rod cGMP-phosphodiesterase 6 determine the selectivity of the enzyme dimerization. *J Biol Chem* **278**, 10594-10601
- 120 Rybalkin, S. D., Rybalkina, I. G., Shimizu-Albergine, M., Tang, X. B. and Beavo, J. A. (2003) PDE5 is converted to an activated state upon cGMP binding to the GAF A domain. *Embo J* **22**, 469-478
- 121 Corbin, J. D. and Francis, S. H. (1999) Cyclic GMP phosphodiesterase-5: target of sildenafil. *J Biol Chem* **274**, 13729-13732
- 122 Hulko, M., Berndt, F., Gruber, M., Linder, J. U., Truffault, V., Schultz, A., Martin, J., Schultz, J. E., Lupas, A. N. and Coles, M. (2006) The HAMP domain structure implies helix rotation in transmembrane signaling. *Cell* **126**, 929-940
- 123 Cusanovich, M. A. and Meyer, T. E. (2003) Photoactive yellow protein: a prototypic PAS domain sensory protein and development of a common signaling mechanism. *Biochemistry* **42**, 4759-4770

References

- 124 Morais Cabral, J., Lee, A., Kohen, S., Chait, B., Li, N. and Mackinnon, R. (1998) Crystal structure and functional analysis of the HERG potassium channel N-terminus: a eukaryotic PAS domain. *Cell* **95**, 649–655
- 125 Repik, A., Rebbapragada, A., Johnson, M. S., Haznedar, J. O., Zhulin, I. B. and Taylor, B. L. (2000) PAS domain residues involved in signal transduction by the Aer redox sensor of *Escherichia coli*. *Mol Microbiol* **36**, 806-816
- 126 Giorgetti, A., Raimondo, D., Miele, A. E. and Tramontano, A. (2005) Evaluating the usefulness of protein structure models for molecular replacement. *Bioinformatics* **21 Suppl 2**, ii72-76
- 127 Wu, A. Y., Tang, X. B., Martinez, S. E., Ikeda, K. and Beavo, J. A. (2004) Molecular determinants for cyclic nucleotide binding to the regulatory domains of phosphodiesterase 2A. *J Biol Chem* **279**, 37928-37938

My academic professors during my study in Jordan University of Science and Technology (JUST), Irbid, Jordan, were ladies and gentlemen:

M. Abuirjeie	Medicinal chemistry
F. Alali	Analytical chemistry
N. Al-Bashir	Biochemistry
H. Alhadidi	Pharmacology
K. AlKhamis	Advanced physical pharmacy
A. Al-Kofahi	Pharmacognosy
S. Assaf	Drug delivery systems
B. Al-taani	Drug stability
Z. Bataineh	Anatomy
R. Batchoun	Parasitology
Z. Elnasser	Microbiology
M. Hasan	Pharmacology and pathology
M. Hassan	Organic chemistry
N. Idkaidek	Industrial pharmacy
J. Jilani	Medicinal chemistry
M. N. Khawam	Physical pharmacy
S. Khateeb	Physiology
A. Obaidat	Pharmacokinetics
A. Qandil	Medicinal chemistry
F. Ridha	Analytical chemistry
B. Tashtoosh	Drug design

LEBENS LAUF

Name	Iman Abdel-Salam Megbel Mansi	
Geburtsdatum	26. Oktober 1973	
Geburtsort	Irbid- Jordanien	
Schulausbildung	1979-1985	Grundschule, Irbid, Jordanien
	1985-1988	Gymnasium, Irbid, Jordanien
	1988-1991	Abitur, Irbid, Jordanien
Studium	1991-1996	Bachelor in Pharmazeutische Naturwissenschaften an der Fakultät für Pharmazie, Jordanische Universität für Wissenschaft und Technologie (JUST), Irbid, Jordanien
	1998-2000	Master in Pharmazeutische Naturwissenschaften (pharmazeutische Technologie) an der Fakultät für Pharmazie, Jordanische Universität für Wissenschaft und Technologie (JUST), Irbid, Jordanien
Promotion	2004-2007	Gottlieb Daimler und Karl Benz Stipendiatin an der Fakultät für Chemie und Pharmazie der Universität Tübingen. Der experimentelle Teil der vorliegenden Arbeit wurde zwischen August 2004 und September 2007 unter der Leitung von Herrn Prof. Dr. J.E.Schultz angefertigt
Berufserfahrung	1996-2000	Lehr und Wissenschaftlicher Assistentin an der Fakultät für Pharmazie, Philadelphia Universität, Amman, Jordanien
	2001-2004	Ganztägig Dozentin an der Fakultät für Pharmazie, Jordanien Universität für Wissenschaft und Technologie, Irbid, Jordanien

CURRICULUM VITAE (C.V.)

Name	Iman Abdel-Salam Megbel Mansi	
Date of birth	26 th , October 1973	
Place of birth	Irbid- Jordan	
School education	1979-1985	Primary school, Irbid, Jordan
	1985-1988	Preparatory school, Irbid, Jordan
	1988-1991	Secondary school, Irbid, Jordan
	June, 1991	General secondary education certificate, Irbid, Jordan
University education	1991-1996	Bachelor of science (Pharmacy), faculty of Pharmacy, Jordan University of Science and Technology (JUST), Irbid, Jordan
	1998-2000	Master in pharmaceutical technology, Faculty of Pharmacy, Jordan University of Science and Technology (JUST), Irbid, Jordan
PhD	2004-2007	Gottlieb Daimler und Karl Benz scholarship holder at the faculty of chemistry and Pharmacy, University of Tübingen. The experimental part of this work was performed within the period from August 2004 to September 2007 under the supervision of Prof. Dr. J.E.Schultz
Work experience	1996-2000	Teaching assistant, faculty of pharmacy, Philadelphia university, Amman, Jordan
	2001-2004	Full-time lecturer, Faculty of pharmacy, Jordan University of science and Technology (JUST), Irbid, Jordan